Stratos III - Mission Planning

A conceptual design for a mission involving a sounding rocket capable of reaching at least 120 km

Shiv Appiah	4115635	Jason Gahagan	4042468
Pieter Gilissen	4024222	Byeongjun Kim	1544357
Junhyeon Lee	4089286	Lars Pepermans	4144538
Mark Rozemeijer	4141733	Bram Strack van Schijndel	4100662
Leon Turmaine	4139690	Stefan van Buuren	1374028

Final Review

Design Synthesis Exercise

TU Delft Delft University of Technology

Faculty of Aerospace Engineering

January 27, 2015(Final Version)

Preface

Dear Reader,

In 2009, DARE launched their Stratos I rocket to an altitude of 12.3 km [1]. The follow-up mission, Stratos II, is ready and waiting for launch in DARE's Korolev lab, designed and built to reach an altitude of 50 km. Looking forward, DARE is hoping to complete their objective with the Stratos program: reach space. This milestone achievement will fall under the responsibility of the newest DARE mission: the Stratos III project.

We would like to thank Chris Verhoeven for acting as principal tutor for this project. We would also like to thank Giuseppe Correale and Haiyang Hu for their guidance and advice in their role as coaches. In addition, we would like to thank the members of DARE for setting up this project and for their work in the past. In particular we would like to thank DARE members Maneesh Kumar Verma, Martin Olde BSc, Tobias Knop BSc and Geert Henk Visser BSc for their assistance to the team and their feedback on the work. We also like to thank Tessa Voogt for her creative input for the mission patch. Finally, we want to thank Ir. Barry Zandbergen for his guidance and input into our propulsion system.

Stratos III DSE team (Fall 2014-2015): Shiv Appiah, Pieter Gilissen, Junhyeon Lee, Mark Rozemeijer, Leon Turmaine, Jason Gahagan, Byeongjun Kim, Lars Pepermans, Bram Strack van Schijndel, Stefan van Buuren

Summary

In 2004, the Civilian Space Exploration Team became the first amateur team to launch a rocket into space, setting a record at an altitude of 116 km [2]. In 2009, DARE launched Stratos I, a two-staged rocket that reached an altitude of 12.3 km. After the successful launch of the Stratos I, the dream was to reach higher altitudes and eventually break into space. An altitude of 50 km was considered the next milestone and this led to the Stratos II, a rocket designed to reach 50 km altitude carrying a scientific payload to be recovered after the launch. The goal of this Design Synthesis Exercise (DSE) was to carry out the mission planning of the Stratos III, a sounding rocket designed to reach an altitude of more than 120 km and, therefore, break the current amateur record. This report presents the design process for the Stratos III rocket and the mission around it.

In conjunction with DARE's experience from Stratos II and the key requirements of the DSE, system-level requirements were generated that were used to determine the functions and subsystems of the rocket and mission. Each subsystem and the mission also generated their own sets of requirements. From there, subsystems used design option trees and trade-off tables to choose the best options that could be used for the Stratos III rocket concept generation. From the 32 concepts generated, one was chosen based on a normalized, quantitative scoring system. The major components of this design included a single-stage, hybrid engine using Nytrox as oxidizer and Paraffin-Al as solid fuel and an active canard control system. From this point, the rocket underwent further design on a subsystem level that required constant iteration for proper system integration.

After 18 major iterations, a final conceptual design was built. The 5.65 m tall, 310 kg rocket is simulated to reach Mach 5.2 after a 29 second engine burn providing a total impulse of 428 kNs. Following a 156 seconds coasting phase the now 138 kg rocket reaches an apogee of 134 km. The rocket will be steered via an active canard control system to keep the rocket on track during both ascent and descent. A ballute followed by a main parachute will slow down the rocket to its water landing location 11 minutes after launch.

Following the design of the rocket, the report describes the mission aspects that are not directly related to the rocket subsystem; from launch site and launch day procedures to logistics and public relations. This also incorporates the development strategy, production plan, management plan, and resources. The final part of the report includes an explanation of the marketability of this mission, which is crucial for the project to appeal to third parties and potential sponsors.

The design provided in this report has a number of uncertainties that must be addressed in the following phases of the Stratos III mission. The performance of the rocket is very sensitive to the specific impulse of the propulsion system. As a result it will be necessary that the rocket will undergo a re-sizing to match the expected performance from small-scale engine testing. Also, the capabilities of the active canard control system are uncertain. It is important to carefully develop and test this system. Finally, around the target altitude of 120 km, a single kilogram of dry mass can have an effect of around 2 km in maximum altitude using the same mass of propellant. Putting constant effort in minimizing weight wherever possible can keep the rocket at a weight that the fully designed engine will be capable of launching into space.

From an organizational point of view also constant effort is required in order to keep the project on schedule. As Stratos III should act as an important pillar program within DARE, it is vital that DARE develops a comprehensive knowledge management system to keep control over the flow of information within the Stratos III project as well as DARE as a whole.

Contents

Preface I

Summary II

Table of Contents V

List of Tables VII

List of Figures IX

List of Symbols X

1 Introduction 1

2 Project Overview 2
- 2.1 Stratos III Mission Breakdown . . . 3
- 2.2 RAMS . . . 3
  - 2.2.1 Reliability . . . 3
  - 2.2.2 Availability . . . 3
  - 2.2.3 Maintainability . . . 3
  - 2.2.4 Safety . . . 5

3 System Design 6
- 3.1 Design Approach . . . 6
  - 3.1.1 Concept Selection . . . 6
  - 3.1.2 Subsystem Design . . . 8
  - 3.1.3 Final Concept Design . . . 8
- 3.2 Final Design Characteristics . . . 9
  - 3.2.1 Resource Budgets . . . 9
  - 3.2.2 Astrodynamics . . . 10
  - 3.2.3 Aerodynamics . . . 12
  - 3.2.4 System Sensitivity Analysis . . . 16

4 Detailed Design 18
- 4.1 Layout . . . 18
  - 4.1.1 External Layout . . . 18
  - 4.1.2 Internal Layout . . . 18
- 4.2 Propulsion . . . 21
  - 4.2.1 Propellant Characteristics . . . 21
  - 4.2.2 Propulsion Subsystem Performance Simulation Model . . . 21
  - 4.2.3 Liquid Oxidizer Tank Design . . . 25
  - 4.2.4 Feed System Design . . . 29
  - 4.2.5 Solid Grain Design . . . 30
  - 4.2.6 Material Compatibility . . . 31
  - 4.2.7 Performance . . . 31
  - 4.2.8 Sensitivity Analysis . . . 32
  - 4.2.9 Mass, Power, and Cost Budget . . . 33
- 4.3 Structure . . . 34
  - 4.3.1 Assumptions . . . 34

4.3.2 Fuselage . . . 34
4.3.3 Nosecone . . . 35
4.3.4 Thermal Loads . . . 37
4.3.5 Design Summary . . . 37
4.3.6 Sensitivity Analysis . . . 39
4.3.7 Mass and Cost Budget . . . 40
4.4 ADCS . . . 40
4.4.1 Attitude and Position Determination . . . 41
4.4.2 Canard and Fin Sizing . . . 43
4.4.3 Rocket Stability Sensitivity Analysis . . . 50
4.4.4 Mass and Cost Budget . . . 51
4.5 Power . . . 51
4.5.1 Power Budget . . . 51
4.5.2 Battery Selection . . . 51
4.5.3 Architecture . . . 52
4.5.4 Sensitivity Analysis . . . 56
4.5.5 Mass and Cost Budget . . . 56
4.6 Communications . . . 56
4.6.1 Antenna Sizing . . . 56
4.6.2 Thermal Control . . . 58
4.6.3 Sensitivity Analysis . . . 58
4.6.4 Mass and Cost Budget . . . 58
4.7 Payload . . . 59
4.8 Recovery . . . 59
4.8.1 Approach . . . 59
4.8.2 Configurations . . . 61
4.8.3 Chosen Re-entry Attitude . . . 61
4.8.4 Main Parachute . . . 62
4.8.5 Ballute . . . 65
4.8.6 Deployment System . . . 68
4.8.7 Simulation . . . 68
4.8.8 Sensitivity Analysis . . . 71
4.8.9 Ground Phase Recovery . . . 72
4.8.10 Mass, Cost, & Power Budget . . . 72
4.9 Flight Termination System . . . 73
4.9.1 System Overview . . . 73
4.9.2 Radio Uplink . . . 74
4.9.3 Receiver Antennas Type and Placing . . . 75
4.9.4 Power . . . 75
4.9.5 Flight Termination Logic . . . 75
4.9.6 Powered Flight Termination Methods . . . 76
4.9.7 Recovery after Flight Termination . . . 76
4.9.8 Mass and Cost Budget . . . 77

5 Verification and Validation **78**
5.1 The System . . . 78
5.2 Subsystems . . . 79
5.2.1 Propulsion . . . 79
5.2.2 Structure . . . 79
5.2.3 ADCS . . . 79
5.2.4 Power . . . 80
5.2.5 Communications . . . 80
5.2.6 Recovery . . . 80
5.2.7 FTS . . . 81
5.3 Rocket Compliance Matrix . . . 81

6 Mission Analysis **83**
6.1 Stratos III Team . . . 83
6.2 Design and Development Logic . . . 84
6.3 Planning of the Stratos III Project . . . 86
6.3.1 Milestones . . . 86
6.4 Development Strategy . . . 90
6.4.1 Propulsion . . . 90
6.4.2 Structure . . . 90
6.4.3 ADCS . . . 90
6.4.4 Power . . . 91
6.4.5 Communications . . . 91
6.4.6 FTS . . . 92
6.4.7 Recovery . . . 92
6.5 Production, Manufacturing and Assembly Plan . . . 92
6.5.1 Propulsion . . . 92
6.5.2 Structure . . . 93
6.5.3 ADCS . . . 93
6.5.4 Power . . . 93
6.5.5 Communications . . . 93
6.5.6 Recovery . . . 93
6.5.7 FTS . . . 94
6.6 Operations . . . 94
6.6.1 Transport . . . 94
6.6.2 The Launch . . . 94
6.7 Resources . . . 98
6.7.1 Materials . . . 98
6.7.2 Financial . . . 98
6.7.3 Knowledge . . . 98
6.7.4 Work and Experience . . . 99
6.7.5 Testing and Launching . . . 99
6.8 Mission Compliance Matrix . . . 99
6.9 Budget . . . 100
6.10 Risk Analysis . . . 101

7 Marketability **104**
7.1 Sustainability . . . 104
7.2 Market Analysis . . . 105
7.2.1 The Sounding Rocket Market . . . 105
7.2.2 Market Trends . . . 106
7.3 'WOW' Factor . . . 106
7.4 Public Relations . . . 106
7.5 Comparison to Other Amateur Sounding Rockets . . . 107
7.5.1 Student Rockets . . . 107

8 Conclusion and Recommendations **109**
8.1 Conclusion . . . 109
8.2 Recommendations . . . 109

Bibliography **113**

A Stratos III Key Parameters **114**

B Requirements **116**
B.1 Subsystems . . . 117
B.2 Mission . . . 119

C DSE Team Organization **121**
C.1 Internal Team Organization . . . 121
C.2 Work Distribution . . . 122

D Project Gantt Chart **123**

List of Tables

2.1 Overview of the Different Nomenclature Used in the Stratos III Project . . . 2
2.2 The Key Requirements for the Stratos III Program . . . 3

3.1 System Requirements for the Stratos III Rocket . . . 6
3.2 Mass Budget for the Stratos III Rocket . . . 10
3.3 Cost Budget for the Stratos III Rocket . . . 10
3.4 Stratos III Key Times . . . 10
3.5 Results of System Sensitivity Analysis . . . 16
3.6 Percent Results of System Sensitivity Analysis . . . 17

4.1 The Ranges for the OF, P_c, A_c/A_t and A_e/A_t. . . . 23
4.2 Variance of T_c and $c^\star$. . . . 23
4.3 Regression Rate Constants . . . 23
4.4 Effect of Addition of Aluminum Powder . . . 31
4.5 Propulsion Key Performance Parameters . . . 32
4.6 Results of Sensitivity Analysis . . . 33
4.7 Percent Results of Sensitivity Analysis . . . 33
4.8 Propulsion Subsystem Item List . . . 33
4.9 Final Rocket Dimensions . . . 39
4.10 Material Properties . . . 39
4.11 Sensitivity Analysis on the Shell Thickness . . . 40
4.12 Sensitivity Analysis on the Oxidizer Tank Thickness . . . 40
4.13 Cost Budget for the Structure Subsystem . . . 40
4.14 Mass Budget for the Structure Subsystem . . . 40
4.15 Final Geometry for Control Surfaces . . . 47
4.16 Mass and Cost Budget of ADCS . . . 51
4.17 Power Budget of Each Subsystem . . . 51
4.18 Specifications of the Battery . . . 52
4.19 Mass and Cost Budget of Power Subsystem . . . 56
4.20 Mass and Cost Budget of Communication Subsystem . . . 58
4.21 Different Options for the Main Parachute . . . 63
4.22 Main Parachute Properties . . . 63
4.23 Main Parachute Forces . . . 65
4.24 Main Parachute Design Properties . . . 65
4.25 Ballute Properties . . . 65
4.26 Ballute Design Properties . . . 67
4.27 Ballute Forces and Temperature . . . 67
4.28 Ballute Material Properties . . . 68
4.29 Recovery Subsystem Sensitivity Analysis . . . 72
4.30 Recovery Subsystem Mass Breakdown . . . 73
4.31 Recovery Subsystem Cost Breakdown . . . 73
4.32 Recovery Subsystem Power Breakdown . . . 73
4.33 Link Budget of the FTS . . . 74
4.34 FTS Antenna Trade-off Matrix . . . 75
4.35 Mass and Cost Budget of the FTS . . . 77

6.2 Overall Mission Cost Budget . . . 100
6.3 Risk Map for Stratos III Program . . . 102

6.5 Risk Map for Stratos III Program after Risk Mediation . . . 103

7.1 Table Comparing Different Amateur Sounding Rockets Comparable to the Stratos III . . . 107
7.2 Table Comparing Different Student Sounding Rockets Comparable to the Stratos III . . . 108

A.1 Rocket Mass . . . 114
A.2 Rocket Geometry . . . 114
A.3 Propulsion . . . 115
A.4 Astro- & Aerodynamics . . . 115
A.5 Recovery . . . 115
A.6 Electronics . . . 115

B.1 The Key Requirements for the Stratos III Program . . . 116
B.2 System Requirements for the Stratos III Program . . . 116
B.3 Requirements for the ADCS Subsystem . . . 117
B.4 Requirements for the Communication Subsystem . . . 117
B.5 Requirements for the Power Subsystem . . . 117
B.6 Requirements for the Propulsion Subsystem . . . 118
B.7 Requirements for the Recovery Subsystem . . . 118
B.8 Requirements for the Structures Subsystem . . . 118
B.9 Requirements for the Flight Termination Subsystem . . . 118
B.10 Build Requirements for the Stratos III Program . . . 119
B.11 Environmental Requirements for the Stratos III Program . . . 119
B.12 Flight Profile Requirements for the Stratos III Program . . . 119
B.13 Logistics Requirements for the Stratos III Program . . . 119
B.14 Resource Requirements for the Stratos III Program . . . 119
B.15 Safety Requirements for the Stratos III Program . . . 120

C.1 Table of Work Distribution . . . 122

List of Figures

2.1 The Different Elements of the Stratos III Project . . . 2
2.2 Functional Breakdown for the Stratos III Mission . . . 4

3.1 N2 Chart . . . 7
3.2 Simulated Rocket Altitude vs Time . . . 11
3.3 Simulated Rocket Drift vs Time . . . 11
3.4 Simulated Rocket Velocity vs Time . . . 12
3.5 Simulated Rocket Altitude vs Mach Number . . . 13
3.6 Simulated Rocket Drag Coefficient vs Mach Number . . . 13
3.7 Simulated Rocket Drag Force vs Mach Number . . . 14
3.8 Simulated Rocket Drag Force During Powered Flight . . . 15
3.9 Simulated Rocket Drag Force During Descent . . . 15

4.1 Two Diagrams Showing the Layouts of the Rocket . . . 20
4.2 Nytrox and Paraffin Performance . . . 21
4.3 Propulsion Subsystem Modelling Flow Diagram . . . 22
4.4 Liquid oxygen Mass Fraction . . . 26
4.5 Temperature of Oxidizer Tank vs. Time without Insulator . . . 28
4.6 Temperature of Oxidizer Tank vs. Time with Insulator . . . 28
4.7 Propulsion Feed System Schematics . . . 29
4.8 Engine Thrust Profile . . . 32
4.9 The Thickness Profile of the Entire Nosecone . . . 36
4.10 The Stress Profile for the Stratos III Rocket . . . 37
4.11 Temperatures on the Nosecone of the Stratos III Rocket . . . 38
4.12 Temperatures at t=100 [s] . . . 38
4.13 Block Diagram for the ADCS . . . 41
4.14 Pinhole with Quad Diode Setup [32] . . . 42
4.15 Tandem Surface Orientation Options, A is In-Line and B is Interlocked . . . 44
4.16 Center of Gravity Shift over Time . . . 45
4.17 Static Margin Shift over Time . . . 46
4.20 Lift Generated by One Canard at Varying Angle of Attack and Mach Number . . . 47
4.18 Fin Geometry . . . 48
4.19 Canard Geometry . . . 49
4.21 Stratos III Electrical Block Diagram [Part I] . . . 54
4.22 Stratos III Electrical Block Diagram [Part II] . . . 55
4.23 Received Power and SNR as a Function of Altitude . . . 57
4.24 Recovery Subsystem Design Flow Chart . . . 60
4.25 All Recovery Stages . . . 62
4.26 Force Reduction Factor as a Function of Canopy Loading . . . 64
4.27 Ballute Geometry . . . 66
4.28 Geometric Profile of the Ballute . . . 67
4.29 Altitude, Drift, Drag, and Mach Number as Functions of Time of the Rocket in a Ballute and Cross Shaped Main Parachute Configuration at Different Apogee Heights . . . 70
4.30 Total Velocity, Acceleration, Horizontal Velocity, and Vertical Velocity as Functions of Time of the Rocket in a Ballute and Cross Shaped Main Parachute Configuration at Different Apogee Heights . . . 70
4.31 Total Temperature and Dynamic Pressure as Functions of Time of the Rocket in a Ballute and Cross Shaped Main Parachute Configuration at Different Apogee Heights . . . 71

4.32 Functional Block Diagram of the FTS . . . 74
4.33 State Diagram Indicating the FTS Logic . . . 75
4.34 Approximation of the Drag Force Generated by the Ballute as a Function of Altitude in case of Immediate Deployment after Mission Abort . . . 76

5.1 The V-model of the Systems Engineering Process . . . 78

6.1 Diagram Showing the Different Teams and Board Members . . . 83
6.2 Diagram Showing the Communication between the Different Stratos III Members . . . 84
6.3 Design and Development Logic . . . 85
6.4 Milestones Overview for Stratos III Mission (1/3) . . . 87
6.5 Milestones Overview for Stratos III Mission (2/3) . . . 88
6.6 Milestones Overview for Stratos III Mission (3/3) . . . 89
6.7 Functional Flow Diagram for the Stratos III Mission . . . 95
6.8 The Flight Path of the Stratos III Mission with the Relevant Altitudes . . . 97

7.1 Two Diagrams Showing the Different Ordering of Sustainability . . . 104

C.1 Internal Communication Flow of the DSE Team . . . 121

List of Symbols

Roman letters

Symbol	Description	(value) Unit
A_c	Inlet area	$[m^2]$
A_e	Exit area	$[m^2]$
A_p	Port area	$[m^2]$
A_t	Throat area	$[m^2]$
AR	Aspect ratio	$[-]$
a	Speed of sound	$[m/s]$
C_a	Axial drag coefficient	$[-]$
C_D	Drag coefficient	$[-]$
$(C_D S)_0$	Drag area	$[m^2]$
C_F	Thrust coefficient	$[-]$
C_{Db}	Drag coefficient of ballute	$[-]$
C_n	Normal drag coefficient	$[-]$
C_x	Opening force coefficient	$[-]$
c	Speed of light	$[m/s]$
c	Chord length	$[m]$
c_p	Heat capacity	$[J/K]$
c_r	Chord root length	$[m]$
c_t	Chord tip length	$[m]$
$c^\star$	Characteristic velocity	$[m/s]$
C	Constant of the distributed drag force	$[-]$
C_{N_α}	Normal force coefficient per angle of attack	$[-]$
D	Rocket Diameter	$[m]$
D_0	Nominal parachute diameter, including area of openings	$[m]$
D_b	Ballute maximum diameter	$[m]$
D_c	Constructed parachute diameter	$[m]$
D_p	Inflated parachute diameter	$[m]$
d	Rocket diameter	$[m]$
F_t	Thrust	$[N]$
F_{or}	Reefed opening force of main parachute	$[N]$
F_{odr}	Disreef opening force of main parachute	$[N]$
F_D	Drag force	$[N]$
f	Frequency	$[Hz]$
f_D	Distributed drag force	$[N/m]$
G	Shear modulus	$[Pa]$
G_{ox}	Oxidizer mass flux	$[kg/(m^2 s)]$
g_0	Gravitational acceleration at sea level	$[m/s^2]$
h	Heat transfer coefficient	$[W/m^2 K]$
I_{sp}	Specific Impulse	$[s]$
$I_{sp_{eq}}$	Equivalent Specific Impulse	$[s]$
L_{solid}	Solid grain length	$[m]$
L	Length of the rocket	$[m]$
L_e	Length of suspension lines	$[m]$

L_p	Length of 3 crosses of parachute	$[m]$
l	Antenna length	$[m]$
m	Mass	$[kg]$
$\dot{m}_{fuel}$	Fuel mass flow	$[kg/s]$
$\dot{m}_{ox}$	Oxidizer mass flow	$[kg/s]$
$\dot{m}_{total}$	Total mass flow	$[kg/s]$
M	Mach number	$[-]$
Nu	Nusselt number	$[-]$
O/F	Oxidizer to fuel ratio	$[-]$
P	Pressure	$[Pa]$
p_a	Atmospheric pressure	$[Pa]$
p_c	Chamber pressure	$[Pa]$
p_e	Exit pressure	$[Pa]$
p_0	Atmospheric pressure at sea level	$[Pa]$
Pr	Prandtl number	$[-]$
R	Rocket radius	$[m]$
R_c	Port radius	$[m]$
$R_{c,0}$	Initial port radius	$[m]$
Re	Reynolds number	$-$
$\dot{r}$	Regression rate	$[m/s]$
S	Surface area	$[m^2]$
S_0	Nominal surface area	$[m^2]$
S_b	Ballute surface area	$[m^2]$
T_c	Chamber temperature	$[K]$
t	Thickness	$[mm]$
t_{nose}	Nose thickness	$[m]$
V_i	Impact velocity	$[m/s]$
V_b	Volume of ballute	$[m^3]$
V_t	Terminal velocity	$[m/s]$
V_x	Velocity in x-direction earth frame	$[m/s]$
V_y	Velocity in y-direction earth frame	$[m/s]$
V_z	Velocity in z-direction earth frame	$[m/s]$
W_p	Width of one cross of parachute	$[m]$
X_1	Opening force reduction factor	$[-]$
x	Distance along the rocket	$[m]$
x_e	x-coordinate in Earth reference system	$[m]$
x_{cg}	Center of gravity	$[m]$
x_{cp}	Center of pressure	$[m]$
y_e	y-coordinate in Earth reference frame	$[m]$
z	Distance from the tip from the nosecone	$[m]$
z_e	z-coordinate in Earth reference frame	$[m]$

Greek letters

Symbol	**Description**	**(value) Unit**
α	Conical half angle	$[deg]$
α	Canard angle of attack	$[deg]$
α_e	Angle of attack earth reference frame	$[deg]$
β	Sideslip angle Earth reference frame	$[deg]$
Γ	Vanderkerckhove function	[-]
γ	Specific heat ratio	[-]
γ	Flight path angle	[deg]
γ_e	Yaw angle earth reference frame	[-]
λ	Wavelength	$[m]$
λ	Taper	$[-]$
λ	Payload Ratio	$[-]$

λ	Thermal conductivity	$[W/mK]$
ρ	Air density	$[kg/m^3]$
ρ_0	Air density at sea level	$[kg/m^3]$
ρ_{fuel}	Fuel Density	$[kg/m^3]$
θ	Nosecone constant	[-]
θ_{nose}	Local half angle	[deg]
σ_l	Meridional stress	$[Pa]$
σ_r	Radial stress	$[Pa]$
σ_v	Von Mises Stress	$[Pa]$
σ_z	Longitudinal stress	$[Pa]$
σ_{z_F}	Longitudinal stress due to pressure	$[Pa]$
$\sigma_{z_{pres}}$	Longitudinal stress due to pressure	$[Pa]$
σ_θ	Hoop stress	$[Pa]$
$\sigma_{\theta_{pres}}$	Hoop stress due to pressure	$[Pa]$
τ	Shear stress	$[Pa]$
τ_c	Shear stress of canopy	$[Pa]$
ϕ_q	Energy flow	$[W]$
ψ_e	State vector	$[-]$

Abbreviations

Symbol	Description
ADCS	Attitude determination and control subsystem
ADR	European agreement for international transport of dangerous goods by road (Accord européen relatif au transport international des marchandises Dangereuses par Route)
AN	Ammonium nitrate
AP	Ammonium perchlorate
APP	Aerospace Propulsion Products
BAE	British Aerospace
CATIA	Computer Aided Three-dimensional Interactive Application
CDE	Carbon Dioxide Equivalent
CFD	Computational fluid dynamics
CFRP	Carbon-fiber Reinforced Plastics
CNC	Computer Numerical Control
CoCom	Coordinating Committee for Multilateral Export Control
COESA	Committee on Extension to the Standard Atmosphere
COM	Communication
CON	Construction
COSPAR	Committee on Space Research
COTS	Commercial off-the-shelf
DARE	Delft Aerospace Rocket Engineering
DLR	German Aerospace Center (Deutsches Zentrum für Luft- und Raumfahrt)
DOF	Degree of freedom
DSE	Design Synthesis Exercise
ECU	Engine Control Unit
ENV	Environmental
ERP	Effective Radiated Power
ESA	European Space Agency
FTS	Flight termination subsystem
FP	Flight path
GPS	Global positioning system

HTPB	Hydroxyl-terminated polybutadiene
IFA	Inverted-F Antenna
IMU	Inertial measurement unit
INTA	National Institute for Aerospace (Instituto Nacional de Técnica Aeroespacial)
IRIG	Inter-Range Instrumentation Group
IRU	Inertial reference unit
LiPo	Lithium-ion polymer battery
LOG	Logistics
LS	Launch site
MCU	Main Control Unit
MEMS	Micro-electromechanical systems
MP	Mission profile
NC	Normally Closed
NO	Normally Open
NFPA	National Fire Protection Association
O/F	Oxidizer to fuel ratio
PCB	Printed circuit board
PD&D	Project design and development logic
PR	Public relations
PRO	Propulsion
PWR	Power
RAMS	Reliability, Availability, Maintainability, Safety
REC	Recovery
RES	Resources
RLV	Reusable launch vehicle
RPA	Rocket Propulsion Analysis
RSO	Range Safety Offices
SARG	Suborbital Applications Researchers Group
SAVE	Safety
SNR	Signal-to-noise ratio
STR	Stratos
STRU	Structure
SUB	Subsystem
SYS	System
TBD	To be determined
TER	Flight termination system
TNO	Applied Physics Research (Toegepast Natuurwetenschapelijk Onderzoek)
TUD	Delft University of Technology

Chapter 1

Introduction

In 2004, the Civilian Space Exploration Team became the first amateur team to launch a rocket into space, setting a record at an altitude of 116 km [2]. In 2007, there was an objective to set the European altitude record for non-commercial rockets. This led to the launch of Stratos I in 2009 by DARE, a two-staged rocket that reached an altitude of 12.3 km. After the successful launch of the Stratos I, the dream was to reach higher altitudes and eventually break into space. An altitude of 50 km was considered the next milestone and this led to the Stratos II, a rocket designed to reach 50 km altitude carrying a scientific payload to be recovered after the launch.

The goal of this Design Synthesis Exercise (DSE) is to carry out the mission planning of the Stratos III, a sounding rocket designed to reach an altitude of more than 120 km and, therefore, break the current amateur record. This DSE will be completed in cooperation with Delft Aerospace Rocket Engineering (DARE) and will build upon previous designs, namely the Stratos I and II. The design should be able to perform the mission while abiding to a number of requirements and constraints relating to reliability, performance, safety, sustainability and cost. Commercial off-the-shelf (COTS) and in-house-developed technology will be used because the resources provided by the TU Delft, the Korolev Lab, and DARE are limited.

The Project Plan provided systematic planning and procedures to ensure the success of the project. It presented the team organization and human resources allocation to structure the team. The Baseline Report provided the foundation upon which the project could be built upon. All the requirements and risks were identified and a market analysis was carried out. The Midterm Report provided the necessary details required for the future detailed conceptual design. The feasible design options were listed, a trade-off method was devised to rank the options based on particular criteria, and concepts were generated. The Final Report follows from the Midterm Report and is the last report of the DSE. It provides a detailed analysis of the chosen conceptual design and the future of the project is defined.

Chapter 2 details the overall system design and the process used to reach it. Chapter 3 begins with a design overview and the final design characteristics of the rocket. Then, all the subsystems are described and the chapter ends with a section on the integration of the subsystems. Then it is followed by a detailed design description of each subsystem. Chapter 5 comprises of the verification and validation procedures both on system and subsystem levels and also includes a compliance matrix to show whether the requirements have been met. Chapter 6 describes the Stratos III mission. This includes the mission breakdown, the development and production strategies, the allocation of resources and the risk analysis. Chapter 7 shows the marketability of the Stratos III and describes its selling points. Finally, the report sums up the main points and the recommendations in Chapter 8, the conclusion.

Chapter 2

Project Overview

In order to launch the Stratos III rocket, the project surrounding it must be clearly defined. This mission includes a description of all the phases of the Stratos III missions and its safety aspects. This chapter also shows the continuation of the project and the future milestones. Next, it gives an overview of the different resources DARE will need for the successfully completion of this mission. Finally, an overview of all the risks involved in the project will be given.

Four different terms will be used for the Stratos III mission, these are listed in the table and figure below. The arrow in Figure 2.1 indicates that the project can only be transferred to DARE after the DSE is complete.

Terminology	**Description**
Stratos III Project	The Stratos III project is the all encompassing part. It contains anything that is related to the rocket and mission.
Stratos III	The Stratos III is the actual rocket and any hardware related to the system or subsystems
Stratos III Mission	This contains all the non-hardware related parts such as resources, development plan, and production plan.
Stratos III DSE	The DSE was the kick-off of the Stratos III project; it laid the foundation for DARE to develop upon.

Table 2.1: *Overview of the Different Nomenclature Used in the Stratos III Project*

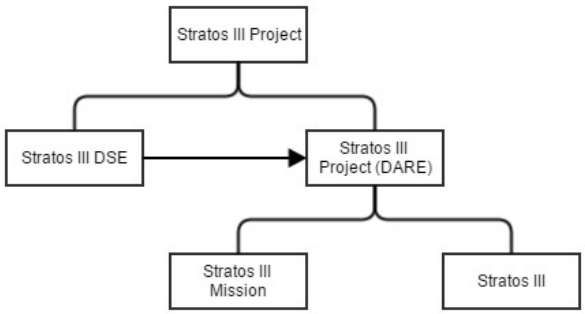

Figure 2.1: *The Different Elements of the Stratos III Project*

2.1 Stratos III Mission Breakdown

The mission need statement for the Stratos III was the following: To launch from the ground a safe, reliable, and sustainable rocket reaching at least 120 km carrying a 15 kg payload using COTS technology within TU Delft resources. From this mission need statement the following key requirements were derived:

Table 2.2: *The Key Requirements for the Stratos III Program*

Designation	Description
STR-KEY-01	System must reach an altitude of 120 km
STR-KEY-02	System must be able to carry a payload of at least 15 kg
STR-KEY-03	System must be built with commercial off-the-shelf and self-designed parts

The detailed mission of the Stratos III rocket is a very complex one. In order to analyze the mission of the Stratos III rocket two diagrams are made. The first diagram is the Functional Breakdown Structure. This diagram shows the mission being broken down in three different phases: the launch, ascend, and recovery phase. An ordered version of the functional breakdown structure, called the functional flow diagram, is shown in figure 2.2.

2.2 RAMS

There are four aspects considered to be important for the construction and operation of the Stratos III rocket: reliability, availability, maintainability, and safety or RAMS for short. It is true that the contribution of successfully designed subsystems to the mission takes up a large part of the mission success, but ignoring these four aspects will hinder the procedures throughout the mission from design to launch.

2.2.1 Reliability

Reliability of components for the Stratos III is something that needs to be taken seriously. No rocket mission around the world is carried out without ensuring that every part of the rocket is verified and validated. This, however, does not mean that rocket launches are without risk; the slightest failure in any subsystem could cause mission failure. Many organizations or companies like NASA or ESA have increased the reliability of their rockets after launching them multiple times. However, missions within DARE are one-time missions, which means that DARE neither re-uses previously launched rockets, nor reconstructs the same rocket for another mission. This means that it is impossible for DARE to collect data for modification to enhance the reliability of the whole system. Therefore it is of utmost priority to design and manufacture the rocket exactly according to the requirements and specifications to maximize its reliability. This can be done by verifying and validating each of the rockets subsystems. The verification and validation procedure is listed in Chapter 5. It is also for this goal of reliability that subsystems have been designed with high safety factors and redundancy.

2.2.2 Availability

Availability can comprise technological readiness and COTS technology. DARE expects to launch Stratos III within two years of the successful launch of Stratos II [1], so it is important to apply the technology that either already exists or will be available within two years. Furthermore, one of the key requirements of the Stratos III mission, **STR-KEY-03**, states that the system must be built with COTS and self-designed parts, which is listed in Appendix B.1. Not following this guideline may result in the delay of development or launch. To prevent this a series of trade-offs were carried out in the Midterm Review to eliminate the design options that are not technologically ready and/or do not use COTS materials.

2.2.3 Maintainability

Although the rocket will be launched only once and will not be used again in the future, it is important to build the rocket with maintainability in mind. This allows the build and launch crews to easily work and repair the rocket. Examples of good maintainability for the Stratos III rocket are the secondary batteries which can simply be recharged after testing and the modular design of the payload, avionics, recovery, and nosecone section that allows for easy access and construction.

[1] The Stratos II launch is planned for October 2015

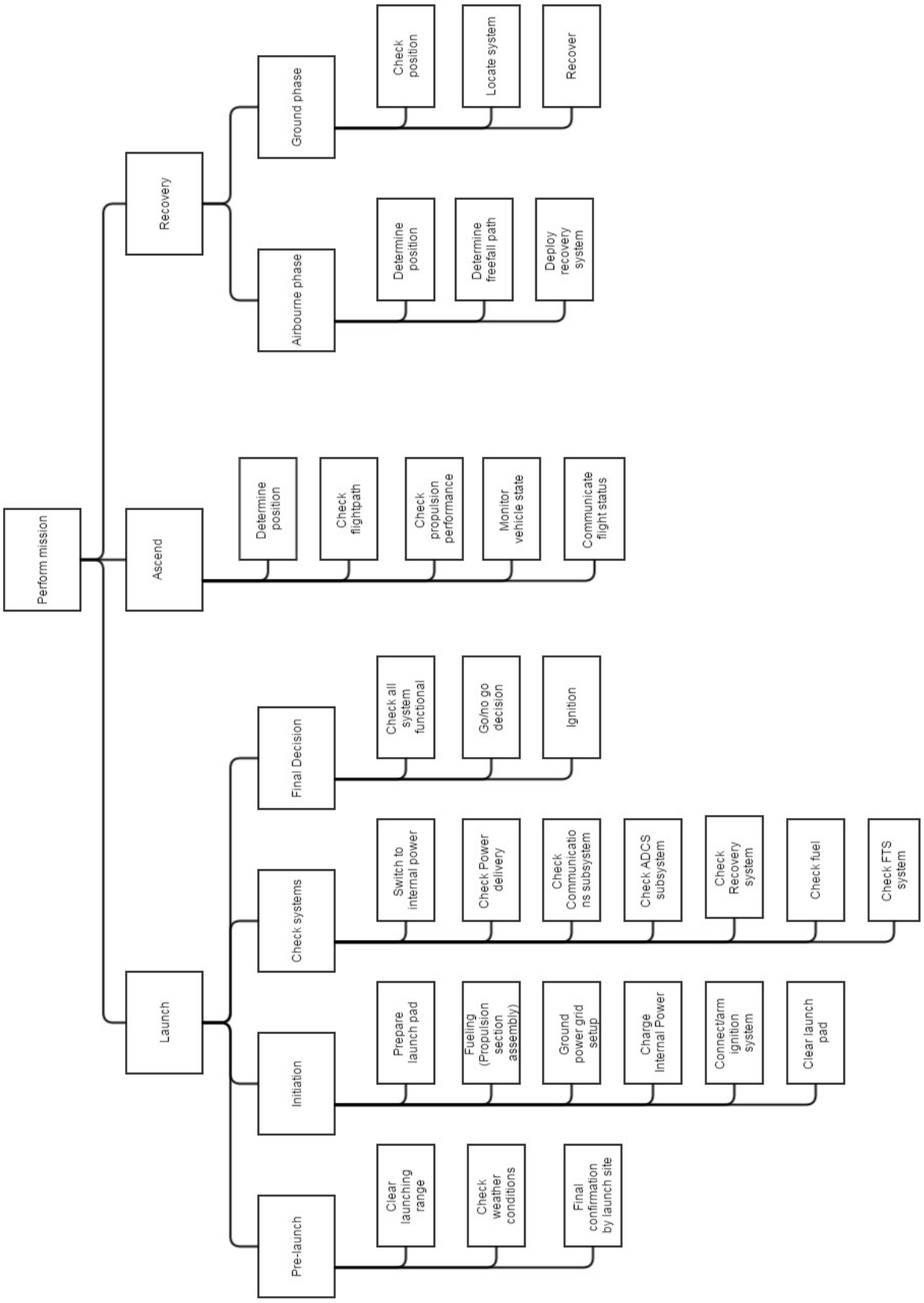

Figure 2.2: *Functional Breakdown for the Stratos III Mission*

2.2.4 Safety

Safety is of great concern for any project, especially when one chooses to launch a rocket into space. There are several aspects that pose a risk during this project.

The most obvious one is the engine and its propellant. The mixture of paraffin and Nytrox is a flammable one and should therefore be handled with care. The team prevents any serious accidents with the fuel and oxidizer by keeping them separated until ignition. Also, the oxygen handling is done by a third party company that will have all the required papers and licenses for handling the oxygen. The only moment that the rocket is fully fuelled and pressurized is after the rocket has been fully checked and the hardware is ready to fly.

The second dangerous part of the rocket is the recovery system. The recovery system utilizes a mortar that uses pressurized gas that fires the ballute through a hole in the hull. In order to prevent the mortar from firing whilst the crew is working with it, a safety valve is attached to the mortar. This means that, should the gases expand whilst on the ground, they can simply escape through the safety valve. Just before the launch the recovery system is armed, and this is the point where the safety valve is closed and the mortar deployment system is activated.

During the entire construction and handling of the rocket all local rules and regulations are followed to minimize the risk of human injury, environmental damage, or damage to the workplace. For this reason the teams are given proper instructions for the different pieces of equipment. At all times there will be a responsible person supervising the work. This person must have intensive experience working with the equipment.

Since the team will launch from a military testing zone, launch safety is largely covered by the base personnel. For any in-flight problems the team can possibly change flight path or terminate the flight.

Chapter 3

System Design

The largest component of the Stratos III Project design is the rocket itself. This chapter will contain the major details concerning the overall system design, starting with the process used to reach this final conceptual design in Section 3.1. Then, an overview of the main design characteristics are provided in Section 3.2. Further details on both system and subsystem levels are discussed in the following chapter.

3.1 Design Approach

The entire project was approached using systems engineering. System requirements were generated that had to be met by the Stratos III rocket as a whole as seen in Table 3.1. These were used to generate the functional flow diagram and functional breakdown structure shown in Chapter 2.

Table 3.1: *System Requirements for the Stratos III Rocket*

Designation	Description
STR-SYS-04	Stratos III shall be safe to work with on a student level.
STR-SYS-05	Stratos III shall send flight information during the entire flight.
STR-SYS-06	Stratos III shall reach an altitude of 120 km.
STR-SYS-07	Stratos III shall carry a 15 kg payload.
STR-SYS-08	Stratos III shall prove that it has reached an altitude of 120 km.
STR-SYS-09	Stratos III shall be recovered with minimal damage.
STR-SYS-10	Stratos III shall have a method of terminating the flight.
STR-SYS-11	Stratos III shall remain within a predetermined flight path.
STR-SYS-12	The Stratos III shall be launched from a ground-based launch site.

3.1.1 Concept Selection

Following the generation of these systems engineering tools, the rocket was able to be divided into key subsystems that could be designed in parallel, providing inputs to each other as shown in Figure 3.1. The key subsystems the rocket design was divided into were: Propulsion, Attitude Determination and Control (ADCS), Structure, Recovery, Communications, Power, and Flight Termination (FTS). These subsystems were designed through the use of individual requirement discovery trees and trade-off tables to arrive at the best subsystem concepts. Subsystems went through a first phase trade-off designed to eliminate those concepts that were unfeasible, unrealistic, or severely under-performing. A second trade-off on a subsystem level was performed based on criteria key to each subsystem including various measures of performance, sustainability, cost, and weight.

ADCS	Gather/store flight data			Determine altitude and location		Anomaly in trajectory
	COM	Check performance	Check performance			
	Send performance status to ground	**PRO**			Resist thermal impact	Anomaly in performance
Provide power for operation	Provide electric power for transmission	Start ignition and control fuel flow	**PWR**	Provide power for initiation		
				REC	Resist impact during lading	
Geometric limitation	Geometric limitaion and radio transparence	Geometric limitation	Geometric limitation	Geometric limitation	**STRU**	Geometric limitation
		Cut fuel feed		Activate REC system		**FTS**

Figure 3.1: *N2 Chart*

From the remaining subsystem options, concepts were generated through combinations of three key parameters: rocket propulsion configuration, rocket engine fuel, and attitude control method. From these parameters, 32 concepts were generated that were traded off on the following criteria:

- **Propulsion Score (35%).** Each engine configuration was assigned a weighted score based on payload ratio, carbon dioxide equivalent emissions, tank mass, and cost. The top performing engine configuration received a maximum score while other options were graded based on relative performance to the best result. The largest component of score-based sustainability for the rocket comes from the carbon dioxide equivalent emissions of the fuel. For this reason, this was given a high weight within the propulsion scoring system.
- **Control Score (30%).** The attitude control systems were rated based on three key criteria: performance, complexity, and technological readiness. Like the propulsion score, the best result was awarded the maximum score with other options assigned a relative score.
- **Cost (10%).** As the rocket itself, outside of propulsion testing, is a low cost of the overall mission, the cost of the system was assigned a relatively low score. Nevertheless, it is an important component of the project that must be considered.
- **Simplicity (10%).** This served as a measure of the complexity of the design. A concept that is simpler to manufacture and has fewer potential means of failure is awarded a higher score for this criteria.
- **Marketability (15%).** Marketability encompasses the concept's ability to sell itself to potential sponsors based on its sustainability, innovation, and overall 'wow' factor.

Following this trade-off, the concept with the highest overall score was selected. The selected concept was a single stage rocket powered by a hybrid engine using Nytrox as the oxidizer and a Paraffin-Aluminum blend as the solid grain. It would also be designed with an active canard control system to provide stabilization throughout the launch.

3.1.2 Subsystem Design

Following concept selection, subsystems were able to be further designed and iterated to match the selected base design. The interactions between these subsystems had to be taken into consideration at a much greater level, which required a dedicated System Integration Engineer and integration software to keep track of the evolution of the overall design and simulate the results of each iteration.

The N^2 Chart demonstrates how highly connected these subsystems are and, therefore, the subsystem design sensitivity, margins of error, and risks all had to be considered within the main integration software. These subsystem components are described along with their key design details in Chapter 4.

3.1.3 Final Concept Design

The final conceptual design of the rocket, after 18 recorded iterations, was agreed upon following results from the system integration software. The software logic is described in Section 3.1.3.1.

3.1.3.1 System Integration Software Logic

One main simulation software was generated to accommodate the selection of the propulsion system with respect to the overall design. This design was iterated many times to arrive at this final design taking into account all subsystems in terms of their weight and position.

The MATLAB program used to calculate the engine properties as described in Section 4.2.2.1. Given a chosen oxidizer mass flow, the MATLAB function `thrust2.m` outputs all combinations of port radius, throat radius, and solid grain length that satisfy chamber pressure and mass flux requirements. Along with this data comes the fuel and propellant masses based on the Paraffin-Al calculated regression rate and the provided tank diameter and thicknesses. Finally, after the engine burn is simulated, the time-dependent specific impulse, O/F ratio, total mass flow, and exit pressure are output.

With the engine thrust data provided from `thrust2.m`, the mass of the aluminum tank is calculated based on the solid grain length and oxidizer fuel length as seen in Equation 3.1. The mass of the paint and graphics is also found through Equation 3.2.

$$m_{\text{tank}} = L_{\text{tank}} \cdot \pi \cdot \rho \cdot d \cdot t \tag{3.1}$$

$$m_{\text{paint}} = 0.20(S_{\text{tank}} + S_{\text{capsule}}) \tag{3.2}$$

These masses, along with the estimated masses for the engine nozzle, bulkheads, and plumbing were summed up to calculate the total mass of the propulsion system. In addition to this, the currently known masses of the other subsystems (including the payload) placed in the capsule above the fuel tank, the mass of the lower fins, and the mass of the glass fiber nosecone were added to the rocket to determine the overall dry mass.

This simulation package provides a 2D track that combines all phases after ignition: powered flight, cruise, and recovery phases. Since the effectiveness of the active control system in the face of zonal winds is not well known yet, zonal winds are largely neglected during rocket ascension. The recovery phase initiates immediately after apogee, after which zonal winds are considered as ballute and main parachute dynamics come into effect.

Atmospheric data is approximated using the ISA model of 1976 [3], implemented in the MATLAB function `isaatmosfun.m` that determines temperature, speed of sound, pressure, and air density at a certain altitude. Wind models are provided by the built-in COSPAR 1986 model to provide the mean annual winds for the latitude of the INTA launch site. The altitude of the rocket has an effect on the specific impulse of the engine as it is dependent on the difference between the exit and atmospheric pressures. Thus, the equivalent specific impulse is computed using Equation 3.3. This is used to calculate the thrust force as shown in Equation 3.4. Finally, Tsiolkovsky's rocket equation is applied to determine the velocity change via Equation 3.5.

$$I_{\text{sp}_{\text{eq}}} = I_{\text{sp}} + \frac{p_{\text{exit}} - p_{\text{atm}}}{\dot{m}} \frac{\pi r_{\text{exit}}^2}{g_0} \tag{3.3}$$

$$F_{\text{thrust}} = I_{\text{sp}_{\text{eq}}} \cdot \dot{m} \cdot g_0 \tag{3.4}$$

$$dV_{\text{thrust}} = I_{\text{sp}_{\text{eq}}} g_0 \cdot \log\left(\frac{m_{\text{total}}(t - dt)}{m_{\text{total}}(t)}\right) \tag{3.5}$$

The speed of sound calculated at the current altitude for each time step is used to determine the Mach number via the basic equation $M = V/a$. The Mach number is used in the look-up tables generated by Missile

DATCOM for the rocket's generated aerodynamic data in order to fine the drag coefficient corresponding to the rocket's Mach number, flight path angle, and altitude.

This drag coefficient is output in the form of two components: the axial coefficient C_a and the normal coefficient C_n. These are transformed to the reference frame used by the system integration software by use of Equations 3.6 and 3.7, which are then converted to drag forces per component using Equation 3.8

$$C_{D_z} = \cos(\gamma)C_a + \sin(\gamma)C_n \tag{3.6}$$

$$C_{D_x} = \sin(\gamma)C_a + \cos(\gamma)C_n \tag{3.7}$$

$$F_{\text{drag}} = \frac{1}{2}\rho V^2 C_D S \tag{3.8}$$

Height and drift after each time step is calculated through simple dynamics using Equations 3.9 and 3.10 with respect to a right-handed reference frame wherein the z-axis points up from the Earth and the x-axis points in the direction of rocket travel based on the flight path angle.

$$\dot{z} = (V_{\text{thrust}_z} + V_{\text{parachute}_z} - V_{\text{gravity}} - V_{\text{drag}_z})dt \tag{3.9}$$

$$\dot{x} = (V_{\text{thrust}_x} + V_{\text{parachute}_x} - V_{\text{drag}_x} + V_{\text{wind}})dt \tag{3.10}$$

The parachute velocity components only come into effect after the rocket reaches its apogee. The drag as a result of the parachute are calculated here according to the equations discussed in Section 4.8. The simulation ends when the rocket reaches sea level, where the final velocity is below 20 m/s before the engine section makes contact with water.

A simulation is done for all of the valid thrusts and a table of all valid options that reach the target altitude are output. Finally, the rocket with the highest payload ratio is selected, where payload ratio is defined by Equation 3.11.

$$\lambda = \frac{m_{\text{capsule}}}{m_{\text{total}} - m_{\text{capsule}}} \tag{3.11}$$

3.1.3.2 System Software Sensitivity Analysis

Initial simulation iterations relied on very rough, preliminary information provided by each subsystem in terms of mass and volume that caused up to a 25% swing in key design parameters between iterations, particularly as the propulsion system portion of the simulation was refined. However, by the final iterations, key parameters only varied by, at most, 5%. The neglected effect of weathercocking is due to the assumption of a highly effective attitude control system. While it is known that the active canard control system developed by DARE can result in more than a 20% improvement in maximum altitude by counteracting the weathercocking effect [4], it will not be known just how effective the design for Stratos III will be until tests are performed. The masses used in the simulation are generally conservative or rounded up to the nearest kilogram in cases where masses are known more precisely.

3.2 Final Design Characteristics

In this section, some key characteristics of the final design are given. First, the resource budgets are given. These will give an overview of the total mass and cost for the hardware of the rocket. Next is the astrodynamics, in which the mission profile are given. Then the aerodynamic characteristics of the Stratos III will be given. Finally, a sensitivity analysis is discussed for the entire system. A full list of all the key parameters related to the Stratos III rocket can be seen in Appendix A.

3.2.1 Resource Budgets

Mass As there were no system level mass requirements for this project, the mass budget serves only as an overview of the breakdown of the rocket into its major components. From the mass breakdown shown in Table 3.2, it is clear that the propulsion system makes up the largest share of the dry mass, with the engine nozzle, plumbing, and tanks composing of 55.2% of the total dry mass and 24.3% of the wet mass. The fuel takes up a majority of the wet mass, making up 55.5% of it.

Table 3.2: *Mass Budget for the Stratos III Rocket*

Component	Mass [kg]	Dry Mass Fraction [%]	Wet Mass Fraction [%]
Payload	15	10.9	4.9
ADCS	10.2	7.4	3.3
Recovery	13	9.4	4.2
FTS	0.3	0.2	0.1
Power	2	1.5	0.7
Communication	1	0.7	0.3
Capsule Structure	19.4	14.1	6.4
Engine Nozzle/Plumbing	38.9	28.2	12.3
Tank Structure	37.1	27	12
Paint	0.9	0.6	0.3
Dry Mass	**137.8**	**100**	**44.5**
Nytrox	144	-	46.5
Paraffin-Al	27.7	-	9
Wet Mass	**309.5**	-	**100**

Cost Provided in Table 3.3 is the cost breakdown for the Stratos III rocket based on the total cost of each subsystem. As expected from the mass breakdown, the fuel makes up the largest cost of the rocket, followed by the propulsion system. Due to the amount of research and development needed for the active control system, the ADCS costs are just below that of the propulsion system. It should be noted that this breakdown is representative only of a single rocket. The entire mission cost, including testing and launch, will be covered in Section 6.9.

Table 3.3: *Cost Budget for the Stratos III Rocket*

Component	Cost [€]	Cost Fraction [%]
Propulsion	1520	16.62
Fuel (1 Tank)	3977	43.49
Structure	813	8.89
ADCS	1490	16.30
Power	120	1.31
Communication	110	1.20
FTS	180	1.97
Recovery	935	10.22
Total	9145	100

3.2.2 Astrodynamics

As shown in Section 3.1.3.1, the rocket simulates the thrust, drag, and force of gravity to determine the overall velocity and trajectory of the Stratos III rocket. The specific equations related to these calculations can be seen in that section. The vertical velocity change was found to be 1.536 km/s, which is consistent with the 1.52 km/s found in the Baseline Review for 120 km. The final design resulted in a simulated altitude of 134.41 km with an average drift of 51.01 km that results from sustained, average wind speeds throughout the flight and a 4 degree flight path angle. It should be noted that this drift does not account for the effect of weathercocking during flight. The additional drift due to weathercocking, as well as a subsequent decrease in apogee altitude, will be dependent on the efficacy of the active canard control system to counteract this weathercocking effect. As engine burnout occurs at 28.9 seconds, the rocket will have reached an altitude of 18.23 km at the end of the powered flight phase.

Table 3.4: *Stratos III Key Times*

Component	Time [s]
Engine Burnout	28.9
Apogee	185.4
Ballute Deployment	310.8
Main Parachute Deployment	489
Splashdown	662.5

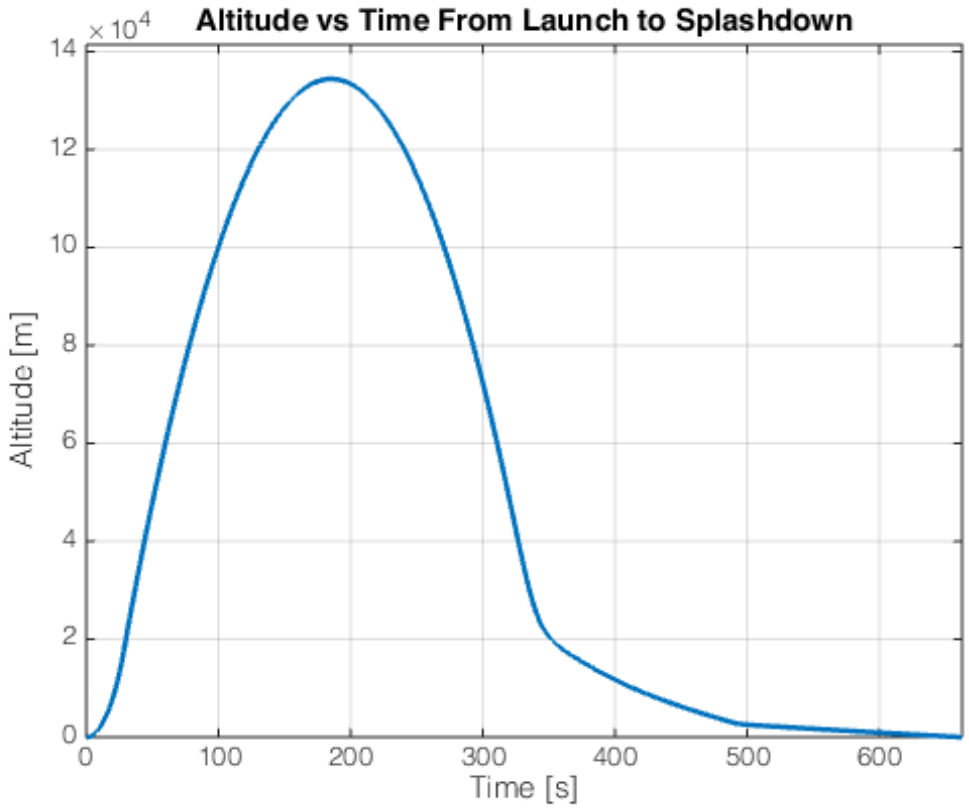

Figure 3.2: *Simulated Rocket Altitude vs Time*

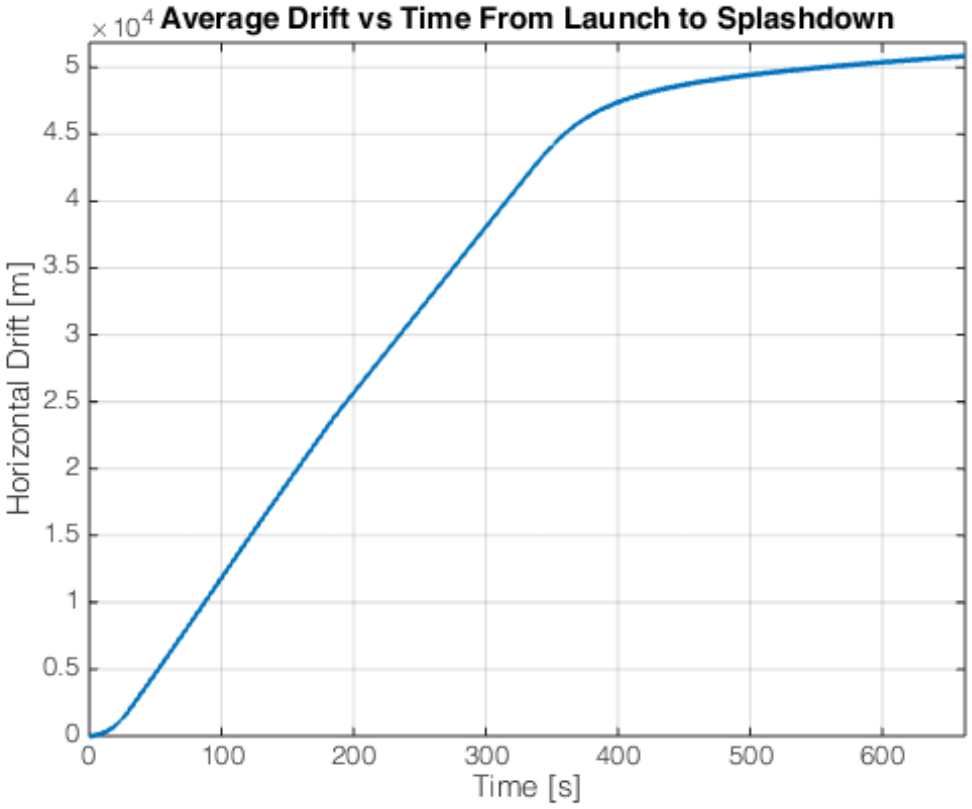

Figure 3.3: *Simulated Rocket Drift vs Time*

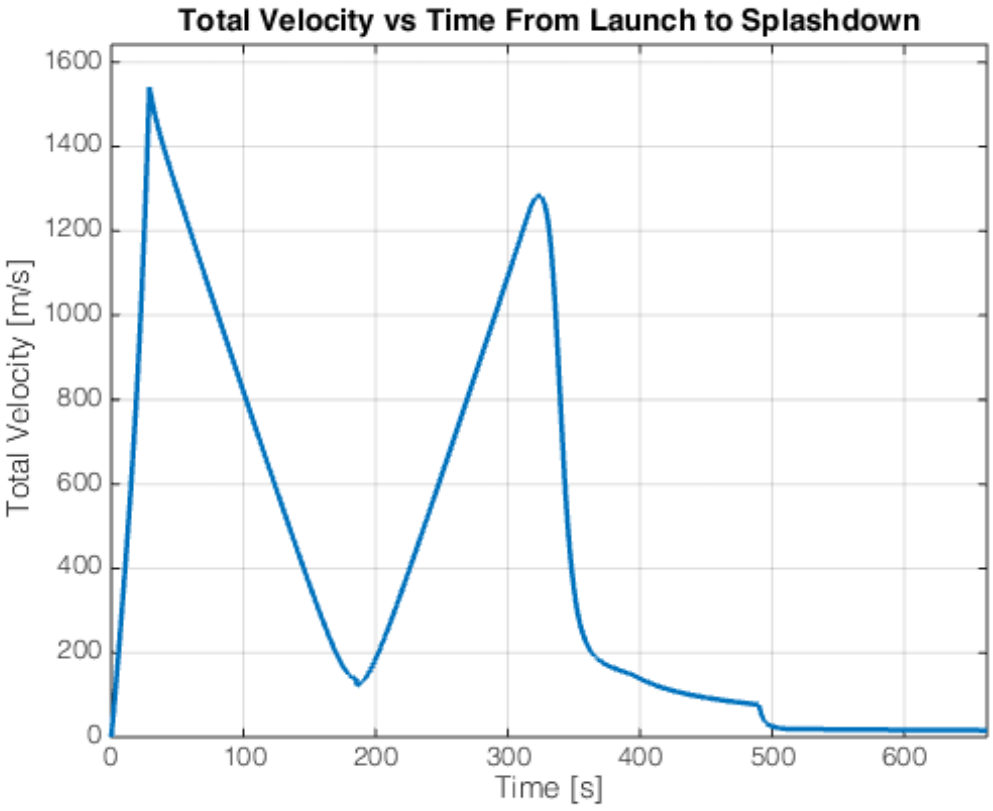

Figure 3.4: *Simulated Rocket Velocity vs Time*

3.2.3 Aerodynamics

The main geometric parameters of the rocket are dictated by two main factors: propulsion and aerodynamics. Thus, these two subsystems had to be designed in tandem to create a rocket capable of overcoming both gravity and drag. As is the case with all rockets, the bigger the engine and fuel tank, the greater the total drag on the rocket which will require a slightly bigger engine to overcome. The diameter of the rocket, shape of the nosecone, and sizes of the fins and canards all affect the aerodynamic profile of the rocket.

For each iteration in the design, the rocket profile was input into Missile DATCOM to provide the expected drag component for set altitudes, flight path angles, and Mach numbers. Within the system integration MATLAB file, the drag component C_D is determined via interpolation from the look-up tables generated by Missile DATCOM. Relevant aerodynamic equations are discussed in Section 3.1.3.1.
Figures 3.5 to 3.7 demonstrate the altitude, drag coefficient, and drag force found for the rocket during a simulated run with a flight path angle of 4 degrees. Thus, the C_D and F_{drag} shown in those graphs are affected by the altitude that is changing along with the Mach number.

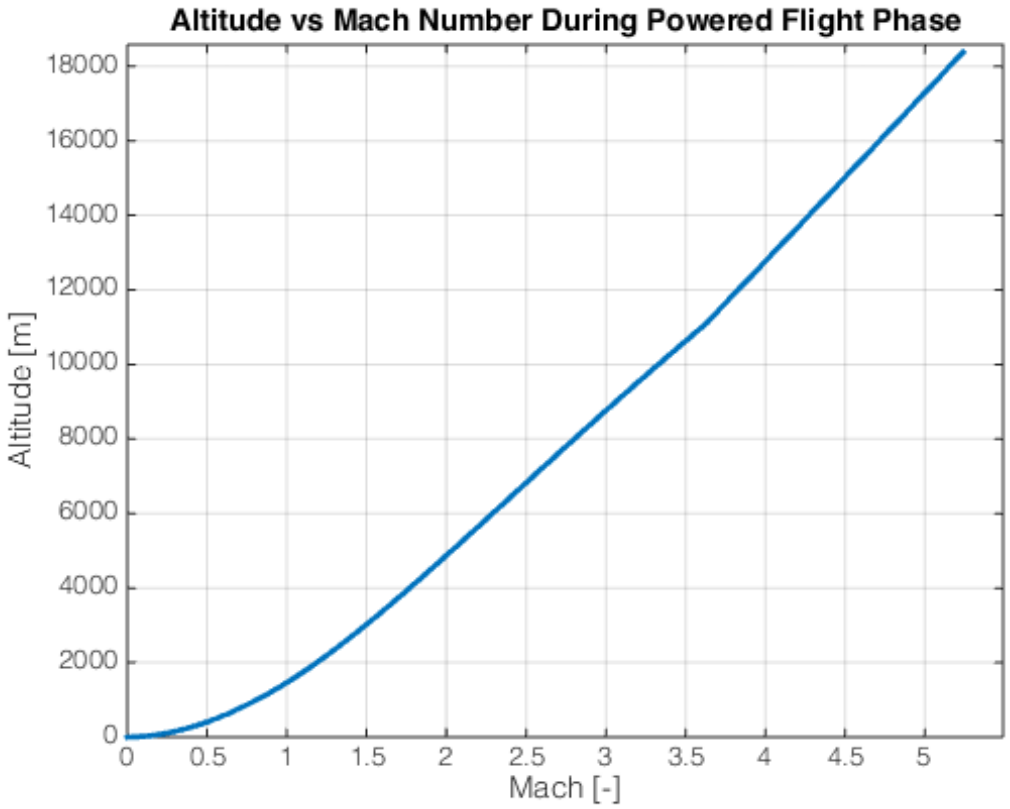

Figure 3.5: *Simulated Rocket Altitude vs Mach Number*

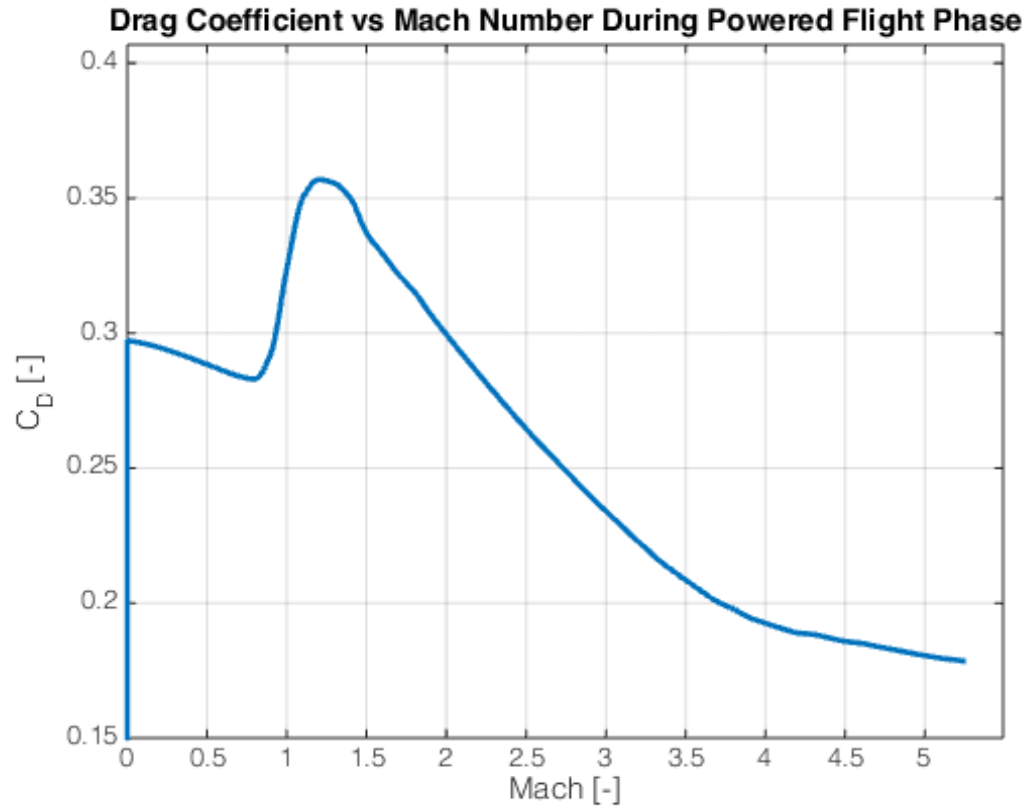

Figure 3.6: *Simulated Rocket Drag Coefficient vs Mach Number*

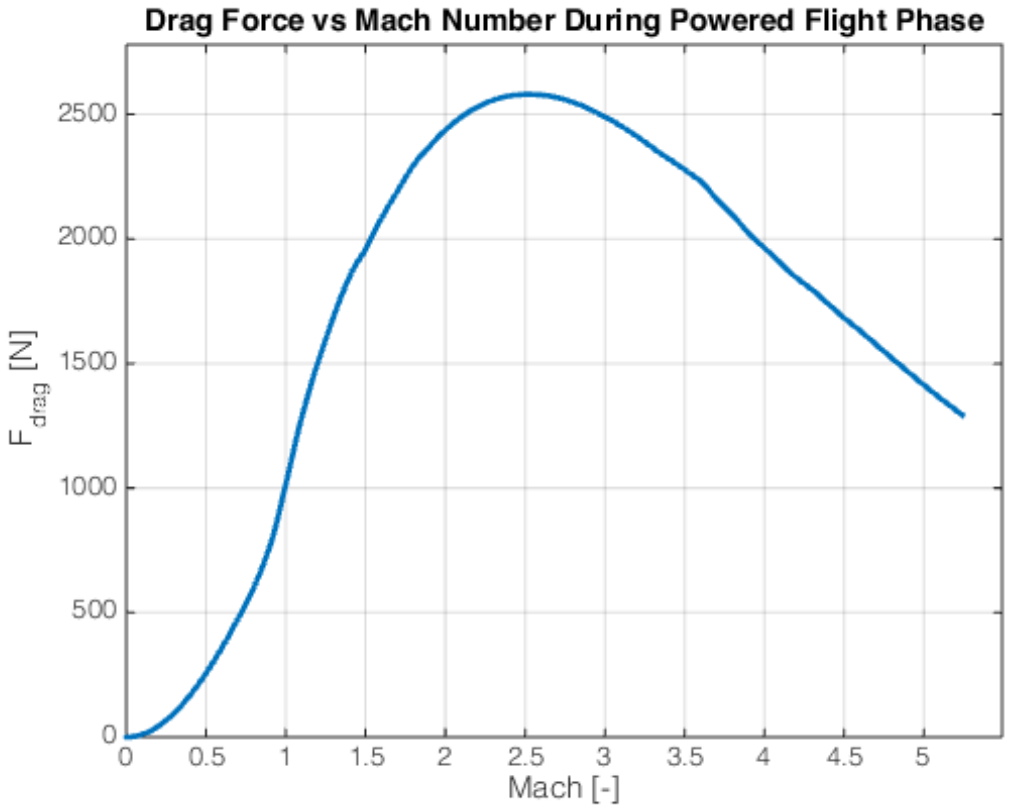

Figure 3.7: *Simulated Rocket Drag Force vs Mach Number*

Figures 3.8 and 3.9 show the drag force of the rocket with respect to time in both the powered flight phase and the descent phase following apogee. This drag force does not include the drag introduced by the recovery system, only the rocket itself. As in the Mach graphs, these graphs show the drag as a result of a 4 degree flight path angle.

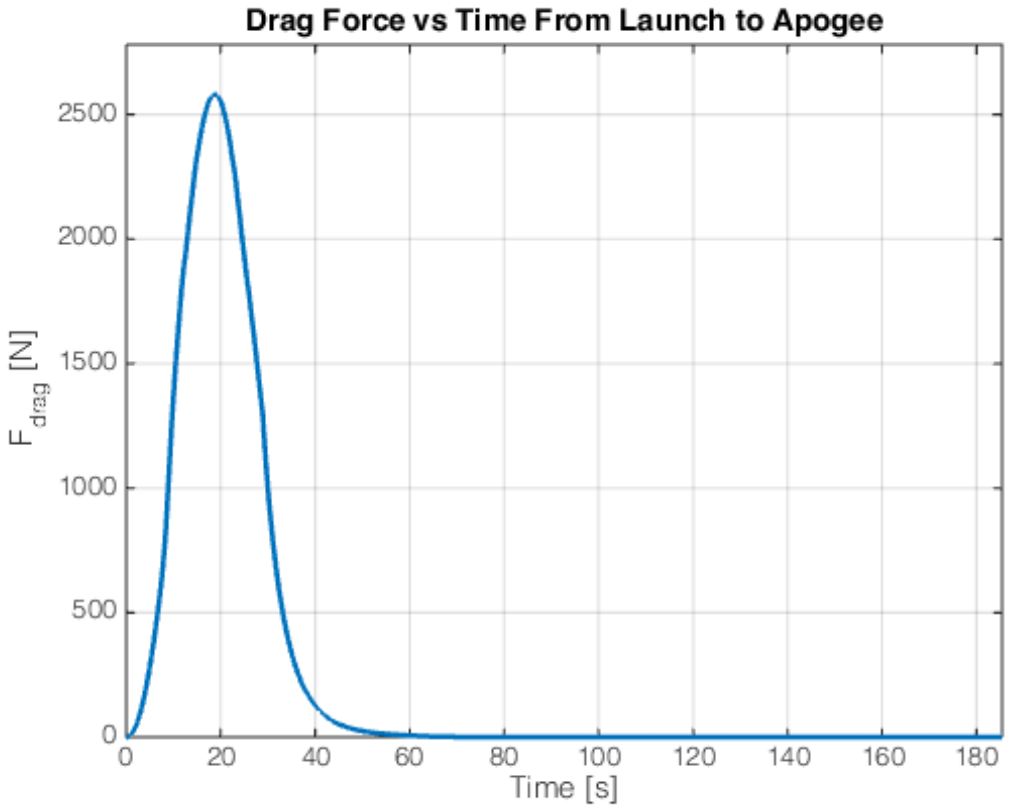

Figure 3.8: *Simulated Rocket Drag Force During Powered Flight*

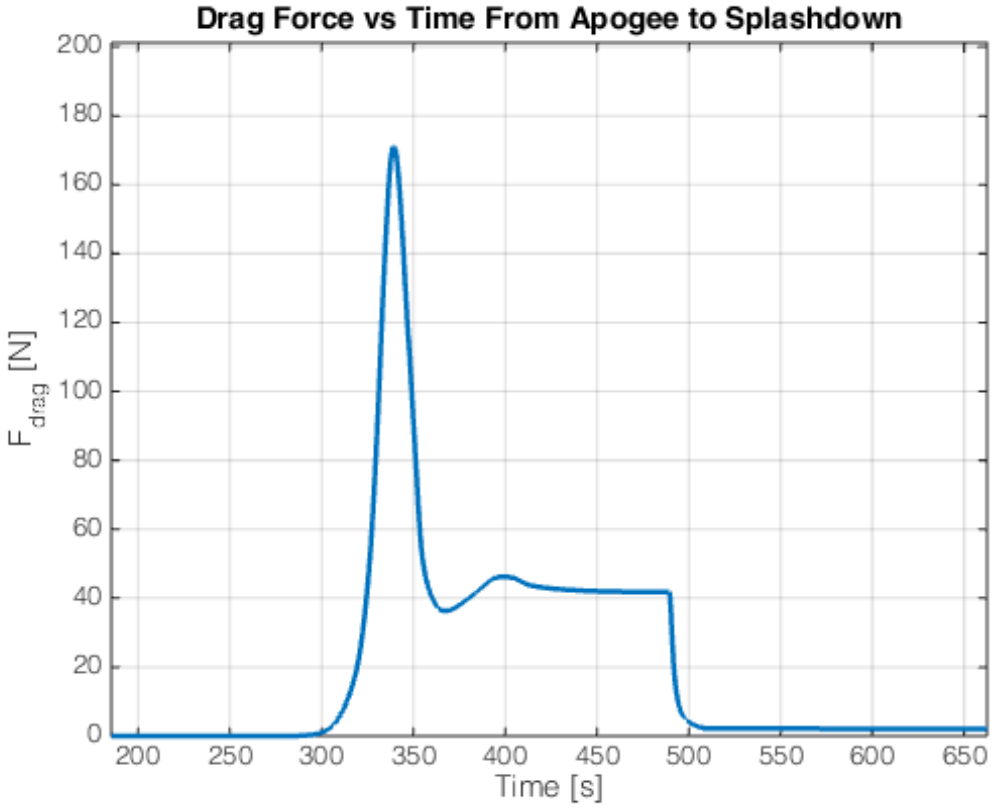

Figure 3.9: *Simulated Rocket Drag Force During Descent*

3.2.4 System Sensitivity Analysis

As a system, the Stratos III rocket has many different parameters it is sensitive to in terms of mass and the apogee height reached. The final design of Stratos III was simulated with 10% changes in payload mass, tank thickness, drag, grain length (and corresponding oxidizer mass), tank diameter, and engine specific impulse. Their direct impacts on mass and apogee height can be seen in Table 3.5.

Table 3.6 puts each change in perspective. Where both mass and apogee height changed, the $\frac{km}{kg}$ column shows the effective change in apogee height per kg change. It is natural that changing the payload mass has an inverse effect on the maximum height given that all other parameters are held constant. The largest effect would come from changing the tank thickness. Not only does this decrease the mass of the tank, but it will also decrease the volume of the oxidizer tank, decreasing the length of the rocket. During system iterations, it was apparent that the easiest way to increase maximum apogee height was to simply increase the diameter. This had the side benefit of increasing the burn time, lowering the average thrust needed from the engine and subjecting the rocket to lower drag forces. Comparable in effect is increasing the grain length which effectively increases the oxidizer mass. This is, in essence, simply a measure of increasing the total propellant which predictably increases the rocket's height and mass. Finally, a look at the engine performance in terms of specific impulse shows how drastic an effect it can have. One of DARE's biggest challenges will come in developing this engine that is significantly more efficient than the current engine used in Stratos II. A change in I_{sp} of only 10% has a massive effect on the capabilities of the engine and the rocket will undoubtedly have to be re-designed based on the tested performance of the engine.

One important observation gained from this analysis is that a 10% change in a parameter that changes the apogee height will increase the maximum height more than an equivalent inverse change will decrease the height. As an example, decreasing the tank thickness by 10% will increase the height by 10.7 km for every 1 kg saved. However, increasing the thickness will decrease the height by only 10 km for each kilogram added. This shows that, at this altitude, each kilometer added in height is reached "easier" than the previous one. At the sacrifice of the payload ratio, the rocket can easily be designed to reach a much greater altitude.

Table 3.5: *Results of System Sensitivity Analysis*

Design	**Percentage Change** [%]	**Mass** $[kg]$	**Apogee Height** $[km]$
Current Design	0	309.6	134.4
Increase Payload	+10	311.1	132.1
Decrease Payload	-10	308.1	136.8
Increase Tank Thickness	+10	311.4	126.3
Decrease Tank Thickness	-10	307.7	143.1
Increase Drag	+10	309.6	129.9
Decrease Drag	-10	309.6	138.9
Increase Grain Length	+10	313.1	138.1
Decrease Grain Length	-10	306	130.7
Increase Diameter	+10	363.6	185
Decrease Diameter	-10	260	89.2
Increase I_{sp}	+10	309.6	177.3
Decrease I_{sp}	-10	309.6	97.7

Table 3.6: *Percent Results of System Sensitivity Analysis*

Design	**Percentage Change [%]**	**% Change of Mass**	**% Change of Apogee Height**	**Height/Mass Ratio** $[\frac{km}{kg}]$
Current Design	-	-	-	-
Increase Payload	+10	+0.5	-1.7	3.5
Decrease Payload	-10	-0.5	+1.8	3.6
Increase Tank Thickness	+10	+0.6	-6.0	10.0
Decrease Tank Thickness	-10	-0.6	+6.5	10.7
Increase Drag	+10	0.0	-3.3	-
Decrease Drag	-10	0.0	+3.4	-
Increase Grain Length	+10	+1.1	+2.7	2.4
Decrease Grain Length	-10	-1.1	-2.7	2.4
Increase Diameter	+10	+17.5	+37.7	2.2
Decrease Diameter	-10	-16.0	-33.6	2.1
Increase I_{sp}	+10	0.0	+31.9	-
Decrease I_{sp}	-10	0.0	-27.3	-

Chapter 4

Detailed Design

The rocket is more than just the sum of its parts. This chapter will detail the overall layout of the rocket, both externally and internally. Following that, each rocket subsystem will be described in great detail in terms of its current design and the methodology and governing equations used to arrive at each design.

4.1 Layout

The general layout of the rocket consist of two major parts. First is the external layout which shows all the protruding parts of the rocket and the skin. The second is the internal layout showing the solid fuel, oxidizer tank, and payload/avionics capsule.

4.1.1 External Layout

The Stratos III rocket will be a 5.65 m high rocket with a width of 0.26 m. The nosecone of the rocket is 0.78 m in length, which connects to the capsule below it. The active control canards connected to this capsule begin 1.32 m from the tip of the rocket, extending down to 1.47 m. The fins used for passive stabilization are located 0.08 m from the base of the combustion chamber and 0.42 m from the base of the nozzle, with a root chord length of 0.35 m. The nozzle of the propulsion system extends out of the combustion chamber just beyond the throat, extending 0.36 m beyond the combustion chamber.

4.1.2 Internal Layout

The internal layout is made up of all of the subsystems. These subsystems are listed in the list below.

- **Propulsion** The Propulsion subsystem is responsible for delivering the required energy to accelerate the rocket to 1.52 km/s. This is split into a few key components. The oxidizer tank is 2.35 m in length, holding the 144 kg of Nytrox that will be expelled during flight. This is located just below the capsule, starting at 1.83 m from the tip of the rocket. Below this is a 30 cm section designated for the designed plumbing system connecting the oxidizer to the combustion chamber. This combustion chamber is about 0.7 m in length to hold the 27.7 kg of Paraffin-based solid grain. Finally, below this is the nozzle which has its first 10 cm within the combustion chamber and the remaining 36 cm below it.
- **Structures** The Structure subsystem is responsible for delivering the supportive structure where that protects and mounts all other subsystems. It has to be strong enough to support all the stresses delivered during the entire flight. The rocket external structure is comprised of two main components. First is the glass fiber nosecone with a titanium tip, weighing 6.5 kg and extending 0.78 m in length. The second is the aluminum 6061 alloy tube that extends from the nosecone down to the end of the combustion chamber, for a combined capsule and tank length of 4.51 m.
- **Flight Termination System (FTS)** The FTS subsystem is responsible for terminating the flight in case of emergency. It prevents the rocket from flying so far off course. For safety reasons, the FTS system is completely separated from all other subsystems of the rocket. Antennae will be located on the tip edge of the fins while the main computer of the FTS will be inside the capsule.
- **Recovery** The Recovery subsystem is responsible for the flight phase from apogee to touch down. It will have to slow the rocket down to acceptable velocities so that the payload and the rocket survive the impact. This system is located at the bottom of the capsule, just above the oxidizer tank.

- **Attitude determination and control system (ADCS)** The ADCS subsystem is responsible for keeping the rocket on the most effective course. It constantly determines its heading and orientation and adjusts accordingly. This is located just above the Recovery subsystem.
- **Avionics** The Avionics are all the electronics that can be considered the brains of the rocket. The avionics consist of the Power, Communications, and Flight Computer.
  - **Power** The Power subsystem consist of all the batteries and wires that are required to activate the rocket and allow for operations of the rocket. These are located near the connection points of the capsule for ease of access.
  - **Communication** The communication subsystem consist of the electronics required to transmit data back down to the ground during the flight. It allows for a down link from the rocket to the ground station. The main antenna is located within the nosecone.
  - **Flight Computer** The Flight Computer is the system that gives the input to the servos controlling the canards of the rocket as well as determining the attitude of the rocket. It is also responsible for processing and storing all the data gathered from the sensors. It will also determine which data to send to the telemetry. This is located just above the actuation system for the canards.
- **Payload** In order to cover a bit of the costs, a payload is taken on board. This payload will weight 15 kg and will be completely independent from the rest of the rocket. Its space is reserved above the ADCS system, extending 10 cm into the nosecone.

(a) Internal Layout *(b) External layout*

Figure 4.1: *Two Diagrams Showing the Layouts of the Rocket*

4.2 Propulsion

The Propulsion subsystem is an essential part of the rocket with its purpose to propel the rocket to sufficient velocity for reaching target altitude. Other than its main function of bringing the rocket upwards, combustion stability, safety, and propellant efficiency have to be considered. After creating an extensive trade off table comparing different rocket propellants to one another, one fuel-oxidizer combination has been chosen. For the Stratos III mission, Nytrox and Paraffin-Aluminum-Carbon black are chosen as oxidizer and fuel.

4.2.1 Propellant Characteristics

The Nytrox-Paraffin propulsion concept is mostly based on research done by the Space Propulsion Group [5]. Its high specific impulse and self-pressurizing characteristics make the Nytrox-Paraffin option highly favorable for a single stage amateur rocket seeking to break the altitude record. However, the design challenge lies in the Nytrox mixture where the oxidizer is to be kept at temperatures lower than -60°C. Increased temperature causes more oxygen molecules to evaporate and would lead to decreased propulsion performance of the engine due to decreased percentage of oxygen in liquid state as shown in Figure 4.2 [5].

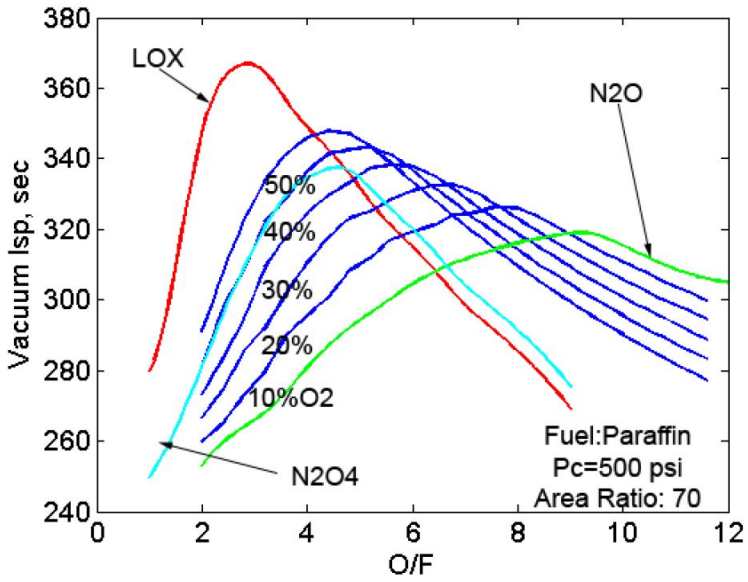

Figure 4.2: *Nytrox and Paraffin Performance*

4.2.2 Propulsion Subsystem Performance Simulation Model

For the propulsion subsystem, many variables can be altered to change the performance of the engine. From Figure 4.3, one can observe interdependent variables. The main input variables are initial port radius, oxidizer mass flow, solid grain length, throat area, exit area, and regression rate. With these parameters, time-varying specific impulse and propellant mass flow rate at the exit can be determined. Once the mass flow rate and specific impulse have been determined, the values can then be used as input variables to the trajectory simulator.

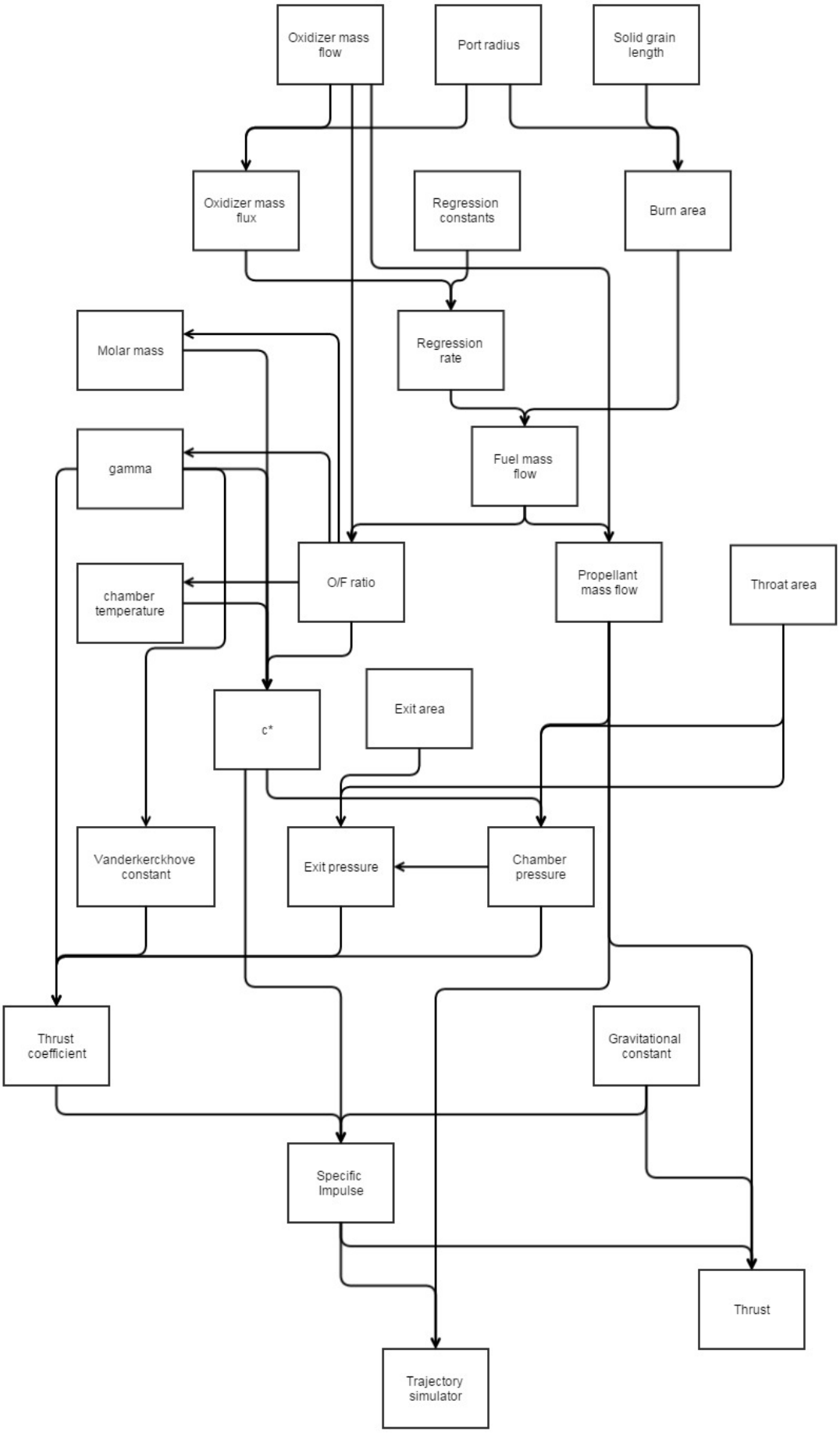

Figure 4.3: *Propulsion Subsystem Modelling Flow Diagram*

Combustion Characteristics

In order to calculate time-dependent performance parameters, the thickness and rocket tube diameter were fixed. Later, these values were also varied in order to optimize rocket design. For the combustion characteristics, RPA was used to calculate the chamber temperature (T_c) and the characteristic velocity ($c^\star$) over varying O/F ratio, chamber pressure (P_c), nozzle inlet ratio (A_c/A_t) and nozzle exit ratio (A_e/A_t). The ranges can be seen in Table 4.1. For the simulated $c^\star$ and (T_c) values, the differences between the maximum and minimum values to the mean value are taken as percentages in order to determine percentage wise fluctuation. For T_c and $c^\star$ the results are given in Table 4.2.

Table 4.1: *The Ranges for the OF, P_c, A_c/A_t and A_e/A_t.*

Parameter	**Maximum**	**Minimum**	**step**
OF $[-]$	3	9	0.5
P_c $[MPa]$	3	10	0.5
A_c/A_t $[-]$	1	50	5
A_e/A_t $[-]$	1	40	5

Table 4.2: *Variance of T_c and $c^\star$.*

Parameter	**Mean**	**Maximum**		**Minimum**	
	$[-]$	$[-]$	$[\%]$	$[-]$	$[\%]$
T_c $[K]$	3,381	3,575	105	2,946	87
$c^\star$ $[m/s]$	1,556	1,626	104	1,465	94

From Table 4.2, it becomes clear that for all parameters varied, the combustion properties change very little. Therefore, T_c and $c^\star$ are set to be fixed at the mean values. Because T_c and the $c^\star$ are set, the specific heat ratio can also be fixed at 1.17.

Performance Calculations

With the combustion characteristics known, the performance of the rocket can be calculated. First, Γ was calculated using the Vanderkerckhove function [6].

$$\Gamma = \sqrt{\gamma}\left(\frac{2}{\gamma+1}\right)^{\frac{\gamma+1}{2}} \tag{4.1}$$

Using the oxidizer mass flow and the port radius, the oxidizer mass flux can be calculated by using Equation 4.2 [6]:

$$G_{ox} = \frac{\dot{m}_{ox}}{A_p} \tag{4.2}$$

Test results from the Peregrine project [7] indicate that the oxidizer mass flux should not exceed 650 kg/m^2 because of flame holding instability occurring at higher mass flux.

Following that the regression rate can be calculated by using Equation 4.3 [6]:

$$\dot{r} = aG_{ox}^n \tag{4.3}$$

a and n are constant and are only dependent on the propellant mixture used. Regression rate coefficients for a similar propellant mixture are found to be $a = 0.15$ and $n = 0.53$ [8]. Using these values and oxidizer mass flux, time varying regression rate can be determined. Detailed regression rate modelling throughout the length of the solid grain can be done once the regression rate tests are performed using specified propellants.

Table 4.3: *Regression Rate Constants*

Constant	**Value**
a	0.15
n	0.53

With the regression rate and the initial port radius the port radius is determined at each time interval. Then the regression rate is again calculated for the next time interval with different oxidizer mass flux due to increased port radius. The port radius at a time t can be calculated using Equation 4.4.

$$R_c(t) = R_{c,0} + \int_0^t \dot{r} dt \tag{4.4}$$

From the above equation, the regression rate and port radius are calculated. Then using the length of the solid grain (L_{solid}), and the fuel density ρ_{fuel} as additional input, the fuel mass flow and subsequently the total mass flow can be calculated using Equation 4.6 [6].

$$\dot{m}_{fuel} = \dot{r} \rho_{fuel} 2\pi R_c L_{solid} \tag{4.5}$$

$$\dot{m}_{total} = \dot{m}_{fuel} + \dot{m}_{ox} \tag{4.6}$$

Knowing the mass flows for the oxidizer and the fuel, O/F ratio can be calculated by simply dividing the two.

$$OF = \frac{\dot{m}_{ox}}{\dot{m}_{fuel}} \tag{4.7}$$

The O/F ratio can be used to check if the performance is in the correct range, the optimum O/F range is 5-6 according to simulations in RPA. Using the throat radius the total mass-flow and $c^\star$ the chamber pressure can be calculated by using Equation 4.8 [6].

$$p_c = \frac{\dot{m}_{total} c^\star}{\pi R_c^2} \tag{4.8}$$

With exit radius and the throat radius used as input, the exit pressure can be calculated using Equation 4.9 [6]. Since this equation is not easily reversible, the exit pressure is calculated iteratively until the correct A_e/A_t ratio is reached.

$$\frac{A_e}{A_t} = \frac{\Gamma}{\sqrt{\frac{2\gamma}{\gamma-1}\left(\frac{p_e}{p_c}\right)^{\frac{2}{\gamma}}\left(1-\left(\frac{p_e}{p_c}\right)^{\frac{\gamma-1}{\gamma}}\right)}} \tag{4.9}$$

Using the exit pressure and the Γ, γ and p_c, the thrust coefficient can be calculated [6].

$$C_F = \Gamma \sqrt{\frac{2\gamma}{\gamma-1}\left(1-\left(\frac{p_e}{p_c}\right)^{\frac{\gamma-1}{\gamma}}\right)} + \left(\frac{p_e}{p_c} - \frac{p_a}{p_e}\right)\frac{A_e}{A_t} \tag{4.10}$$

Using the thrust coefficient the parameter which is of the interest can be calculated the specific impulse. This is done using Equation 4.11[6].

$$I_{sp} = \frac{C_F * c^\star}{g_0} \tag{4.11}$$

Finally the thrust can be calculated by using Equation 4.12[6]

$$F_t = \dot{m}_{total} I_{sp} g_0 \tag{4.12}$$

4.2.2.1 Optimization

There are four main parameters which can be varied to optimize propulsion subsystem modelling.

- Initial port radius
- Grain length
- Oxidizer mass flow
- Throat area

Initial port radius with oxidizer mass flow effectively determines the burn time of the rocket engine. As it can be seen in Equation 4.3, regression rate depends on the oxidizer mass flux. Not only does the initial port radius determine the web thickness of the solid grain, it also alters the oxidizer mass flux by altering the flow cross sectional area. If the initial port radius is increased, burn time of the rocket engine will decrease for fixed rocket diameter. And for the rocket engine to provide the same amount of total impulse compared to that of smaller port radius, the grain length has to be increased. In terms of providing higher thrust, increasing the port radius and grain length is beneficial due to increased burn area and therefore larger propellant mass flow.

As discussed above, grain length determines the burn area of the rocket engine. With larger burn area, provided that enough oxidizer is supplied to maintain combustion, the thrust of the rocket engine will be increased. However, the length of the solid propellant should be kept under a certain limit to ensure rocket length to diameter ratio does not exceed the limit.

Oxidizer mass flow is largely dependent on the oxidizer tank pressure. Higher oxidizer tank pressure will lead to higher oxidizer mass flow. Higher oxidizer mass flow would then result in higher regression rate and therefore higher propellant mass flux. For maximum performance, the oxidizer mass flow should be kept as high as possible while retaining optimum oxidizer to fuel ratio.

The throat area should be sized in such a way to ensure that optimum expansion is achieved at desired altitude for maximum propulsive efficiency. If the nozzle is designed for sea level operations, the nozzle will be under expanded throughout its climb and vice-versa. Throat area also determines the chamber pressure by controlling the exit mass flow rate of the nozzle as shown in Equation 4.14.

$$\dot{m}_{in} = \dot{m}_{out} \tag{4.13}$$

$$\dot{m}_{propellant} = \frac{P_c A_t}{c*} \tag{4.14}$$

After the optimization process, the oxidizer and solid propellant tank can be sized. In the following sections, liquid oxidizer tank design, feed system design and solid propellant grain design will be discussed.

4.2.3 Liquid Oxidizer Tank Design

4.2.3.1 Liquid oxidizer Tank Sizing

For the design of liquid oxidizer tank, the mass of required oxidizer calculated from the trajectory simulator needs to be used as input. And assuming the oxidizer temperature of -60°C and design pressure of 6.6 MPa the required tank volume can be calculated using equations shown below.

$$M_{ox} = M_{\Delta v} + M_{margin} + M_{expulsion} + M_{boiloff} + M_{error} \tag{4.15}$$

Boil-off for liquid oxygen is estimated to be about 0.5-1% for the duration of 30 days [6]. However, considering the short duration of Stratos III mission compared to other missions to moon or other planets, the boil-off mass of oxidizer is negligible. Expulsion mass of oxidizer is estimated to be 5% [9]. M_{error} arising from loading uncertainty is assumed to be 0.5% [6].

Once the mass of the oxidizer has been determined, the volume of the oxidizer tank can be calculated. Volume of the oxidizer tank can be split up into two parts, volume taken by the liquid phase oxidizer and ullage volume (the volume allowed for expansion.)

$$V_t = V_{ox} + V_u \tag{4.16}$$

Liquid phase oxidizer can be simply determined by knowing the mass fraction and densities of nitrous oxide and oxygen. From Figure 4.4 it can be seen that at the design temperature of -60°C and design tank pressure of 6.6 MPa, the mass fraction of oxygen in liquid phase is found to be 15% [5].

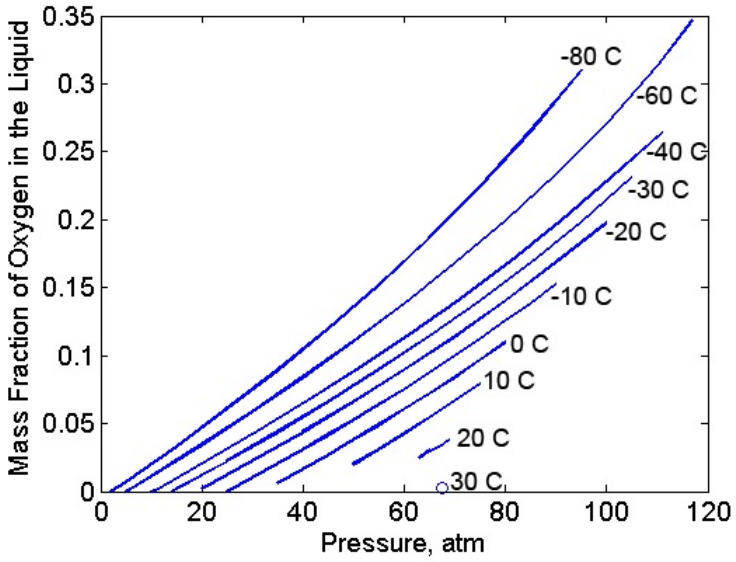

Figure 4.4: *Liquid oxygen Mass Fraction*

Then using the equation shown below: the volume of liquid oxidizer can be calculated.

$$V_{ox} = \left(\frac{M}{\rho}\right)_{oxygen} + \left(\frac{M}{\rho}\right)_{N_2O} \tag{4.17}$$

Ullage volume is necessary in a tank to prevent tank rupture. With no ullage, temperature increase can lead to substantial increase of pressure within the tank [6]. Ullage volume of 3-10% of the total tank volume can be assumed [9]. In the sizing of the final concept, 10% ullage volume was used.

4.2.3.2 Temperature Control

Liquid oxidizer for the Stratos III rocket has to be kept at -60°C. Temperature control of the liquid oxidizer within the rocket is crucial to ensure that the rocket delivers predicted performance. As mentioned before, the propulsion performance of the rocket greatly depends on the temperature of the oxidizer. Possible solutions for oxidizer temperature control are discussed below.

Temperature control through cold oxygen injection to the oxidizer tank during oxidizer injection stage is suggested. In the ground phase when the rocket is connected to feed lines and dump line, liquid nitrous oxide will first be injected into the rocket. After an equilibrium has been reached for the nitrous oxide within the tank, liquid oxygen will then be added to the oxidizer tank while vaporous nitrous oxide and oxygen will be vented from the rocket to decrease the temperature within the tank.

A rough temperature simulation based on energy balance equation taking into account heat conduction, convection and radiation is created. The main purpose of this simulator is to show the effects of feed mass flow regulation and insulation. Shown below is a list of assumptions made for the simulation.

- The temperature of oxygen fed into the tank is assumed to be 190 K.
- It is assumed that the heat transfer between substance within tank with substance being added is instant.
- The composition of mass flow out of the tank is only dependent on mass fraction of substances within mixture.
- It is assumed that the oxidizer within the tank is an evenly mixed mixture.
- Ambient temperature of air around the rocket is assumed to be constant at 303.15 K.
- Ambient air velocity around the tank is assumed to be 5 m/s.
- Reynolds number of air is calculated assuming constant airspeed of 5 m/s and temperature of 30°C.
- Reynolds number of oxidizer within tank is assumed to be 10000.
- Nusselt number for h_1 is calculated using equation for long cylinder perpendicular to the flow.
- Nusselt number for h_3 is calculated using equation for turbulent flow in tubes.

The main equation of the simulation is the energy balance equation.

$$\frac{dE}{dt} = \phi_{q,in} - \phi_{q,out} + P_E \tag{4.18}$$

In this case no work is done by the system, therefore the term P_E can be neglected.
First, heat conduction from oxygen mass flow in and Nytrox mass flow out will be considered.

$$\frac{dE}{dt} = \dot{m}_{in} * c_{p,o2} * T_{oxygen} - \dot{m}_{out} * c_{p,n2o} * T_{n2o} \tag{4.19}$$

Since specific heat capacity of the mixture within the oxidizer tank will change as composition mixture changes, a separate equation needs to be used to calculate average specific heat capacity [6].

$$c_p = \frac{n_{n2o} * c_{p,n2o} + n_{o2} * c_{p,o2}}{n_{o2} + n_{n2o}} \tag{4.20}$$

Where n is number of molecules.
Second, heat convection between ambient air, tank wall, and oxidizer is considered [10].

$$\frac{dE}{dt} = \left(\frac{1}{h_1} + \frac{1}{h_2} + \frac{1}{h_3}\right)^{-1} \cdot \Delta T \cdot A \tag{4.21}$$

where A is the surface area of the oxidizer tank excluding bulk heads.
Heat transfer coefficients h_1, h_2, and h_3 each belonging to forced convection or ambient air, tank wall convection and oxidizer convection are calculated using equations shown below.
The equation used to calculate h_1 and h_3 are as follows [10].

$$h = Nu * \frac{\lambda}{d} \tag{4.22}$$

where d is characteristic length, in this case the diameter of the oxidizer tank. Thermal conductivity, lambda, can be found in material property table. In this calculation they are assumed to be 0.026 for ambient air and 0.26 for oxidizer within the tank.
Nu needs to be calculated using separate equations for each. Nusselt number for h_1 is calculated using equation for long cylinder perpendicular to the flow [11].

$$Nu = 0.5 * Re^{0.5} * Pr^{0.33} \tag{4.23}$$

Reynolds number is found to be 81250 and the Prandtl number is found to be 0.712.
Nusselt number for h_3 is calculated using equation for turbulent flow in tubes [11].

$$Nu = 0.027 * Re^{0.8} * Pr^{0.33} \tag{4.24}$$

Reynolds number is assumed to be 10000 and Prandtl number is assumed to be 0.72, the Prandtl number of Nitrous Oxide.
Now that h_1 and h_3 have been found, h_2 needs to be found.
Heat flux of hollow cylinder can be calculated using the following equation [10].

$$q = \frac{2 * \Delta T * pi\lambda * L}{ln\left(\frac{R_2}{R_1}\right)} \tag{4.25}$$

And the equation for heat transfer coefficient is given by the following equation [10].

$$h = \frac{q}{A * \Delta T} \tag{4.26}$$

Combining the above two equations

$$h = \frac{2 * pi * \lambda * L}{ln(\frac{R_2}{R_1}) * A} \tag{4.27}$$

Where L is the length of tank, λ is thermal conductivity of tank, R_2 is the outer radius, R_1 is the inner radius and A is surface area of tank.
Finally, heat radiation from sun can be taken into account.
Assuming that solar radiation in Spain is 479.17 W/m^2 and that a white smooth surface of the rocket tank has an absorption factor of 0.3, solar radiation energy absorbed by the tank can be roughly estimated.

$$\frac{dE}{dt} = 479.17 * 0.3 * A \tag{4.28}$$

Using the equations shown above, the temperature change over time of the oxidizer tank can be simulated. With the temperature of oxygen fed into the system assumed to be 190 K, the following plot can be shown in Figure 4.5

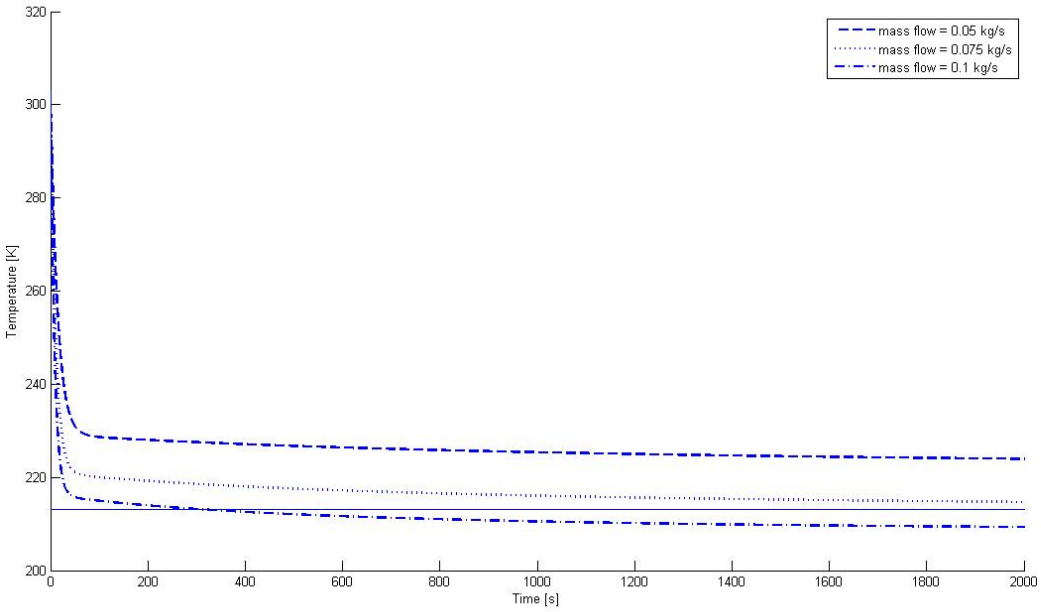

Figure 4.5: *Temperature of Oxidizer Tank vs. Time without Insulator*

From the Figure 4.5, it can be seen that only with the oxygen being supplied at a mass flow rate of 0.1 kg/s is it possible for the oxidizer to be cooled to the desired oxidizer temperature of 213.15 K or -60°C within 33 minutes. A detachable insulator coat around the oxidizer tank can be considered to ensure temperature control at a lower mass flow rate of oxygen.

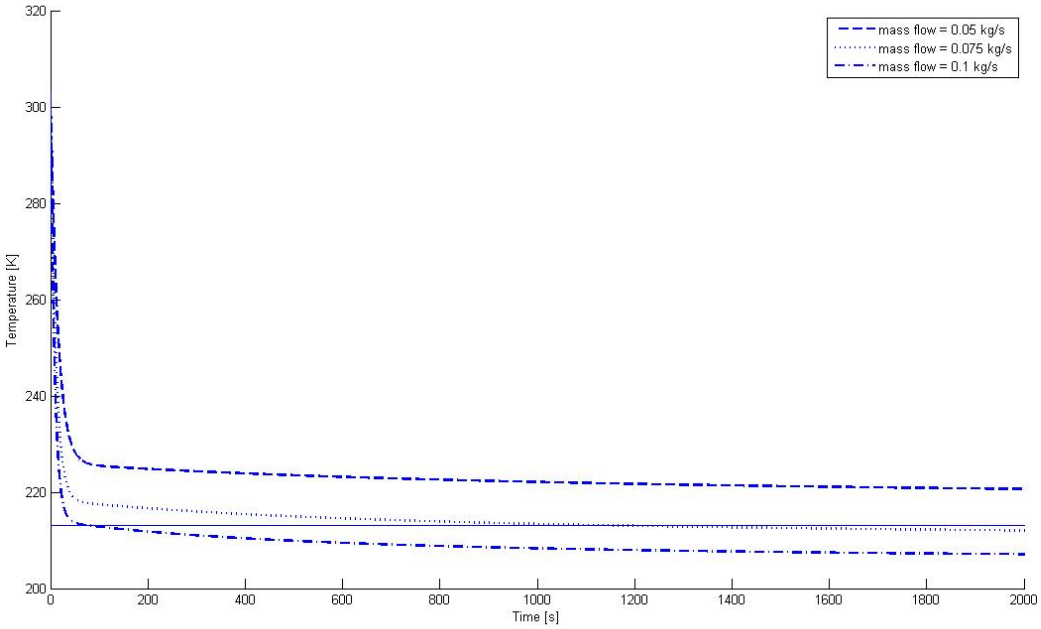

Figure 4.6: *Temperature of Oxidizer Tank vs. Time with Insulator*

The Figure 4.6 shows the temperature over time of the oxidizer given that an 5 mm thick insulator with

thermal conductivity coefficient of 0.25 is wrapped around the tank. It can be seen that now with a oxygen mass flow rate of 0.075 kg/s, the desired temperature can be reached within 33 minutes.

4.2.4 Feed System Design

The chosen self-pressurizing oxidizer does not require an external pressurizing system. But due to the lack of such system, the maximum oxidizer flow into the combustion chamber is limited by the pressure difference between oxidizer tank and combustion chamber. In order to prevent rocket engine backfire where combustion takes place in the plumbing or the oxidizer tank, a pressure difference of 1.5 MPa needs to be kept between the combustion chamber and oxidizer tank pressure. Also, all parts of the feed system that come in contact with Nytrox have to be proven to be compatible with liquid oxygen and nitrous oxide to ensure safety of personnel and success of mission.

The Stratos III rocket will utilize regulated self-pressurized oxidizer feed system. The following Figure 4.7 shows the oxidizer tank and feed system schematics.

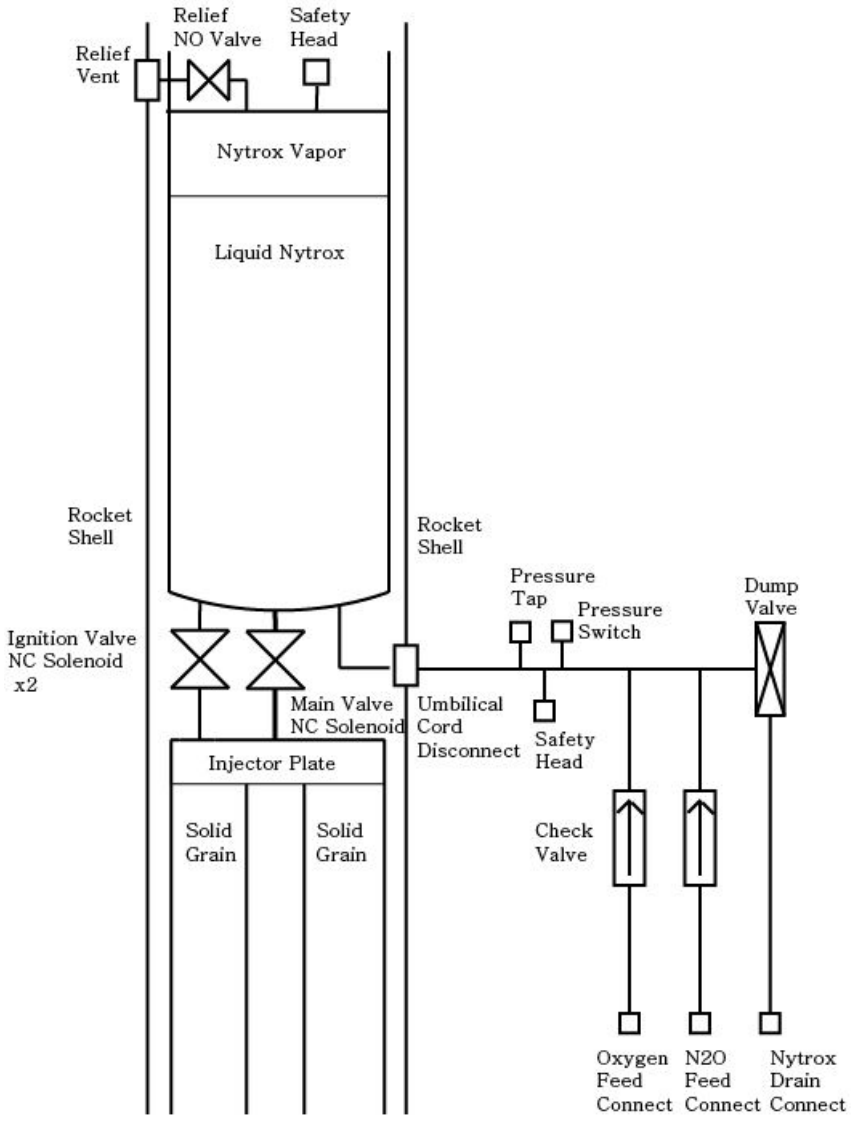

Figure 4.7: *Propulsion Feed System Schematics*

The propulsion feed system schematics show the plumbing of the oxidizer tank to various valves/taps and solid propellant. The following list can be generated to itemize components within the feed system.

- **Feed Connect** is required to connect nitrous oxide tank or oxygen tank to the oxidizer tank of the rocket. From the schematics it can be seen that the feed connect for oxygen is at the bottom of the

oxidizer tank while the nitrous oxide feed connect is located on top. This is to allow gas blending of oxygen and nitrous oxide. Once liquid nitrous oxide has been fed to the oxidizer tank, oxygen will be bubbled through liquid nitrous oxide.

- **Check Valve** is to ensure fluid to flow in one direction. Check valves connected to external feed lines are to ensure that contents of the oxidizer tank do not flow back into the external oxidizer tanks.
- **Pressure Switch** are installed in the feed lines between storage and internal oxidizer tanks to stop the oxygen or nitrous oxide feed when desired pressure within the internal oxidizer tank has been reached.
- **Pressure tap** exists within the feed line between storage and internal oxidizer tank to measure the pressure at which the oxidizers are delivered to the oxidizer tank.
- **Safety Head** are utilized as safety measurements against pipe line rupture. A rupture disc installed within a safety head will rupture at predetermined pressure to prevent over pressurization within the pipe line.
- **Relief valve** serve the same function as the safety head. Its main advantage being that it can be closed after pressure relief. Compared to the rupture disc, it will have a disadvantage of leakage. However its advantage outweighs its disadvantage considering that the relief valve will serve the purpose of controlling oxidizer composition within the tank.
- **Relief Vent** is an opening connected to relief valve exposed to atmosphere to vent gaseous oxidizer.
- **Dump Valve** controls the Nytrox flow out of the oxidizer tank. Together with the relief valve, it is used to control the mixture ratio within the oxidizer tank to reach desired mixture.
- **Drain Connect** is required to connect dump pipe to the ground storage tank. It will mainly handle liquid drainage.
- **Filter** is placed to remove any impurities before the oxidizer enters the combustion chamber. In this case
- **Injector Plate** is placed on top of the combustion chamber to increase atomization of oxidizer and mixing of propellants near the injector plate. This will in turn ensure even burn of solid propellant along its length.

The main and auxiliary valves conveying oxidizer flow to the combustion chamber need to be properly insulated to prevent valve freezing due to condensation. For this purpose, the valves will be encased in diffusion proof insulation. Thermal "antifreeze" jackets can be used to wrap and insulate the valve to prevent freezing.

4.2.4.1 Preliminary Feed System Sizing

In order to size the feed system and get a mass estimation some rough preliminary sizing of the feed system has to be done. The main valve is expected to take up a large fraction of the feed system mass, therefore the focus will be on the main valve. In order to keep the oxidizer flow choked at the injector plate, the flow area of the valve and piping has to be larger than the flow area of the injector. Thus, the area of the injector plate will be estimated first.

Estimation is done using Equation 4.29 [12]. Since this equation assumes steady frictionless flow, a fairly low discharge coefficient (C_d) of 0.5 is assumed. The oxidizer mass flow ($\dot{m}_{ox}$) is assumed to be 6 kg/s, the pressure drop over the injector plate is expected to be at least 0.5 MPa. Filling in the equation gives the following injector flow area:

$$A_{\text{injector}} = \frac{\dot{m}_{\text{ox}}}{C_d\sqrt{2\rho_{\text{ox}}\Delta P}} = 3.6\ cm^2 \tag{4.29}$$

Now the maximum flow area of the injector plate is known, the maximum diameter of the valve and piping can be estimated. Equation 4.30 gives the diameter of the piping assuming the flow area has to be twice the flow area of the injector.

$$d_{\text{piping}} = 2\sqrt{\frac{A_{\text{injector}} \cdot 2}{2\pi}} = 21\ mm \tag{4.30}$$

Thus the diameter of valve and piping are estimated to be 21 mm.

4.2.5 Solid Grain Design

The solid propellant grain of the Stratos III mission is composed of paraffin, aluminum powder and carbon black. One of the main benefit of adding aluminum powder to the solid compound is that it decreases the optimum oxidizer to fuel ratio while retaining similar specific impulse value as can be seen in Table 4.4. Therefore the oxidizer tank size can be reduced which leads to increased overall rocket propulsion efficiency.

Another benefit from the addition of aluminum powder is suppression of combustion instability [13]. However from the propulsion tests conducted by DARE on sorbitol based solid propellants, high percentage composition of aluminum in the solid compound showed undesirable thrust fluctuation due to unburnt aluminum [14]. In addition to paraffin and aluminum powder, carbon black is added to the solid fuel compound to act as blocking agents for possible penetration of heat radiation through paraffin.

Table 4.4: *Effect of Addition of Aluminum Powder*

Percentage Composition of Aluminum	**Ideal Vacuum Specific Impulse**	**O/F ratio**
0	332.9	3.1
5	333	2.9
10	333.2	2.8
15	333	2.6
20	333.4	2.4

Given parameters for this simulation are: a chamber pressure of 7 MPa, 8:2 N_2O O_2 oxidizer ratio, and an expansion area ratio of 17.

As can be seen from Table 4.4, addition of aluminum powder has little effect on specific impulse while reducing the O/F ratio significantly. Additionally, aluminum powder has much higher density than that of paraffin. Therefore, an increase of volumetric specific impulse can be expected as well. Maximum performance can be achieved if the percentage composition of aluminum powder is maximized without causing thrust fluctuations. In conclusion, a mixture of 79.5:20:0.5 of paraffin-aluminum-carbon black is proposed as solid fuel.

4.2.6 Material Compatibility

Nytrox contains both liquid and gaseous forms of oxygen. Nitrous oxide is compatible with a wide variety of metal alloys including: carbon steel, stainless steel brass and aluminum alloy [15]. However, oxygen is the second most reactive material of all elemental materials [16]. Apart from the special attention required for liquid oxygen handling, any material within the Stratos III rocket that come into contact with the oxidizer need to be compatible with oxygen. Under high pressure, up to 7500 psi or 51.7 MPa, research showed that Inconel alloy 600, brass, Monel alloy 400, and nickel displayed favorable characteristics while aluminum and stainless steel showed least satisfactory results [17]. Considering that the tests have been performed under 7000 psi pressure loads which greatly surpasses required oxidizer tank pressure, both aluminum and stainless steel can be considered as well. Additionally for aluminum alloys, aluminum alloy 2219, 6061 and 7020 and lithium aluminum alloy are recommended for use with liquid oxygen [6]. For the main structure of the oxidizer tank and the rocket fuselage, aluminum alloy 6061 is used. As for composite materials, its performance under high pressure loads and at low temperatures is questionable with possibilities of leakage due to micro-cracking of composite laminates and will not be considered. Therefore, all piping, valves and tank that come into contact with liquid or gaseous oxygen need to be manufactured with one of the materials listed below. Further testing of the oxidizer tank and feed system need to be considered to ensure material compatibility.

- Inconel alloy 600
- Brass
- Monel alloy 400
- Nickel
- Stainless steel
- Aluminum alloy 2219
- Aluminum alloy 6061
- Aluminum alloy 7020
- Lithium aluminum alloy

4.2.7 Performance

The thrust profile of the Stratos III rocket designed to reach target altitude of 120 km during burn time is shown in Figure 4.8. The key performance parameters are shown in Table 4.5

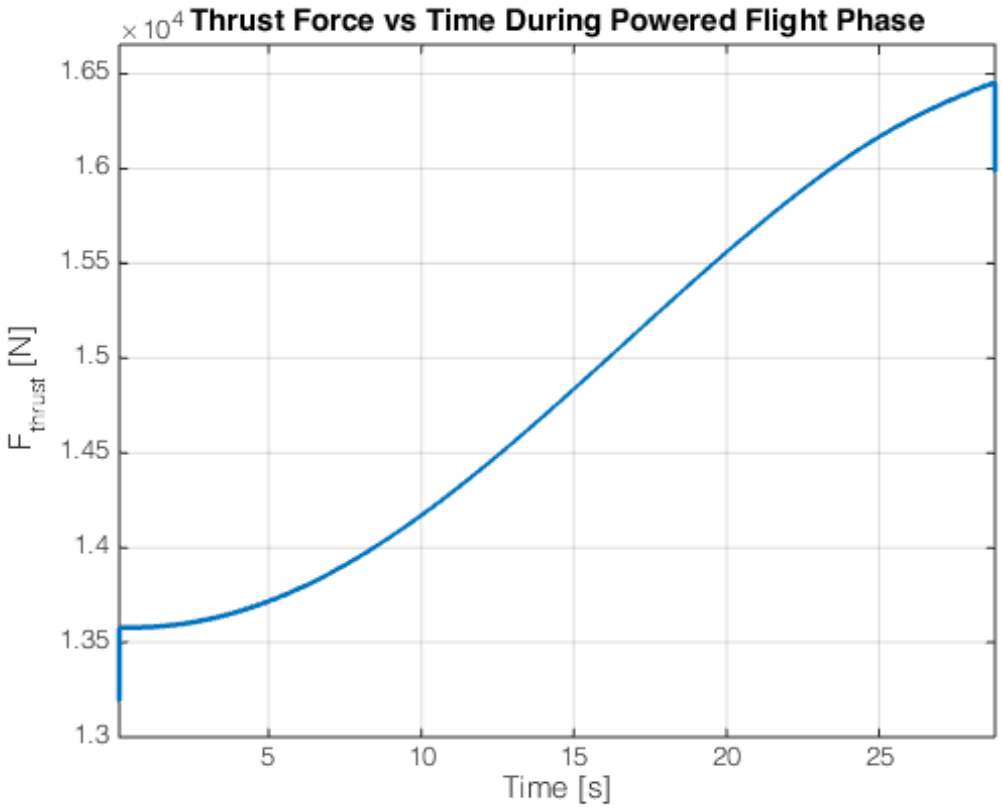

Figure 4.8: *Engine Thrust Profile*

Table 4.5: *Propulsion Key Performance Parameters*

Burn Time	28.9 $[s]$
Sea Level I_{sp}	232 $[s]$
Burnout I_{sp}	282
Average Mass Flow	5.96 $[\frac{kg}{s}]$
Average O/F Ratio	5.17
Optimum Expansion Altitude	13 $[km]$
Optimum Expansion Time	25 $[s]$
Total Impulse	427.8 $[kN]$
Δ-V	1.548 $[km/s]$

4.2.8 Sensitivity Analysis

The propulsion thrust function uses a nozzle efficiency of 85% instead of a more typical 90-99%. Additionally, the Propulsion subsystem uses a combustion efficiency of 95% to accommodate the likelihood that the solid grain will not be a perfect blend. The nozzle efficiency in particular acts to compensate for the assumption used that the mass flow of the oxidizer will remain constant at 5 kg/s. Due to the nature of Nytrox, there will be a certain amount of gaseous oxygen that has percolated through and separated from the nitrous oxide, which could cause a decrease in oxygen mass fraction of the oxidizer mass flow at the end of the burn. Additionally, the decreased number of oxygen molecules within the oxidizer tank will decrease the pressure within the tank and, therefore, decrease oxidizer mass flow towards the end of the burn time. It is estimated that this could result in a 5% decrease in total performance which, along with an assumed 5% of fuel that remains trapped in plumbing or otherwise unburned, balances out the conservative nozzle efficiency estimate.

There are many factors which could alter either specific impulse, thrust or burn time of the rocket engine. Oxidizer mass flow, initial port radius of solid grain, and throat area of the nozzle are varied by 10% to study the sensitivity of the simulation model used to design the rocket propulsion subsystem. The effect of increasing or decreasing solid grain length and therefore grain mass has already been covered in Chapter 3.

Table 4.6: *Results of Sensitivity Analysis*

Parameter change	**Change [%]**	**Average I_{sp} $[s]$**	**Average Thrust $[\times 10^3\ N]$**	**Burn Time $[s]$**
Current Design	0	276.6	16.2	28.8
Increase $\dot{m}_{ox}$	+10	276.6	17.7	27.7
Decrease $\dot{m}_{ox}$	-10	276.6	14.7	30.4
Increase R_c	+10	276.6	16.2	27
Decrease R_c	-10	276.6	16.2	30.3
Increase A_t	+10	281.1	16.4	28.8
Decrease A_t	-10	272.2	15.9	28.8

Table 4.7: *Percent Results of Sensitivity Analysis*

Parameter change	**Change [%]**	**Change of Average I_{sp} [%]**	**Change of Average Thrust [%]**	**Change of Burn Time [%]**
Current Design	0	0	0	0
Increase $\dot{m}_{ox}$	+10	0.0086	9.2	-3.8
Decrease $\dot{m}_{ox}$	-10	0.0016	-9.2	5.6
Increase R_c	+10	-0.0012	-0.018	-6.25
Decrease R_c	-10	0.000036	0.018	5.2
Increase A_t	+10	1.6	1.6	0
Decrease A_t	-10	-1.6	-1.6	28.8

4.2.9 Mass, Power, and Cost Budget

Shown below is a list of parts, including fuel and oxidizer, within the Propulsion subsystem with their mass and power requirements. Note that this budget has been approximated by amount of fuel/oxidizer approximated by the main integration simulation, CATIA modelling, and product specifications given on manufacturer catalogs. Only parts carried within the rocket are itemized. As for the cost breakdown table, the values are only given as a rough estimate to determine the magnitude of each component cost since it does not include costs of shipping and import taxes. Also note that for the budget, costs for oxidizer tank, combustion chamber, and nozzle are included in the Structure subsystem.

Table 4.8: *Propulsion Subsystem Item List*

Section	**Item**	**Quantity**	**Mass $[kg]$**	**Power $[W]$**	**Cost [€]**
Fuel	Oxidizer	-	144	0	3793
Fuel	Solid Propellant	-	27.7	0	184
Tank	Oxidizer Tank	1	-	-	-
Combustion Chamber	Combustion Chamber	1	0	0	-
Feed system	Pipe	0.6 meters	0.5	0	60
Feed system	Umbilical cord disconnect	1	0.2	0	30
Feed system	Pressure tap	1	0.05	0	20
Feed system	Safety head	1	0.15	0	20
Feed system	Relief valve (NO)	1	2	25	200
Feed system	Relief vent	1	0.1	0	20
Feed system	Main Regulator (NC)	1	4	45	600
Feed system	Auxiliary Regulator (NC)	2	2	20	400
Feed system	Swirl injector plate	1	4	0	50
Feed system	Valve Insulator Jacket	1	0.15	0	50
Feed system	Controller	1	0.15	0.5	30
Feed system	Filter	1	0.1	0	10
Nozzle	Graphite/Steel nozzle	1	-	-	-
Nozzle	Nozzle ring	1	-	-	-

Note that in Table 4.8, the estimated cost of oxidizer doesn't take into account extra oxygen and nitrous oxide that may be used to decrease the oxidizer tank temperature. Further research must be done with small

scale oxidizer tank model to determine the amount of excess oxidizer needed.

4.3 Structure

The Structure subsystem is the one which holds the rocket together during flight. Because of this every part of the flight envelope needs to be analyzed. This includes the stresses during the powered flight and the pressures just before launch. The thermal loads on the nosecone are discussed as well to give an total overview of the structure. Finally, a sensitivity analysis is done to see how vulnerable the structure is to changes.

4.3.1 Assumptions

For the structure the following assumptions apply:

- The stress due to the pressure on the nosecone is calculated by using the formula for the pressure on a cylindrical cone and changing the half angle to the angle at that point.
- It is assumed that there is no torsion acting on the rocket.
- The drag is assumed to be a point force acting on the tip of the rocket for the shell of the rocket.
- For the nosecone the drag is modeled as distributed load which is the inverse of the nosecone shape. This means that most of the drag is found at the tip of the nosecone and near the end where the straight fuselage begins the drag is zero.
- The thrust is assumed to be a point force acting on the bottom of the rocket.
- It is assumed that the maximum drag and maximum thrust occur at the same time and that this point is in a complete vacuum. This is not the case during flight and this is therefore a conservative design.
- For the oxidizer tank where two materials are used it is assumed that the stress is evenly distributed over the two materials.
- There is no shear force or shear stress on the main fuselage due to complete symmetry and in-line forces.
- The structure is assumed to be thin-walled until the solid tip.
- The stress caused by the weight of the structure is assumed to be much smaller than the forces acting on it and is therefore neglected.

4.3.2 Fuselage

For the straight fuselage the equation for a cylindrical section under pressure is used. The stresses caused by the internal pressure on a thin-walled cylinder can be calculated by using Equations 4.31a and 4.31b [18].

$$\sigma_{z_{\text{pres}}} = \frac{\Delta P D^2}{(D + 2t_{\text{nose}}) - D^2} \tag{4.31a}$$

$$\sigma_{\theta_{\text{pres}}} = \frac{\Delta P R}{t_{\text{nose}}} \tag{4.31b}$$

For the fuselage the forces are assumed to be point forces acting on the top and bottom, this means that the stress due to the force can be calculated by using Equation 4.32:

$$\sigma_{z_F} = -\frac{F_T + F_D}{2\pi R t_{\text{nose}}} \tag{4.32}$$

Putting Equations 4.32 and 4.31 together, the principle stresses for the cylindrical parts can be calculated. The Von Mises yield criterion from the principle stresses can be calculated using Equation 4.33. Following that, the minimum wall thickness for a particular section of the rocket can be calculated.

To choose a suitable material, a single stress is needed to compare this to the yield stress of the chosen material. If for any material there is no yield stress, such as in the case of composites, the ultimate stress is taken. This critical stress is then compared to the Von Mises yield criterion for only principle stresses, which is given in Equation 4.33 [19].

$$\sigma_v = \sqrt{0.5\left[(\sigma_r - \sigma_\theta)^2 + (\sigma_\theta - \sigma_z)^2 + (\sigma_z - \sigma_r)^2\right]} \tag{4.33}$$

Since the structure is assumed to be thin-walled σ_r is zero and therefore Equation 4.33 can be reduced to:

$$\sigma_v = \sqrt{0.5\left[(\sigma_\theta^2 + (\sigma_\theta - \sigma_z)^2 + \sigma_z^2\right]} \tag{4.34}$$

This is done for all the different sections of the main fuselage - the oxidizer tank and the solid propellant tank - to find the minimum thickness required. The first thickness to be calculated is the shell thickness required for the combustion chamber thickness, then following that a check is done to see that it also fits the parts of the rocket where the payload and the electronics are. If this is not the case a new thickness is calculated. The oxidizer tank will be a separate tank to make maneuverability easier. Since the minimum thickness available for a multitude of manufacturers is 5 mm, this is chosen as a starting point in the design process. This starting point of 5 mm is also enough to handle all the stress on the fuselage.

4.3.3 Nosecone

Nose Fineness and Geometry The nosecone is a Von Kármán nosecone, which is the best overall nosecone for the entirety of the Mach range Stratos III will go through and particularly for the supersonic region after Mach 1.6 [20]. The top is made out of two regions: the first region has to be made out of a temperature resistant material since the temperature at the top during re-entry will get high.

The Von Kármán nosecone follows the formula given in Equations 4.35a and 4.35b.

$$y = \frac{R}{\sqrt{\pi}}\sqrt{\theta - \frac{\sin(2\theta)}{2}} \tag{4.35a}$$

$$\theta = \arccos\left(1 - \frac{2z}{L}\right) \tag{4.35b}$$

For the drag distribution a six-degree polynomial was taken to approximate Equation 4.35 but then in the form $z = f(y)$. This is then used to create the distribution in the form of:

$$f_D(y) = C \cdot f(y) \tag{4.36}$$

In Equation 4.36 C is a constant which can only be obtained by integrating the equation and setting it equal to half of the total drag, which can be seen in Equation 4.37. This is because $f(y)$ is only the shape for half of the nosecone.

$$\frac{F_D}{2} = \int_0^R Cf(y)dy = C\int_0^R f(y)dy \tag{4.37}$$

Solving this for C leads to:

$$C = \frac{F_D}{2\int_0^R f(y)dy} \tag{4.38}$$

To accurately approximate the stresses on the nosecone the angle of the gradient has to be known since this determines if this is a normal stress or a shear stress. The angle can be found by differentiating Equation 4.35 with respect to z and then taking the tangent of the results leading to Equation 4.39:

$$\theta_{\text{nose}} = \arctan\left[\frac{d}{dz}\left(\frac{R}{\sqrt{\pi}}\sqrt{\theta - \frac{\sin(2\theta)}{2}}\right)\right] \tag{4.39}$$

Now that the complete geometry of the nosecone and force distribution is known, the stress calculation can begin. Just as with the main fuselage the stress due to pressure is calculated first. This is done using the stress equation due to pressure for a conical structure these can be seen in Equations 4.40a and 4.40b [21]:

$$\sigma_\theta = \frac{\Delta PR}{t\cos(\alpha)} \tag{4.40a}$$

$$\sigma_l = \frac{\Delta PR}{2t\cos(\alpha)} \tag{4.40b}$$

Equations 4.40a and 4.40b are combined with Equations 4.35a, 4.35b and 4.39 to get the following equations:

$$\sigma_{\theta_{\text{nose,pres}}} = \frac{\Delta Py(z)}{t_{\text{nose}}\cos(0.5\pi - \theta_{\text{nose}})} \tag{4.41a}$$

$$\sigma_{l_{\text{nose,pres}}} = \frac{\Delta Py(z)}{2t_{\text{nose}}\cos(\theta_{\text{nose}})} \tag{4.41b}$$

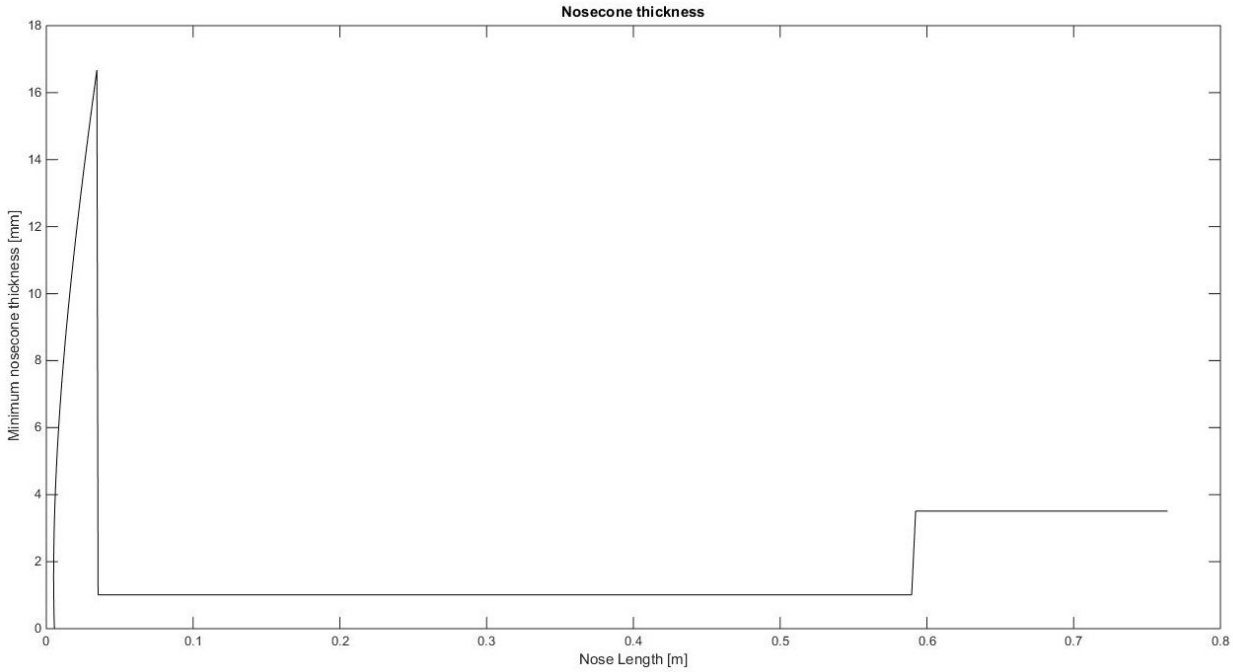

Figure 4.9: *The Thickness Profile of the Entire Nosecone*

Now that the stress due to the pressure is known the stress due to the forces can be calculated. The forces are a point force thrust and the distributed drag force from Equation 4.36. The normal stress at a position z measured from the tip can be calculated by using Equation 4.42:

$$\sigma_{l_{\text{nose,force}}} = -\int_0^{y(z)} \frac{f_D(y)\cos(0.5\pi - \theta_{\text{nose}}(y))}{2\pi y(z) t_{\text{nose}}} dy - \frac{F_T}{\pi y(z)^2} \tag{4.42}$$

In Equation 4.42 $y(z)$ is the local radius at a z location along the length of the rocket. But because the nosecone is curved and the drag is always oriented in the z-axis there is also a shear stress. The shear stress can be calculated by using formula Equation 4.43 [22].

$$\tau = q/t \tag{4.43}$$

Where q is the shear flow in N/m. This shear flow is the component of the distributed load which is normal to the surface.

$$q = f_D \sin(0.5\pi - \theta_{\text{nose}}) \tag{4.44}$$

So the shear stress for the rocket becomes:

$$\tau = \frac{f_D \sin(0.5\pi - \theta_{\text{nose}})}{t_{\text{nose}}} \tag{4.45}$$

Using the stresses from Equations 4.41a, 4.41b, 4.42 and 4.45 and filling them in into the Von Mises equation which this time includes one shear stress. The Von Mises stress can be seen in Equation 4.46

$$\sigma_v = \sqrt{0.5\left[(\sigma_\theta^2 + (\sigma_\theta - \sigma_z)^2 + \sigma_z^2\right] + 3\tau^2} \tag{4.46}$$

Because there is a distributed load there will be a minimum thickness for every position along the z-axis. But because of limitations if the minimum thickness for the glass fiber cannot be lower than 1 mm. To make the process of creating the nosecone easier, a choice has been made to create a nosecone with two thicknesses, one with the minimum thickness of 1 mm and one with the maximum thicknesses needed on the other part of the nosecone. So using all the equations above concerning the nosecone the thickness profile can be seen in Figure 4.9 As can be seen for the first 3.5 cm the thickness increases immensely this is because of the solid titanium tip to handle the thermal loads on the tip, but this is discussed in Section 4.3.4. Know knowing the thicknesses on every part of the rocket the stress profile can be seen in Figure 4.10

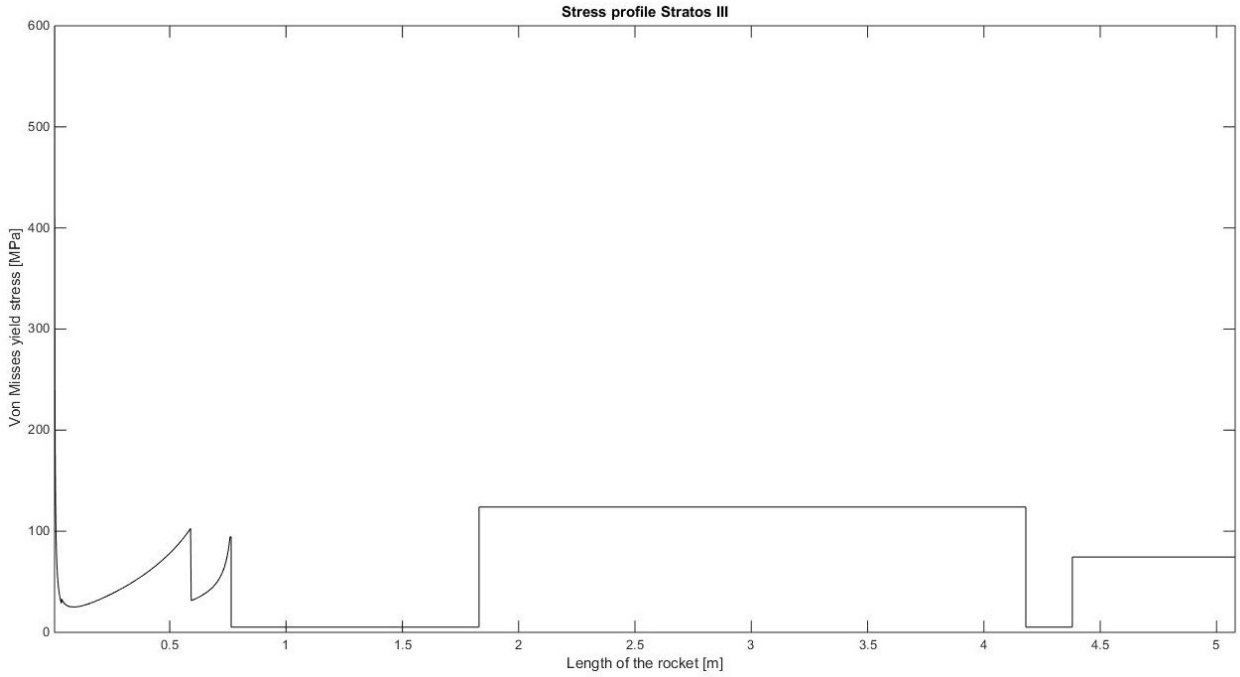

Figure 4.10: *The Stress Profile for the Stratos III Rocket*

4.3.4 Thermal Loads

For the temperature on the tip a very crude estimation is used. This estimation entails that the temperature on the tip is the same as the temperature after the normal shock wave at the speed the rocket finds itself. The temperature profile on the tip of the rocket can be seen in Figure 4.11. From Figure 4.11 it can be seen that the highest temperatures are around 30 s and another peak can be observed at 320 s. These are the two important points for the thermal loading case. To find out if the temperature on the nosecone will reach melting temperature a software tool called SimScale [23] was used to calculate the heat transfer along the nosecone. The heat transfer for critical point is given in Figure 4.12

The time step of 100 s was chosen because that is the point where the outside temperature drops below the melting temperature of the glass fiber, therefore it is assumed that after that unless it is heated up again the glass fiber will not melt. This notion in enforced by the fact that just after 100 s Stratos III will not be going supersonic and will therefore be exposed to outside temperatures in the atmosphere and outside the atmosphere over the entire rocket which will be cooler than the temperature on the rocket.

4.3.5 Design Summary

Know that the stresses on the rocket are known as-well as the thermal loads the final design can be given in Table 4.9.

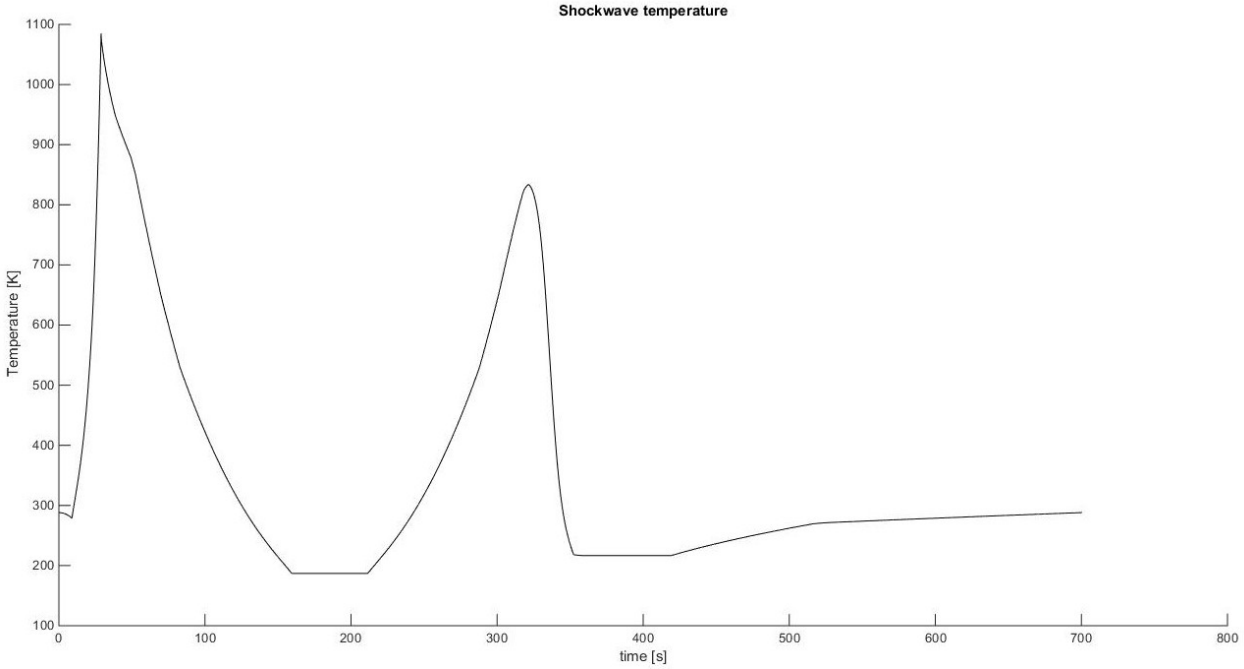

Figure 4.11: *Temperatures on the Nosecone of the Stratos III Rocket*

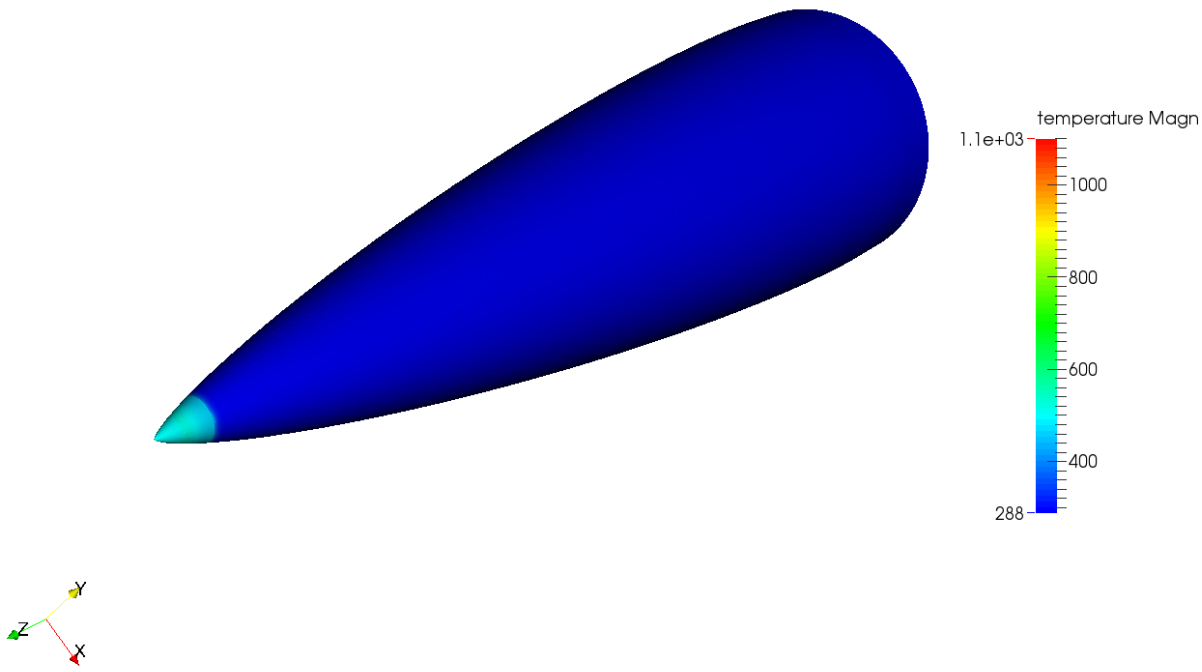

Figure 4.12: *Temperatures at t=100 [s]*

Table 4.9: *Final Rocket Dimensions*

Nosecone Design	
Tip Material	Titanium
Main Material	Glass fiber
Profile	Von Kármán
Length	0.78 $[m]$
Base Diameter	0.26 $[m]$
Glass fiber Thicknesses	1 $[mm]$ from tip to 0.58 $[m]$ 3.5 $[mm]$ from 0.58 $[m]$ to 0.78 $[m]$
Fuselage Design	
Main Material	Aluminum
Length	4.51 $[m]$
Thickness	5 $[mm]$
Diameter	0.26 $[m]$
Overall Design	
Total Length	5.65 $[m]$

Knowing know the dimensions the only thing remaining is the material properties which can be seen in Table 4.10 [24, 25].

Table 4.10: *Material Properties*

Material	**Density** $[kg/m^3]$	**Yield Strength** $[MPa]$	**Ultimate Strength** $[MPa]$	Melting Temperature $[C]$
Aluminum 6060	2630	185	220	635
Titanium TiAl6V4	4430	1030	1150	1650
Glass fiber PA6 GF30	1400	-	190	220
Steel 316L	8000	280	650	1400
Graphite	2260	-	151	3500

4.3.6 Sensitivity Analysis

All structural thicknesses were calculated with a safety factor of 1.5. With the exception of the tip of the nosecone, this safety factor still means the required material thickness is much lower than what is commercially viable. In the case of the glass fiber nosecone, the required thicknesses after the safety factor are far below 1 mm, which is considered the thinnest thickness DARE will be capable of producing effectively. Thus, using COTS structures, the rocket will be many times stronger than is needed.

Also the different input variables which are not major design changes like the increase in diameter will be increased by 10%. These variables and their impact can be seen in Table 4.11 and 4.12. For this sensitivity analysis the minimum thicknesses are removed to see the impact of the changes. For the sensitivity two parts are calculated the minimum thickness for the main shell this is the thickness at the combustion chamber and the thickness for the oxidizer tank.

Table 4.11: *Sensitivity Analysis on the Shell Thickness*

Parameter	**Initial minimum thickness**		**Increased thickness** $[mm]$	
	$[mm]$	$[\%]$	$[mm]$	$[\%]$
Thrust	2.42	100	2.42	100
Drag	2.42	100	2.42	100
Chamber Pressure	2.42	100	2.66	109.92
Oxidizer pressure	2.42	100	2.42	100
Oxidizer mass	2.42	100	2.42	100
Maximum g-loading	2.42	100	2.42	100

Table 4.12: *Sensitivity Analysis on the Oxidizer Tank Thickness*

Parameter	**Initial minimum thickness**		**Increased thickness** $[mm]$	
	$[mm]$	$[\%]$	$[mm]$	$[\%]$
Thrust	4.83	100	4.83	100
Drag	4.83	100	4.83	100
Chamber Pressure	4.83	100	4.83	100
Oxidizer pressure	4.83	100	5.31	109.94
Oxidizer mass	4.83	100	4.83	100
Maximum g-loading	4.83	100	4.83	100

4.3.7 Mass and Cost Budget

For the budgeting of the structures the only budget is the cost and mass budget, these can be seen in Table 4.14, the mass of the graphite nozzle is bigger than the actual nozzle because the specific nozzle cannot be bought off the shelf and has to be made by hand from a graphite block. The table is divided into two parts the cost budget for the individual materials and the mass budget for the parts.

Table 4.13: *Cost Budget for the Structure Subsystem*

Material	**Euro/Unit**	**cost**
Aluminum	162 per m [26]	734€
Titanium	12.16 per kg [27]	0.1€
Glass fiber	7.92 per kg [28]	51.35€
Steel	0.76 per kg [29]	8.44€
Graphite	1.284 per kg [30]	19.35€
Total		813.24€

Table 4.14: *Mass Budget for the Structure Subsystem*

Part	**Mass** $[kg]$	**% of Total**
Aluminum tubes	56.5	69.28
Fasteners	2	2.45
Glass fiber	6.5	7.97
Graphite part Nozzle	5.586	6.85
Steel skirt nozzle	10.961	13.44
Titanium Tip	0.006	0.01
Total	81.5526	100

4.4 ADCS

The attitude determination and control system is the system that functions as the rockets eyes and ears. It follows everything during flight and determines the location and orientation of the rocket. It includes the flight computer, which analyses everything from battery levels to engine status. If the computer deems it

to be necessary, it will send a signal to the canards such that it can correct the course of the rocket. An overview for the ADCS subsystem is given in block diagram form in Figure 4.13.

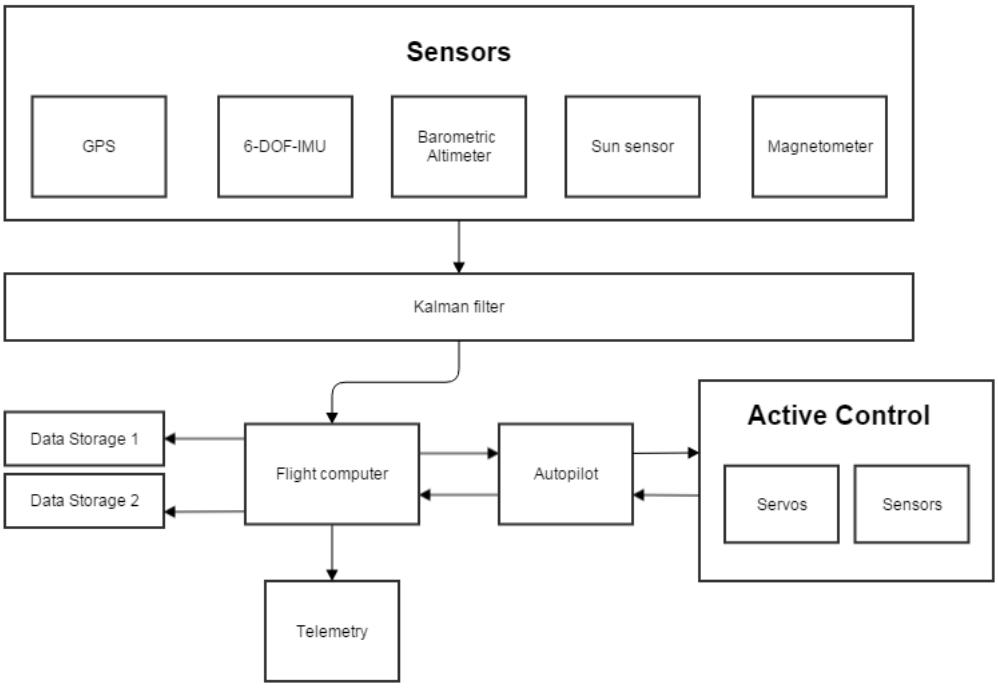

Figure 4.13: *Block Diagram for the ADCS*

4.4.1 Attitude and Position Determination

The main capability of the attitude determination system is to produce a state vector for the rocket with values in the earth fixed reference system as given in Equation 4.47. The last four state variables are quaternions. These are a commonly used method in spacecraft attitude dynamics for showing angular rates about axes without fear of gimbal lock.

$$\psi_e = [x_e, y_e, z_e, V_x, V_y, V_z, \alpha, \beta, \gamma, q_i, q_j, q_k, q_r] \tag{4.47}$$

In requirement form, this is the following:

- The ADCS must be able to determine altitude to within 10 m accuracy.
- The ADCS must be able to determine yaw angle to within 1 deg accuracy.
- The ADCS must be able to determine pitch angle to within 1 deg accuracy.
- The ADCS must be able to determine velocity to within 50 m/s accuracy.
- The ADCS must be able to determine geographical location to within 20 m accuracy.

The state vector will be generated with a sample rate of 10 Hz from each of the following sensors after being input into the flight computer. To give the necessary accuracies, two separate measurement vectors are needed. After burn out, this is especially difficult because the IMU begins to drift. This is solved by using a multitude of sensors given in the following paragraphs.

4.4.1.1 Sun Sensor

The sun sensor will provide one of the two vectors for attitude determination after burn out. As the rocket may roll slightly during ascent, Stratos III must have four sun sensors spaced equally apart around its fuselage. From the many different types, an in-house-built quad diode sensor is the most promising. This type of sun sensor has been successfully developed for the Delfi-n3xt project [31]. The selection of this sun sensor is primarily due to its low mass, power, and cost. Fairly simple manufacturing methods and rocket structure integration are also large advantages.

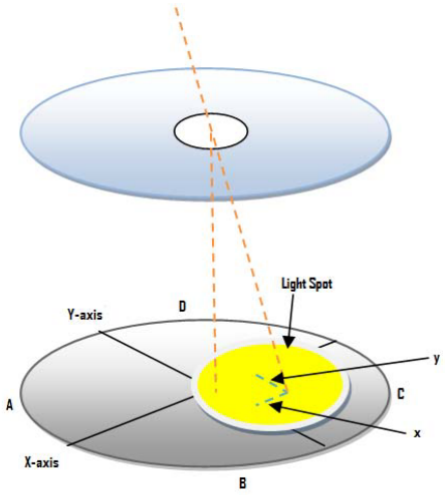

Figure 4.14: *Pinhole with Quad Diode Setup [32]*

A quad diode sun sensor is a configuration of four different diodes located next to each other. This can be seen in Figure 4.14, where the sections A,B,C and D are the four separate diodes. Direct sunlight falls through a pinhole which is drilled in the side of the fuselage and filled by acrylate polymers, which are transparent. The incidence angles in the earth fixed reference frame can be found from the four different currents running through the diodes. These angles can then be converted into the Earth reference system to give the yaw and pitch angles of the rocket [33].

4.4.1.2 Magnetometer

Magnetometers are reliable, lightweight, cheap and, can function at high altitudes. For this reason, a three-axis magnetometer will be used to create a second position vector. This is done by measuring the direction and intensity of the Earth's magnetic field and comparing it to a mathematical model [33]. Usually the Earth's magnetic field is modelled as a dipole magnet, which is approximately 95% accurate. Measurements received from magnetometers first need to be normalized and then need to be converted to the Earth reference system.

4.4.1.3 GPS

An unrestricted GPS would be highly useful in redundancy for both attitude and altitude. Previously, problems have arisen with the CoCom limit, where GPS receivers lock out at 18 km altitude and $1.9km/s$. This is to avoid the export of the parts to build inter-ballistic missiles, according to International Traffic in Arms Regulations. However, an exception is made for self-built or modified GPS receivers. This can be seen in 22:CFR:125.4c and 22:CFR:121.1 Category XV [34][35]. Buying an open source GPS receiver and altering the code is much easier and will be cheaper in terms of necessary man-hours to design and manufacture DARE's own unrestricted GPS. An example for the purchase of an open source GPS receiver is given in reference [36]. Another option is having the part sponsored. Some examples of companies that have done so in the past are ACTE and GOMSPACE; both sponsored Copenhagen Suborbital, a non-profit organization similar to DARE [37].

4.4.1.4 Altimeter

One of the ways to measure the altitude will be with a barometric altimeter. It requires a static pressure port, which connects to the outside air. This will be done by drilling a small hole in the fuselage and mounting the altimeter in an encasing around it on the inside. Problems also occur at supersonic Mach numbers, where shockwaves can fluctuate the measured pressure and thus altitude. This is why it is important to have altitude inputs from the accelerometer and GPS as a reference to accurately determine the rockets altitude.

4.4.1.5 IMU

The IMU or Inertial Measurement Unit is the main component of an inertial navigation system and will be used to determine the rockets heading. It will be a 6-DOF system, with three accelerometers and three MEMS gyroscopes. This will then be augmented with additional measurement systems using Kalman filtering for

increased accuracy [38]. An IMU can be bought off-the-shelf or self-built using accelerometers and gyroscopes. Specifications are given at the end of the section.

After receiving signals from each sensor, an algorithm for getting multiple sensor inputs and receiving a single accurate output is then used in the computer. Precisely how this is done is beyond the scope of this project. What is known is that to determine the position of the rocket during flight, two different measurement vectors are needed [33]. Until burnout these vectors can be supplied by the 6-DOF IMU and magnetometers. However, the accelerometers in the IMU will receive inaccurate values after burn out, the gyroscopes in the IMU will drift over time, and erroneous measurements will ensue. A sun sensor will be used to provide an additional measurement vector extending up to the target altitude. A GPS chip will be used as an additional fail safe, also providing the altitude measurement additionally to the barometric altimeter. All position vectors are determined in the Earth reference frames.

4.4.1.6 Active Control

Active control is necessary for flights of this altitude to reduce weathercocking into the wind. This occurs with passive rockets, because the side winds move the velocity vector away from the 'vertical' direction. The sensory inputs need to be evaluated before a signal can be sent to the servos to correct any deviations from the ideal flight path. This is done using an algorithm that uses a series of measurements observed over time, containing noise and other inaccuracies, and produces estimates of unknown variables that tend to be more precise than those based on a single measurement alone. This is more commonly known as Kalman filtering. The filter is already implemented in the Stratos II, but becomes a lot more important for the Stratos III. The algorithm will run on the flight computer along with the autopilot which gives the inputs to the canard servos based on the outputs of the Kalman filter. Some autopilot software and algorithms are already available within DARE, however further development is needed because at the moment there is only experience in controlling subsonic flight.

Flight Computer The primary function of the flight computer will be the autopilot and Kalman filtering. However it will also be responsible for the opening and closing of the propulsion valves, sending/storing data, and processing the communication with the ground station.

4.4.2 Canard and Fin Sizing

Because the target altitude is the only major requirement, it is crucial for the rocket to follow its predetermined flight path. Any sideways orientation or 'weathercocking' is inefficient and will lower the maximum altitude. For this reason Stratos III will be equipped with movable canards located above the oxidizer tank to provide aerodynamic control and tail fins to provide sufficient stabilization.

4.4.2.1 Configuration

For the configuration of the control surfaces, the following parameters are of importance:

- Number of planar surfaces
- Tandem surface orientation
- Control surface geometry

Control systems have either two (mono-wing), three (tri-tail), four (cruciform), six, or eight planar surfaces. At least three control surfaces are needed for static stability. Using a set up with more than four control surfaces results in less induced roll, but comes at the price of increased drag. Because Stratos III will fly at a very low angle of attack, induced roll will be unlikely to occur. Thus, the remaining choice was between tri-tail and cruciform configurations. The tri-tail is considered more difficult and since the cruciform is already under development within DARE it was chosen over the tri-tail configuration. The cruciform configuration uses 'skid-to-turn' maneuvering [39].

The tandem surface orientation is a choice between interlocking and in-line orientation of canards and tail fins. Here, an in-line orientation was chosen due to lower drag. Interlocking orientations are used primarily to decrease induced roll, which should not be a problem for Stratos III. For clarity these orientations are shown in Figure 4.15 with a top view of the rocket.

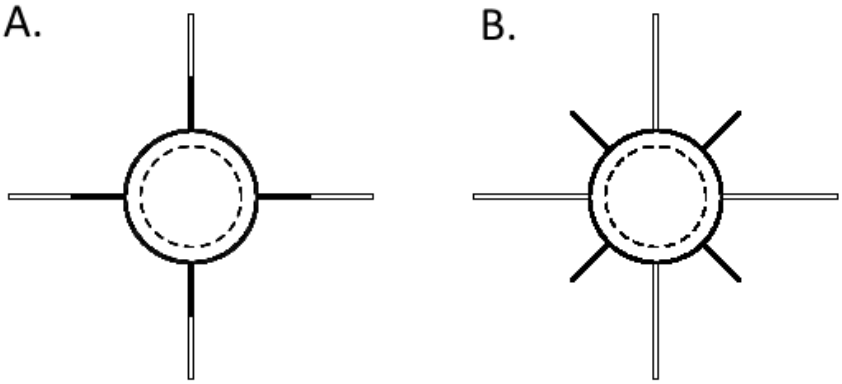

Figure 4.15: *Tandem Surface Orientation Options, A is In-Line and B is Interlocked*

Control surface deflection can be either flap control or balanced actuation control. The first is the use of a small movable surface on the end of the canard. The second is a fully movable surface. Because the Active Control Group Minor have already started on balanced actuation control and due to flap control being highly complex, fully movable surfaces are selected [39].

4.4.2.2 Control Surface Geometry

The geometries of the fins and canards have the following design parameters.

- Control surface shape
- Control surface airfoil
- Control surface material
- Control surface thickness
- Control surface size

For the control surface shape a choice had to be made between rectangular, trapezoidal, triangular (delta), bow tie, and double swept leading edge shapes. For the tail fins, a trapezoidal shape was chosen because it has high control effectiveness and performs sufficiently well in drag, aeroelastic stability, and varying aerodynamic center. For the canard surfaces a delta shape is preferred. Delta shapes have the lowest drag at supersonic velocities and cause a low bending moment on the canards, which will make actuator specifications lower. Increased sweep angles result in lower normal velocities over the canards and reduce supersonic drag. Delta wings do, however, provide less control than trapezoidal surfaces and will have a larger shift in center of pressure of the canard with increasing velocity. This needs to be taken into account when sizing the control surfaces and needs further research [39] [40].

The cross-sectional shape of the fin and canards also needs to be selected. The choice came down to two options: a symmetrical double wedge airfoil and a symmetrical biconvex airfoil. Both produce good lift to drag ratios in supersonic flow. However, the symmetrical double wedge airfoil is easier to manufacture and is thus selected for both the tail fins and the canards [41].

The material for the fins and canards will be pure aluminum. The aerodynamic heating will be minimal, because the nose cone will carry the largest shock waves. Once again, it is important to reanalyze this after supersonic analysis has been made. If aerodynamic heating were to occur, a possible solution could be to add aramid fibers to the leading edge. This could also be counteracted by increasing thickness, but in order to save weight this would be the best option.

The canard and tail fin geometries are sized by starting with Stratos II's fin geometries. The center of gravity is then found by summing all the elements contributing to the mass of the rocket together, as can be seen in Equation 4.49. The center of pressure for each contributing element is also added together to give the center of pressure for the rocket, as can be seen in Equation 4.50. Problems arise with both the center of gravity and center of pressure shifting during flight. Thus accounting for the shift, the static margin, which is the distance between the center of pressure and the center of gravity divided by the rocket diameter, must be between 1 and 2 for the largest part of the flight. This can be seen in Equation 4.48.

$$\frac{x_{cg} - x_{cp}}{2R} = \text{margin} \tag{4.48}$$

$$x_{cg} = \frac{\sum_{j=1}^{n} (x_j m_j)}{\sum_{j=1}^{n} m_j} \tag{4.49}$$

$$x_{cp} = \frac{\sum_{i=1}^{n} x_i (C_{N\alpha})_i}{\sum_{i=1}^{n} (C_{N_\alpha})_i} \tag{4.50}$$

x_{cg} and x_{cp} are found by summing all the contributing elements of the rocket together [42]. The parts of the rocket that contribute to the center of pressure, x_{cp}, are:

- Canards
- Fuselage
- Tail fins

The parts of the rocket that contribute mass to the system are:

- Nozzle
- Oxidizer and tank
- Solid grain and tank
- Rocket plumbing
- ADCS, Communications and Power
- Recovery
- Payload

A rough sizing will be completed by taking the center of pressure generated by Openrocket, which uses the Barrowman equation mentioned in Equation 4.50 and a self-written code in Matlab to give the shift in center of gravity over time, which is plotted in Figure 4.16.

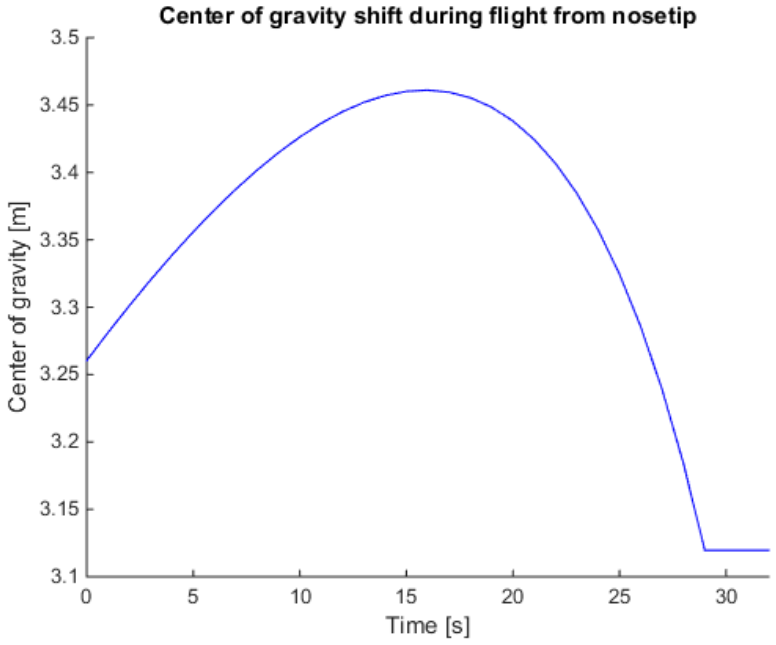

Figure 4.16: *Center of Gravity Shift over Time*

Because the supersonic pressure coefficient becomes inaccurate for Openrocket, a constant value is assumed after Mach 1.5. Generally, once the rocket surpasses the transonic region, little change occurs in the center of pressure [43]. Using this assumption, it is possible to get an indication of the change in static margin over time, as seen in Figure 4.17.

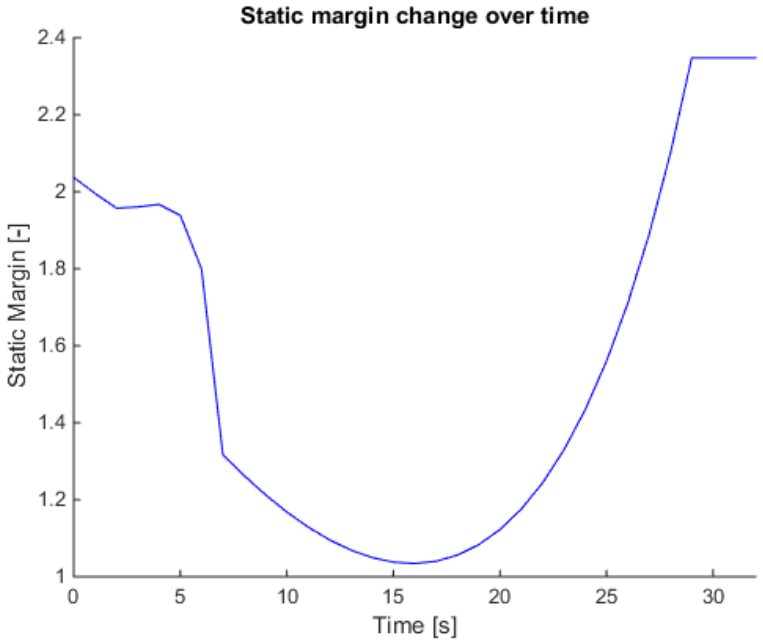

Figure 4.17: *Static Margin Shift over Time*

Although it is recommended that the static margin stay between 1 and 2, it is acceptable that the static margin is above 2 at the end of the flight, the canards would be able to correct for this overstability. Over stability is preferred over an unstable rocket anyway in case the active canards cause failure. Furthermore, weathercocking will not have much influence in the higher atmosphere because of low air density.
Further study on the exact shape and size of the fins and canards must be done using a more advanced CFD method accounting for high Mach numbers. This is done to check whether the assumption of constant center of pressure from Mach 1.5 onwards is acceptable. Changes in center of pressure could also be caused by canard-body-tailfin integration. This analysis was not possible in the time span of the DSE and requires future research.

The thickness of the control surfaces should be as small as possible in order to reduce drag and mass. This minimum thickness is determined by analyzing divergence and flutter characteristics of the canards and fins. After reaching a certain velocity, control surfaces can become dynamically unstable and oscillate at their natural frequencies. This leads to control surfaces shearing off and the rocket possibly becoming unstable. The velocity this occurs at, is called the flutter velocity. A rough estimation is done using a subsonic method based on the aspect ratio of control surfaces [44]. This method will be applied for the flutter velocity at point of burnout with an input of fin geometry. The maximum velocity of the rocket at point of engine burnout may not exceed the flutter velocity, an additional safety factor of 25% is added to ensure structural stability. From this condition a thickness is chosen in an iterative manner. Sufficient flutter velocities around Mach 6-7 give a thickness of 6 mm for the canards and 8 mm for the fins. A more accurate estimation for the necessary thickness can be completed using the Theodorsen method, which accounts for supersonic velocities [45]. Although an attempt was made, it was not possible to find this value within the DSE timeframe.

$$V_f = \frac{a \cdot S}{\frac{p}{p_0} \cdot \frac{\lambda+1}{2} \cdot \frac{39.3 \cdot AR^3}{\left(\frac{t}{c}\right)^3 (AR+2)}} \tag{4.51}$$

4.4.2.3 Overview of Control Surface Geometry

This paragraph shows the final geometry of the fins and canards. Afterwards, a rough calculation of the lift that the canards supply for further calculations. For this, linearized supersonic theory is used, which is applicable at angles of attack up to 10 deg [43].

Table 4.15: *Final Geometry for Control Surfaces*

Control surface	**Location** $[m]$	**Root chord** $[m]$	**Tip Chord** $[m]$	**Height** $[m]$	**Thickness** $[mm]$	**Number**
Canard	1.35	0.15	0	0.10	6	4
Tail fin	5.17	0.35	0.15	0.20	8	4

Next, the lift coefficient for the canards was calculated in order to get an indication for the torque on the actuators and the lift the canards can provide. The assumptions for this calculation are as follows [43]:

- Small angles of attack ($\alpha < 10\,\text{deg}$)
- 3D lift coefficient is assumed to be equal to 2D lift coefficient
- Thin airfoil, flat plate assumed

Finding the 2D-lift coefficient using Equations 4.52 and 4.53 [43]. For M<1:

$$C_l = \frac{4\alpha}{\sqrt{1 - M^2}} \tag{4.52}$$

For M>1:

$$C_l = \frac{4\alpha}{\sqrt{M^2 - 1}} \tag{4.53}$$

Then calculating the lift with Equation 4.54.

$$L = \frac{1}{2} C_l \rho (Ma)^2 S \tag{4.54}$$

This results in a graph showing the lift at different angles of attack for varying Mach numbers for one canard. As seen in Figure 4.20. The shape is expected, as the density also reduces steeply with increasing Mach number.

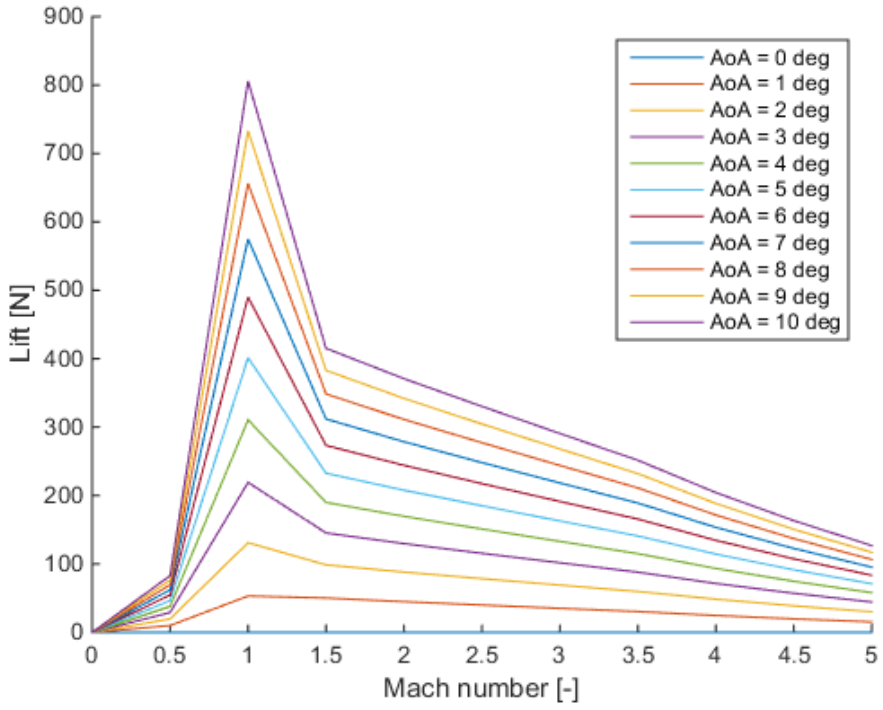

Figure 4.20: *Lift Generated by One Canard at Varying Angle of Attack and Mach Number*

The actuator will be assumed to be at 0.6 of the root chord from the front of the canard, this is because the hinge line should be in front of the center of pressure but still be as close as possible to it in order to reduce torque on the actuator. The torsion working on the actuator can then be calculated by taking the arm of

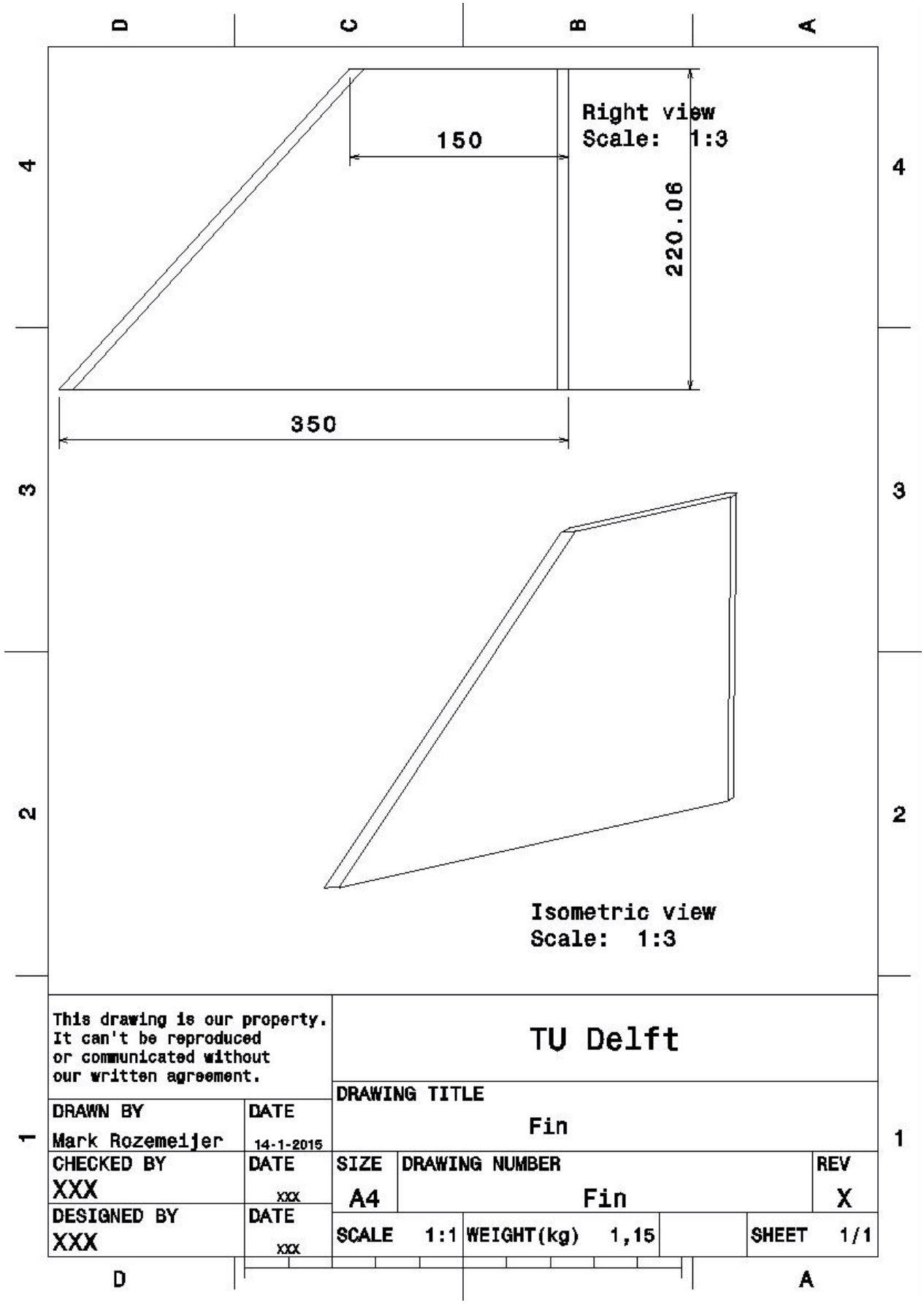

Figure 4.18: Fin Geometry

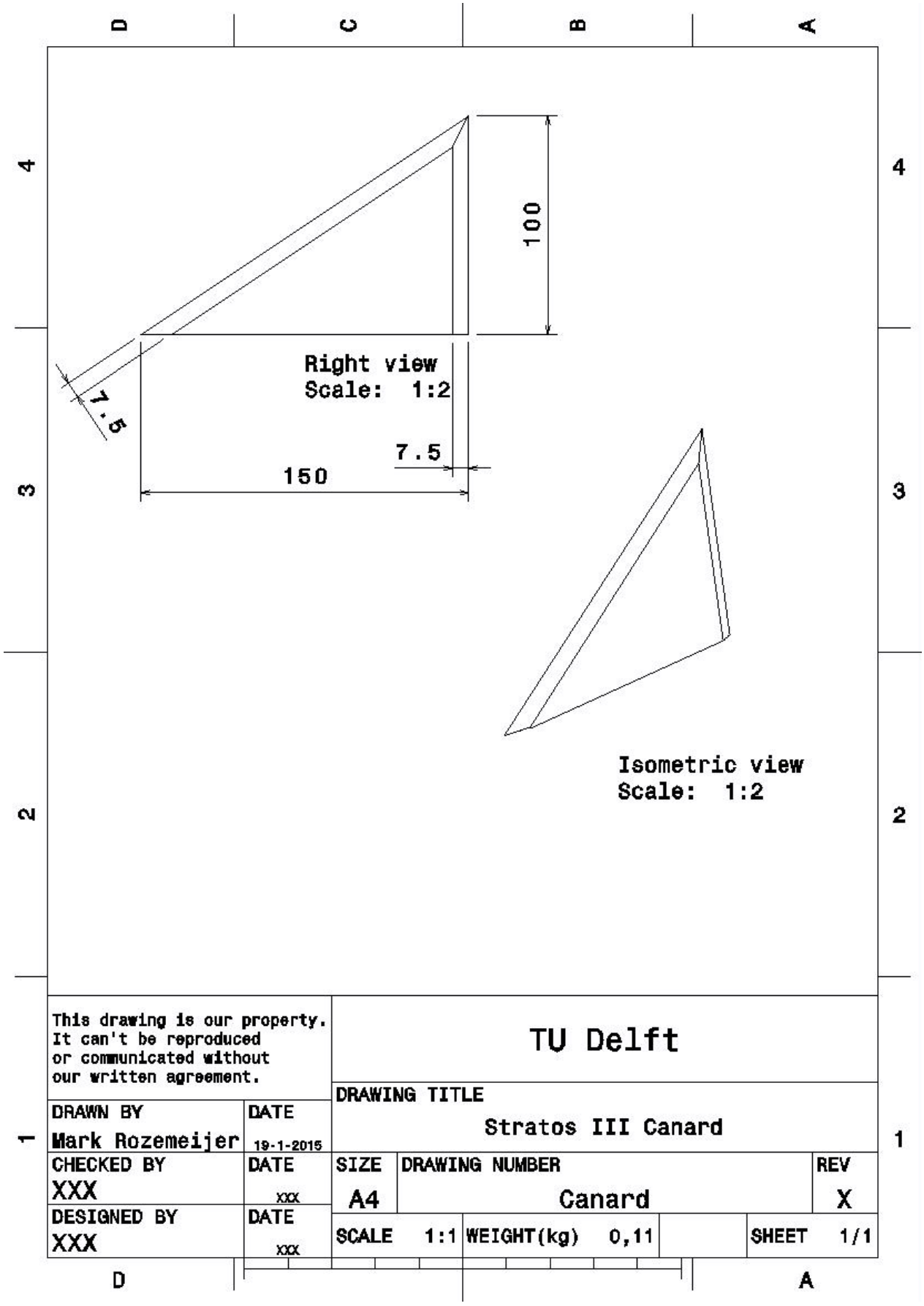

Figure 4.19: Canard Geometry

the lift to the hinge line of the canard. The subsonic MAC is given in Equation 4.55, where λ is the taper. Where the mean aerodynamic chord for supersonic situations is assumed to be at 11 % distance from the subsonic location of mean aerodynamic chord [40]. The maximum lift occurs at a subsonic velocity, thus the subsonic MAC is used. Once the maximum torsion is found, it can be used to select a set of actuators.

$$x_{mac_{sub}} = \frac{2}{3} c_r \frac{(1 + \lambda + \lambda^2)}{1 + \lambda} = 0.67 c_r \tag{4.55}$$

$$T_{max} = (x_{mac_{sub}} - 0.6 c_r) L = 4.5 Nm \tag{4.56}$$

As this is only a rough estimation, the selection for the actuators can only be completed after a more detailed supersonic analysis has been completed after which a similar computation for torque must be completed.

4.4.2.4 Canard Sizing Sensitivity Analysis

Canard design was developed with a safety factor of 25% when calculating its geometric properties to counter the possibility of flutter. The overall active canard control system effectiveness is, at this stage, only theoretical. Based on the subsonic results of the active control system designed by DARE, it is known that altitude can be increased by up to 20% through the use of active control [4]. However, it's efficiency in transonic and supersonic flow is yet unknown. For this reason, design, development, and testing of the active control system will need to be one of the preliminary projects completed during the early development stages of Stratos III.

4.4.3 Rocket Stability Sensitivity Analysis

The primary element which needs a sensitivity analysis is the stability of the rocket. The influence on the static margin, which should stay between 1-2 is dependent on several elements:

- Oxidizer tank length
- Oxidizer burn time
- The mass budgets for each separate system
- Control surface size

Increasing the oxidizer tank length and burn time would lead to a larger shift in center of gravity and would make need for larger control surfaces for stability. Furthermore, the same holds for different mass budgets for the subsystems. After each subsystem changes their mass, an iteration is needed on the control surface sizing.

Another element which needs sensitivity analysis is the torque acting on the canards. The factors influencing the torque on the canard are:

- Mean aerodynamic chord location
- Hinge line location of actuator
- Canard surface area

Increasing the arm by either changing the hinge line location of the actuator or a shift in MAC, will cause a larger torque on the actuator, resulting in higher specifications for the actuator. Furthermore, increasing the surface area of the canard will increase lift and also result in a higher torque.

4.4.4 Mass and Cost Budget

Table 4.16: *Mass and Cost Budget of ADCS*

Section	Item	Quantity	Mass $[kg]$	Power $[W]$	Total Cost [€]
Sensors	GPS	1	0.05	2	500
Sensors	Sun sensor	1	0.1	1	20
Sensors	6-DOF IMU	1	0.3	1	150
Sensors	Magnetometer	3	0.05	0.5	20
Sensors	Altimeter	1	0.05	0.5	20
Sensors	Structure	-	2.0	-	30
Sensors	Other	-	2.0	-	50
Data handling	Flight computer	1	0.1	3	80
Data handling	Heat sinks & fans	1	0.5	1	20
Data handling	Structure	-	1.0	-	20
Active control	Actuators	4	6.0	154	500
Active control	Fins & Canards	4	5.2	-	80

4.5 Power

The Power subsystem delivers the required electricity to every subsystem. The power subsystem is sized according to the power required by the different subsystems and the available COTS technology.

4.5.1 Power Budget

The power budget for the different subsystems of the Stratos III is shown in Table 4.17. This provides the baseline from which the batteries can be sized. It should be noted that the power budget is an estimation and the most accurate way of determining the required number of batteries and their capacity is to build and test a model or the rocket itself. This is because the batteries are cheap and light compared to the rest of the rocket and a change in the type of battery will not significantly influence the whole design. Moreover, the power required for the FTS is not included because that system is a stand-alone one.

Table 4.17: *Power Budget of Each Subsystem*

Subsystem	Power $[W]$	Time $[s]$	Energy $[mWh]$
ADCS	160	150	6670
Communication	4	810	900
Propulsion	105	60	1750
Recovery	2	1	0.6
Total	271	1021	9320

4.5.2 Battery Selection

The electronic components can be powered by either primary or secondary batteries. The electrochemical reaction in primary batteries is not reversible and this makes them not rechargeable. Secondary batteries, on the other hand, are rechargeable. The average unit price of primary batteries is usually lower than that of secondary batteries. However, throughout the Stratos III project, the electronic components will have to be repeatedly tested and verified and this is why rechargeable batteries prove to be more cost effective. Furthermore, it would be more beneficial for Stratos III to use secondary batteries for sustainability reasons, since one the key requirements of the Stratos III mission is to be sustainable.

The most widely used type of secondary batteries for sounding rockets is the lithium-ion polymer battery, or LiPo in short, which is also used in the Stratos II. LiPo batteries are advantageous over other batteries in a number of ways. Firstly, they are light-weighted, which is important for maximum performance of the rocket. Secondly, they have a high energy density, which means they can provide more energy than other batteries with the same size. Thirdly, they have no memory effect which means that they can be recharged many times without the battery capacity being significantly influenced. Finally, when damaged, they have less chances of exploding when compared with other batteries. Table 4.18 describes the battery specifications intended for the Stratos III.

Table 4.18: *Specifications of the Battery*

Parameter	Battery type 1	Battery type 2
Seller	StefansLipoShop GmbH	
Battery type	Lithium-ion Polymer	
Voltage $[V]$	7.4	11.1
Capacity $[mAh]$	800	1000
Mass/unit $[kg]$	0.051	0.099
Price/unit	€6.99	€11.99

4.5.3 Architecture

The Power subsystem is responsible for providing the required power to the various subsystems. Figures 4.21 and 4.22 give a preliminary overview of the electric circuitry of the rocket. A decentralized system is used to distribute power because of reduced complexity and mainly because of redundancy. If one of the batteries fails, only one component will stop functioning but since most components include redundancies, the power subsystem as a whole will not be affected.

Therefore, the Power subsystem can be considered to be robust because of the technological readiness level, low complexity and redundancies. In Figure 4.21, it can be seen that there are measurements A and B as well as actuations A and B. These represent two identical electronic boards which perform the same functions and are used in parallel both as a means of data validation and safety measure, and they are considered as a 'voting' system. Measurement A is compared with measurement B and if both are within a predefined margin, the required action is taken. If the measurements differ, the main control unit compares them with predicted values and then decides on the required action. It should be noted that, due to the high data rate required for the active control system, the measurements and actuators should be put in one board for faster data access.

Moreover, each battery powers a separate board. It is useful to include components that monitor the status of the battery such as voltage. The current going through each board can also be determined and hence, the power that each board uses can be easily found. In establishing the required battery capacity, one of the best ways is to build a prototype of the electronics module and test it with respect to the processes it will perform during flight. The battery state can be checked at the end of the test and a stipulation can be made that the battery is not allowed to be drained by more than a specified amount of its fully-charged state. This is the preferred way to optimize the battery selection by choosing the battery that just fulfils the drainage condition.

The rocket will be subjected to a number of conditions such as gravitational forces, vibrations, and temperature and pressure gradients. While some of the rocket status data such as altitude and GPS coordinates will be downlinked to the ground station, all the data will be stored inside the rocket in memory cards. These memory cards are kept in casings which are able to withstand shocks, high temperature variations and sea water immersion. The retrieval of the memory cards is of great importance to the mission because if the apogee altitude cannot be confirmed, the record cannot be validated.

As for the batteries, they are stacked between plates to provide structural compression so that a loss in pressure due to altitude will not severely influence their performance. A problem that the Stratos II experienced was the recharging of batteries after testing. The actual problem arises because the batteries are located inside the nosecone or in the section between the oxidizer tank and the combustion chamber and every time they need to be recharged, the particular section needs to be disassembled, the batteries taken out, recharged, put back in and the section needs to be reassembled. This process is tedious and time-consuming but unfortunately, there is not a really feasible solution.

For redundancy and simplicity reasons, the power subsystem has been chosen to be decentralized. A centralized power distribution with one battery would have helped greatly with logistics but there would have been the problem of voltage regulation which would have increased the complexity. For the decentralized system, it is still possible to have all the individual batteries stacked up together and put in two key locations. However, for easy access to the batteries, a small hatch can be made but this would have repercussions on the structure of the rocket. One addition can be the use of two or even three battery stacks so that when one is in the rocket the other can be charged. Hence, to speed up the change of batteries, the charged stack can be readily exchanged for the one which was in the rocket.

A noteworthy point is that the temperature between the oxidizer tank and the combustion chamber drops rapidly and becomes very low once the main valve is open and Nytrox flows through it. At low temperatures, the internal resistance of the batteries increase and this reduces their energy and power densities [46], which implies that their performance is reduced. Therefore, the batteries should be wrapped in thermal insulation so that they can still perform and not negatively influence the mission. During the testing phase, the battery

performance can be determined in those cold conditions and the degree of insulation can be chosen. Moreover, if the battery still shows a certain percentage decrease in performance, they can be re-sized to compensate for the losses.

In Figure 4.22, it can be seen that there are two military-style launch boxes, one at the control point and one on the launch pad. When activated simultaneously, they provide the ignition sequence start signals. The external and internal engine control units are connected to the launch box which is on the launch pad. The external engine control unit operates the filling up of the oxidizer tank and also provides the igniter output signal to start the pyrotechnics. Pressure and temperature sensors take readings of the oxidizer tank and the combustion chamber and are connected to the internal engine control unit.

While the rocket is on the launch pad, the electronics inside will be powered externally through an umbilical cord until seconds before launch. The umbilical cord also transfers data from the rocket to the launch box and vice-versa. Thus, the internal batteries are not drained before the rocket goes airborne. At lift-off, the umbilical cord breaks and separates from the rocket and then, a simple diode system switches to internal power. Before lift-off, the decoupler system also disconnects the oxidizer tank from the external oxidizer supply. For safety reasons, some LED lights are placed on the rocket and these are switched on when the rocket is in arm mode.

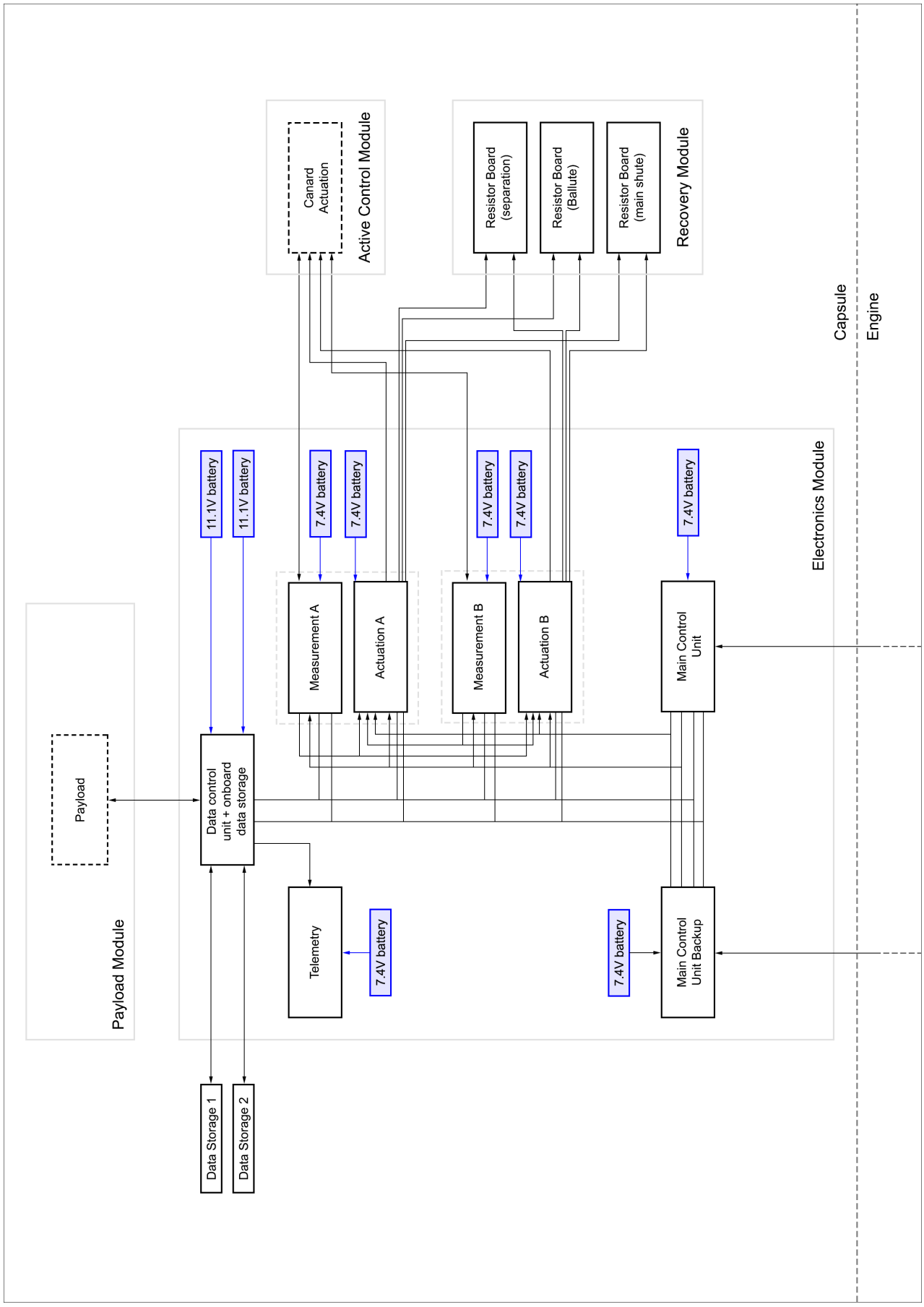

Figure 4.21: *Stratos III Electrical Block Diagram [Part I]*

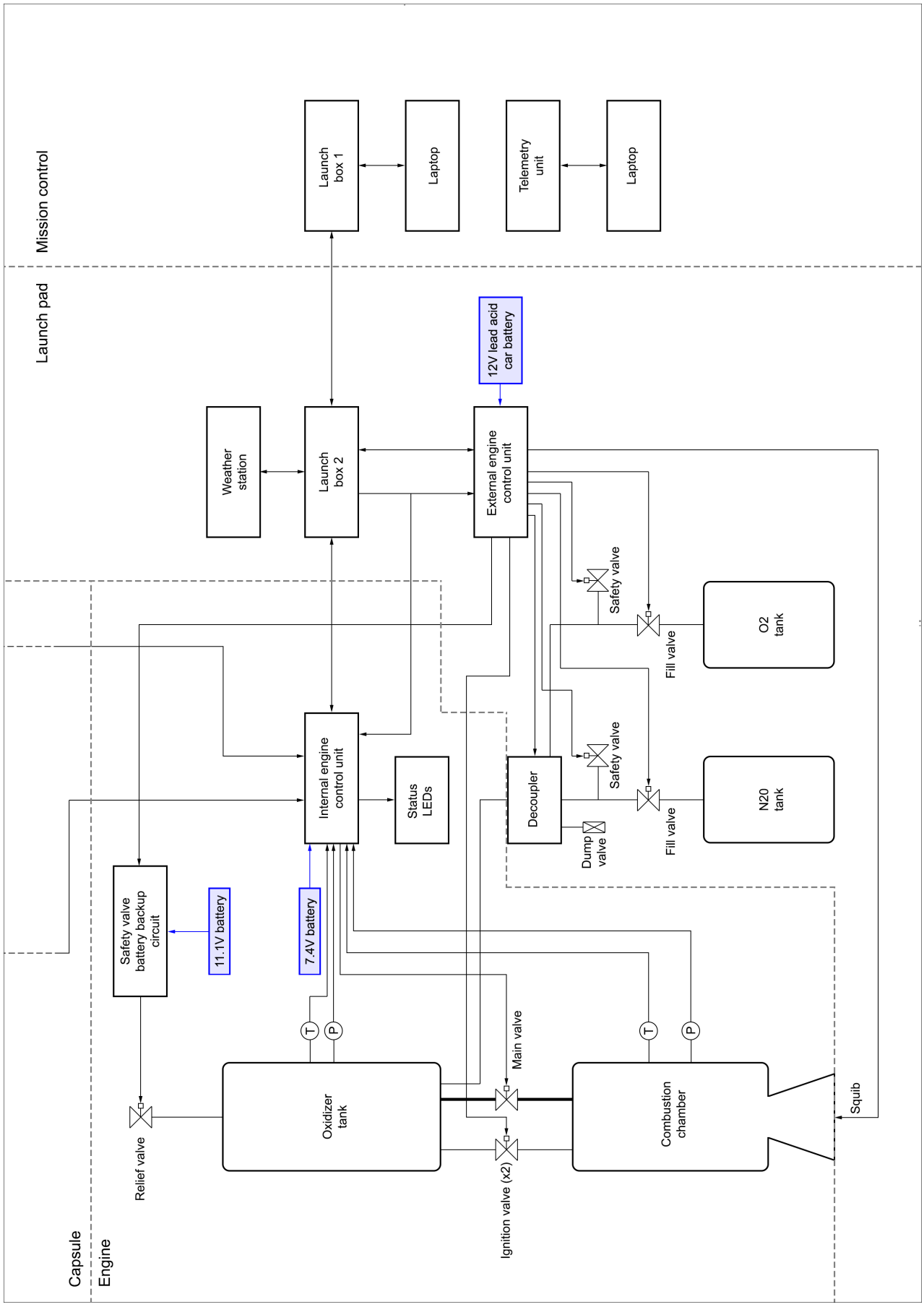

Figure 4.22: *Stratos III Electrical Block Diagram [Part II]*

4.5.4 Sensitivity Analysis

The Power subsystem has been designed conservatively. The power requirement for each component was determined first, then the price and the cost estimates were calculated for each battery type. These estimates are quite an overshoot, because they were determined after considering several aspects: redundancy, performance and functional environment. For Stratos II, two batteries are used for each component for redundancy. Also, the batteries are not allowed to discharge more than a certain amount to ensure constant performance. As the battery discharges the voltage drops, and this can negatively influence the performance of the battery. Finally, the battery usually performs less than intended when exposed to extreme conditions like heat or cold. Therefore it is wise to aim for oversize instead of designing the Power subsystem exactly according to the requirement. As a result, the mass of the battery stated in Table 4.19 with the oversize is about eight times the original estimate. The reason why the batteries can be oversized is that the increased mass is far less than 1% of the total mass of the rocket. Therefore this will have minimum effect on the thrust performance.

4.5.5 Mass and Cost Budget

Two types of batteries are chosen because of the different voltages and currents at which different components function. StefansLiposhop GmbH is listed as seller because Stratos II acquired its batteries from them and so, there is already a liaison between DARE and that particular seller. The mass budget and the cost estimate of the Power subsystem is shown in Table 4.19. The mass of the cabling as well as its cost have been presented as an estimate. The supporting structure represents additional materials which may be used, for instance, to hold the batteries together or insulation of the cables or batteries at certain points.

Table 4.19: *Mass and Cost Budget of Power Subsystem*

Component	**Mass** $[kg]$	**Cost** [€]
Batteries	0.7	70
Cabling	0.5	20
Supporting structure	0.5	30
Total	1.7	120

From Section 4.5.1 which gave the power budget for each subsystem, the batteries have been sized. The exact number of batteries depends on the architecture and the degree of redundancy that is required. At this stage and especially at the system integration level, the mass of the batteries is more important than the number of batteries. Some estimations can be given about other parameters. From StefansLipoShop GmbH, the mass per capacity of the batteries rated at 7.4 V and 11.1 V are about 0.07 g/mAh and 0.1 g/mAh respectively. The price per battery capacity is about 1.2 $cents/mAh$. Using a conservative safety factor as was be explained in Section 4.5.3 and redundancies, the total mass and the cost of the batteries can be estimated to be 0.7 kg and €70.

4.6 Communications

Communications is the subsystem that allows the rocket to send back telemetry to the ground regarding its orientation, altitude, and health. This allows the ground to make track the rockets status and allows them to verify the record of 120 km.

4.6.1 Antenna Sizing

The rocket is required to provide communication with the ground station during most flight stages. The design is approached with low complexity and high technological readiness level in mind. The communication system of the Stratos III is heavily based on that of the Stratos II and despite the unsuccessful launch of the latter, it is assumed that the communication system would have delivered the necessary performance. The following assumptions are considered for the design:

- The downlink rate is 20 $kbit/s$
- The downlink frequency is 800 MHz
- The antenna efficiency is 0.2
- The antenna is omnidirectional and has a gain of 1
- The receiver is a parabolic reflector with a diameter of 1 m

- The receiver dish has an efficiency of 0.95
- The noise temperature is 290 K
- The atmospheric loss is 5 dB
- The losses due to the radio transparency of the rocket is 10 dB
- The receiver and transmitter losses amount to 2 dB

The assumptions are of conservative nature without significantly leading to an over-designing of the communication system. The downlink rate of 20 $kbit/s$ is twice as much as what was used for the Stratos II and this allows the transfer of more data. The atmospheric loss is 5 dB and this accounts for the temperature, pressure, humidity and wind. The antenna is located inside the nosecone and the losses due to the radio transparency of the glass-fiber and the rocket itself is estimated to be 10 dB. Finally, the receiver and transmitter losses amount to 1 dB. Using the script that was written to compute the parameters of the antenna, at an altitude of 120 km and a transmit power of 1 W, the received power at the ground station is -94 dBW and the signal-to-noise ratio (SNR) is 18.5 dB. The received power and SNR are only about 10% less than at an altitude of 50 km and hence, it is justified that the Stratos III communication system can be based on its predecessor. Figure 4.23 shows the received power and the SNR as a function of the altitude.

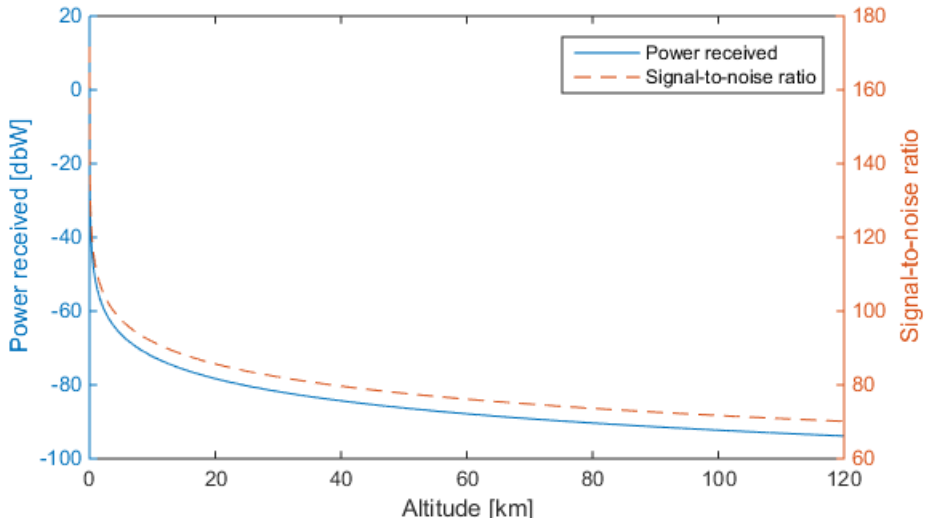

Figure 4.23: *Received Power and SNR as a Function of Altitude*

The radio antenna itself is a simple monopole one which consists of a straight rod-shaped conductor which is mounted perpendicularly on a ground plane. The size of the antenna depends on the wavelength of the radio waves it receives. The most common way of sizing a monopole antenna involves the quarter-wave principle which means that the antenna is approximately 1/4 the size of the wavelength of the radio waves. The antenna size is calculated using Equation 4.57.

$$l = \frac{1}{4}\lambda = \frac{1}{4}\frac{c}{f} \tag{4.57}$$

A radio wave frequency of 800 MHz yields an antenna size of 9.4 cm. The antenna size decreases as the frequency used increases. A smaller antenna has a smaller mass and is logistically easier to fit inside the nosecone and so, a high frequency is advantageous. It should be noted that Stratos II used a frequency of 433 MHz for communication which resulted in an antenna length of 17.3 cm. However, INTA uses a frequency range of 400 to 550 MHz for the FTS and this caused the communication antenna to experience interference problems.

Similar to the Stratos II, the telemetry receivers can be placed at two different locations. The secondary station can be 5 km from the launch pad with the goal of receiving the first few seconds of data after lift-off and it also acts as a backup to the primary station. The primary location can be located about 50 km from the launch site to allow for a direct line of sight and a stable link of the antenna located in the nosecone up to the apogee at 120 km. It is not suitable to have the telemetry receivers close to the launch site because the transmitter antenna points upwards along the rocket's longitudinal axis and the radiation pattern is null along that axis.

4.6.2 Thermal Control

One of the main problems caused by the communication subsystem is the heat generated. The antenna has an efficiency of about 20% and the rest of the energy is lost as heat. As a result, a lot of heat can accumulate in the nosecone and this has to be dealt with. Otherwise, some components such as batteries and printed circuit boards (PCBs), which have to be maintained within a specific temperature range, run the risk of loss of performance or even failure.

One of the simplest ways of maintaining an environment in which the electronic equipment can function is to install heat exchangers. The PCBs are stacked in towers and these towers can be cooled by fan-cooled heat sinks. However, at an altitude of only 30 km, the air pressure is about 1% of that at sea level and at higher altitudes, the pressure is even less. This means that if the nosecone is not pressurized, there will be almost no air inside it and a cooling system based on air flow will be useless. Therefore it needs to be pressurized.

Furthermore, after burnout, which occurs at an altitude of about 20 km, the rocket coasts up to the apogee at 120 km and then falls back to Earth in the recovery phase. During the coasting phase, the rocket experiences weightlessness and so, the heat will not by itself undergo convection. The Stratos II had two fans blowing inside pressurized nosecone to create a convection current to dissipate the heat produced. Stratos III will use two fans as these are light and cheap.

One of the main heat generators is the amplifier for the antenna and this can be counteracted by connecting it with a fin heat sink. This usually consists of a plate as a base and pins or straight flat surfaces which extend from the base to increase the surface area and hence, the efficiency. The heat sink is made of a high thermal conductivity material such as copper or aluminum. Copper has about twice the thermal conductivity of aluminum and has faster and more efficient heat absorption. However, it is three times as heavy and more expensive. This is why aluminum is chosen since it is also one of the most common heat sink materials.

Based on the Stratos II, an aluminum heat sink weighing 0.3 kg is enough to dissipate the heat generated from the amplifier. Thermal grease is a thermally conductive adhesive that improves the performance of the heat sink by filling the air gaps between the heat sink and the component to be cooled. When combined with the thermal grease, the heat sink provides the necessary performance and makes the the cooling system robust. However, the best way to optimize the cooling system is to build a prototype, test it, and iterate the design. The two fans, the fin heat sink and the thermal grease weigh about 0.5 kg and are powered using the same battery that is connected to the PCBs or the antenna.

4.6.3 Sensitivity Analysis

The assumptions that have been made in the design of the communication subsystem are conservative without leading to an over-design. The downlink rate accounts for about 20% more than the predicted one. The satellite dish size and efficiency at the ground station are likely to be higher than what was assumed. Moreover, the losses have been overestimated by about 50% for a worst-case scenario. Eventually, the parameters that influence the rocket during integration are the mass and the power consumed. Since the mass of the communication subsystem is less than 1% of the rocket dry mass, optimizing or scaling up the system will not significantly influence the design of the whole rocket.

4.6.4 Mass and Cost Budget

The PCBs are designed and built by DARE. The heat sinks and fans are relatively light and cheap and can be easily purchased in stores selling computer parts. The antenna is essentially a 9.4 cm rod made of copper because of its high electrical conductivity. Aluminum is an alternative material that can be used because it is lighter and cheaper but has lower electrical conductivity than copper. Table 4.20 shows the mass and cost estimate of the communication subsystem.

Table 4.20: *Mass and Cost Budget of Communication Subsystem*

Component	**Mass** $[kg]$	**Power** $[W]$	**Cost** [€]
Transmitter	0.2	1	50
Heat sink	0.3	-	30
Fans	0.2	3	30
Total	0.8	4	110

4.7 Payload

The top-level payload mass requirement for Stratos III is 15 kg. No requirements were given considering the shape or volume. In order to facilitate a convenient integration of the payload into the rocket it is preferable to use some commonly used standard. The CubeSat standard [47] was used in the Stratos II rocket and will also work for Stratos III.

Assuming a mass of 1.33 kg per CubeSat unit a 15 kg payload corresponds to a volume of 12 L consisting of 10 cm cubes. Because the diameter of the rocket is designed to be 0.26 cm, two stacks of CubeSats can be placed next to each other resulting in a payload section length of the rocket of 0.6 m. Around the CubeSat stacks is enough space for wiring and/or antennas.

The Stratos III rocket does in principle not provide any other resources to the payload bay other than the space. However, there is space available to place experiments with custom sizes, or place a power system for the payload if needed.

4.8 Recovery

The Recovery subsystem is responsible for the part of the flight from apogee to the ground. It consists of a two-stage inflatable decelerator configuration. A ballute will stabilize the descent and slow the rocket down enough for the main parachute to open reliably. The main parachute will then slow down the rocket to its final impact velocity. First the approach of design will be explained, then different configurations will be elaborated on and finally every step in the detailed design will be shown and explained.

4.8.1 Approach

In order to reach the final design of the entire Recovery subsystem a flow chart is followed, this chart can be found in Figure 4.24.

The input of the flowchart given in Figure 4.24 is the dry mass or recoverable mass and the maximum impact velocity. Based upon these parameters the main parachute is sized and designed. Then the ballute is sized based upon the velocity and altitude the main parachute will be opened. When the main parachute and the ballute have been sized, the envelope of the Recovery subsystem generated.

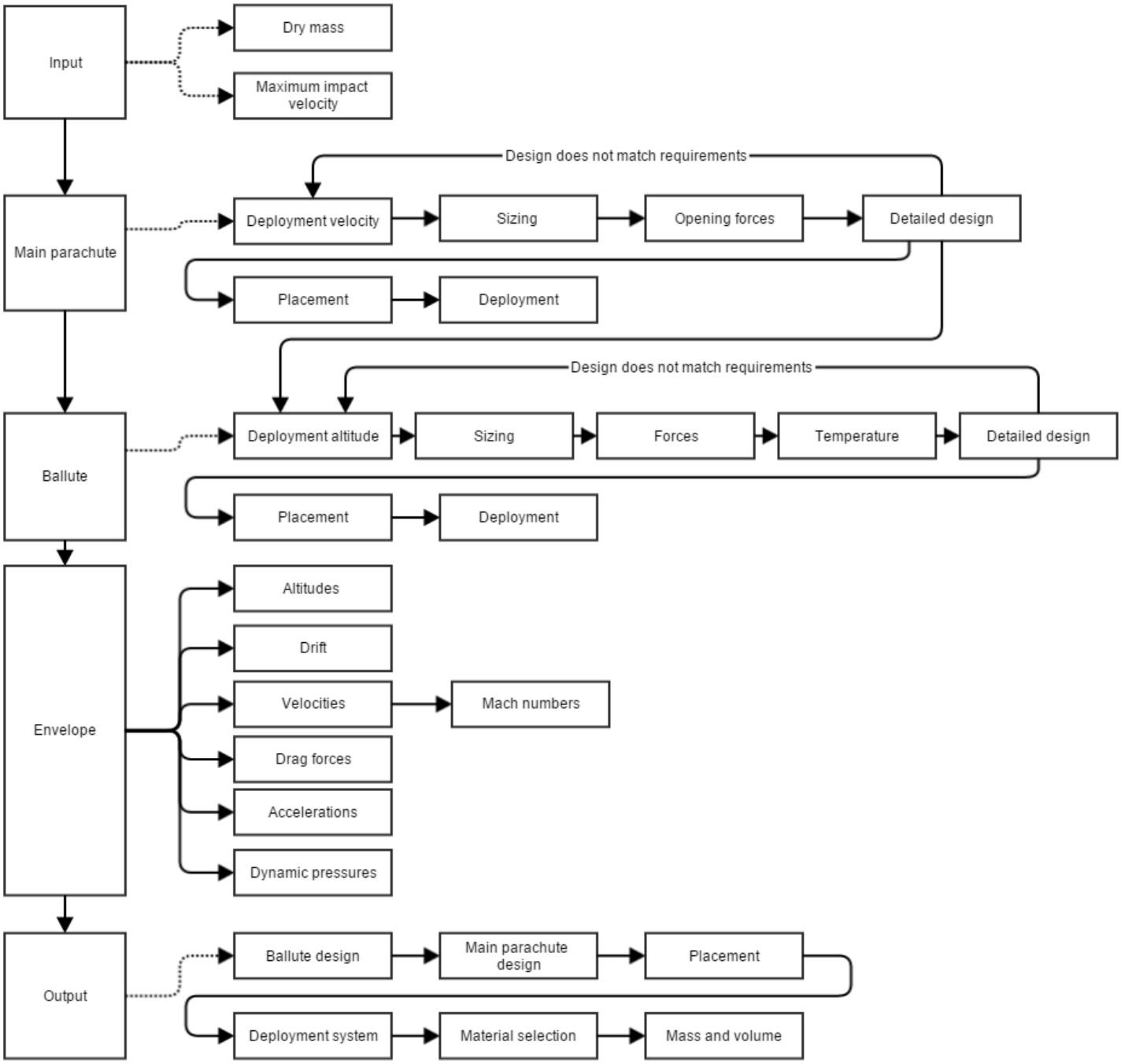

Figure 4.24: *Recovery Subsystem Design Flow Chart*

4.8.2 Configurations

The main considerations in the Recovery subsystem are the ballute and main parachute placement inside the rocket. Two configurations have been considered: A nose-down re-entry attitude and a nose-up re-entry attitude.

4.8.2.1 Nose-down Re-entry Attitude

It is favorable to have the rocket re-enter the atmosphere in a nose-down attitude. This is because of pendular and transverse oscillations, and the severe heating of re-entry can be absorbed by the nosecone. Two options were considered to ensure a nose-down re-entry:

The ballute will be deployed from as close to the nozzle as possible It is likely that there is room for the ballute just below the oxidizer tank. This will result in changing the shape of the oxidizer feed system and drilling holes near the engine. Fuselage separation here is too complex, so this means that the ballute will have to be deployed sideways. There will not be enough room for both the ballute and main parachute below the oxidizer tank, so the main parachute will be stored in the capsule section. The ballute can be used to pull out the main parachute or another deployment system can be installed.

The ballute will be deployed from just below the nosecone A line is already in place, attached onto or into a groove in the side of the rocket, connecting the ballute to an explosive bolt on the rear of the rocket. Main parachute deployment is then initiated by ejecting the explosive bolt, which results in the ballute pulling out the main parachute and flipping the rocket into a tail-first attitude. The advantages of this option are that there is only one mortar required and no drogue gun, the whole Recovery subsystem is lighter and difficult engineering below the oxidizer tank is not necessary.

4.8.2.2 Nose-up Re-entry Attitude

Fuselage separation is a more conventional configuration of recovery. Both the ballute and the main parachute are stored in the capsule. At first-stage deployment the nosecone separates from the main fuselage and the ballute inflates. Both the fuselage and nosecone are attached to the ballute. The length of the risers are chosen such that the nosecone and fuselage cannot collide. When the rocket has decelerated enough the main parachute will be deployed from the nosecone. The advantages of this configuration is that after the engine hits the water, the capsule will rapidly slow down before it hits the water and that this is a proven design. The disadvantages of this configuration are that the rocket will be in a nose-up attitude during reentry, which can introduce heavy oscillations, and the separation system of the nosecone is complex and a weak point.

4.8.3 Chosen Re-entry Attitude

The nose-down re-entry attitude with ballute and main parachute deployment from below the nosecone has been selected. The following detailed design will be in occurrence with this configuration. First the main parachute will be selected and sized, after which the ballute can be sized. The forces and stresses on all stages will be calculated and materials can be selected. It should be noted that when changing the configuration the sizing and material selection will for a large part stay the same. Only the deployment systems need to be completely revised. A figure of the different stages can be seen in Figure 4.25.

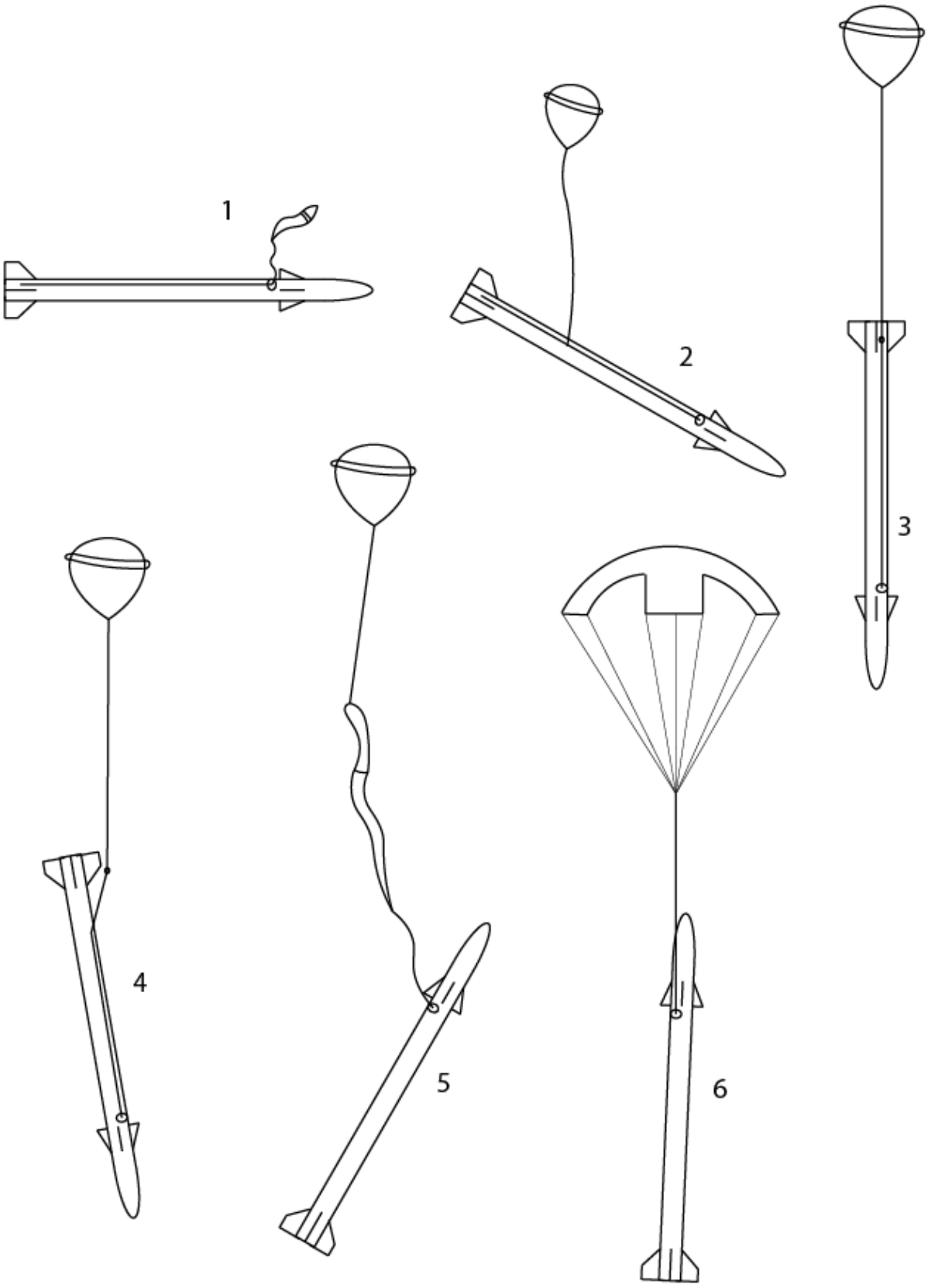

Figure 4.25: *All Recovery Stages*

4.8.4 Main Parachute

The following sections will discuss the shape selection and sizing, forces and material selection of the main parachute.

Selection and sizing: The main parachute system has the following requirements.

- The main parachute system shall be able to recover a rocket with a dry mass of 140 kg
- The main parachute system shall be able to deploy at velocities up to 75 m/s
- The main parachute system shall be able to deploy at an altitude of down to 2000 m
- The main parachute system shall ensure an impact velocity of no more than 20 m/s for the engine section
- The main parachute system shall ensure an impact velocity of no more than 15 m/s for the capsule section
- The main parachute system shall have a mass no more than 4 kg
- The stored main parachute system shall fit in a volume of 0.01 m^3
- The diameter of the stored main parachute system shall be no more than 0.25 m

As a main parachute the annular and cross type parachutes are considered. The main advantage of a cross the parachute is the experience within DARE, the Stratos II will also fly a cross parachute, and a low opening force coefficient. The annular parachute has as major advantages the high drag coefficient and a high shape efficiencies. Both parachutes are compared in Table 4.21 [48]. A cross shaped parachute has been selected, mainly because of DARE's experience with cross shaped parachutes.

Table 4.21: *Different Options for the Main Parachute*

Parachute	C_{D0}	C_x	D_c/D_0	D_p/D_0
Annular	0.85-0.95	1.4	1.04	0.94
Cross	0.60-0.85	1.1-1.2	1.15-1.19	0.66 - 0.72

The forebody, in this case Stratos III, produces a wake that effects the parachute. According to Knacke [48] the parachute should be ejected to a distance of preferably six times the forebody diameter into good airflow behind the forebody. This sets the minimum suspension lines and riser length combined. The length of the suspension lines also affects the parachute effectiveness. Short suspension lines will result in a parachute that will not fully inflate. The paramter to be considered is the ratio suspension lines length to parachute diameter L_e/D_0. A ratio of at least 1 should be taken. The riser length should be long enough to extend beyond the Stratos III nosecone. A length of 2 m should be sufficient. The required drag area $(C_DS)_0$ of the main parachute can be calculated using the equation below. Because the engine and capsule are not separated the impact velocity has been set to a value of 15 m/s.

$$(C_DS)_0 = \frac{2mg_0}{{V_i}^2\rho_0} \tag{4.58}$$

Using a drag coefficient of 0.70 for a cross shaped parachute the parachute surface area can easily be calculated and the nominal and inflated diameters can be found using the equation below, where the diameter ratio has been assumed to be 0.69, from Table 4.21. The difference between D_0 and D_p is that the D_0 is the diameter when stretching the parachute and D_p is the inflated parachute diameter.

$$D_0 = \sqrt{\frac{4S_0}{\pi}} \tag{4.59}$$

$$D_p = D_p/D_0 \cdot D_0 \tag{4.60}$$

The arm width to length ratio W/L affects the drag, stability and opening forces. A low W/L ratio produces better stability and a lower opening force coefficient, but also a lower drag coefficient. Cross parachutes have a tendency to rotate, so a shivel connecting the riser and suspension lines will be required. For simplicity a W/L ratio of 0.33 can be selected, so that the parachute basically consist of 5 squares. A higher W/L ratio should be considered in case the main parachute will make use of a reefing system. Table 4.22 summarizes the main parachute system properties.

Table 4.22: *Main Parachute Properties*

Parachute shape	C_{D0} [−]	C_x [−]	S_0 [m^2]	D_0 [m]	L_e/D_0	W_p/L_p
Cross	0.70	1.15	14	4.22	1.2	0.33-0.40

Main parachute forces: Parachute reefing allows a stepwise opening of the parachute canopy. Reefing has been found to dramatically reduce the opening forces with a factor of approximately 5. Therefore it has been decided to make use of reefing. The simplest form of reefing is slider reefing. In slide reefing an octagon or square, in case of a cross parachute, piece of cloth is attached onto the suspension lines. At deployment the slider keeps the canopy closed and prevents a high snatch force. The spreading action of the inflating canopy pushes the slider down along the suspension lines, allowing for a controlled opening of the canopy. The strength of the connection points of the slider onto the suspension lines determines the time it takes to completely disreef. The fully reefed drag area of a cross parachute can be as low as 10 % of the fully open drag area according to Knacke [48]. The force when the parachute has fully opened for the first time after disreefing is the highest. This is in accordance with the program *Recover.m*.

$$F_{or} = 0.5\rho V t^2 C_{D0} S_0 C_x X_1 0.1 \tag{4.61}$$

$$F_{odr} = 0.5\rho V t^2 C_{D0} S_0 C_x X_1 0.9 \tag{4.62}$$

The first equation corresponds to the reefed deployment and the second equation corresponds to the disreef opening force. The air density has been taken at an altitude of 2000 m and the terminal velocity is 75 m/s in order to create a limit case. The terminal velocity at disreef has been found to be 58.5 m/s. The opening force coefficient C_x is 1.15, from Table 4.21. The opening force reduction factor has been derived from Figure 4.26. Using the two canopy loadings the reduction factor has been found to be 0.73 for reefed opening and 0.28 for disreef. It should be noted that the actual maximum opening force will be lower, because the slider will increase the opening time.

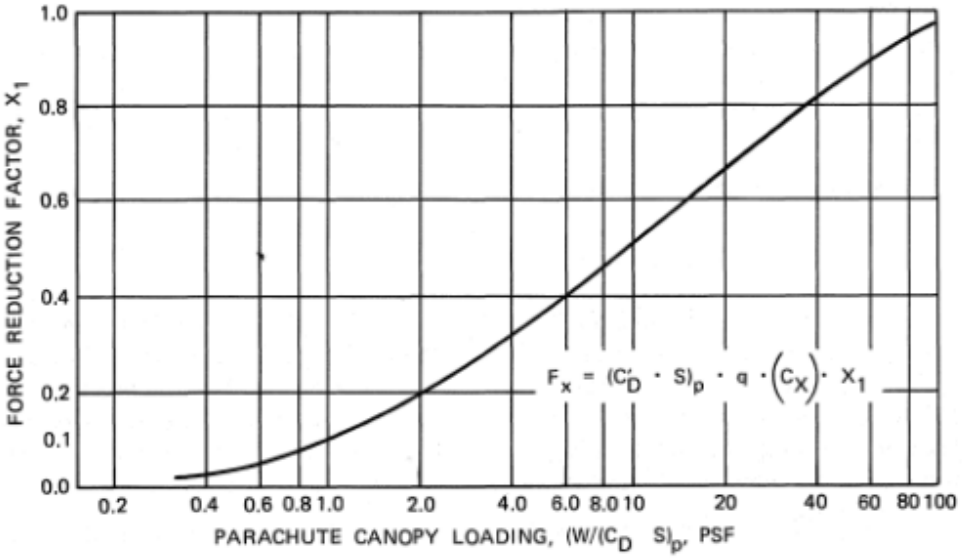

Figure 4.26: *Force Reduction Factor as a Function of Canopy Loading*

The canopy, riser, and suspension lines should be able to withstand the force resulting from Equation 4.62. It was concluded that 24 suspension lines will be enough. This number has been chosen so that the lines will not experience extraordinary high loads and thus can be made from COTS materials and are a multiplication of 8, which is easy to work with because of the cross-shape. The riser will have to be able to withstand the entire maximum loading F_o. The suspension line forces can be found by simply dividing the maximum force by the amount of suspension lines. No precise method has been developed for calculating canopy stresses. An estimation can be made by using the following equation:

$$\tau_c = \frac{F_o dr}{D_p 12} \tag{4.63}$$

Table 4.23: *Main Parachute Forces*

	Amount [−]	**Force** [N]	**Design factor** [−]	**Design Force** [N]
Canopy	1	140 [N/m]	1.85	259 [N/m]
Suspension lines	24	204	1.93	393
Riser	1	4890	2.1	10270

Now the design forces are known, materials can be chosen. When considering suspension lines nylon kern-mantle ropes referred to as 'parachute cords' are strong enough as they have breaking strengths ranging from 450 N to 3350 N. The particular rope type I has a breaking strength of close to 450 N and a diameter of 3 to 4 mm. The riser needs to be able to hold an impact force of 10 kN, as the average loading will decrease rapidly immediately after parachute opening. Dynamic ropes should therefore be considered as they reduce the peak load by elongating. Kevlar ropes are a good choice, because of their high tensile strength, but are not used in applications where shock loads are experienced. If using Kevlar ropes, they should be strong enough to be used as a static rope. A single braid Kevlar rope with a diameter of 6.35 mm can withstand a force of 30 kN. The canopy stress loading is relatively low, because of the relative large parachute size used. This means that a standard nylon ripstop cloth can be used. With good materials options selected an accurate mass budget can now be made. Some aspects like shivels, stitches and other connection points have been estimated to take up 300 g. This can be seen in Table 4.24.

Table 4.24: *Main Parachute Design Properties*

	Material	**Length** [m]	**Thickness** [mm]	**Mass** [kg]
Canopy	Ripstop nylon	15.5 [m^2]	0.1	0.77
Suspension lines	Type I parachute chord	5.07	1.85	0.21
Riser	Single braid Kevlar	2	6.35	0.060
Misc.	-	-	-	0.30
Total	-	-	-	1.34

4.8.5 Ballute

The following sections will discuss the shape and sizing, forces and material selection of the ballute.

Design and sizing: The ballute has the following requirements.

- The drogue system shall be able to slow down the rocket to at least 75 m/s at 3000 m altitude
- The drogue system shall be able to deploy at dynamic pressures of up to 3000 Pa
- The drogue system shall be able to withstand a dynamic pressure of up to 10000 Pa
- The drogue system shall have a mass no more than 9 kg
- The stored drogue system shall fit in a volume of 0.005 m^3
- The diameter of the stored drogue system shall be no more than 0.25 m

The ballute being used is the Goodyear ballute. It consists of a balloon-shaped rear part, burble fence center part, and a conical forward part. The rear part and burble fence act as a tension shell and the conical forward part carries the loads to a junction point for connection with the riser. Air inlets in front of the burble fence ram-air inflate the ballute. Air inlets will not function in vacuum conditions, because there is no dynamic pressure in space. Therefore another method of inflation should be used to initially inflate the ballute. Two options were considered: A small pressurized gas tank and an elastic burble fence. A pressurized gas tank can inflate the ballute by expelling the gas from the gas tank into the ballute. An elastic burble fence can force the ballute in the inflated shape by making use of material properties. As the dynamic pressure begins to rise, the air scoops will keep the ballute inflated. The properties of the Goodyear ballute can be seen in Table 4.25. It should be noted that the drag coefficient is related to the ballute diameter instead of the surface area. More material is therefore needed than conventional drogue parachutes.

Table 4.25: *Ballute Properties*

C_{Db} [−]	C_x [−]	D_c/D_0	D_p/D_0
0.60 - 1.20	1.05	0.51	0.51

The size of the ballute is determined using the requirements that the ballute has to be able to slow down the rocket to at least 75 m/s at an altitude of 3000 m. The drag area can then be calculated using the following equation:

$$(C_D D)_b = \frac{2mg_0}{{V_t}^2 \rho} \tag{4.64}$$

Then taking into account that the drag coefficient is 0.6 at subsonic airspeeds, the ballute diameter can easily be calculated.

$$D_b = \frac{(C_D D)_p}{C_{Dp}} \tag{4.65}$$

The exact geometry of the ballute has been taken from Supersonic Parachutes [49]. This can be seen in Figure 4.27.The results have been summarized in Table 4.25. The volume and surface area have been calculated using a Matlab program. The values in the table include the burble fence, but not the air inlets. Two images of the Matlab figure can be seen in Figures 4.28a and 4.28b. It should be noted that the symbol D_c in Figure 4.27 is in this report being referred to as D_b.

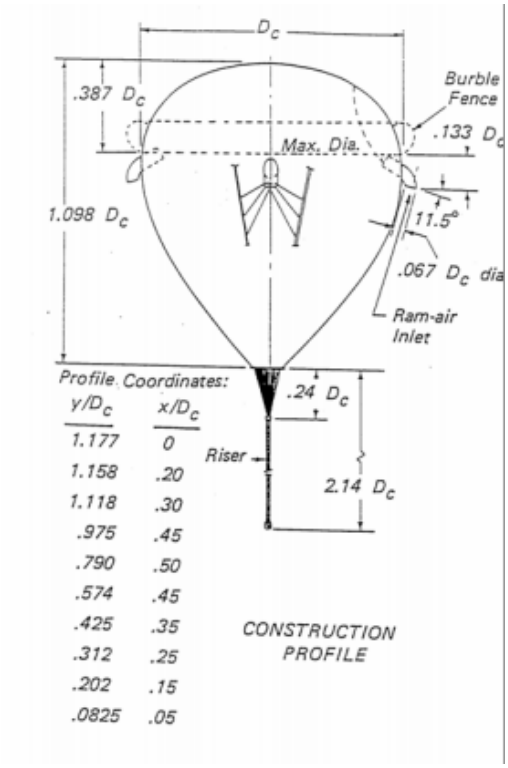

Figure 4.27: *Ballute Geometry*

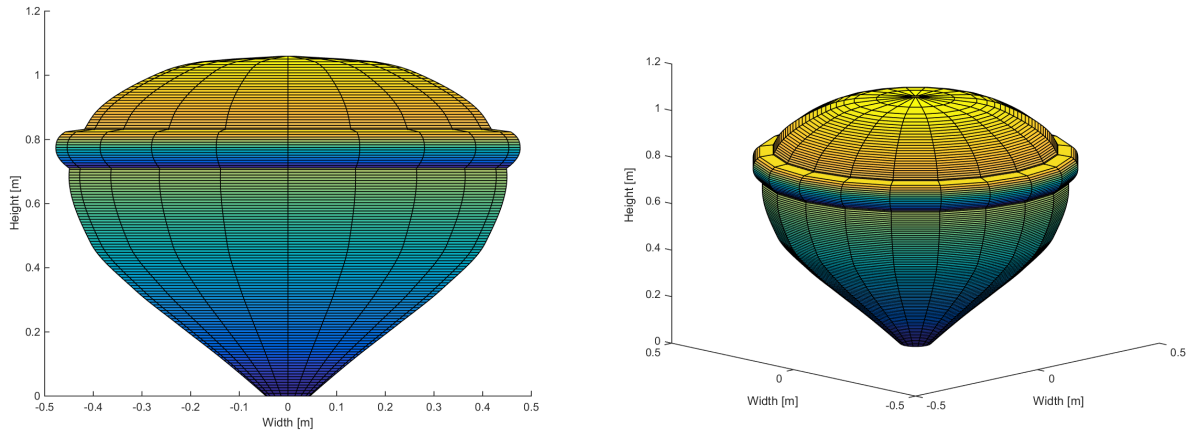

(a) 2D Ballute Matlab profile *(b) 3D Ballute Matlab profile*

Figure 4.28: *Geometric Profile of the Ballute*

Table 4.26: *Ballute Design Properties*

Ballute shape	$D_b[m]$	$V_b[m^3]$	$S_b[m^2]$
Goodyear	0.9	0.47	2.47

The air inlets of the ballute require special attention. The Armadillo Aerospace group [50] also uses a ballute for their sounding rockets. They concluded that the inlets pictured in Figure 4.27 are not reliable. Also the Copenhagen Suborbitals group [51] designed other air inlets. It is therefore advised to start with a copy of the air inlets used by the Copenhagen Suborbitals group, since their ballute has been tested and clear pictures are available, and make design changes afterwards if deemed necessary.

Ballute forces and temperature: First the maximum forces and temperature should be found, because the opening forces are not the maximum forces due to the low air density at deployment. Simulations from *Recover.m* have been used to find these forces when an apogee of 132 km will be reached. They can be seen in Table 4.27

Table 4.27: *Ballute Forces and Temperature*

Drag force $[N]$	**Design force** $[N]$	**Temperature** $[K]$	**Design Temperature** $[K]$
9568	30809	1010	700

The length of the first riser is defined by a short length in the mortar tube and the distance between the mortar tube and the explosive bolt located on the rear of the rocket. In order to make accurate mass estimations this length has been estimated to be 5 m. A single braid Kevlar rope with a diameter of 9.525 mm has a tensile strength of over 53 kN and can withstand the temperatures. This exceptionally strong riser may not be required, but can be useful when the flight termination system demands a deployment at higher dynamic pressures. The second riser connecting the explosive bolt and the main parachute needs to be taken into account as well. This riser will experience loads comparable to the opening loads of the main parachute, but will experience the same temperatures as the ballute. Therefore a Kevlar rope has been selected.

The temperature in this table represents the air temperature behind the shock wave of the rocket. Because the ballute will be far away from the rocket due to the long riser, the air temperature will already be cooled down significantly around the ballute. It is therefore acceptable to assume that the ballute will not experience this temperature. The main temperature contributor will be due to aerodynamic heating. Knowing that the nosecone will reach temperatures of 800 to 900 K at a Mach number of around 5, it is acceptable to design the ballute so it can withstand a temperature of 700 K. Two materials were being considered: Nomex and Zylon. Zylon is the better performing material in terms of tensile strength and heat resistance but also more expensive. It was concluded that Kevlar reinforced Nomex type 455 is strong enough. Some aspects like shivels, stitches, the explosive bolt and other connection points have been estimated to take up 250 g. The resulting material properties can be seen in Table 4.28.

Table 4.28: *Ballute Material Properties*

	Material	**Length** $[m]$	**Thickness** $[mm]$	**Mass** $[kg]$
Riser 1	Single braid Kevlar	5	9.5	0.30
Riser 2	Single braid Kevlar	5	6.35	0.15
Ballute	Type 455 Nomex	3.06 $[m^2]$	0.7	2.37
Misc.	-	-	-	0.20
Total	-	-	-	3.02

4.8.6 Deployment System

The deployment system is responsible for reliable deployment of the first and second stage decelerators. A deployment system can easily take up 50 % of the total mass and volume of the Recovery subsystem and should therefore be designed in detail. The deployment system will consist of a mortar tube containing the ballute in a deployment bag or harness, an expulsion gas responsible for firing the mortar, a deployment bag for the main parachute and a bulkhead which will connect the main parachute to the rocket. The explosive bolt connection the ballute to the rocket also falls under the Recovery subsystem. Of course all these items need to be fixed into place.

Ballute Deployment

The ideal moment to deploy the ballute is when the dynamic pressure is small, but not zero. At zero dynamic pressure there is still no drag force so the ballute riser will be prone to entanglement and the ballute will not stay inflated. If the dynamic pressure is large, opening forces will be very high and may result in line break, ballute failure or bolt tear out. Ideally there is a small dynamic pressure, and thus drag force, to ensure line stretch, stabilized descent and inflation. According to *Recover.m* this leaves a deployment window of around 25 s. Inputs from ADCS, accelerometers and altimeters, should be used to initiate deployment. It is also advised to predefine a certain time window in which the ballute can deploy. Outside this time window, ascent and peak dynamic pressure, the ballute should not be deployed. The FTS should be able to overwrite this window of deployment in case of a terminated flight. When the flight computers has determined the ballute should be deployed an impulse current runs through an electrical wire to a detonator in the mortar tube. This detonator is attached to a small gas tank, which will then build up the pressure inside the mortar tube. When a certain pressure difference has been reached, the bolts attached to the mortar cap will fail and the ballute will be fired away from the rocket. This force in combination with the drag generated by the ballute will rip the riser free from the side of the rocket and flip the rocket into a nose-first attitude. It is advised to fix a small gas cartridge inside the ballute which will initially inflate the ballute immediately after deployment. Air inlets will then keep the ballute inflated.

Main Parachute Deployment

The main parachute has been designed to reliably deploy at 75 m/s and down to 2000 m altitude. The target opening altitude however is 3000 m so there is a larger time window between initiated deployment and terminal velocity and the opening forces are lower at higher altitudes, because of the lower air density. The deployment is also initiated by the flight computer and based on ADCS input. Similar to the first stage decelerator an electrical impulse will run through a wire connected to the explosive bolt. The charge placed around the bolt will ignite and disconnect the riser from the fuselage. The ballute then pulls the entire riser from the side of the rocket and eventually pulls out the main parachute through the same hole the ballute was fired from. This requires that the force applied on the main parachute is large enough for the mortar tube to break. A way of solving this problem is breaking the mortar tube up in two parts. One strong part build to be able to withstand the pressure and one part where the ballute and mortar cap will simply slide through and the main parachute can puncture through. Since the riser of the main parachute is connected to a bulkhead below the canards, the rocket will flip into a tail-first attitude. In order to ensure that the suspension lines do not get entangled with the canards, the force of the ballute has to be strong enough to ensure immediate line stretch. The reefing system of the main parachute does not require any input.

4.8.7 Simulation

The entire descent phase of Stratos III has been simulated in the program called *Recover.m*. The assumptions used in this program have been summarized below:

- The isentropic expansion factor γ equals 1.4.

- The earth's radius is constant.
- The drag coefficient of the main parachute does not vary with velocity.
- The surface area of the first stage inflatable decelerator does not vary during flight.
- The surface area of the main parachute does not vary during flight.
- The wind does not rotate.

The results of the program can be seen in the Figures 4.29, 4.30, and 4.31. The values used in this program correspond to the values used in the design for the Recovery subsystem, i.e. dry mass is 140 kg, main parachute surface area is 14 m^2, and the ballute diameter is 0.9 m. Two apogee heights have been simulated, 120 km and 132 km, because the target altitude is 120 km, but the design altitude is 132 km. It can be seen that using the design parameters determined in the previous sections, all the requirements have been met.

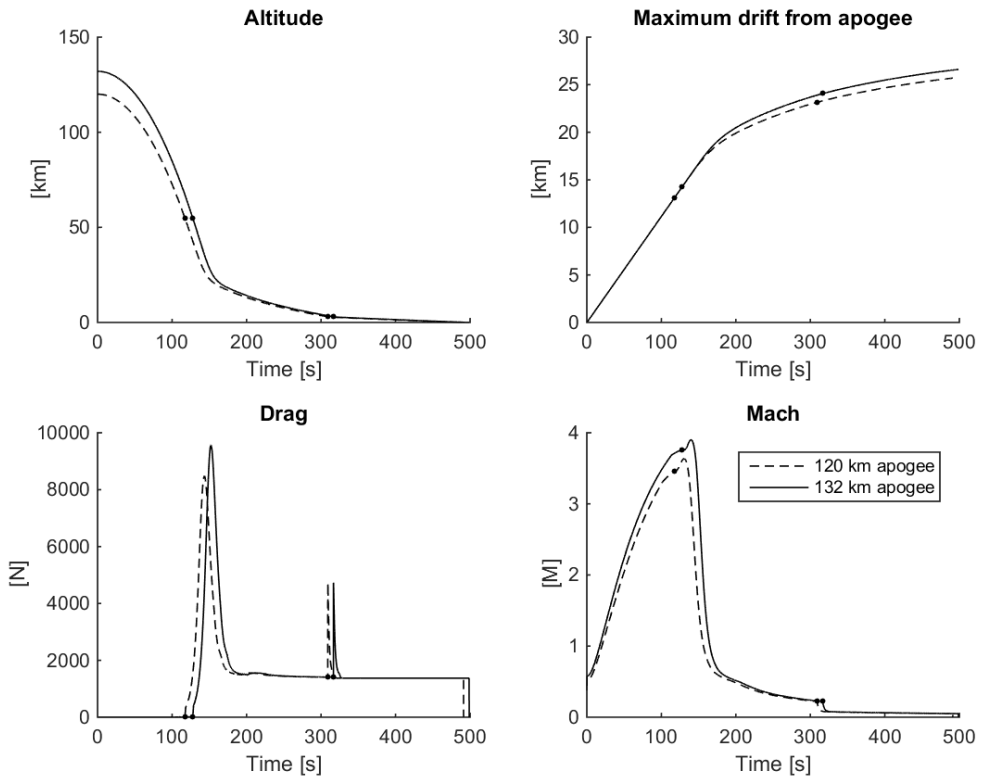

Figure 4.29: *Altitude, Drift, Drag, and Mach Number as Functions of Time of the Rocket in a Ballute and Cross Shaped Main Parachute Configuration at Different Apogee Heights*

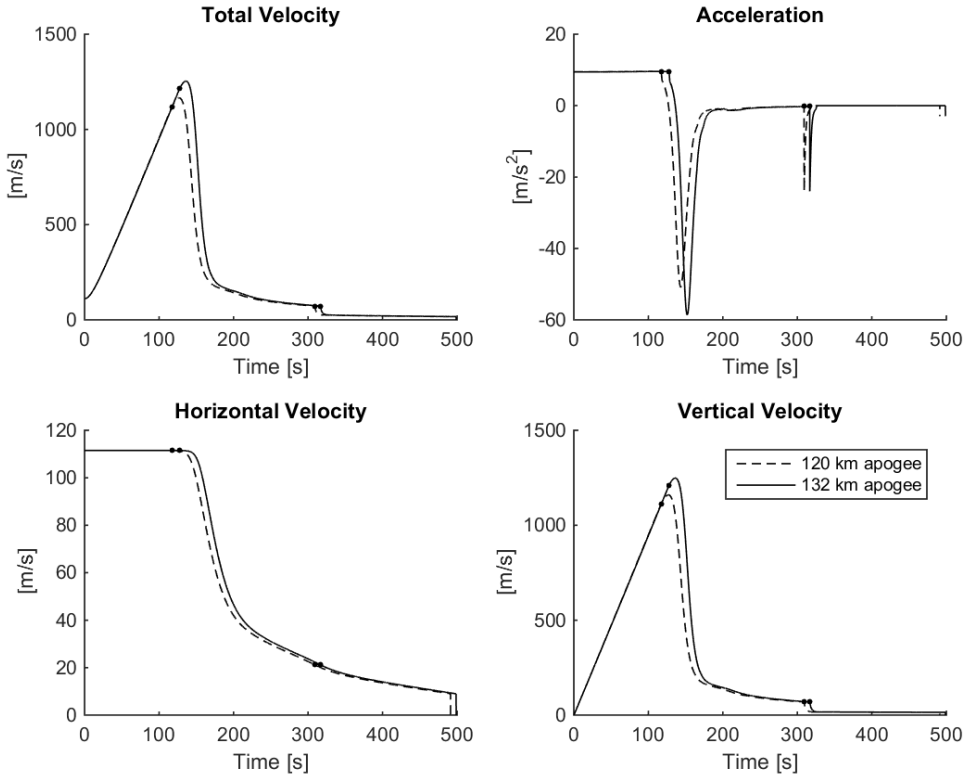

Figure 4.30: *Total Velocity, Acceleration, Horizontal Velocity, and Vertical Velocity as Functions of Time of the Rocket in a Ballute and Cross Shaped Main Parachute Configuration at Different Apogee Heights*

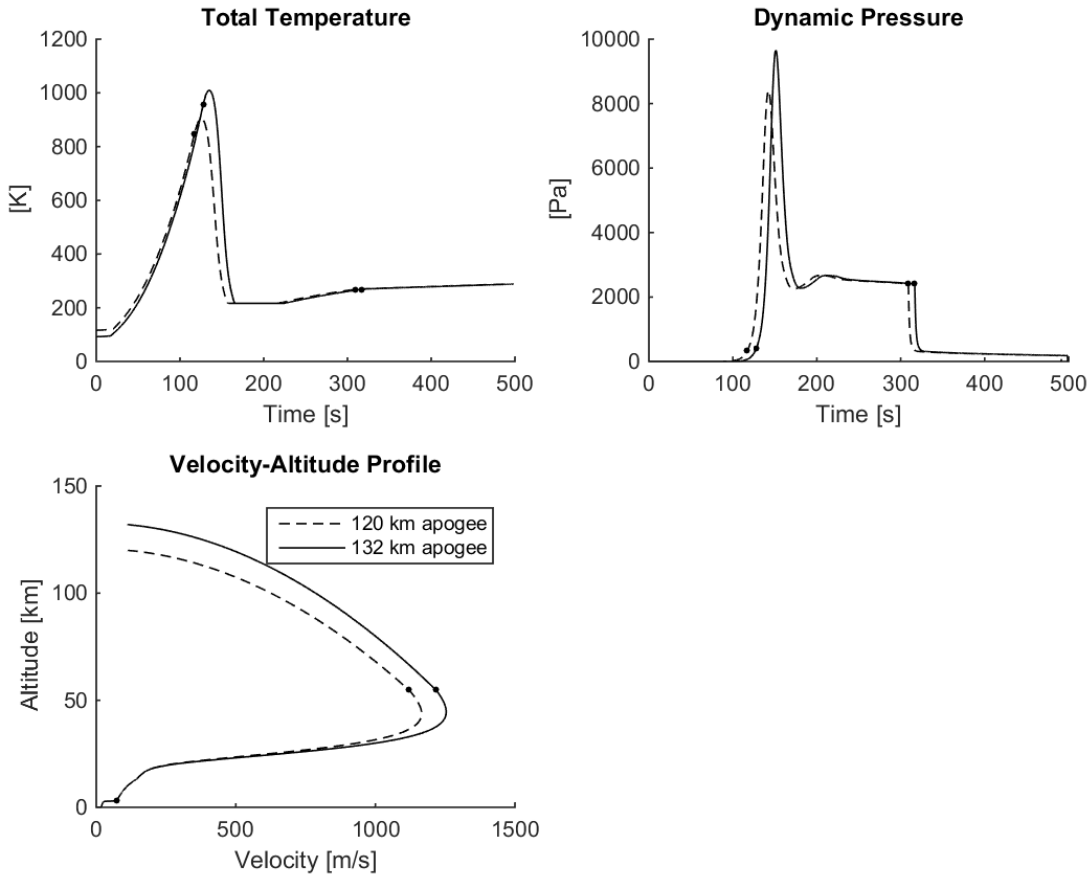

Figure 4.31: *Total Temperature and Dynamic Pressure as Functions of Time of the Rocket in a Ballute and Cross Shaped Main Parachute Configuration at Different Apogee Heights*

4.8.8 Sensitivity Analysis

A sensitivity analysis has been conducted to determine what effects changing parameters have on the Recovery subsystem. Table 4.29 shows the effect when the dry mass or the apogee height changes. Increasing the dry mass will result in a drag increase of around 10% at every phase of descent and a corresponding higher dynamic pressure. This could result in the need for stronger materials and therefore higher costs and possibly a higher subsystem mass. The materials currently selected however would still be strong enough to recover a rocket with a dry mass of 154 kg. The impact velocity changes with approximately 1 $m/$. If deemed unacceptable the main parachute size would have to be increased, leading to a slightly higher subsystem mass. Decreasing the dry mass with 10% will result in the opposite effects. Increasing the apogee height only influences the forces on the ballute. This is because the ballute still has enough time to reach the same terminal velocity. A higher maximum drag force, maximum velocity, maximum acceleration, maximum temperature, and maximum dynamic pressure are the result of a 10% increase in apogee height. These effects cannot be ignored, but they seem not to affect the performance so much that the ballute would be likely to fail. In conclusion, using the same requirements, an increase in dry mass results in the need for a slightly bigger and stronger ballute and main parachute and an increase in apogee height results in the need for a stronger ballute.

Table 4.29: *Recovery Subsystem Sensitivity Analysis*

Changing parameter	Effect
+10% Dry mass	20 seconds shorter descent time 10% higher drag force 1 m/s higher impact velocity 1000 Pa higher dynamic pressure
-10% Dry mass	20 seconds longer descent time 10% lower drag force 1 m/s lower impact velocity 1000 Pa lower dynamic pressure
+10% Apogee height	8 seconds longer descent time 1000 N higher maximum ballute drag force 100 m/s higher maximum velocity 8 m/s^2 higher maximum deceleration 100 K higher maximum temperature 1200 Pa higher maximum dynamic pressure
-10% Apogee height	1000 N lower maximum ballute drag force 100 m/s lower maximum velocity 8 m/s^2 lower maximum deceleration 100 K lower maximum temperature 1200 Pa lower maximum dynamic pressure

Design factors

The Recovery subsystem is designed with a large range of conservative safety factors. First of all the Recovery subsystem has been designed to be able to recover a rocket with a dry mass of 140 kg from an apogee of 132 km. The main parachute has been designed to deploy at velocities up to 75 m/s. Furthermore design factors ranging from 1.85 to 3.22 have been used. These high design factors do not affect the material selection for all parts. Finally the Recovery subsystem is capable of successfully deploying the main parachute within a 2000 m altitude range of its target and the ballute within a 25 s time window.

4.8.9 Ground Phase Recovery

Requirement **STR-SUB-REC-06** states that the recovery system has to produce a clear proximity indicator after splashdown. The best options were decided to be a colored canopy design and a sea dye marker, because of their low mass and low costs. A sea dye marker contains a fluorescent powder that will spread over the surface of the water after splashdown. This can be placed inside the Recovery system area and weighs only 100 g.

4.8.10 Mass, Cost, & Power Budget

The mass, cost, and power budget breakdowns will be shown and elaborated on in the following subsections.

Mass

The Recovery subsystem was designed to have a mass of no more than 13 kg. This value has been defined based on experience from Stratos II, payload-altitude interpolations and after a feel of what was possible after literature and initial calculations were performed. The main parachute and ballute were calculated to have masses of 1.34 kg and 3.17 kg respectively. This includes suspension lines, risers and connection points. This leaves 8.49 kg for the deployment bags, mortar tube and bulkheads. They have been estimated in this conceptual design. The detailed mass budget can be seen in Table 4.30.

Table 4.30: *Recovery Subsystem Mass Breakdown*

Main Parachute		Ballute		Deployment System		Miscellaneous	
Canopy	0.77	Canopy	0.77	Mortar tube	1.00	Deployment bags	0.50
Suspension lines	0.21	Riser 1	0.30	Gas tank	0.30	Harness	1.00
Riser	0.060	Riser	0.15	Explosive bolt	0.050	Bulkheads	4.00
Misc.	0.30	Misc.	0.25	Detonators	0.060	Misc.	0.30
Total	1.34	Total	3.17	Total	1.41	Total	5.8

The total mass of the Recovery subsystem has been estimated to be 11.57 kg while the rocket has been designed to contain a 13 kg Recovery subsystem. This leaves room for 1.43 kg of additional weight.

Cost

A detailed cost breakdown can be seen in Table 4.31. These costs have been taken from various sources on the web and are only to be used as an order of magnitude estimate, because some parts will come with shipping costs and others will have to be custom made. This cost breakdown also concerns the cost of all the parts once, so for example testing is not considered in this section.

Table 4.31: *Recovery Subsystem Cost Breakdown*

Main Parachute		Ballute		Deployment System		Miscellaneous	
Canopy	175	Canopy	120	Mortar tube	20	Deployment bags	50
Suspension lines	200	Riser 1	100	Gas tank	50	Harness	20
Riser	50	Riser	50	Explosive bolt	20	Bulkheads	10
Misc.	10	Misc.	30	Detonators	20	Misc.	10
Total	365	Total	370	Total	130	Total	70

Power budget

The only power the Recovery subsystem will use comes from the two electrical detonators. One detonator is connected to the mortar tube and the other detonator is connected to the explosive bolt. Electrical detonators only require a very short impulse of current. The detailed power budget of the Recovery subsystem can be seen in Table 4.32.

Table 4.32: *Recovery Subsystem Power Breakdown*

Part	**Amount**	**Current** $[A]$	**Power** $[W]$	**Time** $[ms]$	**Watt hour** $[Wh]$
Detonator	2	5	1	5	$1.39 \cdot 10^{-6}$

4.9 Flight Termination System

The following section addresses the Flight Termination Subsystem (FTS). The FTS is a vital requirement for launch safety but it is a risk in itself to the system as its responsibility of termination is potentially catastrophic. Therefore, great care needs to be taken during its design.

4.9.1 System Overview

During Stratos III ascension phase the rocket will travel within a predetermined flight corridor, in which case the rocket will land within a safe zone. However, in case of any failure resulting in deviation from the flight corridor, the RSO will send the flight termination commands.

Stratos III uses a hybrid engine that can be relatively easy to shut down by closing the main valve, which will stop the oxidizer from entering the combustion chamber. This leads to relatively simple and safe FTS design since no pyrotechnic charges are required as is the case for solid propellants.

System Architecture The FTS as a whole consists of two segments: a ground segment and a flight segment. The ground segment sends an IRIG standard monitor, arm or abort signal to the rocket. The RSO of the launch site gives, if needed, the abort decision, based on a predetermined set of rules. It follows that the flight segment should be able to receive the IRIG signals, process them and, if necessary, send the abort signals to the engine and main control unit. As the FTS has to be as independent as possible, it will have its own power supply and communication system. The architecture is shown in Figure 4.32.

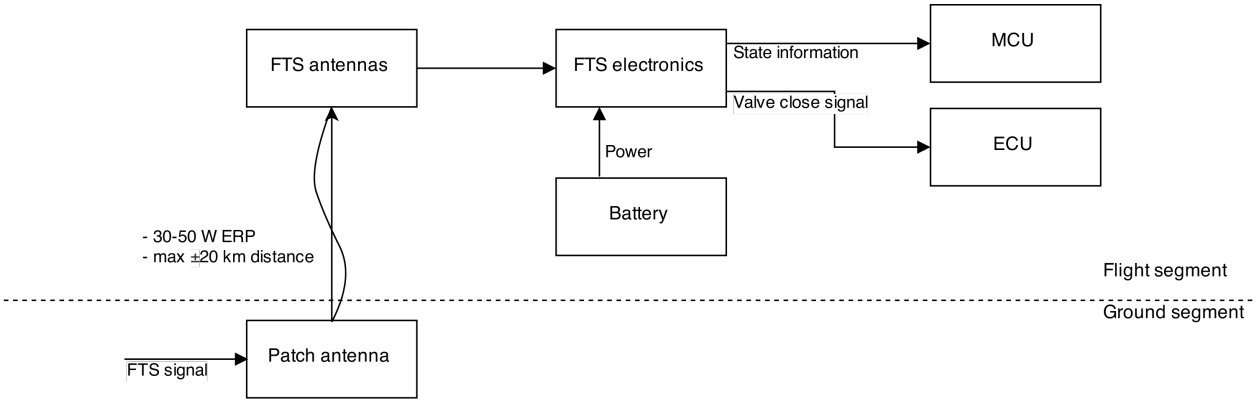

Figure 4.32: *Functional Block Diagram of the FTS*

The following subsections will address the design considerations of the FTS.

4.9.2 Radio Uplink

The FTS needs to receive a clear signal from the ground. If it loses this signal it is impossible to receive an abort signal from the ground so the FTS goes in fail-safe mode as explained in Section 4.9.5. Good positioning, designing and testing of the FTS's antennas is therefore essential.

The FTS uplink provided by INTA has the following properties:

- 400-446 MHz carrier frequency ($\lambda \approx 0.7\ m$)
- IRIG standard (Monitor, termination, arm frequency of respectively 500, 750 and 1250 Hz)
- FM modulation, deviation about 10 kHz to a few MHz
- About 30-50 W ERP
- Patch antenna mounted on optical/radar tracker
- Origin located around 300 m from launch site

Link Budget In order to get some preliminary numbers on the required FTS receiver sensitivity a link budget is made. A maximum link distance of 20 km is assumed given the burnout altitude of 18 km. The antenna gain is dependent on antenna type and placing and therefore unknown at the moment and set to the conservative estimate of zero dB. Table 4.33 shows the resulting link budget.

Table 4.33: *Link Budget of the FTS*

Item	**Quantity**
Link distance	20 km
Frequency	433 MHz
Transmit power (ERP)	45 dBm (30 W)
Free space loss	-111 dB
Propagation and polarization loss	-3 dB
Antenna gain	0 dB
Receiver line loss	-3 dB
Received power	-72 dBm

During detailed design the noise power and resulting SNR needs to be computed, as well as the resulting antenna gain in order to complete the link budget.

4.9.3 Receiver Antennas Type and Placing

Since the FTS transmitter antenna is relatively close to the launch site, the FTS transmitter antenna is, under nominal conditions, pointing to the underside of the rocket. This implies that the FTS receiver antenna system should have a sufficient gain in downside direction.
In order to minimize interference with the telemetry system and/or video downlink the antennas should be positioned far away from the nose cone. Also, if the antennas are placed inside the nose cone, the rocket itself shields the downward radiation so placing the FTS antennas in the nose cone is not considered an option.

Possible options of antenna types and position combinations are:

1. Blade antennas on the fuselage near main valve
2. Monopoles at the trailing edge of the fins
3. Inverted F antennas (IFA) between the combustion chamber and the oxidizer tank

Table 4.34: *FTS Antenna Trade-off Matrix*

Option	Coverage	Aerodynamics	Mass performance	Development risk
1	Less predictable than other options	Good	Average	Average
2	Probably good	Best	Extra wiring needed	Low
3	Good [52]	Average	Average	High

In order to minimize development risk and cost it is advised that option 2, the monopole at the trailing edge of the fins is used. Two monopole antennas at two opposite fins are estimated to be sufficient but proper simulation and testing should be done in order to verify this. The fuselage of the rocket and the fins perpendicular to the monopoles will serve as a ground plane. Potential problems and integration issues that have to be accounted for are:

- Ionization of the exhaust plume and as a result reduced gain because of shielding by the exhaust plume
- Wiring from the FTS electronics to the antennas
- Integration of the monopoles on or into the tail fins
- Interaction between the antennas

4.9.4 Power

The FTS will be a stand-alone system. Therefore it has its own power supply since it cannot rely on the main power supply. The power supply consists of batteries and is included in the FTS mass budget.

4.9.5 Flight Termination Logic

The design of the flight termination logic as seen in Figure 4.33 is driven by the requirements from INTA. The goal is to minimize the probability of a false positive, while still having a 'fail-safe' option in case of a communications failure between the ground and flight segment.

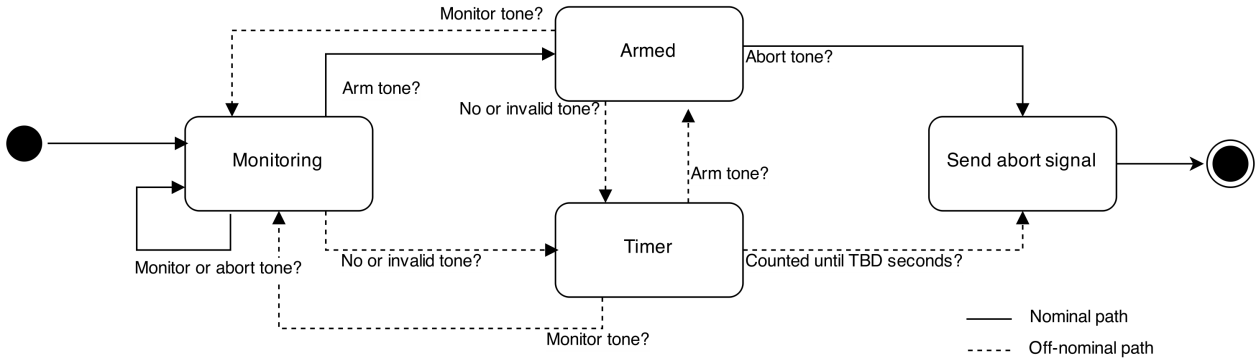

Figure 4.33: *State Diagram Indicating the FTS Logic*

There can be three possible valid tones received by the FTS:

Monitor Flight can continue

Arm Abort cannot happen without this tone received prior to the abort tone

Abort Abort flight if arm tone was send immediately prior to it

If no tone or some invalid tone is received by the FTS, the FTS goes into the 'fail-safe' mode. The timer starts and the FTS will autonomously abort the flight after a predetermined amount of time. From a FTS point of view this is off-nominal behavior as indicated as such in Figure 4.33.

4.9.6 Powered Flight Termination Methods

There are two main methods of terminating powered flight:

- The first method is simply closing the main valve that feeds oxidizer to the combustion chamber. The main valve is a NC valve which means that the valve will automatically close if no current is flowing through. By utilizing an NC valve, the situation in which the loss of power resulting in loss of valve control can be avoided.
- The second method is opening the relief valve located at the top of the oxidizer tank to reduce pressure within the oxidizer tank. By lowering the pressure within the oxidizer tank, pressure difference between the combustion chamber and the oxidizer tank will be reduced. This would in turn result in decreased oxidizer mass flow, significantly reducing the thrust of the rocket engine. The relief valve needs to be sized large enough to accommodate fast pressure relief, more research needs to be done in this area.

Both flight termination methods can be performed in parallel to complement each method. In case of valve failure where the main valve fails to be closed, the relief valve can still be used to significantly reduce thrust.

Depending on launch site requirements, the FTS can be modified or altered to incorporate alternative methods such as shape charge on the oxidizer tank.

4.9.7 Recovery after Flight Termination

Being able to recovery the rocket in case of a mission abort is desirable. Dissipating energy is the first concern after a mission abort. This would imply an immediate deployment of the ballute and eventually the main parachute for final recovery. However the concern existed that the ballute would not be able to cope with the forces of deploying at high dynamic pressures, therefore an analysis has been performed to investigate this.

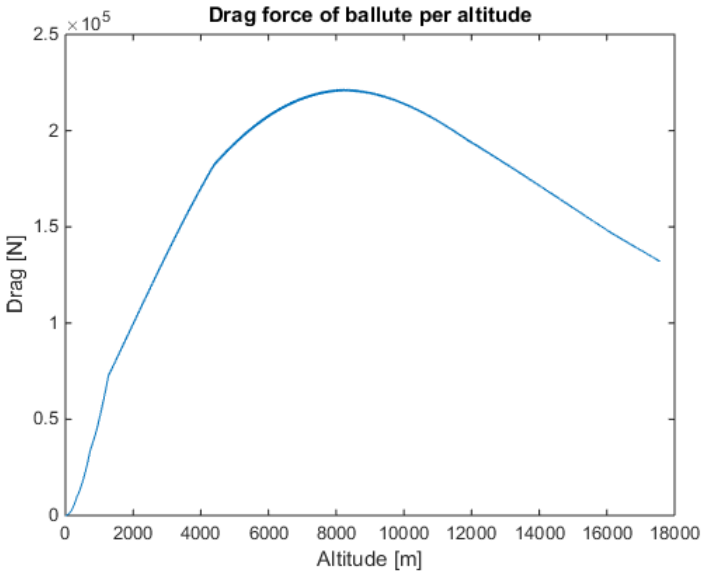

Figure 4.34: *Approximation of the Drag Force Generated by the Ballute as a Function of Altitude in case of Immediate Deployment after Mission Abort*

Figure 4.34 shows that the maximum drag force would be close to 250 kN at an altitude of approximately 8000 m. The current drogue system is designed to withstand a load of 31 kN. This means that in the current design it is not advised to immediately deploy the ballute after a mission abort. The ballute would not be

able to hold deployment at altitudes higher than 700 m or after 6.2 s of burn time, because this will result in a recovery system failure and thus in the loss of the rocket. There are several options of preventing rocket loss like increasing the drogue system strength by choosing stronger or thicker materials or by setting a delay of deployment after mission abort. Requirements of the launch site will come into play here. From a design point of view it is best to leave the recovery subsystem as it is and setting a delay of deployment. This will allow the rocket to first slow down to an acceptable dynamic pressure before deployment. The launch site may however demand immediate energy dissipation. In which case the drogue system will need serious reinforcements.

4.9.8 Mass and Cost Budget

The mass of the FTS can be estimated as being around 200-300 g based on the experience with Stratos II.

The FTS electronics can be developed in-house by DARE. By doing this the costs will be limited to the cost of the components, which are expected to be low, thus limiting the cost of the FTS.

Table 4.35: *Mass and Cost Budget of the FTS*

Part	**Mass** $[g]$	**Cost [€]**
Antennas (2)	100	20
Antenna wiring	80	40
Battery + wiring	70	20
FTS electronics	50	50
Total	300	180

Chapter 5

Verification and Validation

Verification and validation contains the procedures of confirming if key requirements are met and determining whether the final product meets the requirements. Verification and validation can be done on every level of the (sub)system. The verification and validation process according to the V-diagram can be seen in the figure below:

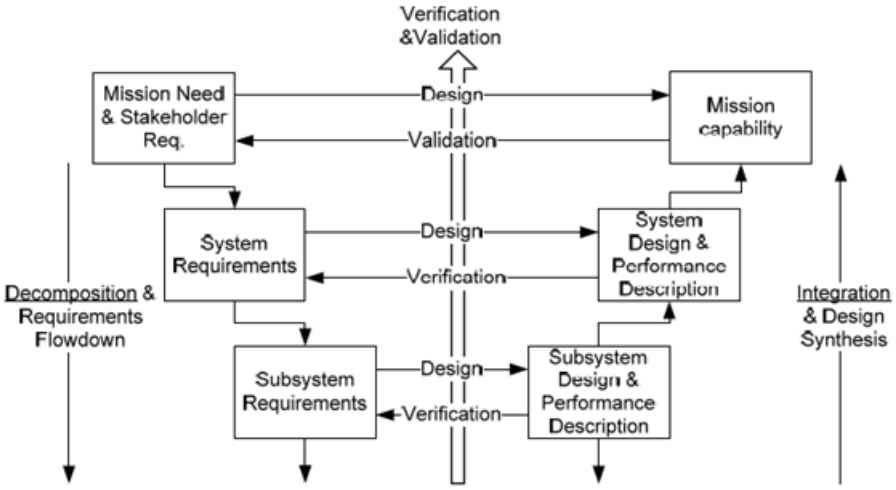

Figure 5.1: *The V-model of the Systems Engineering Process*

Verification for the Stratos III can be done in four different ways; by inspection, analysis, demonstration or testing. This chapter contains the validation and verification procedures for the rocket and finishes with a compliance matrix that ticks off all the passed requirements.

5.1 The System

The System requirements can be easily verified by inspecting and analyzing the system. By inspection one can easily see that the system has a flight termination system, communication system, recovery system and ADCS system. This covers requirements **STR-SYS-01, STR-SYS-05, STR-SYS-06, STR-SYS-07, STR-SYS-08, STR-SYS-09, STR-SYS-10, STR-SYS-11**. Furthermore by inspection the remaining requirements can be verified. The validation of the system can only be done with a full scale launch.

5.2 Subsystems

Each subsystems has its own approach on how to validate and verify the subsystem. The methodology is described in the following sections.

5.2.1 Propulsion

Requirements for the Propulsion subsystem can be seen in Table B.3 in Appendix B.

Requirements **STR-SUB-PRO-01** through **STR-SUB-PRO-06** can be verified by a number of tests. First of which will be the solid propellant regression rate test. Determining the regression rate of solid propellant is crucial to estimate the thrust profile of the engine and therefore the performance. Regression rate coefficients of specific solid propellant compounds are often not disclosed to public and therefore regression rate coefficients have been estimated in this final design review. Second, oxidizer tank needs to be tested for liquid Nitrous Oxide and Oxygen mixing and their temperature and pressure under varying conditions. Depending on the temperature of the liquid oxidizer within the tank, the performance of the rocket engine will vary due to changing oxygen mass ratio in liquid phase. As for pressure of the oxidizer tank, not only should this be tested for safety, maximum tank pressure, but also for the performance of the engine deriving from the fact that the oxidizer need to be self-pressurized. Third, the feed system need to be tested for its ability to deliver Nytrox at specified temperature, pressure and mass flow rate. This test should check for possible valve and pipe leakage, freezing or rupture. Also, the safety heads and pressure sensors need to be checked as to whether the rupture disc ruptures at rated pressure and whether the pressure sensor gives correct pressure readings. Finally, a firing test of the entire propulsion subsystem need to be conducted to verify that the propulsion subsystem delivers sufficient thrust to reach target altitude of 120 km. Requirements **STR-SUB-PRO-07** through **STR-SUB-PRO-08** can be verified through inspection of all chemicals stored within the propulsion subsystem, propellant exhaust product analysis.

Validation of the propulsion subsystem model is difficult at this point as there are little or no information provided for a similar rocket propulsion subsystem. Therefore, it is essential to build and test a small scale model early in the development phase to validate the model.

5.2.2 Structure

The requirement for the Structure subsystem can be found in Table B.8 in Appendix B. There are five tests which need to be done in order to verify the structures subsystem. The first is a static force test where forces simulating thrust drag and pressure differences are tested for the various cases applicable to the Stratos III mission. This is done using a simple compression load given to a pressurized cylinder. This test verifies requirements **STR-SUB-STR-01** and **STR-SUB-STRU-08**.

Secondly a dynamic force test must be done in order to see if the rocket will survive impact during landing or a by a foreign object during transport. This is done by impacting a model of the main body of the rocket with an impulse force which it has to sustain. This test will verify requirement **STR-SUB-STRU-02**.

Thirdly is the vibrations test in order to see that the structure will vibrate within its limits and will never reach its natural frequency. This is done by trying to map every frequency under every condition. This test verifies requirements **STR-SUB-STRU-04** and **STR-SUB-STRU-05**.

Fourth is a temperature test to see if the required temperatures during re-entry do not impede the structural integrity of the rocket. This can be done by taking a small sample of material used in the rocket and heating it to the estimated temperature during re-entry and observing if the material still has the required properties to function properly. This will verify requirement **STR-SUB-STRU-03**.

The final test is the simplest one, this test is to see if the communications which are inside the rocket are not impeded by the rocket. This can be done by putting a simple radio transmitter inside the rocket and conclude if the signal is coming through or not. This will verify requirement **STR-SUB-STRU-07**.

5.2.3 ADCS

The requirements for the ADCS subsystem are given in Table B.3 in Appendix B. IMU test: The IMU needs to be tested for three different aspects: accuracy, digital interface and temperature drift. The MEMS gyroscopes, accelerometers and magnetometers in the IMU need to have error estimates and require calibration. These errors are determined using a rate table, the accuracy of these rate tables should first be determined using previous sensors. This can be done using TU Delft facilities. This test verifies the following requirements: **STR-SUB-ADCS-DET-04**,**STR-SUB-ADCS-DET-05** and **STR-SUB-ADCS-DET-06**.

During this accuracy test, the digital interface can also be verified by using the same processor and flash memory as the rocket in the processing of test data. This test verifies the following requirement: **STR-SUB-ADCS-DET-07**.

GPS test Although some tests to determine GPS accuracy can be made by moving the chip and measuring locations, it is difficult to verify whether or not the GPS is unrestricted. This is due to the altitude and velocity requirements of COCOM, which causes lockdown. An option for testing would be to send the unrestricted GPS chip on another sounding rocket mission and analyze whether or not it can operate above 18 km at 1,900 km/h. If obtained in time, it can be included as a payload on Stratos II. Another option, which would be much cheaper but less convincing, is to test the chip by simulating supersonic input signals. These tests verify the following requirements: **STR-SUB-ADCS-DET-01**,**STR-SUB-ADCS-DET-02** and **STR-SUB-ADCS-DET-03**.

Control surface test More precise sizing of the canards will have to be an iterative process. First an analysis of supersonic flow must be made and validated using wind-tunnel tests. Furthermore, the effect of the nose cone and canards on the tail fins must be checked. Once again, this has to be done through wind-tunnel tests and/or modeling using computational fluid dynamics. The assumption of a constant center of pressure after Mach 1.5 for the shift in overall center of pressure needs to be analyzed for supersonic conditions. These tests verify the following requirements: **STR-SUB-ADCS-CON-02**, **STR-SUB-ADCS-CON-03**, **STR-SUB-ADCS-CON-04**.

Flight computer test The flight computer and all the algorithms running on it can be verified using a Hardware-in-the-Loop simulation. A simulation must include electrical emulation of sensors and actuators. These electrical emulations act as the interface between the simulation and the flight computer. The value of each electrically emulated sensor is controlled by the simulation and is read by the flight computer. Likewise, the flight computer implements its control algorithms by outputting actuator control signals. Changes in the control signals result in changes to variable values in the simulation. After these tests an actual test flight can be flown to make sure everything works as intended before the final version is placed on the Stratos III. These tests verify the following requirement: **STR-SUB-ADCS-CON-01**.

5.2.4 Power

Requirements for the Power subsystem can be seen in Table B.5 in Appendix B. Electrical systems should be tested on a part-by-part basis when possible. Wires can be tested for their capability to carry the required current and batteries will be tested during subsystem verification tests. Requirements **STR-SUB-PWR-01** through **STR-SUB-PWR-05** and **STR-SUB-PWR-09** can be tested through a full system test, verifying the system's capability to provide all power needed for the full duration of the anticipated mission time including the maximum time on the launch pad. Providing simulated acceleration data to the main flight computer can be used to test that the electrical system can work for all parts of the mission.

5.2.5 Communications

The requirements for the Communications subsystem are given in Table B.4 in Appendix B. Providing communication between the rocket and the ground station during most flight stages **STR-SUB-COM-01** can be verified by analysis using a simulation software. The rocket could experience communication blackouts, especially during re-entry through the Earth's atmosphere. This is caused by a region of ionized air around the rocket which is caused by the heat from the compression of the atmosphere by the rocket. This phenomena will be evaluated in more detail in the next design phase and its effects will be minimized as far as possible.

During the selection of components, it should be inspected that flight-proven ones are used **STR-SUB-COM-03** as far as possible to minimize possible sources of failure such as low pressure, radiation and vibrations. This reduces the time and costs of building and testing new components. Transmitting status reports in real time **STR-SUB-COM-02** can be verified by analysis of a simulation or by testing a prototype. The visible outside indication that the rocket is in safe or arm mode **STR-SUB-COM-04** is intended as a safety measure and this can be easily verified by demonstration. Finally, it can be verified by inspection whether or not the system conforms to regulations and protocols **STR-SUB-COM-05**. This minimizes interference by using specified channels and also reduces safety hazards.

5.2.6 Recovery

The requirements for the recovery subsystem can be found in Table B.7 in Appendix B.

Analysis will be performed on the Recovery subsystem on every phase of the descend. Following from this analysis, the first requirement can be verified: **STR-SUB-REC-01**.

Testing the recovery subsystem will a big issue. Supersonic wind tunnels with a large enough test section are rare and testing in them will come with large costs, due to transportation costs and wind tunnel fees. Therefore it may be a better way to test the recovery subsystem by releasing a model rocket at a high altitude from an aircraft or hot air balloon. In this test the ballute will be deployed from the mortar and then at the appropriate altitude pull out the main parachute. The following requirements can be verified in this test: **STR-SUB-REC-02** and **STR-SUB-REC-03**. After this test two more requirements can be verified due to inspection: **STR-SUB-REC-05** and **STR-SUB-REC-06**. The fourth requirement, **STR-SUB-REC-04**, can be verified by demonstration. It is a good idea to demonstrate this during the live test. As the aircraft will have an initial horizontal airspeed and altitude, the drift of the rocket can be demonstrated and then extrapolated in order to show that the maximum drift will stay within the safe zone.

It is recommended to thoroughly test the deployment of the ballute in near vacuum conditions and possibly test a ballute model in a supersonic wind tunnel to ensure it will survive the harsh conditions during reentry. Also the high temperatures the ballute will experience during reentry should be tested in order to ensure the ballute will not lose too much strength. A good way of testing the stability and performance of the air inlets of the ballute at subsonic air speeds can be done by placing the ballute in a vertical wind tunnel used for indoor skydiving.

5.2.7 FTS

The requirements for the FTS can be found in Table B.9 in Appendix B. The most important test to verify requirement **STR-SUB-FTS-01** is a hardware in the loop test during which the reception of the antennas is tested. Preferably this test is done during an engine test, with the antennas attached to the fins, in order to account for the exhaust plume. Other testing can take place in a more convenient setting by simulating different FTS input signals under different simulated flight conditions.

5.3 Rocket Compliance Matrix

In the baseline review several requirements were written down for the system and different subsystems, these requirements can be found in Appendix B. This section looks back at the requirements and shows which requirements are met and which are not. This is done using a compliance matrix, in this matrix the identifier is repeated with the compliance and method of verification is stated.

Identifier	**Compliance (F/P/C/N/X)** [1]	**Verify (I/A/D/T)** [2]	**Notes**
STR-SYS-01	F	A	
STR-SYS-02	F	A	
STR-SYS-03	F	A	
STR-SYS-04	F	A	
STR-SYS-05	P	A	There is as of this moment no certainty at this moment that the rocket will be able to communicate during the transonic phase
STR-SYS-06	F	A	
STR-SYS-07	F	A	
STR-SYS-08	F	A	
STR-SYS-09	F	A	
STR-SYS-10	F	A	
STR-SYS-11	F	A	
STR-SYS-12	F	I	
STR-SUB-ADCS-DET-01	F	A	
STR-SUB-ADCS-DET-02	F	A	
STR-SUB-ADCS-DET-03	F	A	
STR-SUB-ADCS-DET-04	F	D	

[1] F - Full, P - Partial, C - Requirement changed, N - Not complied with ,X - Requirement dropped
[2] I - Inspection, A - Analysis, D - Demonstration, T - Testing

STR-SUB-ADCS-DET-05	F	D	
STR-SUB-ADCS-DET-06	F	D	
STR-SUB-ADCS-DET-07	F	D	
STR-SUB-ADCS-CON-01	F	T	
STR-SUB-ADCS-CON-02	F	T	
STR-SUB-ADCS-CON-03	F	T	
STR-SUB-ADCS-CON-04	F	T	
STR-SUB-COM-01	F	A	
STR-SUB-COM-02	F	D	
STR-SUB-COM-03	F	I	
STR-SUB-COM-04	F	I	
STR-SUB-COM-05	F	I	
STR-SUB-PWR-01	F	A	
STR-SUB-PWR-02	F	D	
STR-SUB-PWR-03	F	D	
STR-SUB-PWR-04	X		No central power system used
STR-SUB-PWR-05	X		
STR-SUB-PWR-06	F	I	
STR-SUB-PWR-07	P		
STR-SUB-PWR-08	F	I	
STR-SUB-PWR-09	F	A/T	
STR-SUB-PWR-10	F	D	
STR-SUB-PWR-11	F	I	
STR-SUB-PRO-01	F	D	
STR-SUB-PRO-02	F	T	
STR-SUB-PRO-03	F	A	
STR-SUB-PRO-04	P	D	The oxidizer level can be estimated and therefore the fuel levels
STR-SUB-PRO-05	F	D	
STR-SUB-PRO-06	P		Safety factor not defined
STR-SUB-PRO-07	F	I	
STR-SUB-PRO-08	F	I	
STR-SUB-REC-01	F	T	
STR-SUB-REC-02	F	D	
STR-SUB-REC-03	F	A	
STR-SUB-REC-04	P	A	The recovery system cannot steer it into a safe zone, however it can descend fast enough to remain within INTA's safe zone
STR-SUB-REC-05	F	I	
STR-SUB-REC-06	F	I	
STR-SUB-STRU-01	F	T	
STR-SUB-STRU-02	F	T	
STR-SUB-STRU-03	F	T	
STR-SUB-STRU-04	F	T	
STR-SUB-STRU-05	F	T	
STR-SUB-STRU-06	F	T	
STR-SUB-STRU-07	F	T	
STR-SUB-STRU-08	F	T	
STR-SUB-FTS-01	F	D	
STR-SUB-FTS-02	F	I	
STR-SUB-FTS-03	F	I	
STR-SUB-FTS-04	F	A	
STR-SUB-FTS-05	F	I	

Chapter 6

Mission Analysis

This chapter introduces the design and planning for the Stratos III mission. It covers the recommended plan of action for DARE to keep moving forward with the design, development, production, and assembly of the rocket. Following this, is an elaboration on the required resources available to DARE. The final mission design is then compared to its requirements in a compliance matrix and the budget and risk analysis are presented.

6.1 Stratos III Team

After the conceptual mission design is completed by the DSE team, DARE will be able to start implementing it on the Stratos III mission. The current DSE team organization can be found in Appendix C. The suggested team setup for DARE can be found in the remaining part of this section.

Just as with the Stratos II, the Stratos III team will be a mixture of different DARE projects. The three main teams will be: Hybrid Rocket Propulsion, Capsule & Recovery and Advanced Control Team. The Stratos III team will be supplemented by an electronics team and a simulations team. For the marketing side of the project there will be a public relations team and a sponsor acquirement team.

The internal organization of the Stratos III team can be found in Figure 6.1. It shows the different positions within the board and the required teams. Note that the same person can take up different spots. For instance the PR board member can also be the PR team leader.

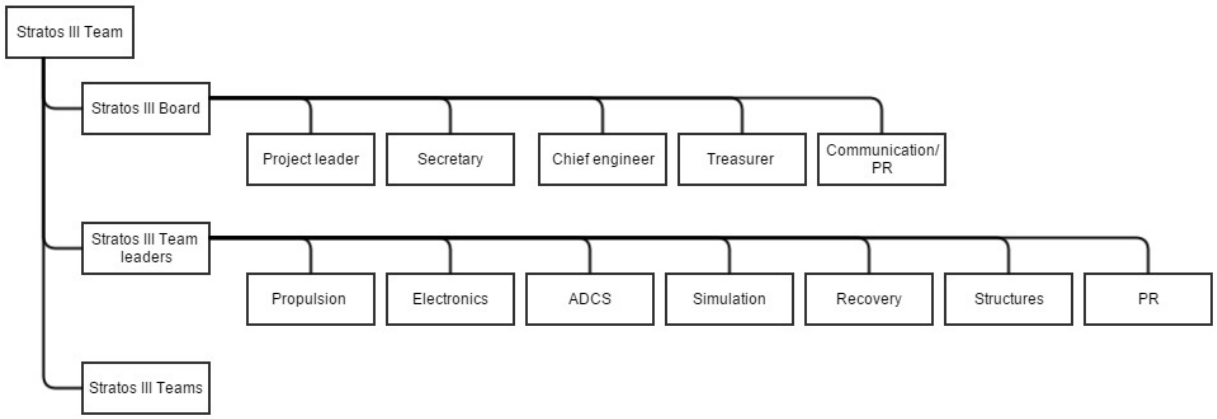

Figure 6.1: *Diagram Showing the Different Teams and Board Members*

The board of the Stratos III team will have the following functions:

- **Project leader** The project leader is the person that is generally responsible for the entire project. It is his job to steer the Stratos III project and ensure mission success.
- **Secretary** The secretary is responsible for all the paperwork and is considered to be the right hand of the project leader.
- **Chief engineer** The chief engineer is responsible for the entire technical aspect of the rocket. He is responsible for keeping an overview of the system and coordinating the subsystem integration.

- **Treasurer** The Treasurer is responsible for all finances within the Stratos III project.
- **Communication/PR** This board member is responsible for all communication to the outside world and is responsible for the sponsors and public relations.

In order to communicate effectively between the teams and board members, the communication flow diagram, shown in Figure 6.2, has to be followed.

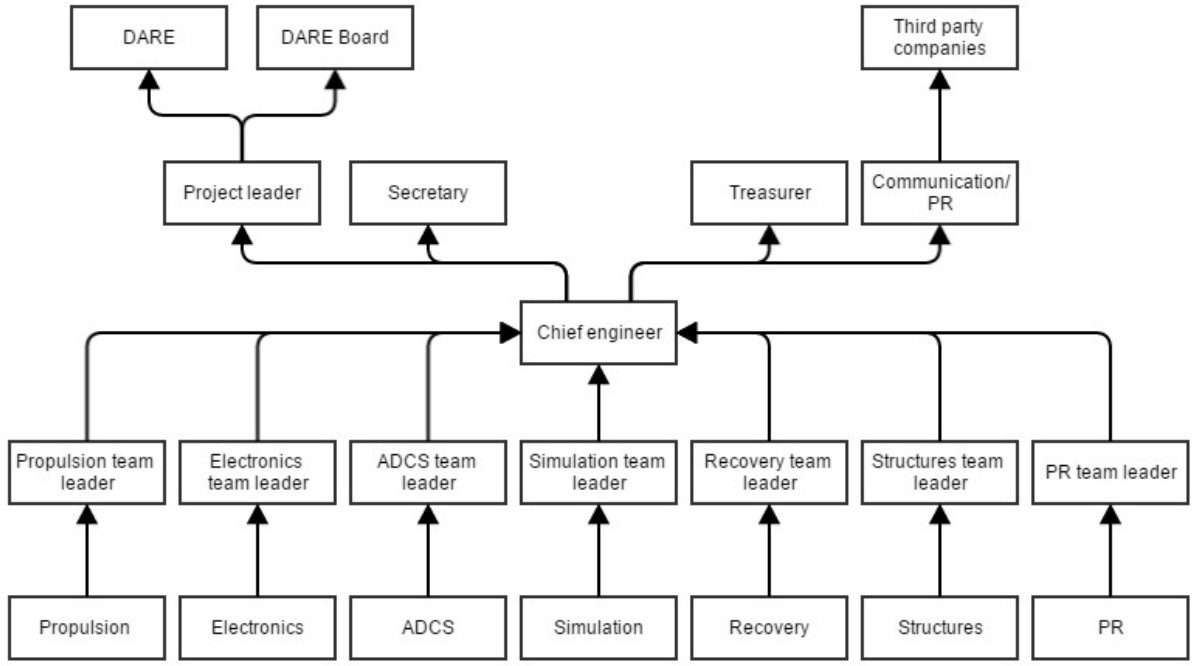

Figure 6.2: *Diagram Showing the Communication between the Different Stratos III Members*

From this diagram it can be seen that the teams will only communicate internally and with their respective team leader. They will hold their regular meetings and test as they see fit complying to the Stratos III time line. The team leaders communicate directly to the Chief engineer. This group of leaders will meet once a month to update each other of the changes and progress within the groups. During these meetings the technical aspects of the mission will be the primary focus. The Chief engineer communicates to the board in a monthly meeting, and the total Stratos III mission progress is discussed. The respective board members communicate the results of the meeting and the progress of the Stratos III mission to the people that require the update. These people include the DARE members and all stakeholders. In order to present the results to stakeholders and anyone interested, DARE will have to hold design reviews quarterly. These reviews will discuss the progress made by the team and the plans for the next quarter.

6.2 Design and Development Logic

The project design & development logic, PD&D, shows the activities that have to be performed from the DSE up to the launch planned in the summer of 2017. The final product of this DSE will be a Phase-A conceptual design, although some subsystems have already moved into the Phase-B preliminary design. The system still has to go through the following phases before the project can be completed.

Final Formulation Phase

- Phase B: Preliminary Design and Technology Completion

Implementation Phase

- Phase C: Final Design and Fabrication
- Phase D: System Assembly, Integration and Test
- Phase E/F: Launch and Closeout

Details of each phase can be found in this chapter, but a basic overview is given in Figure 6.3.

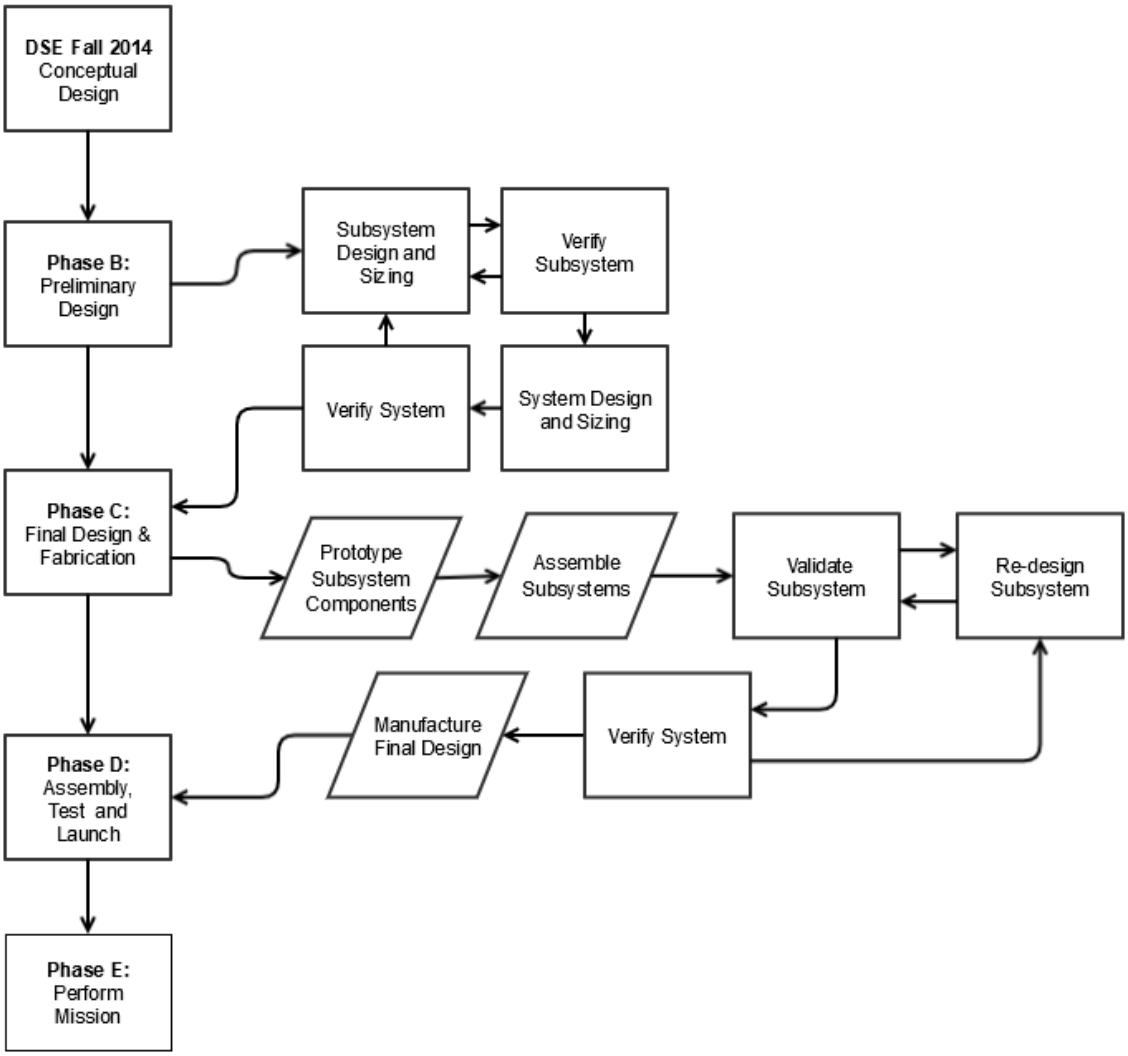

Figure 6.3: *Design and Development Logic*

6.3 Planning of the Stratos III Project

Once the Stratos III DSE is complete, the project will be assimilated into the current DARE inventory and will be the follow-up for the Stratos II mission. This section lists all the required steps over the next years. The next two years will consist of the development and testing for each of the required subsystems. After which the system will be assembled and launched. This section shows the milestones over the next years.

6.3.1 Milestones

Milestones are key achievements that indicate the progress of a project. The milestones for the different subsystems can be roughly categorized in the following way:

1. Project transfer to DARE
2. Internal organization of DARE
3. Design review
4. Small scale testing
5. Design review
6. Large scale testing
7. Integration testing
8. Final design review
9. Manufacturing

The first major milestone is the transfer of the project to DARE. This is done by presenting the results in a presentation and a final technical report. DARE will then have to start organizing themselves. They will need to have different teams, which cooperate and communicate well with each other, in order to get the Stratos III mission off to a good start. A well thought out team structure is important for efficient communication between project members and to keep the project on track. Therefore DARE should take sufficient time for this planning phase.

The next phase is studying the project as outlined in this report. DARE has already been updated regularly on the progress of the DSE team, however not all members have had a chance to review the design. The second phase for DARE is to review the rocket and mission design created by the DSE team. This is the part where DARE can make adjustments to parts of the system and project planning.

As soon as the design is approved by DARE, the development of the different subsystems can begin. Some subsystems have been designed in less detail than others, especially ADCS and Propulsion need more development than the others. A more detailed design should start at soon as possible for these subsystems. Tests are also needed for more detailed design, these tests contain the small scale tests and lets the students get familiar with handling the new materials. A more detailed overview of the required small scale testing can be found in the Gantt chart presented in Appendix D.

After the small scale tests, the design can be refined and uncertainties will be reduced. The design should now slowly start to go toward a finalized design where all the bumps are smoothed out. This is also the phase to re-evaluate the previously made choices based on new information and developments.

After a second design review, large scale testing can commence. These tests will be representative for the final rocket since they will be the same size and use comparable components as the final product. During these tests DARE can see what effects the scaling of the subsystems have and whether there are still errors in the design. However, these tests are very expensive and should therefore be carefully planned and thought out.

Integration testing is done as a last phase of the full scale testing. During these tests the hardware will be implemented in the flight configuration and tested. For the engine, for example, this would mean that it will be tested with the oxidizer tank attached instead of a separate oxidizer feed.

The final design review is done just before building the final rocket. It consists of checking all the drawings and results for one final time. This will also be the moment when the DARE members are shown the final results. After the final design review the building and assembly can start. The assembly is the last step before transport and launching the rocket. A general overview of the milestones for each subsystem is given in Figures 6.4, 6.5, 6.6.

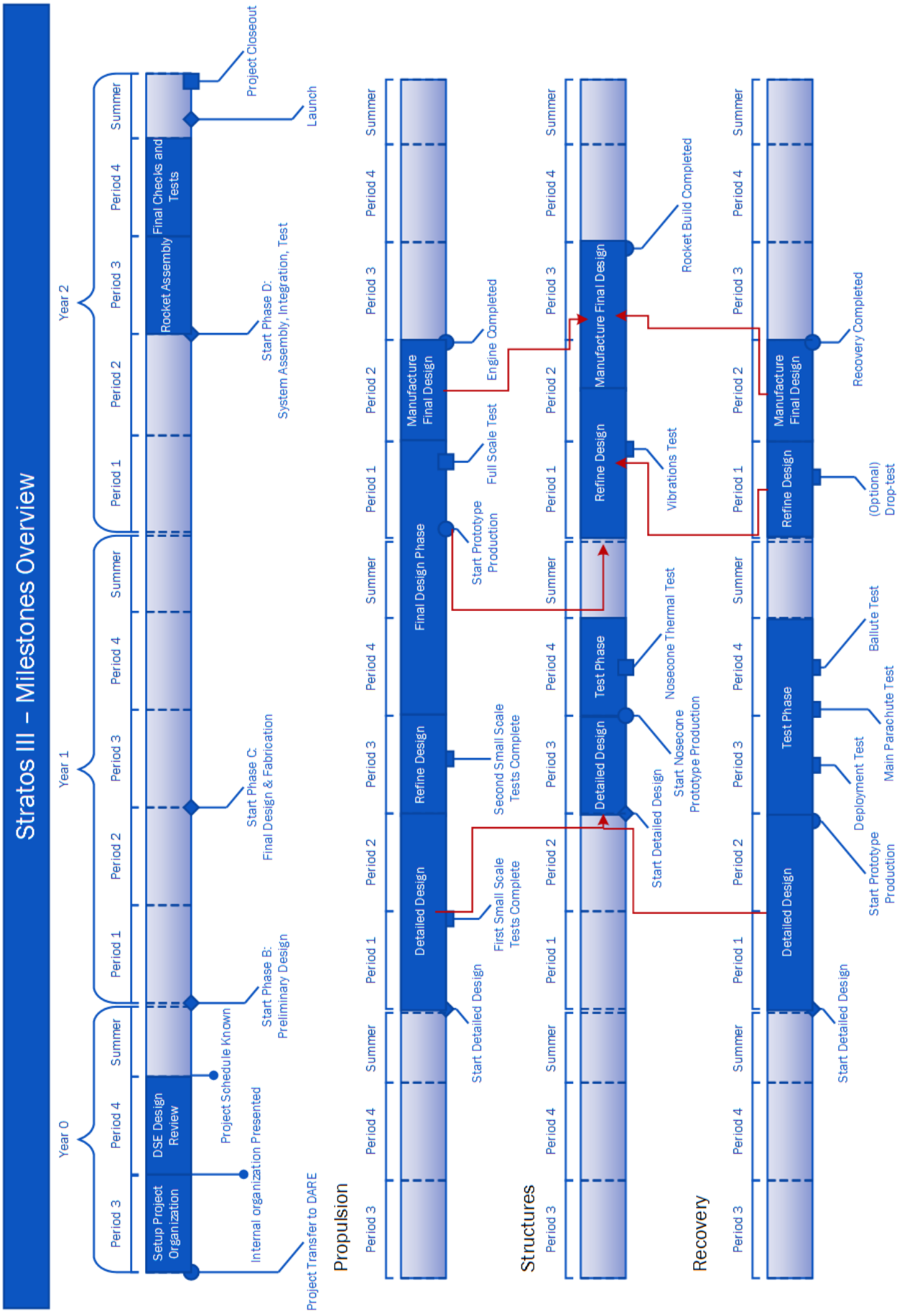

Figure 6.4: *Milestones Overview for Stratos III Mission (1/3)*

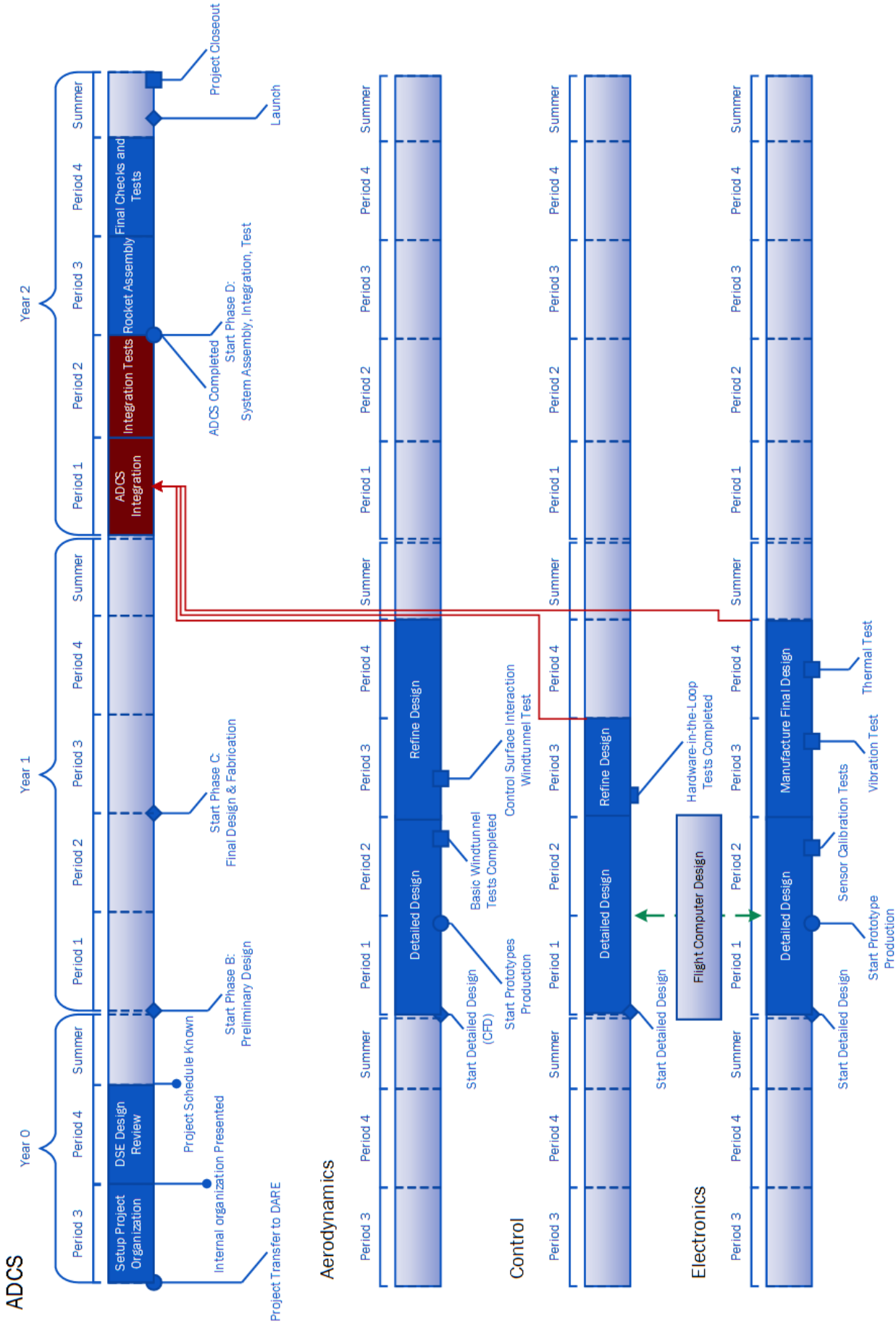

Figure 6.5: *Milestones Overview for Stratos III Mission (2/3)*

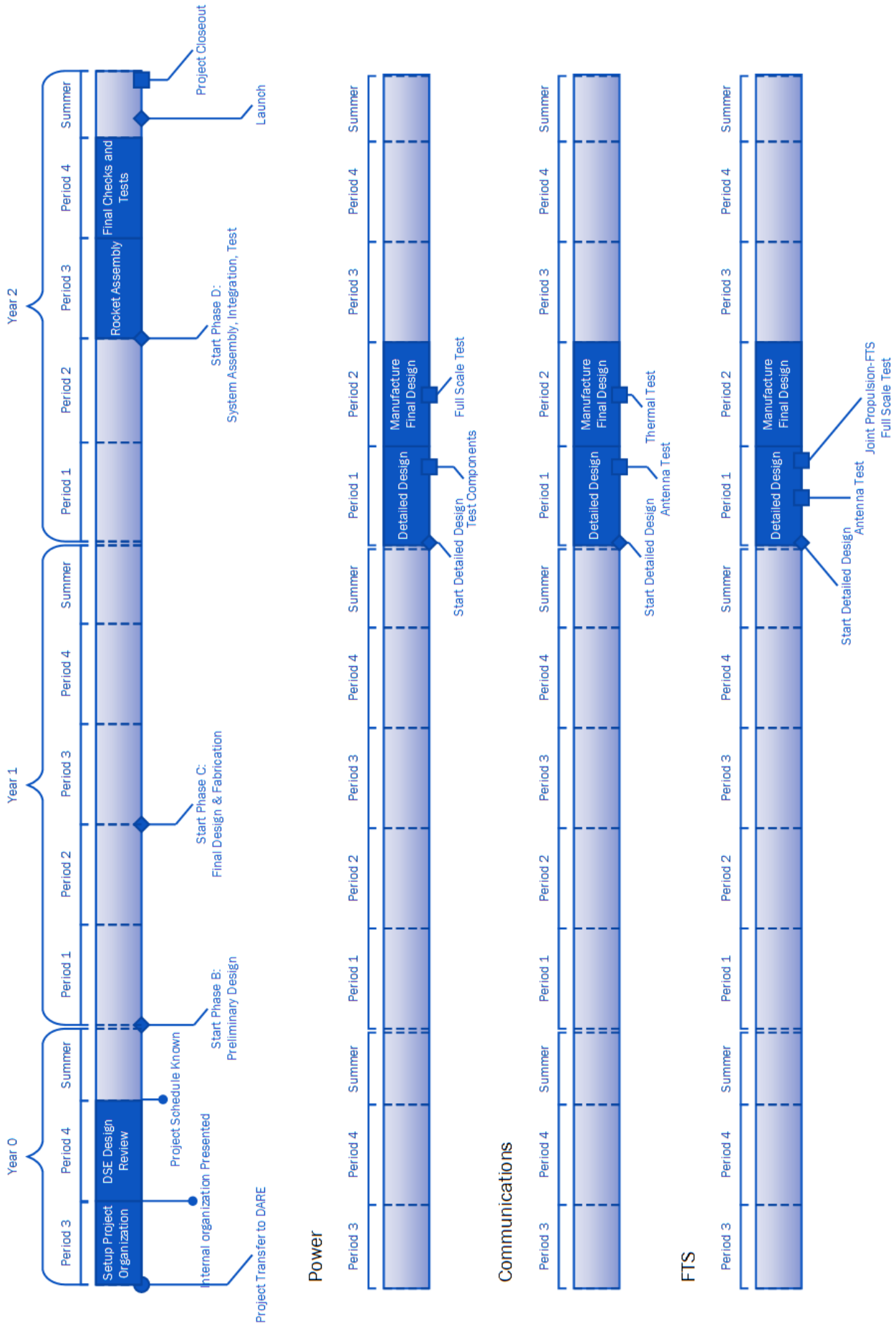

Figure 6.6: *Milestones Overview for Stratos III Mission (3/3)*

6.4 Development Strategy

The DSE will only deliver a conceptual design for the future Stratos III mission. This means that a development process must be undergone for all subsystems. Development will be the detailed design, testing and integration of each subsystem. This development can be done by internal DARE teams, minor teams, and possibly other DSE projects. Stratos III will incorporate COTS material and technology as a major aspect of its development. This COTS includes the materials and technology that have already been used in the past DARE missions or technology present within third party companies. This can significantly reduce the complexity and cost of the development, hence the production will be more convenient and efficient. The development strategy for each subsystem is given below.

6.4.1 Propulsion

The Propulsion subsystem can be split up into three groups in terms of development: the oxidizer tank/feed system, the combustion chamber and the nozzle.

Oxidizer Tank/Feed System The oxidizer tank and feed system group will focus on Nytrox pressure-temperature modelling and control followed by a feed system design. The first step would be to develop an accurate model for the oxidizer state and properties within the tank. Then the next step is to simulate temperature control for the oxidizer tank by using insulation, oxidizer fueling and venting. Once the simulation is complete, it should be validated by a small scale oxidizer tank testing. Running in parallel with the oxidizer tank simulation and modelling would be the feed system simulation and modelling. As soon as the oxidizer state and properties have been defined within the tank, the feed system can be sized. When the oxidizer tank temperature control test is performed, the oxidizer tank can be connected with the feed system to validate feed system sizing and flow properties. Additionally, the feed system should be checked for any anomalies such as frozen valves, ice forming, deformation and leaks.

Combustion Chamber The Combustion chamber group will first determine the solid propellant composition and its material properties. By testing different compounds with different mass fractions to be used as fuel, the regression rate coefficients and structural integrity of the grain can be determined. Then, in parallel with the nozzle group, the combustion chamber is to be integrated with the nozzle and tested. In this test, regression rate, combustion chamber temperature, combustion chamber pressure and thrust profile will be recorded. Anomalies such as combustion instability, incomplete burn and heat concentration over any part of the combustion chamber need to be recorded and dealt with appropriately. Combustion instability can be mitigated by changing solid propellant composition. Typically, reducing the aluminum mass fraction of the compound helps reduce combustion instability. Incomplete burn can be reduced by changing the mixer plate design to better atomize and distribute oxidizer mass flow or by adjusting oxidizer mass flow. Heat concentration can be solved by reinforcing that particular area with thicker material or by reducing combustion chamber temperature by changing the solid propellant composition.

Nozzle The main goal of the nozzle group will be to minimize the weight of the nozzle while retaining structural integrity during burn time. Since the size of the nozzle will mainly be dictated by the combustion chamber pressure, the design of the nozzle will only incorporate at which altitude optimum expansion is desired. However, if graphite/steel nozzle design is to be used on the rocket, extensive thermal tests need to be performed to check the possible deformation or failure of the nozzle. As mentioned above, a prototype nozzle will be integrated with the combustion chamber during a firing test to be validated.

6.4.2 Structure

The structural aspect of the rocket is fully COTS. The aluminum tubes can be bought from the same store as the tubes from the Stratos II rocket. The same goes for the composite nose cone, DARE already has a lot of experience with these and should be able to make it quite easily. The attachment points for the Stratos II were re-evaluated and considered to be capable of flying on the Stratos III mission as well.

6.4.3 ADCS

The ADCS subsystem is split up into three different groups. This is deemed the most efficient way, so groups can work alongside one another before integrating the three systems into the final ADCS. The groups are divided as follows: a control group, an electronics group and an aerodynamics group.

Control group The control group will be focused on the programming of the flight computer. The first step is to review the base flight computer by analyzing shortcomings of the Stratos II computer. Next, the flight computer has to be modified such that it can provide active control. An auto-pilot must be developed, this will be the most intensive problem for the Control group to deal with. When this is complete, a hardware-in-the-loop verification method should be used to check the developed auto-pilot. Artificial inputs must lead to correct deflection of the canards.

Electronics group After reviewing the proposed determination system set up by the DSE, more detailed electrical block diagrams for each PCB must be set up. Knowledge must be gathered on more practical aspects of implementing sensors and microcontrollers. Alongside this, the sun sensor must be developed and tested so its accuracies are known. Communication with the Delfi Space program could prove useful in this phase, as they have already used similar quad photodiode sun sensors in the past. After acquiring an unrestricted GPS, the GPS needs to be tested by a program that can generate signals which simulate velocities past COCOM limits. Also, if possible, it would be ideal to send the unrestricted GPS chip as a payload on Stratos II to verify its unrestricted capabilities. The 6-DOF IMU needs testing and calibrating using a rate table test to maximize accuracy. Next, the Kalman filter for the flight computer needs further research in order to implement it sufficiently. Furthermore, a thermal inspection must be completed on the flight computer in order to determine the weight of heat sinks and fans. Finally a hardware-in-the-loop verification method should be used to check whether the sensors can work together with the flight computer to supply sufficient accuracies.

Aerodynamics group The most intensive part of the active control design will be the aerodynamics. Although a rough estimation has been made with linearized supersonic theory, the interactions in supersonic flow between control surfaces and the body have not been taken into account. The shift in center of pressure was deemed constant after Mach 1.5. These assumptions need to be checked using a CFD model, which analyzes flow over the body at angles of attack from 0 to 10 degrees, where the air flow is still close to linear [53]. Furthermore, a supersonic flutter analysis needs to be completed to check whether the thickness is sufficient to avoid control surface oscillations. The Theodorsen method is the primary method to do this [45]. Once these models have been created, the fins and canards should be adjusted and manufactured. The canards can be put in a supersonic wind tunnel to get the lift at each angle of attack. After this, the actuators can be selected by using the canard lift to find the torque on each canard and size the actuators accordingly. The tail fins are then assembled to the body and the active control system is integrated into the flight computer.

Finally, bringing it all together, a full scale integrated ADCS test must be completed. This comes in the form of a full scale subsonic test and is the final step to check stability and check whether the active control system is working sufficiently with the determination system.

6.4.4 Power

DARE has a lot of experience with designing the Power subsystem for other missions including Stratos I and Stratos II, so the development of the subsystem for Stratos III will not be a very difficult task. The Power subsystem for Stratos III will primarily be based on the Stratos II power system. The electrical architecture is very similar to that of Stratos II with some parts of modification to meet the requirements of Stratos III, so DARE can manage the development with ease. Batteries from the same provider, Stefansliposhop, will be used. The power capacity of the batteries will first be verified and validated by running each component to confirm that they deliver enough electric power. Although the batteries are not going to be used for the entire flight, they need to be tested in extreme conditions like high or low temperature, low pressure and shock for the predefined time of function.

6.4.5 Communications

The Communications subsystem components of Stratos III will be mainly based on those of Stratos II. The subsystem has been actively developed in the past by DARE for other missions including Stratos I and II. The most ideal way of developing the Communication subsystem for the Stratos III is to test the one for the Stratos II during the latter's mission. From the analysis, it has been found that the power received (in dBW) and the SNR ratio at an altitude of 120 km are only about 10% less than at an altitude of 50 km. A lot of valuable information can be used from the Stratos II mission given its success. The power received and strength of signal at the telemetry receiver stations can be recorded and this data can be used to validate the script that was created to analyze the telemetry parameters. The data storage components after retrieval

and analysis can demonstrate whether the antenna amplifier was generating too much heat and whether the thermal control system was adequate.

Moreover, it can be verified that the configuration of the receiver stations and their respective distances from the launch site was appropriate. The extent to which the Stratos III receivers can be scaled up is then determined from the test data of Stratos II. It is important that the rocket can communicate with the ground station (telemetry receiver stations) for as much time during the airborne phase as possible and this can be verified from the Stratos II mission. Finally, the design of the Communication subsystem for the Stratos II can be reviewed for strengths and weaknesses and this can give a good basis for the development of the Stratos III.

6.4.6 FTS

The Stratos III flight termination system development should expand on the knowledge of the Stratos II FTS. First next steps can be to simulate different antenna configurations, start the preliminary design for the electronics and decide on a test plan. Some tests will have to be done in conjunction with the propulsion team in order to test the FTS communications link in presence of the exhaust plume. If the team wants to have the FTS antennas integrated into the fins, some engineering effort has to go into that integration.

6.4.7 Recovery

The Recovery subsystem of Stratos III will be significantly different from the one designed for Stratos II. However, experience and lessons from Stratos II can still be of great use. The first step is to perform a preliminary design review, after which the next design phase can start. In this next design phase thorough calculations will lead to a detailed design as well as a CATIA model and a test plan. It should also become clear how flexible the current system is in terms of scaling and performance. Before production can start, a critical design review will take place. In this review the design will be presented to other team members and eventually the decision to start production and testing can be made. In the construction phase the entire Recovery subsystem will be produced. After construction the system properties should be evaluated to check if anything has changed, e.g. system mass or aerodynamic behavior. The next step is to perform all the tests. After verification and validation all design changes should be implemented and documented. The flight itself is also a part of validation. Post-flight the entire process should be documented as well as giving recommendations for future projects.

6.5 Production, Manufacturing and Assembly Plan

After successful the design and development of the rocket, manufacturing will be done by using all the resources and facilities available for DARE and TUD, such as the Dream Hall. If any technology required is not present within DARE/TUD it will try to be accomplished with the help of external sponsors. In the case of Stratos II, for example, this meant that the hot fire tests of the engine were done at TNO. The following sections describe the different subsystems and their respective production, manufacturing and assembly plan.

6.5.1 Propulsion

A list of parts within propulsion subsystem which need to be produced are shown below.

- Oxidizer tank bulk heads
- Mixer Plate
- Nozzle

The oxidizer tank bulk heads and mixer plate can be machined from solid metal blocks using the CNC machines available at TUD. In a similar way, part of the nozzle can be machined from a solid block of graphite. However, the steel skirt section of the nozzle will need to be specially forged and treated by an outside manufacturing company. If the acquisition of such special part proves to be difficult, the nozzle design can be reverted back to machining solid block of graphite. Other items can be bought from outside companies. These items would include valves, piping, solenoids and sensors.

As for the manufacturing and assembly of the propulsion subsystem, the oxidizer tank will be manufactured first. The top and bottom bulk heads will be fitted into the rocket shell, bolted in place and sealed. The next step is the combustion chamber manufacturing. First the nozzle will be fixed into place within the combustion chamber shell. Then solid propellant will be manufactured by pouring liquid state compound into the combustion chamber. The speed at which the compound is poured and stirring the compound might have

a great impact on the production of evenly distributed solid propellant grain. Once the grain hardens, an igniter holder, a thin wooden plate, will be placed on top of the grain followed by an injector plate which will be bolted against the wall of the combustion chamber completing the combustion chamber section. Finally the oxidizer tank section and the combustion chamber section will be connected together by a coupler ring which will also serve as housing for feed lines and valves. Once the coupler ring has been installed, feed lines, valves and solenoids will be put in place connecting the oxidizer tank to the combustion chamber.

6.5.2 Structure

For the structure part, the production plan can be very similar to Stratos II, the aluminum tubes have to be cut into different parts to produce the chamber pressure, valve space, oxidizer tank and the capsule. These are attached to each other using a simple bolt connection with an inner aluminum ring. For the glass fiber nosecone on the inside, a metal ring needs to be bonded in order to attach it to the metal shell. For the nozzle attachment an aluminum ring needs to be attached at the very end to hold the graphite part of the nozzle in place, that same ring will also hold the metal skirt in its place.

6.5.3 ADCS

After all the necessary parts for the determination system are bought, the Electronics team must solder them on PCBs and create an IMU with 3 gyroscopes, 3 accelerometers and 3 magnetometers. Next, the sun sensor, GPS and altimeter need soldering onto their own PCBs. The structure supporting and connecting all these PCBs then needs machining using the CNC machines at TUD and connecting with the inside of the fuselage. For implementation of the sun sensor and the altimeter holes need drilling in the fuselage and need to be filled by a transparent acrylate polymer and connecting with the sensor. The stabilization fins will be machined from a sheet of aluminum and fitted to the rocket by welding both sides of the fin to the body. The weld must be as symmetrical as possible for each fin. A hole needs to be drilled into the airfoil of each canard so the actuator can be fitted. Inside, a strong structure needs manufacturing to hold the actuators in place.

6.5.4 Power

The batteries will be purchased from Stefansliposhop.de in Germany, the supplier for the Stratos II mission, to reduce the effort of looking for the new supplier. The PCBs will be constructed by DARE members as it has been for the past missions.

6.5.5 Communications

Since DARE has experience with building their own electronics, their dedicated Electronics team will be responsible for acquiring the necessary resources, designing and building the PCBs. The antenna and the amplifier can be bought based on the design requirements. The fans and heat sinks can be bought in stores selling computer parts. Given the work that the Stratos II electronics team performed on its Communication subsystem, it is expected that there exists the necessary expertise within DARE to integrate all the parts and optimize the system.

6.5.6 Recovery

Most materials for the main parachute can be bought from kite shops and shops specialized in skydiving materials. The large canopy will likely have to be custom made, since shops usually don't sell cloths with a larger width than 1.5 m. Sewing the 5 canopy parts together can be done by the shop Naaiattelier Stratos. They also produced the canopy for Stratos II. This is however quite expensive, €200 for Stratos II. It should therefore be considered to do it within DARE. An initial search for shops selling the material used for the ballute, type 455 Nomex, proved fruitless. It may be required to contact specific companies and have the material be custom made. The mortar tube can best be bought off the shelf, because there are a lot of different tubes available. The mortar cap can then be custom made and holes need to be drilled in the cap and tube. The bulkheads connecting the inflatable decelerators to the rocket can be machined from solid metal blocks using CNC machines available at TUD. They can then be attached to the rocket using simple bolt connections. The explosive bolt can be bought of the self and connection to a bulkhead using bolt connections.

6.5.7 FTS

The electronics team will be responsible for acquiring the necessary resources, designing, and building the PCBs. The antenna and the receiver can be bought based on the design requirements.

6.6 Operations

This section describes all of the logistics required to launch the rocket successfully. This includes the transportation of the rocket, fuel, and required materials to and from the launch site and launch procedures.

6.6.1 Transport

Transportation of the rocket and materials from and to the launch site will be done using a rental truck. The DARE members will fly in shifts to the launch site and stay on the base. DARE members pay a certain fee [1] in order to fly to and stay on the base. This fee covers most expenses for housing and food during the launch campaign. The launch campaign contains the full two weeks that the DARE members are required to be present on the base

The materials used in the Stratos III project are non-toxic and non-explosive when kept separate. This means that during transport the risk to the people handling the rocket is minimal. All oxidizer will be delivered to the launch site by a third party company, which means that the safety and transport is of no concern to the students. The transport of the solid fuel, however, is of concern. Fortunately, the paraffin without the oxidizer is non-explosive and safe to handle. The following parts of the rocket can however cause a risk during transport:

- Paraffin is a fuel. This means that it will burn or explode when in contact with an oxidizer and an ignition source. The flash point of paraffin wax is about 200 $^{\circ}C$.
- The mortar deployment system used in the recovery system will be dismantled for transport. However, this means that there is still a pressurized/explosive substance situated.

For all of these points a license has to be obtained with the ADR office [54]. Furthermore, the mixing of the oxidizer is done at the test center. Therefore safety will fall under the responsibility of DARE/INTA members.

6.6.2 The Launch

The entire Stratos III program culminates into the launch of the Stratos III sounding rocket. The goal is to launch Stratos III about two years after the launch of Stratos II+, which would put the launch date in 2017. The following section describes all the aspects required for the launch and all the events leading up to the launch.

6.6.2.1 The Launch Site

The preferred launch site for the Stratos III rocket is INTA's launch range El Arenosillo. This will also be the launch site of Stratos II+ mission. The major advantage of El Arenosillo is that there is already good communication between both organizations. El Arenosillo is also one of the closest launch sites to Delft, INTA offers a very good launch cost to DARE, and they already have the tracking equipment required for the launch.

The El Arenosillo test center is located near Mazagón in Spain in the province of Huelca. According to DARE internal documentation INTA has the capability to scan both the air and sea in order to provide a safe operating space for the launch. In addition, INTA possesses the tracking and communication equipment that allows the ground to follow and see the rocket at all times. During the previous attempted launches with DARE/INTA, the launch crew at INTA assisted the DARE team a lot during procedures.

6.6.2.2 Launch Windows

On every launch day there will be one or two launch windows of several hours. During these windows the firing range and landing zone are cleared and the rocket is prepared for launch. The launch window can be divided into five phases. Before a launch window is started all the preparations that can be done the day before will already have been done. The launch phases are shown in Figure 6.7 and described in the sections below the figure.

[1] The launch fee for the Stratos II launch was €350 per member

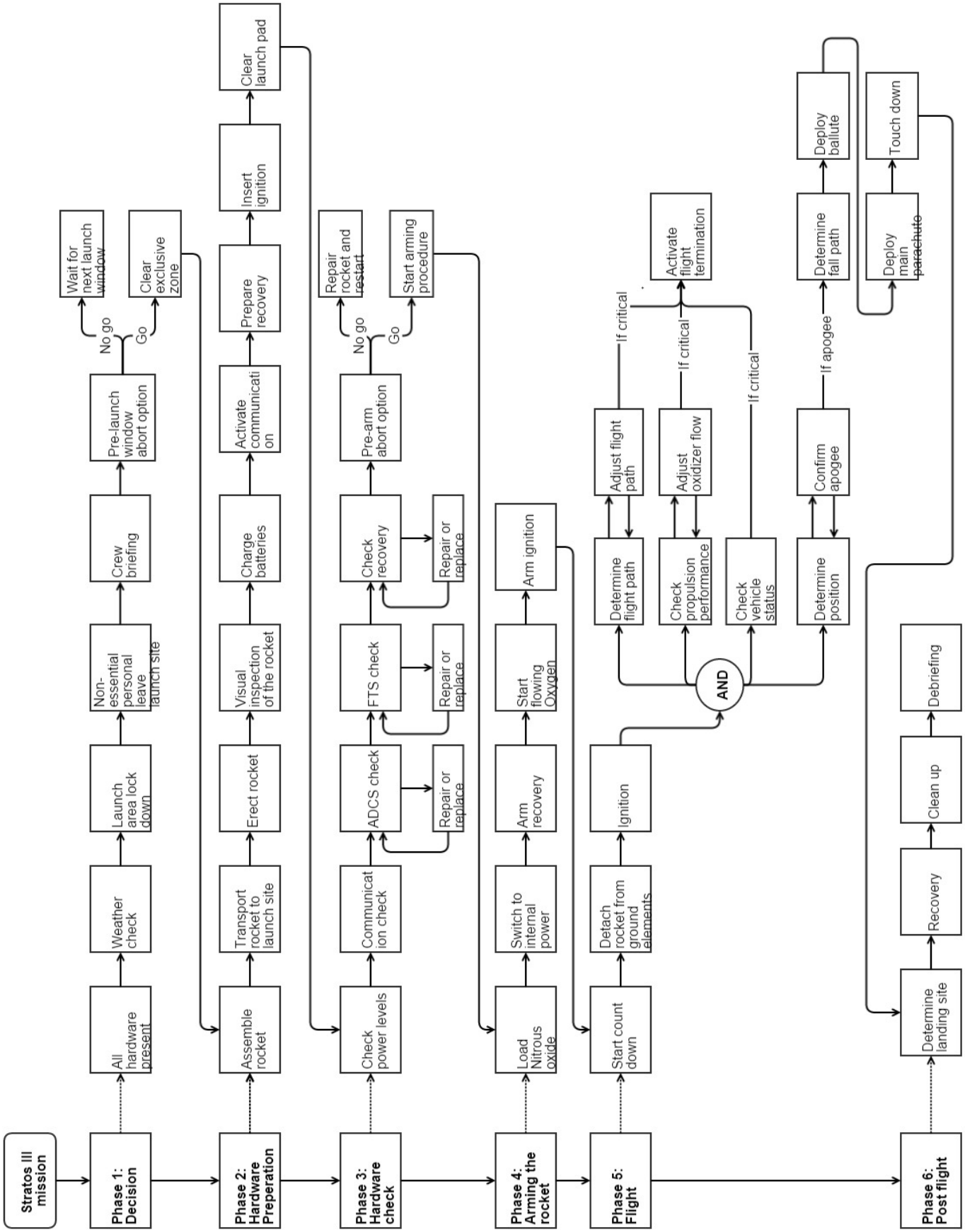

Figure 6.7: *Functional Flow Diagram for the Stratos III Mission*

Phase 1: Decision The first phase of the launch is to make the decision whether to prepare for the launch. This phase includes a weather check with high and low altitude balloons, mission briefing for all personnel involved, and a lock-down of the launch area. By the end of this phase the entire crew knows what they should do for the following launch window, and a go or no-go decision is made in collaboration with INTA.

Phase 2: Hardware Preparation If the launch window is a go, the hardware for the mission can be put in place. This phase means transporting the rocket to the launch pad, erecting the rocket, fueling the rocket, and starting up all subsystems. By the end of this phase the rocket is flight ready. The launch pad is now cleared from personnel. The tracking hardware at INTA will also be activated in this phase.

Phase 3: Hardware Check The rocket is now standing ready on the launch pad and the area is cleared for launch. During phase three the checklist for each subsystem will be run by the responsible crew member. If all systems give a go for flight the mission will continue. By the end of this phase the rocket is powered and cleared for flight.

Phase 4: Arming the Rocket This phase ensures all systems are armed and prepared for flight. The power is switched to internal power, the rocket is fueled, pressurized and armed. By the end of this phase all that is left is the countdown and the actual flight.

Phase 5: Rocket Flight With all systems go, the rocket enters its last minute on the launch pad. From this moment on, the rocket launch can only be aborted should there be serious safety risks. If no such event occurs, the rocket will be launched at T-0. This phase is completed when touchdown occurs. A detailed description of the flight phase can be found in Section 6.6.2.3.

Phase 6: Post Flight As soon as the rocket lands in the ocean the recovery crews will start looking for it. At this moment the tracking and recording operations are stopped and the rocket is recovered. To finalize the operation, a debriefing is held and the mission is celebrated.

6.6.2.3 The Flight

The flight is considered the phase from the moment the countdown is started to the moment the rocket touches down.

During the countdown the rocket is cleared for flight, and the launch will be just seconds away. By the end of the countdown phase the engine is started and the tracking equipment is locked onto the rocket.

For the first part of the flight the Stratos III rocket will fly on the combination of liquid Nytrox inside the oxidizer tank and the paraffin-based solid grain in the combustion chamber. During this phase the rocket has the most thrust and will be flying through the thickest atmospheric layers. After the first powered phase, the liquid Nytrox will be depleted. This means the rocket is literally flying on the last fumes of fuel. This means that the rocket has far less thrust than it had in the first phase but will still be accelerating. Should anything go wrong during this phase of the flight the flight termination system can be activated in order to guarantee safety.

The powered phase is followed by the coasting phase. In this phase the kinetic energy build up during the powered phase is transformed into potential energy. The rocket will slow down as it is increasing in altitude until it finally slows down to zero vertical velocity and reaches apogee. During the coasting phase the rocket will leave the atmosphere, therefore the canards will not be functioning anymore and the rocket will experience weightlessness. At this point the rocket will have to be on course.

As the apogee is reached the altitude record should be broken. After apogee the rocket's altitude is decreasing and the recovery phase starts. The recovery phase begins with a free fall phase. During this phase the rocket will re-enter the atmosphere. As soon as the rocket hits any mentionable atmosphere it will rotate to a nose down position and the ballute is released. After the rocket slows down to acceptable velocities the main parachute can be deployed. If the main parachute is deployed, the rocket will rotate into a tail-first attitude and slowly drift down to the ground. After a long recovery phase the rocket splashes down into the ocean and the flight is complete.

Figure 6.8 shows the flight of the Stratos III with the relevant altitudes and flight phases:

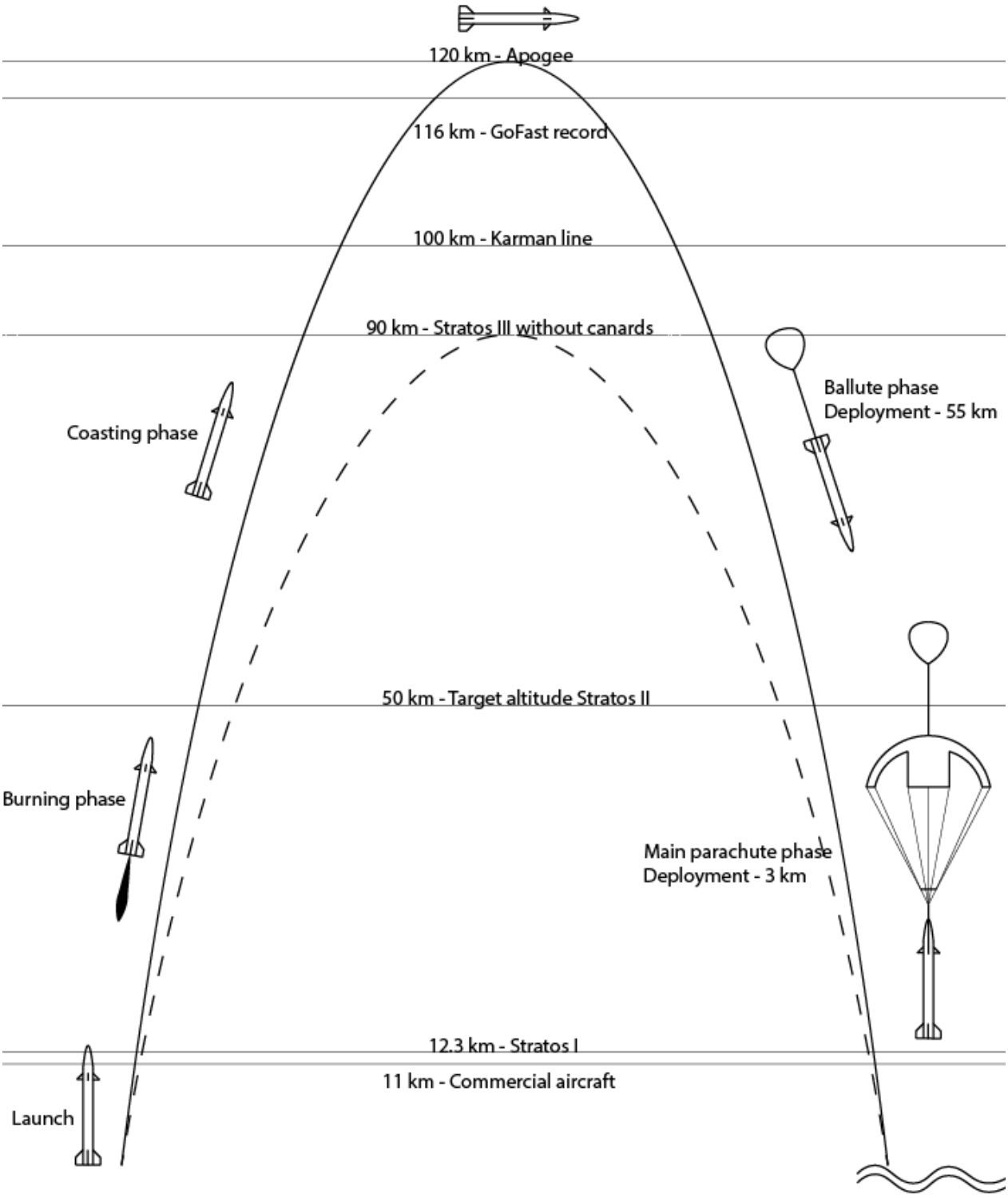

Figure 6.8: *The Flight Path of the Stratos III Mission with the Relevant Altitudes*

6.6.2.4 Abort Modes

There are several reasons why one would want to abort the launch. This section gives the different abort modes used in the Stratos III mission with the respective reasons and consequences of the abort.

Pre-launch Window Abort The launch window can be aborted for several reasons. A launch window abort means that the entire window is scrapped before the rocket even leaves the hanger. This could be done in a scenario where the weather is not good enough or when the launch area is not locked down for the launch

window. The team is now forced to wait for the next launch window.

Pre-arm Abort The decision not to arm the rocket can be made just before the start of the fourth phase in the launch window. This can be done for several reasons, however all reasons are related to the technical aspects of the rocket. Should any part of the rocket not be cleared for flight and cannot be replaced or repaired on the launch pad this abort mode is called in. The team will now have to repair the rocket and wait for the next launch window.

Emergency Abort During any moment of the launch procedure an emergency abort can be called in. This abort mode means that there is a severe enough reason to abort the mission. This could be anything that jeopardizes the life and safety of the launch crew or any other human life. This could be because of unauthorized personnel on the base or exclusive zone or any other unforeseen event. In the best case the launch team can continue within the same launch window. In the worst case, however, they will have to wait for the next launch window.

If the rocket is already armed and fueled the team cannot approach the rocket. The Nytrox is dumped into a separate tank and the rocket is left to vent. During the procedure the team will have to wait for the green light.

In-flight Abort Should the ground team lose control of the rocket in mid-flight, the flight termination system is activated. The design of the FTS system can be found in Section 4.9. The FTS is activated if the rocket cannot maintain its flight path and threatens to leave the exclusive zone and therefore endangers people. Another reason to abort the flight is if the propulsion or structure starts to fail and the team feels they can save the rocket by terminating the thrust.

6.7 Resources

DARE will require a lot of different resources for the Stratos III mission. These different resources come in the categories of materials, financial, knowledge, work, experience, testing, and launching. For all of these categories the DARE teams will be dependent on different third-party people.

6.7.1 Materials

Materials are available within many companies that DARE already has contact with. According to the Stratos II sponsoring team, it is considered to be easier to get material sponsored then money. This has to do with two factors. The first is that the companies already have the facilities to produce these materials and structures. The second is that companies would much rather see their work fly, than have their money hidden somewhere within a large project. Therefore the materials should be relatively easy to find.

6.7.2 Financial

Finances within DARE are divided among the different projects within DARE. This means that part of the Stratos III project will be funded using money from TUD and DARE members. A second source of money comes directly from sponsors, these sponsors will be sought separately from other activities within DARE. Alternatively DARE could set up a crowdfunding/Kickstarter project in order to reach their goal. The Boston University Rocket Propulsion Group showed that a Kickstarter can collect up to $ 17,000 [55]. As stated in the materials subsection, it is easier the get materials sponsored than finances. Therefore the money will primarily be used to perform experiments, transport, construction and launch. Kickstarters are a great way to get a initial sum of money that allows DARE to start showing results and gaining more sponsors.

6.7.3 Knowledge

There is already a lot of knowledge within DARE and TUD. Unfortunately not all knowledge is available to a student team and therefore third party companies are asked to assist the Stratos III team. There are a number of companies that have experience with sounding rockets or space flight in general. The companies that the Stratos III program could ask for help include Airbus Defense and Space Netherlands [2], ESA, APP, BAE Systems, TNO, or Dassault Aviation.

[2] Previously: Dutch Space

6.7.4 Work and Experience

As with knowledge, there is a lot of experience with the rocket building. However, most of these rockets fly at much lower altitudes. Even the Stratos II mission was very hard for DARE to complete. The Stratos III can continue to build on the experience of Stratos II, but a lot of uncharted territory is still to be explored. Besides the teams within DARE that will work on the scaling up the engines and the active control system there are other student resources that DARE could use. These resources are the minors and the bachelor thesis [3]. All faculties have their final thesis programs, which are all available to DARE. The requirements for such projects would have to be set up as the need arrives. Minors are done once every year for the duration of one semester and the DSE projects are done twice every year.

The production of the Stratos III rocket will be done in the Dreamhall situated on the campus of TUD. The Dreamhall possesses a lot of experience with the production and construction of the different Dream projects within TUD.

6.7.5 Testing and Launching

As determined earlier in this section, the launch of Stratos III will most likely be done in El Arenosillo on the launch site of INTA. INTA not only can give DARE a significant reduction in launch cost but also supply the experience in launching sounding rockets that is much needed when launching Stratos III.

Testing for the Stratos II was done mainly on the campus of TUD. The larger rocket tests were done on a test ground of TNO in Germany. Here stands a bunker that allows for full scale testing of the different engines. One other major method of validation for Stratos III is its predecessor, Stratos II. The flight of Stratos II validates the simulation software written for Stratos II and part of the coding for Stratos III. It will also be the flight test for the hardware and reasoning behind the hardware of Stratos II. Other possibilities for testing can be researched by the different sub-teams when the need arrives.

6.8 Mission Compliance Matrix

In the Baseline Review, several requirements were written down for the system and different subsystems, which can be found in Appendix B. This section looks back at the requirements and shows which requirements have been met and which have not.

Identifier	Compliance (F/P/C/N/X) [4]	Verify (I/A/D/T) [5]	Notes
STR-MP-CON-01	F	I	
STR-MP-CON-02	F	I	
STR-MP-CON-03	F	I	The Dreamhall supplies different trainings for the usage of the equipment
STR-MP-CON-04	F	I	All tools required are present in the Dreamhall
STR-MP-CON-05	F	I	This is up to DARE to comply with during the build
STR-MP-CON-06	F	I	
STR-MP-ENV-01	F	I	
STR-MP-ENV-02	F	I	
STR-MP-FP-01	F	I	
STR-MP-FP-02	F	I	
STR-MP-FP-03	F	I	
STR-MP-FP-04	F	I	
STR-MP-FP-05	F	I	
STR-MP-FP-06	F	I	
STR-MP-FP-07	F	I	
STR-MP-LOG-01	F	I	The oxygen is transported by a third party company
STR-MP-LOG-02	F	I	

[3] In the faculty of aerospace engineering the bachelor thesis is called the DSE (Design Synthesis Exercise)
[4] F - Full, P - Partial, C - Requirement changed, N - Not complied with ,X - Requirement dropped
[5] I - Inspection, A - Analysis, D - Demonstration, T - Testing

STR-MP-LOG-03	F	I	
STR-MP-LOG-04	F	I	
STR-MP-RES-01	F	I	
STR-MP-RES-02	F	I	
STR-MP-RES-03	F	I	
STR-MP-RES-04	F	I	
STR-MP-RES-05	F	I	
STR-MP-RES-06	F	I	
STR-MP-SAVE-01	P	I	There is a contingency plan for each mission phase, but not in such a way that the rocket is always saved
STR-MP-SAVE-02	P	I/A	Handling a rocket is always dangerous. Especially the handling of the liquid oxygen during fueling. However, all necessary rules and regulations will be put into place
STR-MP-SAVE-03	F	I/A	
STR-MP-SAVE-04	F	I	
STR-MP-SAVE-05	F	I	
STR-MP-SAVE-06	F	I	
STR-MP-SAVE-07	F	I	All DARE members signed an agreement that they will obey these rules
STR-MP-SAVE-08	F	I	

6.9 Budget

In order to make an accurate estimation for the Stratos III mission budget, costs for each subsystem are required. These costs include the development and testing for all systems. The cost for the rocket hardware is taken into the value listed in Miscellaneous.

Table 6.2: *Overall Mission Cost Budget*

Subsystem	**Description**	**Cost**
Testing and development		
Propulsion	Full scale	40000
Propulsion	Small scale	10000
Recovery	Development and testing	10000
ADCS	Development and testing	20000
Power	Development and testing	2000
Communication		2000
Launch site		
Launch windows		20000
Transport to launch site		3000
Miscellaneous		
Public relations		10000
Rocket	Rounded up	10000
Total:		117000

Note that the budget for the ADCS system includes a Masters Thesis, which has a cost of €10.000.

6.10 Risk Analysis

Risk is always present in any project. However, the risks can be identified by means of a risk analysis so that the chances of mission success are as high as possible. Table 6.3 shows the risks for all subsystems divided into different categories. Failures are listed on the rows by the likelihood that the error will occur. In each column the failures are listed with respect to how serious each failure is and what impact they will have on the mission.
The seriousness of the impact on the mission is defined with the following categories.

- Negligible: Complete mission, rocket intact, launch delay of hours/day
- Minor: Complete mission, rocket intact, launch delay of weeks/months
- Moderate: Partial completion of the mission, minor damage to the rocket, possibility for a retry
- Serious: Mission failure, possibility for retry
- Critical: Mission failure, rocket lost

The risk analysis for the Stratos III mission was done in two steps. In the first table all possible risks are indicated. This table was created at the start of the design process when the team knew nothing about the configuration of the rocket. When the design was complete, the verification of the system provided risk mitigation and altered the risk analysis table. Several entries shift to the lower right or dissapear completely. Any other non-applicable were also discarded from the table.

Examples of non-applicable risks after the final design:

- Stage ignition failure [PRO]
- Stage separation failure [FP]
- Booster separation failure [PRO]
- Power regulation failure [PWR]

The first three risk options are removed because Stratos III will be a single-stage rocket and hence does not consist of stage or booster. Therefore considering the failure of stage or booster is needless. Power regulation failure is also eliminated because the power subsystem will use decentralized power distribution, and therefore does not require power regulation.

The risks that are considered to have less impact on the mission success are moved to other blocks, and are marked with asterisks in Table 6.5.

- Unexpected crew or civilian in the safety zone [SAVE]
- Large construction errors [CON]
- Tank rupture [PRO]

The first risk is moved from "Likely" to "Low likelihood" in the same column because the launch site has a lot of launch experience and it will not be a great problem for INTA to clear the safety zone. Also DARE has experience with building the rocket including Stratos II, so it is likely that there would not be a major fault in the construction of Stratos III. Therefore the second risk in the list above can be moved from "Likely" to "Low likelihood". The minimum required thickness of the fuel tank is 2.14 mm with the safety factor of 1.2, but the COTS aluminum tube that will be used for the construction has the thickness of 5 mm which provides more than enough structural integrity. Therefore this option can be moved to "Not likely" from "Low likelihood".

Table 6.3: Risk Map for Stratos III Program

	Negligible	Minor	Moderate	Serious	Critical
Near certainty	[STRU] Cosmetic damage				
Highly likely	[SAVE] Strong wind during launch window	[CON] Small construction errors	[PRO] Stage ignition failure		
Likely	[SAVE] Unexpected crew or civillian in safety zone	[PRO] Valve freeze [PRO] Ignition failure	[ADCS] Active control determination failure [CON] Large construction errors		
Low likelihood	[LOG] Transportation delay	[PRO] Leakage detected during pre-flight	[PRO] Leakage detected mid-flight [FP] Booster separation failure	[ADCS] Data storage failure [PWR] Power regulation failure [REC] Recovery deployment failure [COM] Communication software failure [COM] Communication hardware failure [FP] Stage separation failure [CON] Larger construction errors	[PRO] Serious leakage detected mid-flight [PRO] Tank rupture [ADCS] Active control system software failure [REC] Failure to deploy REC mechanism
Not likely	[PRO] Pipe blockage on the ground [LOG] Slight damage during transportation	[PRO] Power distribution failure during launch [STRU] Communication blockage [LOG] Minor damage during transportation	[PRO] Wrong fuel mixture [PRO] Pressure sensor failure [PRO] Mid-flight pipe blockage [PRO] Not enough fuel [LOG] Moderate damage during transportation	[ADCS] Stability failure [ADCS] Altitude determination failure [ADCS] Attitude determination failure [REC] Re-entry failure [REC] Lost payload [STRU] Thermal deformation of structure [LOG] Serious damage during transportation	[PRO] Mid-flight pipe blockage [PWR] Energy storage failure [STRU] Disintegration [LOG] Critical damage during transportation [FTS] Power loss in FTS antenna

Table 6.5: Risk Map for Stratos III Program after Risk Mediation

	Negligible	Minor	Moderate	Serious	Critical
Near certainty	[STRU] Cosmetic damage				
Highly likely	[SAVE] Strong wind during launch window	[CON] Small construction errors			
Likely		[PRO] Valve freeze [PRO] Ignition failure	[ADCS] Active control determination failure		
Low likelihood	[SAVE] Unexpected crew or civilian in the safety zone ⋆ [LOG] Transportation delay	[PRO] Leakage detected during pre-flight	[PRO] Leakage detected mid-flight [CON] Large construction errors ⋆	[ADCS] Data storage failure [REC] Recovery deployment failure [COM] Communication software failure [COM] Communication hardware failure	[PRO] Serious leakage detected mid-flight [ADCS] Active control system software failure [REC] Failure to deploy REC mechanism
Not likely	[PRO] Pipe blockage on the ground [LOG] Slight damage during transportation	[PRO] Power distribution failure during launch [STRU] Communication blockage [LOG] Minor damage during transportation	[PRO] Wrong fuel mixture [PRO] Pressure sensor failure [PRO] Mid-flight pipe blockage [PRO] Not enough fuel [LOG] Moderate damage during transportation	[ADCS] Stability failure [ADCS] Altitude determination failure [ADCS] Attitude determination failure [REC] Re-entry failure [REC] Lost payload [STRU] Thermal deformation of structure [LOG] Serious damage during transportation	[PRO] Tank rupture ⋆ [PRO] Mid-flight pipe blockage [PWR] Energy storage failure [STRU] Disintegration [LOG] Critical damage during transportation [FTS] Power loss in FTS antenna

Chapter 7

Marketability

No project is a success if it cannot be sold or if money cannot be raised for the actual build of the project. Stratos III is of no exception to this rule. The predicted cost of the Stratos III project, based on the cost of the Stratos II project, will be around €100,000. In order to impress the potential sponsors the Stratos III team needs to be different from its competitors. This chapter concerns the aspects in which the Stratos III rocket is better than any other amateur rocket.

7.1 Sustainability

Sustainability is the art of performing a mission without causing permanent damage to any of the surroundings. This means that the rocket launch will not endanger the future generations. Sustainability is based on three main factors or pillars: Economy, Society and Environment.

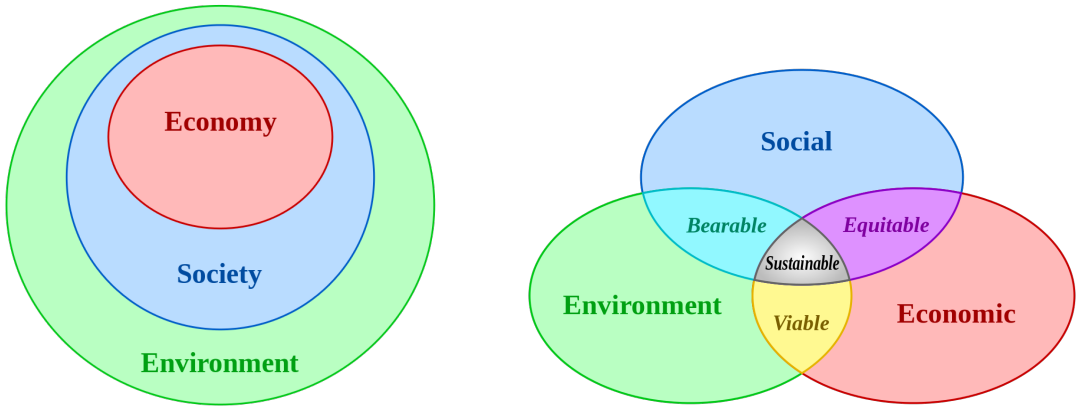

(a) *Diagram showing the three pillars of sustainability in a Nested form [56]*

(b) *Diagram showing the three pillars of sustainability in a Venn diagram [57]*

Figure 7.1: *Two Diagrams Showing the Different Ordering of Sustainability*

In order to be considered sustainable, one must obey three different pillars and with those pillars three different categories where the project will not damage the future. In Figure 7.1a it can be seen that the three pillars are limited by each other. Therefore one cannot be economically sustainable if the society does not want to cooperate or the environment does not permit it.

There are several factors that one could think of when considering a sustainable approach for Stratos III. These factors concern all three pillars.

- No part of the rocket will be left behind in or near the launch site
- No part of the rocket will be dangerous for students to work with, otherwise appropriate precautions will be taken
- No material will be wasted during any phase of the project
- Any waste will be taken to the appropriate recycling institutes
- No material or part of the rocket will be toxic for the environment

- The launch of the rocket will not be disturbing for the people living near the launch site
- The production of the rocket will not be disturbing for the people living near the production site

For the rocket itself this means that it will have to be completely recovered after launch, which means that, unlike normal sounding rockets, the Stratos III cannot simply discard the engine and only recover the payload section. The safety and toxicity requirements severely limit the fuel choice. This means that the sustainability requirements severely impact the propulsion and recovery subsystems.

Keeping these sustainability rules in mind the Stratos III rocket will become a sustainable rocket that will completely fit into the vision the TUD has for sustainability and the future of mankind.

7.2 Market Analysis

This section takes a closer look at the market for sounding rockets. This is done in order to assess the potential impact and marketability of the Stratos III and future projects based on the development of this rocket. A favorable market position means that it would be easier to sell the 15 kg of payload and make cover part of the cost of the Stratos III rocket.

7.2.1 The Sounding Rocket Market

As early as 1947 in the USA, and in the mid-1950s in Europe, a few rockets based on the German V-2, were used as sounding rockets to study unexplored features of the upper atmosphere and near-Earth orbit [58]. Nowadays, sounding rockets are still the main means of transporting objects to sub-orbital space. Currently, the price of launching payloads into sub-orbital space ranges from $50,000 to $350,000 for the type of payloads the Stratos III will be capable of carrying [59]. With these payloads the project intends to fill any remaining gap in the budget after sponsorships and other grants have been taken into account.

7.2.1.1 Research

Sounding rockets are just one of many options for scientists, especially those carrying out microgravity research. Drop towers and parabolic aircraft can provide a few seconds up to half a minute of weightlessness. At the other end of the spectrum, orbiting spacecraft can provide extended exposure to microgravity and other aspects of the space environment. This, however, comes at a steep price and is not required for a lot of experiments. The sounding rocket fills this gap by providing approximately 280 seconds of microgravity and space environment, while limiting costs. According to the Suborbital Applications Researchers Group (SARG), there are many scientists lining up to conduct experiments but the supply of cost-effective sounding rockets is still limited [60]. Although the main goal of DARE is not to provide regular commercial flights, it can use these experiments to cover a part of the costs.
The possible fields of research for sounding rockets are listed below:

- Biological and physical research
- Earth science
- Atmospheric science
- Astronomy
- Space science

7.2.1.2 Education

The DARE Stratos projects provide students with a hands-on rocket program experience. Stratos missions follow the same steps required by any major aerospace mission. A mission includes passing through concept reviews, detailed design, manufacturing, fabrication, assembly, testing, launch, recovery and data analysis. Another market is those of miniaturized satellites, the most notable being the CubeSat programs. The CubeSat programs for schools, universities and companies have been growing over the last few years and can be used to cover costs.

Stratos III and future missions will have the capability to launch CubeSats into lower space and hence provide different departments, universities or other interested parties a means to launch their CubeSat.

7.2.1.3 Advancement in Aerospace Technology

The launches can also be used to provide testing and demonstration of new or improved aerospace technology to meet hardware qualifications and tests. Using a sounding rocket can be an economically efficient way to test new designs before they are applied to an orbital or deep space mission. In cooperation with respective companies, the rocket may be adjusted within certain limits to fit their needs.

7.2.2 Market Trends

Multiple companies are working on reusable launch vehicles (RLVs) with the aim to substantially reduce prices for sub-orbital payloads [61][62]. The sounding rocket may in the future lose its place as the cheapest option to launch objects into lower space, but so far none of the attempts have been hugely successful. Even though there are already privately-owned companies and government programs offering sounding rockets to third parties, the demand outweighs the supply.

7.3 'WOW' Factor

In order to be able to sell, a product needs several selling points. These factors are considered to be the "Wow" factors. They come in two distinct categories: Hardware and mission. The hardware factors are the factors that are revolutionary for amateur rocket design. The mission factors are the factors that make the mission special, these could be the different records the team aims to break. For the Stratos III project the following are the "Wow" factors:

Hardware goals:

- Stratos III will use a new hybrid engine where most amateur sounding rockets use a solid engine.
- Stratos III will use active canard control where most amateur sounding rockets are spin stabilized or passively stabilized.
- Stratos III will become the first DARE rocket to fly a ballute.
- Stratos III will use a new and revolutionary recovery system that is capable of recovering the entire rocket.

Mission factors:

- Stratos III will set the record for amateur sounding rockets.
- DARE will become the first student team to reach space.
- Stratos III will break the European altitude record, this record is currently also in hands of DARE with the Stratos rocket.
- Stratos III will be the first dutch build rocket to reach space. Adding the Netherlands to the list of countries that reached space.
- Stratos III will prove that a student team with minimal resources can reach space.
- Stratos III will be the first sounding rocket to have sustainability as a system requirement.

7.4 Public Relations

Public relations and the media package are the prime source of income for Stratos III and future DARE programs. If the market is aware that DARE is working on this project and showing that there is serious progress within the Stratos III mission, it will increase the chances of obtaining sponsors. The list below shows several options that can be used for the public relations.

- **Mission patch**. The mission patch is the logo of the Stratos III. This shall be on almost every materialistic resource of the program.
- **3D rendering**. 3D rendering is used to allow the crew to build the rocket and the different subsystems. However, a 3D rendering also gives general public a nice visual of the rockets mission.
- **3D printed model**. A printed model gives a great opportunity for the team to show a visual representation of the rocket before it is actually built. As soon as the rocket is built and completed the rocket can be used as a show model for stands.
- **Flight footage**. Stratos II was to take videos from launch and apogee using two GoPro cameras in the nosecone. The images from this altitude speak to the imagination of many people and can lead to a good image and new future sponsors. Should it be possible, a down-looking camera would be great for showing the launch and the entire body at apogee. This is ideal for not only public relations, but also for analysis of the launch. For future launches it could be a source of information for technology used in Stratos III.
- **DARE site blog**. During the DSE, the development and the launch campaign there will be several blogs on the DARE website. These will either be written by DARE members or DSE members. This will give the sponsors a great overview of the progress made. Also it will show the rest of the interested world a good look into the progress of the program.

- **Article in "Leonardo Times"**. The monthly edition of the Leonardo Times is a great way to advertise the Stratos III program and DSE to other students and companies. This could potentially lead to more student engineers and increased sponsorship.
- **Scientific publications**. Since three subsystems are very new and innovative, the team expects that there will be a lot of research done within DARE that is worth publishing. It is expected that there will be at least one publication for the ADCS system, three for the propulsion system, one for the recovery system and two for the overall system.
- **Search Engine Optimization (SEO)**. Any project that aims to reach the market and the sponsors has to be found. This means that the DARE and Stratos III project will have appear on the first page of any intenet search related to student space flight, student sounding rockets or amateur rockets to space.

7.5 Comparison to Other Amateur Sounding Rockets

There are several comparable rockets to the Stratos III. In order to compare these a comparison table was drafted. This table can be found below. Note that there are many more sounding rockets that have been operated comparable to the Stratos III. However, all these rockets were considered to be professional rockets whereas the rockets in the table below are classified as amateur rockets.

Table 7.1: *Table Comparing Different Amateur Sounding Rockets Comparable to the Stratos III*

	Stratos III	**Stratos II**	**GoFast [63]**	**Heat-1X [64]**
Operator	DARE	DARE	CSXT	Copenhagen Sub-orbitals
Goal	Become the first student sounding rocket to fly into space	Fly a rocket to an altitude of 50 km	Become the first amateur rocket to reach space	Prototype for a human rated sounding rocket
Status	Launch date for 2017	Launch attempt failure in October 2014, retry in October 2015	Successfully launch in 2004 and 2014	Launch failure, rocket deviated from course and automatically aborted flight
Altitude	120+ km	50km (goal)	117 km	2.8 km
Payload	15 kg	3 kg	None	None
Length	6.68 m	6.56 m	6.4 m	9.38 m
Diameter	26 cm	20 cm	25.4 cm	64 cm
Engine type	Semi-cryogenic Hybrid	Hybrid	Solid	Cryogenic hybrid
Fuel	Nytrox/paraffin-Al	N2O/Sorbitol-Paraffin-Al	Ammonium perchlorate based	Polyurethane/LOX
Staging	One stage	One stage	One stage	One stage
ADCS	Active canard control	Passive control	Spin stabilized	Passive stabilisation

7.5.1 Student Rockets

DARE is not the only student team that aims to reach space. As of this moment the team is aware of two other student teams that aim to fly a sounding rocket into space. These teams are the "Rocket Propulsion Laboratory" of the University of Southern California (USCRPL) [65] and the "Rocket Propulsion Group" of the Boston University (BURPG) [55]. The following table shows the comparison of the three student teams.

Table 7.2: *Table Comparing Different Student Sounding Rockets Comparable to the Stratos III*

	Stratos III	**Traveler 1/2**	**Starscraper**
Operator	DARE	USCRPL	BURPG
Status	Launch attempt in the summer of 2017	Launch failure in summer 2013 and 2014. Loss of vehicle in both casus	Launch attempt in the summer of 2015
Altitude	120+ km	120 km	140 km
Payload	15 kg	None	40 lbs
Engine type	Semi-cryogenic Hybrid	Solid	Hybrid
Fuel	Nytrox/paraffin-Al	AP/AI	Nitrous oxide/HTPB
Staging	One stage	One stage	One stage
ADCS	Active canard control	Passive control	Thrust vectoring by fuel injecting

At the moment USCRPL does not show any intent to retry their mission to fly the Traveler rocket to space. BURPG however has shown some very promising engine tests and has the intention to test their ADCS system in the near future. In order for DARE to become the leading student team, they will have to keep momentum for the Stratos III mission high.

Chapter 8

Conclusion and Recommendations

8.1 Conclusion

This report detailed the design process for the Stratos III rocket and the mission around it. Throughout the design process, systems engineering tools were used, starting with proper project management of the DSE used to develop this design. At the very start, a mission need statement was developed to properly define the goals of the Stratos III mission. In conjunction with DARE's experience from Stratos II and the key requirements of the DSE, system-level requirements were generated that were used to determine the functions and subsystems of the rocket and mission. Each subsystem and the mission also generated their own sets of requirements.

From there, subsystems used design option trees and trade-off tables to choose the best options that could be used for the Stratos III rocket concept generation. From the concepts created, one was chosen based on a normalized, quantitative scoring system. The major components of this design included a single-stage, hybrid engine using Nytrox as oxidizer and Paraffin-Al as solid fuel and an active canard control system.

From this point, the rocket underwent further design on a subsystem level that required constant iteration for proper system integration. At the same time, the Stratos III mission was designed such that it can accommodate the entire process from the end of this DSE to the rocket recovery following the launch. This encompasses the organization, timeline, market analysis, budget, design, and development surrounding the Stratos III rocket.

After 18 major iterations, a final conceptual design was built. The 5.65 m rocket is simulated to reach 134 km in 185 seconds following a 29 second engine burn providing a total impulse of 428 kNs. The rocket will be steered via an active canard control system to keep the rocket on track during both ascent and descent. A ballute and main parachute will carry the rocket down to its water landing location 663 seconds after launch.

The rocket and its surrounding mission are designed with safety and sustainability in mind every step of the design. The chosen fuel exhibited very low carbon dioxide equivalent emissions, which will minimize the impact on the environment during launch and propulsion testing. Following this rocket design and the processes and development strategy detailed in this report will lead DARE to a record-breaking and sustainable rocket in its first foray into space.

8.2 Recommendations

The design provided in this report has a number of uncertainties that must be addressed in the following phases of the Stratos III mission. On an organizational level, it is highly recommended that DARE establish permanent positions for the highest leadership roles in the Stratos III project, as well as full-time positions for the board of DARE itself.

As Stratos III should act as an important pillar program within DARE, it is vital that DARE develops a comprehensive knowledge management system to keep control over the flow of information within the Stratos III project as well as DARE as a whole. This can be done in the form of a file server and/or wiki. It should be considered good practice to document important observations and research in much the same way a scientific lab requires rigorous logbook entry.

The propulsion system is vital to the rocket's capability to reach space in that the rocket is very sensitive to the specific impulse of the rocket. It will be necessary that the rocket undergo a re-sizing to match the expected performance from small-scale engine testing. No construction of other subsystems should be started until the engine performance is more concrete, as a low specific impulse engine may require a change in the diameter of the rocket to accommodate additional fuel. In addition, a more realistic thrust profile after

testing will need to be accounted for rather than the steady thrust modelled based on the assumptions of a constant oxidizer mass flow and the assumed regression rate model.

The nozzle skirt design in this conceptual design will likely require a re-design. It is recommended that DARE look into a composite nozzle using a phenolic resin as it is believed that it may be better suited than the current steel skirt in the design.

One of the largest uncertainties in the design is the capabilities of the active canard control system. It is important to carefully develop and test this system. The current design assumed a perfect, parabolic flight as it was not known how effective the active control would be. For this reason, an appropriate penalty could not be applied to the flight path. It is best to design for overshooting 120 km in future iterations until the performance of this system can be better estimated.

The current design of the structure has minimal thermal and vibrational analysis, thus the small-scale supersonic nosecone test and vibrational tests are of paramount importance for the structural integrity of the rocket.

Finally, there is room for improvement in all designs to save weight. Around the target altitude of 120 km, a single kilogram of dry mass can have an effect of around 2 km in maximum height using the same mass of propellant. Minimizing weight wherever possible can keep the rocket at a weight that the fully designed engine will be capable of launching into space.

Bibliography

[1] DARE. *History: Stratos I*. Nov. 19, 2014. URL: http://dare.tudelft.nl/stratos-ii/stratos-i/ (visited on 11/19/2014).

[2] Rocketman Enterprises. *Civilian Space Exploration Team*. Nov. 11, 2014. URL: http://www.the-rocketman.com/CSXT/default.asp (visited on 11/11/2014).

[3] International Organization for Standardization. *Standard Atmosphere ISO 2533:1975*. 1975. URL: http://www.iso.org/iso/catalogue_detail?csnumber=7472 (visited on 01/07/2014).

[4] A.L. Hertog. *Incremental Non-Linear Dynamic Inversion Control of a Sounding Rocket*. Tech. rep. TU Delft, 2011.

[5] M. Arif Karabeyoglu. "Mixtures of Nitrous Oxide and Oxygen (Nytrox) as Oxidizers for Rocket Propulsion Applications". In: *Journal of Propulsion and Power* 30.4 ().

[6] B.T.C Zandbergen. *Thermal Rocket Propulsion*. 2.04. Delft University of Technology, 2010.

[7] Eric Doran Jonny Dyer M. Arif Karabeyoglu Brian Cantwell Greg Zilliac Benjamin S. Waxman. "Peregrine Hybrid Rocket Motor Ground Test Results". In: Joint Propulsion Conference & Exhibit 48. Aug. 2012.

[8] M. Arif Karabeyoglu. *AA 284a Advanced Rocket Propulsion - Lecture 10 Hybrid Rocket Propulsion Design Issues*. http://www.spg-corp.com/docs/Stanford_AA284a_Lecture10.pdf. May 14, 2012 (accessed January 6, 2014).

[9] George P. Sutton and Oscar Biblarz. *Rocket Propulsion Elements, 6th Edition*. English. 6th edition. New York: John Wiley & Sons, Inc, 1992. ISBN: 0471529389.

[10] Rob Mudde Harrie van den Akker. *Fysische Transportverschijnselen*. 3rd edition. VSSD, 2008.

[11] M.M.C.G. Warmoeskerken L.P.B.M. Janssen. *Transport Phenomena Data Companion*. 3rd edition. VSSD, 2006.

[12] D.W. Green R.H. Perry. *Perry's Chemical Engineers' Handbook*. 8th ed. VSSD, 2007.

[13] E.W. Price et al. *Behavior of aluminium in solid propellant combustion*. Tech. rep. Georgia Institute of Technology, 1982.

[14] Tobias Knop et al. *Sorbitol-Based Hybrid Fuel Studies with Nitrous Oxide for the Stratos II Sounding Rocket*. 2013. URL: http://arc.aiaa.org/doi/pdf/10.2514/6.2013-4049 (visited on 01/08/2015).

[15] International Organization for Standardization. *Transportable gas cylinders - Compatibility of cylinder and valve materials with gas contents - Part 1:Metallic materials*. 1997. URL: https://law.resource.org/pub/us/cfr/ibr/004/iso.11114-1.1997.pdf (visited on 01/09/2015).

[16] Defense Metals Information Center Battelle Memorial Institue Columbus. *Compatibility of Materials with Rocket Propellants and Oxidizers*. 1965. URL: http://www.dtic.mil/dtic/tr/fulltext/u2/613553.pdf (visited on 01/09/2015).

[17] G.J. Nihart and C.P. Smith. *Compatibility of Materials with 7500 psi Oxygen*. 1964. URL: http://www.dtic.mil/dtic/tr/fulltext/u2/608260.pdf (visited on 01/09/2015).

[18] David Roylance. *Pressure vessels*. Tech. rep. Department of Materials Science and Engineering, Massachusetts Institute of Technology, 2001.

[19] Paul A. Lagace. *Yield and Failure Criteria*. Tech. rep. Department of Aeronautics and Astronautics Massachusetts Institute of Technology, 2009.

[20] US Department of Defense. *Design of aerodynamically stabilized free rockets*. US Department of Defense, 1990.

[21] Frank Keith and D. Yogi Goswami. *The CRC Handbook of Mechnical Engineering*. 2nd. CRC Press, 2004.

[22] T.H.G Megson. *Aircraft Structures for Engineering Students*. Fifth. Elsevier Aerospace Engineering, 2013.

[23] SimScale GmbH. *SimScale*. Online software. 2015.

[24] matbase. *matbase*. Nov. 14, 2014. URL: http://www.matbase.com/material-categories/ (visited on 11/14/2014).

[25] Entergris INC. *Properties and Characterstics of Graphite*. Tech. rep. Entergris INC., 2013.

[26] Gizom.nl. *Aluminium en non ferro metalen - Gizom Veendam*. Nov. 19, 2014. URL: http://www.gizom.nl/ (visited on 11/19/2014).

[27] metalprices.com. *Titanium*. URL: http://www.metalprices.com/metal/titanium/titanium-ingot-6al-4v-rotterdam (visited on 01/15/16).

[28] Chakrapan Tuakta. Tech. rep.

[29] AK Steel. Tech. rep.

[30] Northern Graphite. *Grapite pricing*. URL: http://northerngraphite.com/graphite-labs/graphite-price/ (visited on 01/15/16).

[31] M. Vos. "Delfi-n3xt's Attitude Determination and Control Subsystem". An optional note. MA thesis. Technische Universiteit Delft, Apr. 2013.

[32] Tahir Akram Ishtiaq Maqsood. *Development of a Low Cost Sun Sensor Using Quadphotodiode*. Tech. rep. Technical university of Hamburg-Harburg & Masdar institute of Science and Technology, 2010.

[33] Christopher D. Hall. *Spacecraft Attitude Dynamics and Control*. http://www.dept.aoe.vt.edu/~cdhall/courses/aoe4140/attde.pdf. 2003 (accessed December 18, 2014).

[34] American Government. *International Traffic in Arms Regulations, 22:CFR:121.1*. Aug. 27, 2010. URL: http://www.fas.org/spp/starwars/offdocs/itar/p121.htm#C-XV (visited on 01/07/2015).

[35] American Government. *International Traffic in Arms Regulations exceptions, 22:CFR:125.4*. Aug. 27, 2010. URL: http://www.law.cornell.edu/cfr/text/22/125.4 (visited on 01/07/2015).

[36] Swift Navigation. *Piksi - Swift Navigation*. URL: http://www.swiftnav.com/piksi.html (visited on 11/24/2014).

[37] Alexandru Csete. *GPS without limits*. URL: http://copsub.com/gps-without-limits/ (visited on 11/24/2014).

[38] MathWorks. *Design and use Kalman filters in MATLAB and Simulink*. Nov. 19, 2014. URL: http://nl.mathworks.com/discovery/kalman-filter.html (visited on 11/19/2014).

[39] Eugene L. Fleeman. *Missile Design and System Engineering*. 1st ed. AIAA, 2012.

[40] William E. Palmer and Dale L. Burrows. *A transonic wind-tunnel investigation of the longitudinal force and moment characteristics of two delta wings and one clipped-tip delta wing 4 percent thickness on a slender body*. 1955. URL: http://naca.central.cranfield.ac.uk/reports/1955/naca-rm-l55a07a.pdf (visited on 01/16/2015).

[41] W. E. Rogers and C. J. Berry. *Experiments with Biconvex Aerofoils in Low-Density, and Double-Wedge Supersonic Flow*. 1968. URL: http://naca.central.cranfield.ac.uk/reports/arc/rm/3635.pdf (visited on 01/14/2015).

[42] Sampo Niskanen. *OpenRocket technical documentation*. 2013. URL: http://openrocket.sourceforge.net/techdoc.pdf (visited on 12/14/2014).

[43] John D. Anderson Jr. *Fundamentals of Aerodynamics, 5th Edition*. English. 5th edition. New York: McGraw-Hill Science/Engineering/Math, Feb. 2010. ISBN: 9780073398105.

[44] Dennis J. Martin. *Summary of flutter experiences as a guide to the preliminary design of lifting surfaces on missiles*. 1958. URL: http://naca.central.cranfield.ac.uk/reports/1958/naca-tn-4197.pdf (visited on 11/18/2014).

[45] Theodore Theodorsen. *General theory of aerodynamic instability and the mechanism of flutter*. 1935. URL: http://naca.central.cranfield.ac.uk/reports/1935/naca-report-496.pdf (visited on 01/08/2015).

[46] Yancheng Zhang & Chao-Yang Wang Yan Ji. "Li-Ion Cell Operation at Low Temperatures". In: *Journal of the Electrochemical Society* 160.4 ().

[47] California Polytechnic State University. *CubeSat Design Specification*. 2014. URL: http://cubesat.calpoly.edu/images/developers/cds_rev13_final.pdf (visited on 01/05/2015).

[48] Theo W. Knacke. *Parachute Recovery Systems Design Manual*. Para Publishing, 1992.

[49] Steve Lingard. *Supersonic Parachutes*. https://solarsystem.nasa.gov/docs/11%20-%20Supersonic%20parachutes%20Lingard.pdf. 2005.

[50] Armadillo Aerospace. URL: http://armadilloaerospace.com/n.x/Armadillo/Home (visited on 01/15/16).

[51] Copenhagen Suborbitals. URL: http://copsub.com/ (visited on 01/15/16).

[52] Jae-Deuk Lee Dong-Chul Park Tae-Hyun Kim Sung-Wan Kim. "Analysis of radiation patterns of inverted-F antenna on a cylindrical conducting body like a satellite launcher". In: Microwave Conference Proceedings. Dec. 2005. URL: \url{http://ieeexplore.ieee.org/xpls/icp.jsp?arnumber=1606384}.

[53] Frank G. Moore. *Approximate methods for weapon aerodynamics*. AIAA, 2000.

[54] *Vervoer gevaarlijke stoffen (ADR)*. 2014. URL: https://www.rdw.nl/sites/igk/Paginas/Vervoer-gevaarlijke-stoffen-(ADR).aspx (visited on 07/01/2015).

[55] Starscraper Team. *Starscraper*. URL: http://www.burocket.org/rockets/starscraper/ (visited on 01/14/2015).

[56] M Scott Cato. *Green economics*. Earthscan, 2009.

[57] W.M Adams. *The future of Sustainability: Re-thinking environment and development in the twenty-first century*. Report of the IUCN Renowned Thinkers Meeting, 2009.

[58] Gnther Seibert. *The history of sounding rockets and their contribution to European Space Research*. 2006.

[59] The Tauri Group. *Suborbital Reusable Vehicles: A 10-Year Forecast of Market Demand*. URL: http://www.spaceflorida.gov/docs/misc/srvs-10-year-forecast-of-market-demand-report.pdf.

[60] Alexanda Witze. *Commercial access to suborbital space still on the horizon*. June 7, 2013. URL: http://blogs.nature.com/news/2013/06/commercial-access-to-suborbital-space-still-on-the-horizon.html (visited on 11/17/2014).

[61] FAA. *The U.S. Commercical Suborbital Industry*. 2014.

[62] Brian Orlotti. *Ontario Firm Building Rocket Engines for Space Port America*. Nov. 10, 2014. URL: http://acuriousguy.blogspot.nl/2014/11/ontario-firm-building-rocket-engines.html (visited on 11/14/2014).

[63] *GoFast*. 2004. URL: http://www.ddeville.com/derek/CSXT.htm.

[64] Copenhagen Suborbitals. *HEAT-1X*. 2011. URL: http://copsub.com/rockets-2/heat1x/ (visited on 01/26/2015).

[65] USCRPL. *The Rocket Propulsion Laboratry*. 2013. URL: http://uscrpl.com/index.php (visited on 01/26/2015).

Appendix A

Stratos III Key Parameters

Table A.1: *Rocket Mass*

Dry Mass	137.8 $[kg]$
Wet Mass	309.5 $[kg]$
Paraffin Mass	27.7 $[kg]$
Nytrox Mass	144 $[kg]$

Table A.2: *Rocket Geometry*

Length of Nosecone	0.78 $[m]$
Length of Capsule	1.05 $[m]$
Length of Oxidizer Tank	2.35 $[m]$
Length of Propulsion Plumbing	0.31 $[m]$
Length of Combustion Chamber	0.70 $[m]$
Length of Nozzle	0.46 $[m]$
Total Rocket Length	5.65 $[m]$
Fuselage Diameter	0.26 $[m]$
Location of Canard Root from Tip	1.32 $[m]$
Canard Root Chord	0.15 $[m]$
Canard Length	0.10 $[m]$
Location of Fin Root from Tip	4.76 $[m]$
Fin Root Chord	0.35 $[m]$
Fin Tip Chord	0.15 $[m]$
Fin Length	0.20 $[m]$
Fuselage Thickness	5 $[mm]$
Nosecone Thickness for 0.035-0.58 m	1 $[mm]$
Nosecone Thickness for 0.58-0.78 m	3.5 $[mm]$

Table A.3: *Propulsion*

Oxidizer	Nytrox w/ 15% O2
Fuel	0.75:0.2:0.05 Paraffin/Al/Carbon Black
Engine Burn Time	28.9 $[s]$
Altitude at Burnout	18.2 $[km]$
Specific Impulse at Sea Level	232 $[s]$
Specific Impulse at Burnout	282 $[s]$
O/F Ratio	5.20
Oxidizer Mass Flow	5 $[\frac{kg}{s}]$
Total Mass Flow at Start	5.98 $[\frac{kg}{s}]$
Total Mass Flow at Burnout	5.95 $[\frac{kg}{s}]$
Total Impulse	427.7 $[kNs]$
Maximum Thrust	16.5 $[kN]$
Port Radius	6 $[cm]$
Throat Radius	3 $[cm]$

Table A.4: *Astro- & Aerodynamics*

Altitude at 4°Launch Angle	134.41 $[km]$
Average Drift at 4°Launch Angle	51.01 $[km]$
Vertical Velocity Change	1.536 $[\frac{km}{s}]$
Time to Apogee	185 $[s]$
Time to Splashdown	662.6 $[s]$
Maximum Drag Force	2580 $[N]$
Drag Loss	16.7%

Table A.5: *Recovery*

Ballute Diameter	0.9 $[m]$
Main Parachute Area	14 $[m^2]$
Ballute Deployment Altitude	60 $[km]$
Ballute Deployment Time	310.8 $[s]$
Main Parachute Deployment Altitude	3 $[km]$
Main Parachute Deployment Time	489 $[s]$
Maximum Ballute Drag Force	9568 $[N]$
Maximum Main Parachute Drag Force	4890 $[N]$

Table A.6: *Electronics*

Antenna Transmission Power	1 $[W]$
Antenna Frequency	800 $[MHz]$
Antenna Transmission Rate	20 $[\frac{kb}{s}]$
Antenna Length	9.4 $[cm]$
Design Peak Power	271 $[W]$
Total Energy	9320 $[mWh]$
Flight Computer Transmission Rate	10 $[Hz]$

Appendix B

Requirements

Table B.1: *The Key Requirements for the Stratos III Program*

Identifier	Description
STR-KEY-01	System must reach an altitude of 120 km
STR-KEY-02	System must be able to carry a payload of at least 15 kg
STR-KEY-03	System must be built with commercial off-the-shelf and self-designed parts

Table B.2: *System Requirements for the Stratos III Program*

Identifier	Description
STR-SYS-01	The total cost of the Stratos III project shall be in the order of €100,000.
STR-SYS-02	The rocket shall be transportable from TUD to the launch site.
STR-SYS-03	The Stratos III program shall obey the law with respect to health, safety, and legal regulations.
STR-SYS-04	The Stratos III rocket shall be safe to work with on a student level.
STR-SYS-05	The Stratos III rocket shall send flight information during the entire flight.
STR-SYS-06	The Stratos III rocket shall reach an altitude of 120 km.
STR-SYS-07	The Stratos III rocket shall carry a 15 kg payload.
STR-SYS-08	The Stratos III rocket shall prove that it has reached an altitude of 120 km.
STR-SYS-09	The Stratos III rocket shall be recovered with minimal damage.
STR-SYS-10	The Stratos III shall have a method of terminating the flight.
STR-SYS-11	The Stratos III shall remain within a predetermined flight path.
STR-SYS-12	The Stratos III shall be launched from a ground-based launch site.

B.1 Subsystems

Table B.3: *Requirements for the ADCS Subsystem*

Identifier	Description
STR-SUB-ADCS-DET-01	The ADCS shall determine the altitude of the payload during flight.
STR-SUB-ADCS-DET-02	The ADCS shall determine the geographic coordinates of the payload during flight.
STR-SUB-ADCS-DET-03	The ADCS shall determine the velocity of the payload during flight.
STR-SUB-ADCS-DET-04	The ADCS shall determine the yaw angle.
STR-SUB-ADCS-DET-05	The ADCS shall determine the pitch angle.
STR-SUB-ADCS-DET-06	The ADCS shall determine the roll rate.
STR-SUB-ADCS-DET-07	The ADCS shall store all rocket kinematics data.
STR-SUB-ADCS-CON-01	The ADCS shall reduce deflection from predetermined flight path angle.
STR-SUB-ADCS-CON-02	The ADCS shall be able to change the pitch-rate of the rocket.
STR-SUB-ADCS-CON-03	The ADCS shall be able to change the yaw-rate of the rocket.
STR-SUB-ADCS-CON-04	The ADCS shall be able to change the roll-rate of the rocket.

Table B.4: *Requirements for the Communication Subsystem*

Identifier	Description
STR-SUB-COM-01	The communications subsystem shall provide communication between the rocket and the ground station during most flight stages.
STR-SUB-COM-02	The communications subsystem shall transmit status reports in real-time.
STR-SUB-COM-03	The communications subsystem shall have flight-proven components.
STR-SUB-COM-04	There shall be a visible outside indication that the rocket is in safe or arm mode.
STR-SUB-COM-05	The communications subsystem shall conform to protocols.

Table B.5: *Requirements for the Power Subsystem*

Identifier	Description
STR-SUB-PWR-01	The power subsystem shall have the capacity to store all energy required throughout the entire launch.
STR-SUB-PWR-02	The power subsystem's storage solution shall have the capability to be charged via an external power source.
STR-SUB-PWR-03	The power subsystem shall be capable of providing subsystem status and health information.
STR-SUB-PWR-04	The power subsystem shall be capable of regulating the input and output of power.
STR-SUB-PWR-05	The power subsystem shall be capable of converting power to match the current and voltage requirements of all subsystems on an individual basis.
STR-SUB-PWR-06	The power subsystem shall be designed to minimize its weight and cost.
STR-SUB-PWR-07	The power subsystem shall be designed to take up less than [TBD]% of the overall cost budget.
STR-SUB-PWR-08	The power subsystem shall be designed to abide by international electrical safety standards.
STR-SUB-PWR-09	The power subsystem shall minimize harm and interference with all other subsystems and components.
STR-SUB-PWR-10	The power subsystem shall be designed to minimize power losses during distribution.
STR-SUB-PWR-11	The power subsystem shall use components that are safe to handle according to electrical safety and workplace health standards.

Table B.6: *Requirements for the Propulsion Subsystem*

Identifier	Description
STR-SUB-PRO-01	The propulsion subsystem shall have means of controlled ignition.
STR-SUB-PRO-02	The propulsion subsystem shall deliver sufficient thrust to propel the rocket to an altitude of 120 km.
STR-SUB-PRO-03	The fuel tank shall store sufficient amount of fuel to reach target altitude.
STR-SUB-PRO-04	The propulsion subsystem shall have means of fuel level indication.
STR-SUB-PRO-05	The propulsion subsystem shall have means of thrust level indication.
STR-SUB-PRO-06	The engine shall withstand the combustion with a safety factor of [TBD]
STR-SUB-PRO-07	The propulsion subsystem shall not contain any chemicals with a Degree of Health Hazard above class 2 under NFPA 704 standards.
STR-SUB-PRO-08	The propulsion subsystem shall not contain any government restricted materials.

Table B.7: *Requirements for the Recovery Subsystem*

Identifier	Description
STR-SUB-REC-01	The recovery subsystem shall be able to dissipate a sufficient amount of potential energy.
STR-SUB-REC-02	The recovery subsystem shall ensure an impact velocity of no more than 15 m/s.
STR-SUB-REC-03	The recovery subsystem shall introduce a deceleration of no more than 11 G during recovery.
STR-SUB-REC-04	The recovery subsystem shall ensure the land site is within the predetermined safe zone.
STR-SUB-REC-05	The recovery subsystem shall limit the damage inflicted on the rocket in the period between landing and pick-up.
STR-SUB-REC-06	The recovery subsystem shall produce a clear close proximity location indicator.

Table B.8: *Requirements for the Structures Subsystem*

Identifier	Description
STR-SUB-STRU-01	The structure shall be able to resist all forces acting on it.
STR-SUB-STRU-02	The structure shall be able to resist the impact force when landing.
STR-SUB-STRU-03	The structure shall withstand a temperature without deforming.
STR-SUB-STRU-04	The structure shall withstand certain vibrations.
STR-SUB-STRU-05	The structure shall not reach its natural frequency.
STR-SUB-STRU-06	The structure shall have a safety factor.
STR-SUB-STRU-07	The structure shall not disturb the communications.
STR-SUB-STRU-08	The structure shall protect the payload both from air and water.

Table B.9: *Requirements for the Flight Termination Subsystem*

Identifier	Description
STR-SUB-FTS-01	The FTS shall have a Flight Termination System listening to IRIG flight termination commands and handle accordingly.
STR-SUB-FTS-02	The FTS shall be active only during the burn time.
STR-SUB-FTS-03	The FTS shall work as independently as possible from other systems.
STR-SUB-FTS-04	The FTS shall eliminate the risk of false positives.
STR-SUB-FTS-05	The FTS shall only terminate the flight in clearly defined abort scenarios.

B.2 Mission

Table B.10: *Build Requirements for the Stratos III Program*

Identifier	Description
STR-MP-CON-01	All materials used in the mission shall be within the resources of TU Delft and DARE.
STR-MP-CON-02	All technology used in the mission will be COTS technology.
STR-MP-CON-03	The crew shall be properly trained to operate the tools used during the build.
STR-MP-CON-04	All tools used during the build shall be within reach of TU Delft and DARE.
STR-MP-CON-05	During manufacturing all Dutch "ARBO" laws shall be followed.
STR-MP-CON-06	During manufacturing no material shall be used that risk the well-being of the building crew or its surroundings.

Table B.11: *Environmental Requirements for the Stratos III Program*

Identifier	Description
STR-MP-ENV-01	The Stratos III mission shall not use materials that are hazardous to the environment.
STR-MP-ENV-02	Upon completion of the mission, no rocket part or residual shall be left behind on the launch site.

Table B.12: *Flight Profile Requirements for the Stratos III Program*

Identifier	Description
STR-MP-FP-01	The systems check shall contain every subsystem that is used during flight.
STR-MP-FP-02	During the arming of the rocket, unnecessary personnel shall be clear of the rocket.
STR-MP-FP-03	During the arming of the rocket, a contingency plan shall be in place.
STR-MP-FP-04	During the final check, all subsystems engineers shall give their go/no-go to the flight director.
STR-MP-FP-05	During the entire flight the rocket shall be tracked.
STR-MP-FP-06	The rockets flight path shall not cross over populated areas.
STR-MP-FP-07	There shall be a contingency plan should the rocket fly outside of its predetermined flight path.

Table B.13: *Logistics Requirements for the Stratos III Program*

Identifier	Description
STR-MP-LOG-01	The rocket shall not be a hazard to surrounding environment and involved crew during transport.
STR-MP-LOG-02	During transport the rocket shall conform to the transportation laws of the nations it is travelling through.
STR-MP-LOG-03	The rocket shall conform to the international laws with respect to weapons and ammunition.
STR-MP-LOG-04	The transport cost shall be within the resources of TU Delft and DARE.

Table B.14: *Resource Requirements for the Stratos III Program*

Identifier	Description
STR-MP-RES-01	All the resources used shall be available within the reach of TU Delft and the sponsors.
STR-MP-RES-02	Resource waste shall be minimized during the project, except for spare parts and contingency.
STR-MP-RES-03	All usage of resources shall be logged.
STR-MP-RES-04	All resource sources shall be logged.
STR-MP-RES-05	All technology used shall be COTS or DARE designed technology.
STR-MP-RES-06	All resources used shall be allowed by European and Dutch regulations.

Table B.15: *Safety Requirements for the Stratos III Program*

Identifier	Description
STR-MP-SAVE-01	The rocket shall have a contingency plan for every phase of its flight.
STR-MP-SAVE-02	The rocket shall not endanger any human or animal at any phase of its flight.
STR-MP-SAVE-03	The rocket shall not emit toxic material during any phase of the mission.
STR-MP-SAVE-04	During launch the launch crew and the rocket shall perform according to all the regulations given by the launch site.
STR-MP-SAVE-05	Upon loss of communication during flight the rocket shall have a contingency plan that will prevent it from forming health risks and property damage.
STR-MP-SAVE-06	The rocket shall have a probability of catastrophic failure of less than [TBD]%.
STR-MP-SAVE-07	No technology shall be sold to nations that are under European trade prohibition.
STR-MP-SAVE-08	All systems checks performed shall be performed on all subsystems.

Appendix C

DSE Team Organization

C.1 Internal Team Organization

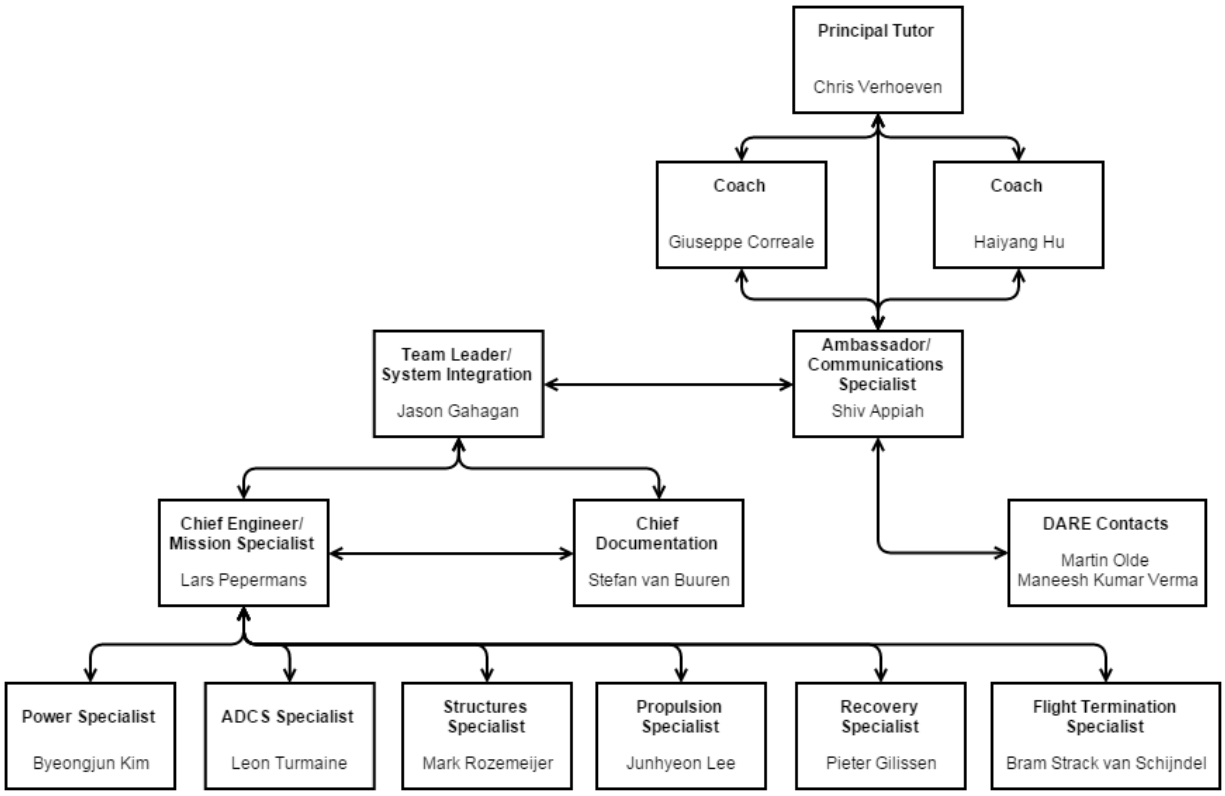

Figure C.1: *Internal Communication Flow of the DSE Team*

C.2 Work Distribution

Table C.1: *Table of Work Distribution*

Shiv Appiah	1, 4.5.3, 4.5.4, 4.6, 5.2.5, 6.4.5, 6.5.5
Jason Gahagan	3, 4.1, 4.2.7, 4.3.5, 8, Appendices A, C, and D, Integration Software
Pieter Gillissen	4.8, 4.9.7, 5.2.6, 6.4.7, 6.5.6, Recovery Software
Byeongjun Kim	2.2, 4.5.1, 4.5.2, 4.5.4, 4.5.5, 5.2.4, 5.2.5, 6.4.4, 6.5.4, 6.10
Junhyeon Lee	4.2, 4.9.6, 5.2.1, 6.4.1, 6.5.1
Lars Pepermans	Preface, 2, 5.1, 5.3, 6.1, 6.2, 6.3, 6.6, 6.7, 6.8, 6.9, 7.1, 7.3, 7.4, 7.5, Appendix B
Mark Rozemeijer	4.1, 4.2.2, 4.3, 5.2.2, 6.4.2, 6.4.6, 6.5.2, Rocket Engine Software, Structural Software
Bram Strack van Schijndel	4.2.4.1, 4.7, 4.9, 5.2.7, 6.5.7, Early Integration Software, Summary
Leon Turmaine	4.4, 5.2.3, 6.2, 6.3, 6.4.3, 6.5.3
Stefan van Buuren	4.4, 5.2.3, 6.3.1, 6.3.2, 6.4.2, 6.5.3, 7.2, Chief Editor

Appendix D

Project Gantt Chart

ID	Task Mode	Task Name	Duration	Start	Finish	Predecessors
25		**Propulsion**	**375 days**	**9/7/15**	**2/10/17**	
26		Preliminary Propulsion Design	23 wks	9/7/15	2/12/16	6
27		Oxidizer tank in-depth modelling	5 wks	9/7/15	10/9/15	6
28		Regression rate testing	5 wks	9/7/15	10/9/15	6
29		Manufacture small scale oxidizer tank	5 wks	10/12/15	11/13/15	28,27
30		Small scale oxidizer tank model validation	5 wks	11/16/15	12/18/15	29
31		Small scale solid propellant RR validation	5 wks	11/16/15	12/18/15	29
32		Detailed nozzle design	5 wks	12/21/15	1/22/16	30,31
33		Small scale engine model	5 wks	1/25/16	2/26/16	32
34		Small scale engine tests	5 wks	2/29/16	4/1/16	33
35		Engine design optimization	30 wks	2/15/16	9/9/16	26
36		Feed system testing	10 wks	4/4/16	6/10/16	34
37		Prototype production	14 wks	6/13/16	9/16/16	36
38		Solid propellant trials	10 wks	9/19/16	11/25/16	37
39		Full scale engine test	21 wks	9/19/16	2/10/17	37
40		**ADCS**	**465 days**	**9/7/15**	**6/16/17**	
41		**Control Group**	**165 days**	**9/7/15**	**4/22/16**	
42		Review base flight computer software	5 wks	9/7/15	10/9/15	6
43		Extend flight computer software	18 wks	10/12/15	2/12/16	42
44		Hardware in the loop verification	10 wks	2/15/16	4/22/16	43
45		**Electronics Group**	**225 days**	**9/7/15**	**7/15/16**	
46		Detailed determination system design	23 wks	9/7/15	2/12/16	6
47		Sun sensor design	10 wks	9/7/15	11/13/15	6
48		Unrestricted GPS testing	15 wks	9/7/15	12/18/15	6

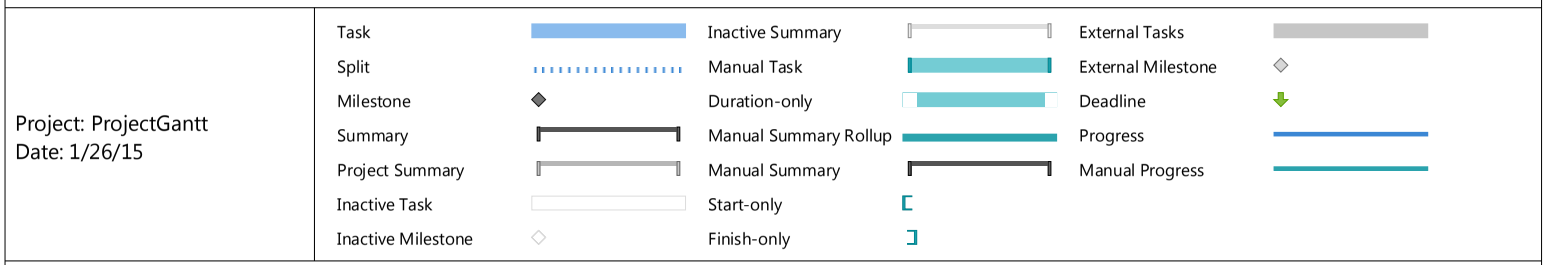

ID	Task Mode	Task Name	Duration	Start	Finish	Predecessors
49		Rate table tests	6 wks	2/15/16	3/25/16	46
50		Computer thermal analysis	11 wks	2/15/16	4/29/16	46
51		Flight computer manufacturing	22 wks	2/15/16	7/15/16	46
52		Sensor Calibration	10 wks	9/7/15	11/13/15	6
53		**Aerodynamics Group**	**165 days**	**9/7/15**	**4/22/16**	
54		Detailed Control Surfaces Design	22 wks	9/7/15	2/5/16	6
55		Supersonic analysis	22 wks	9/7/15	2/5/16	6
56		Detailed flutter analysis	22 wks	9/7/15	2/5/16	6
57		CFD Analysis of Rocket Profile Interaction	22 wks	9/7/15	2/5/16	6
58		Supersonic canard windtunnel test	22 wks	9/7/15	2/5/16	6
59		Small scale supersonic test	11 wks	2/8/16	4/22/16	54
60		Manufacture canards/fins	11 wks	2/8/16	4/22/16	54
61		Actuator selection	10 wks	9/7/15	11/13/15	6
62		Fullscale subsonic test	10 wks	2/8/16	4/15/16	54
63		Integrated ADCS Test	18 wks	2/13/17	6/16/17	62,51,44,21
64		**Recovery**	**450 days**	**9/7/15**	**5/26/17**	
65		Detailed Recovery Design	22 wks	9/7/15	2/5/16	6
66		Manufacture small scale ballute	15 wks	2/8/16	5/20/16	65
67		Vertical windtunnel test	20 wks	2/8/16	6/24/16	65
68		Deployment tests	5 wks	2/8/16	3/11/16	65
69		CFD Ballute Analysis	12 wks	2/8/16	4/29/16	65
70		Main Parachute Reefing Test	12 wks	2/8/16	4/29/16	65
71		Electrical detonator test	5 wks	4/24/17	5/26/17	22
72		Explosive bolt tests	5 wks	4/24/17	5/26/17	22

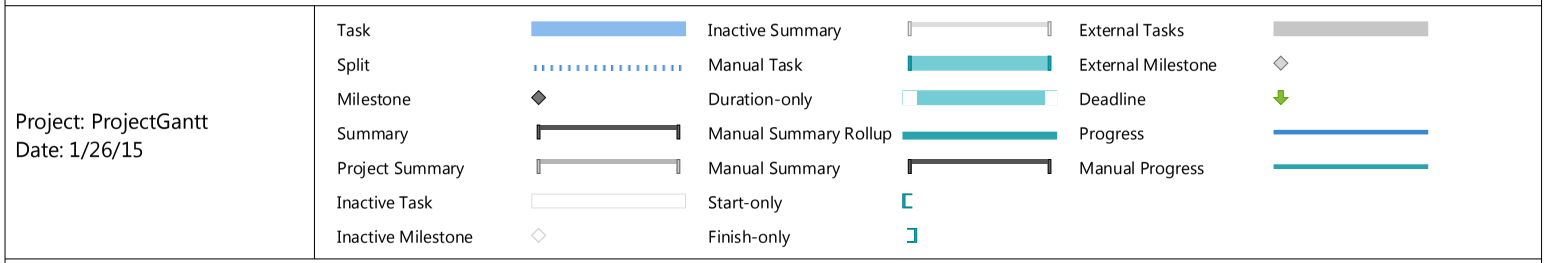

ID	Task Mode	Task Name	Duration	Start	Finish	Predecessors
73		**Structures**	**200 days**	**2/15/16**	**11/18/16**	
74		Detailed Structures Design	11 wks	2/15/16	4/29/16	26
75		Small scale oxidizer tank stress testing	11 wks	5/2/16	7/15/16	74
76		Nosecone thermal tests	5 wks	5/2/16	6/3/16	74
77		Vibration tests	18 wks	7/18/16	11/18/16	75
78		**Communication**	**140 days**	**7/18/16**	**1/27/17**	
79		Detailed Communication Design	28 wks	7/18/16	1/27/17	51
80		Signal Strength Test	19 wks	7/18/16	11/25/16	51
81		Thermal Tests	19 wks	7/18/16	11/25/16	51
82		Radiation Pattern Tests	19 wks	7/18/16	11/25/16	51
83		Bandwidth Test	19 wks	7/18/16	11/25/16	51
84		**Power**	**225 days**	**7/18/16**	**5/26/17**	
85		Detailed Power Design	28 wks	7/18/16	1/27/17	51
86		Pressurization/Temperature Tests	20 wks	7/18/16	12/2/16	51
87		Component Testing	10 wks	12/5/16	2/10/17	86
88		Full-Scale Test	5 wks	4/24/17	5/26/17	22
89		Launch	0 days	8/21/17	8/21/17	17
90		Post-Launch Evaluation	5 wks	8/22/17	9/25/17	89

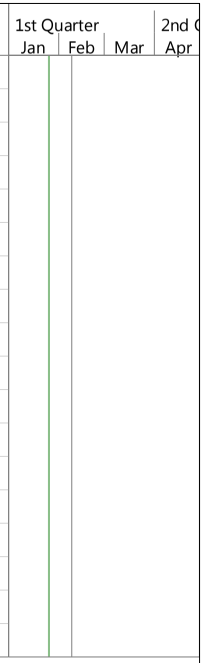

Project: ProjectGantt
Date: 1/26/15

Task
Split
Milestone
Summary
Project Summary
Inactive Task
Inactive Milestone
Inactive Summary
Manual Task
Duration-only
Manual Summary Rollup
Manual Summary
Start-only
Finish-only
External Tasks
External Milestone
Deadline
Progress
Manual Progress

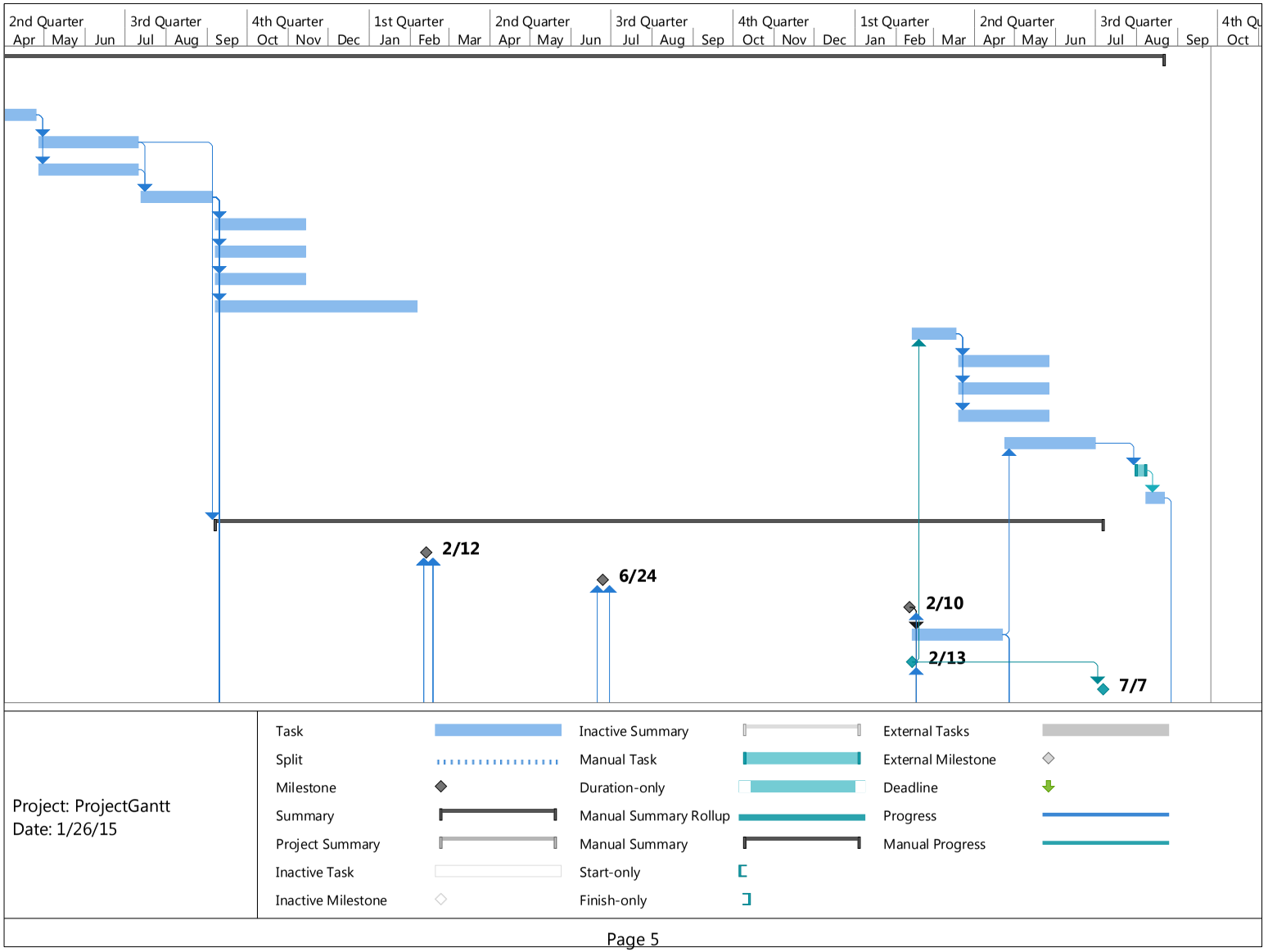
2nd Quarter
Apr May Jun
3rd Quarter
Jul Aug Sep
4th Quarter
Oct Nov Dec
1st Quarter
Jan Feb Mar
2nd Quarter
Apr May Jun
3rd Quarter
Jul Aug Sep
4th Quarter
Oct Nov Dec
1st Quarter
Jan Feb Mar
2nd Quarter
Apr May Jun
3rd Quarter
Jul Aug Sep
4th Qu
Oct
2/12
6/24
2/10
2/13
7/7
Project: ProjectGantt
Date: 1/26/15
Task
Split
Milestone
Summary
Project Summary
Inactive Task
Inactive Milestone
Inactive Summary
Manual Task
Duration-only
Manual Summary Rollup
Manual Summary
Start-only
Finish-only
External Tasks
External Milestone
Deadline
Progress
Manual Progress

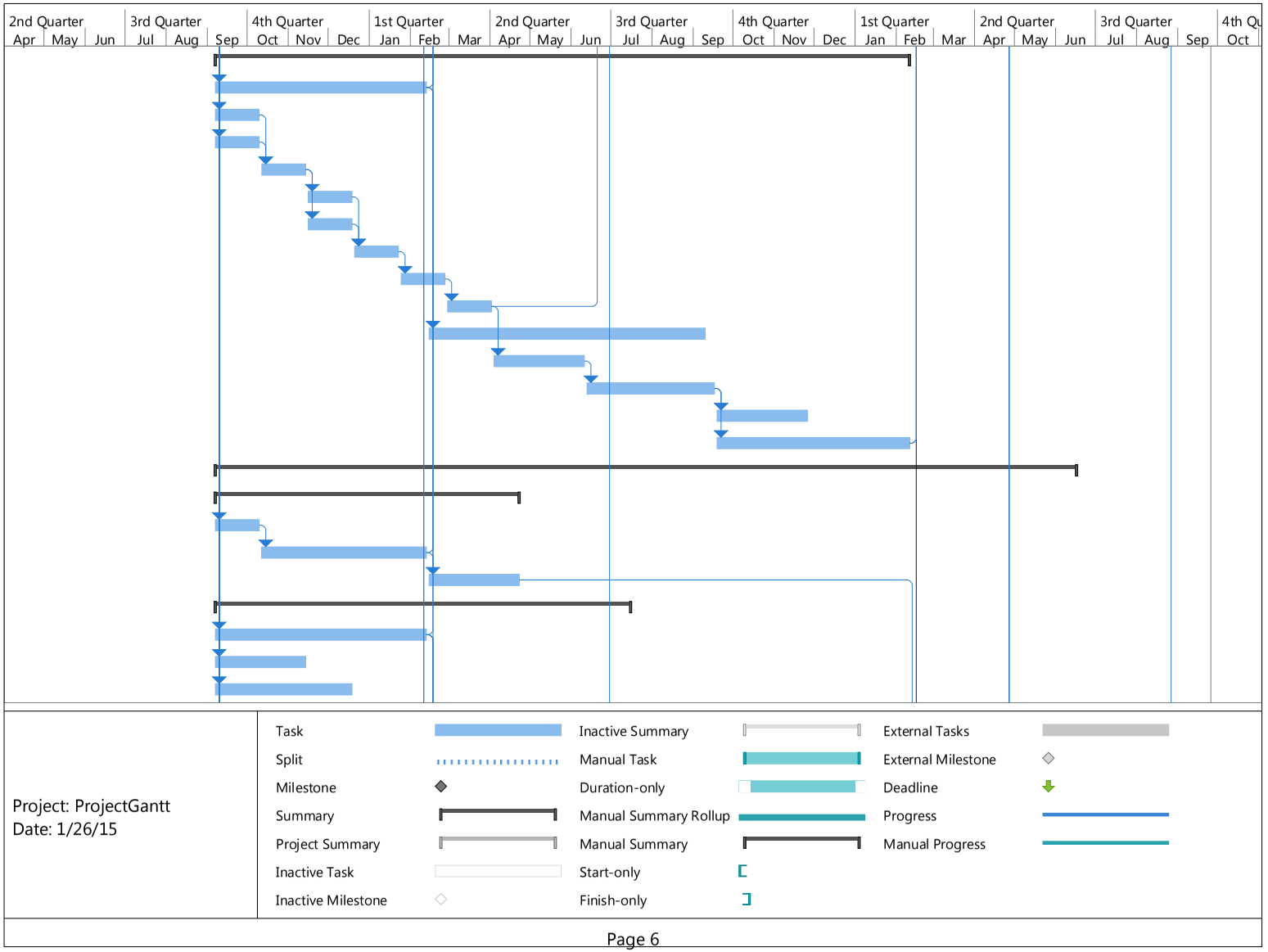
2nd Quarter
Apr
May
Jun
3rd Quarter
Jul
Aug
Sep
4th Quarter
Oct
Nov
Dec
1st Quarter
Jan
Feb
Mar
2nd Quarter
Apr
May
Jun
3rd Quarter
Jul
Aug
Sep
4th Quarter
Oct
Nov
Dec
1st Quarter
Jan
Feb
Mar
2nd Quarter
Apr
May
Jun
3rd Quarter
Jul
Aug
Sep
4th Qu
Oct
Project: ProjectGantt
Date: 1/26/15
Task
Split
Milestone
Summary
Project Summary
Inactive Task
Inactive Milestone
Inactive Summary
Manual Task
Duration-only
Manual Summary Rollup
Manual Summary
Start-only
Finish-only
External Tasks
External Milestone
Deadline
Progress
Manual Progress

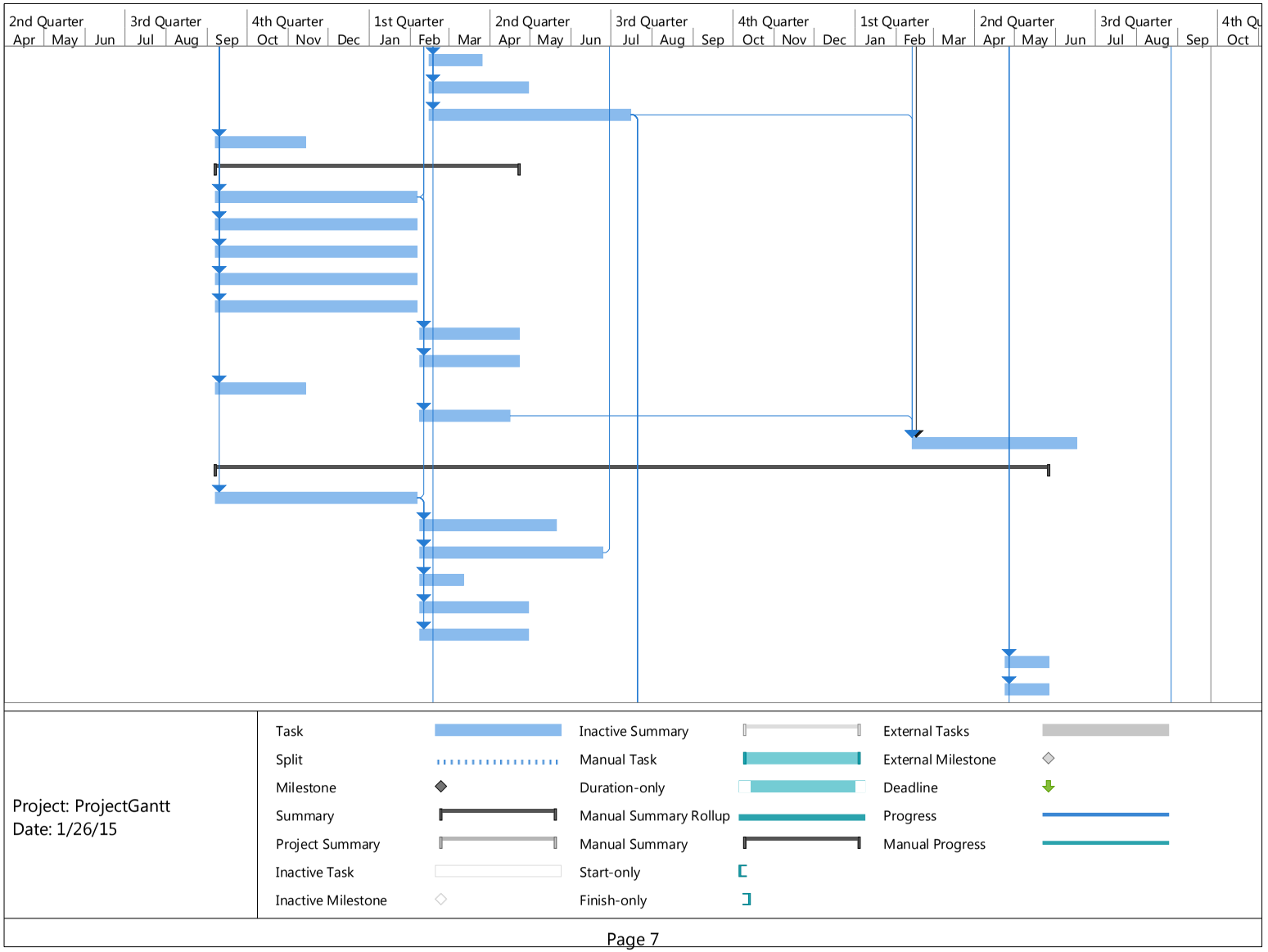
2nd Quarter
Apr May Jun
3rd Quarter
Jul Aug Sep
4th Quarter
Oct Nov Dec
1st Quarter
Jan Feb Mar
2nd Quarter
Apr May Jun
3rd Quarter
Jul Aug Sep
4th Quarter
Oct Nov Dec
1st Quarter
Jan Feb Mar
2nd Quarter
Apr May Jun
3rd Quarter
Jul Aug Sep
4th Qu
Oct
Project: ProjectGantt
Date: 1/26/15
Task
Split
Milestone
Summary
Project Summary
Inactive Task
Inactive Milestone
Inactive Summary
Manual Task
Duration-only
Manual Summary Rollup
Manual Summary
Start-only
Finish-only
External Tasks
External Milestone
Deadline
Progress
Manual Progress

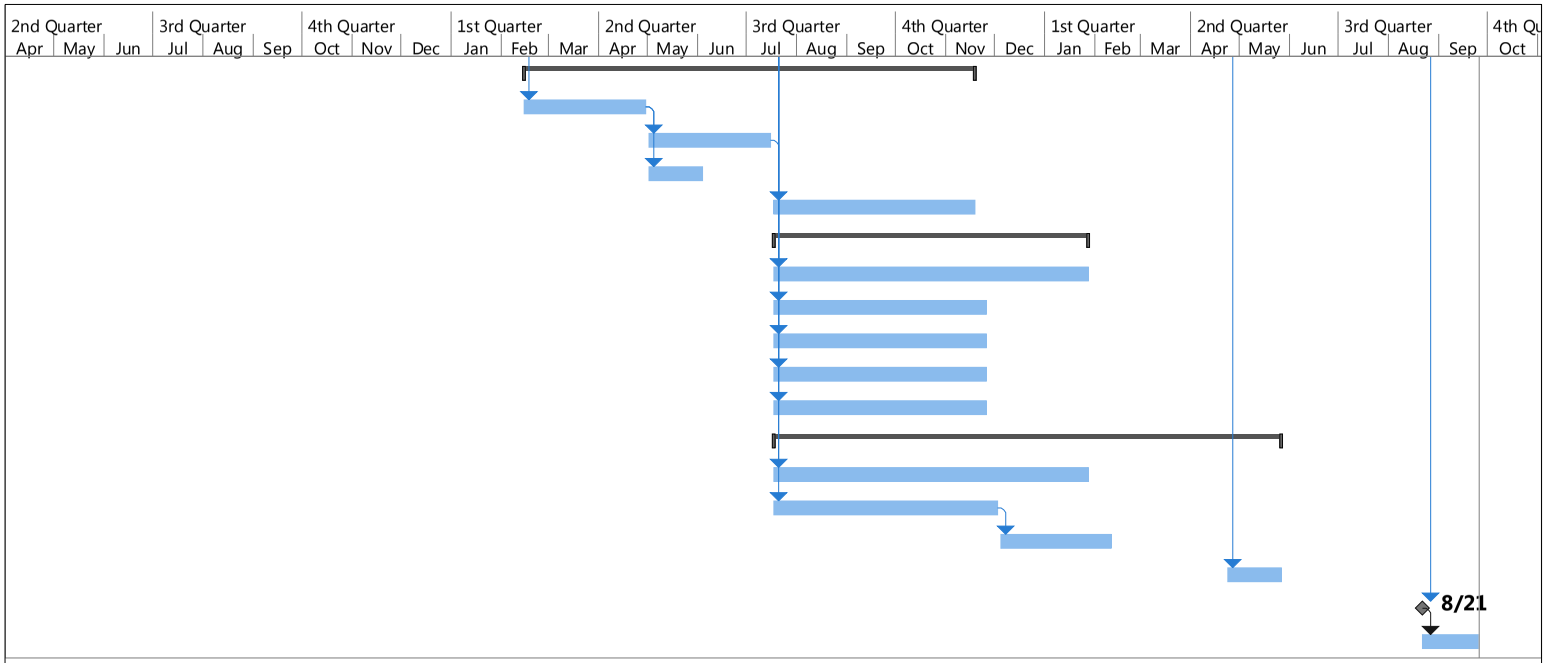

Project: ProjectGantt
Date: 1/26/15

Task		Inactive Summary		External Tasks	
Split		Manual Task		External Milestone	
Milestone		Duration-only		Deadline	
Summary		Manual Summary Rollup		Progress	
Project Summary		Manual Summary		Manual Progress	
Inactive Task		Start-only			
Inactive Milestone		Finish-only			